

# **Advanced Turbine Systems Program**

## **Phase III**

### **Technical Progress**

#### **Final Report**

**Prepared for: US Department of Energy  
National Energy Technology Laboratory  
Morgantown, WV 26507-0880**

**Prepared by: Siemens Westinghouse Power Corporation  
Orlando, Florida 32826-2399**

**Date Issued: April 21, 2004**

**DOE Contract Nos. DE-AC21-93MC30247  
DE-FC21-95MC32267**

## **DISCLAIMER**

“This report was prepared as an account of work sponsored by an agency of the United States Government. Neither the United States Government nor any agency thereof, nor any of their employees, makes any warranty, express or implied, or assumes any legal liability or responsibility for the accuracy, completeness, or usefulness of any information, apparatus, product, or process disclosed, or represents that its use would not infringe privately owned rights. Reference herein to any specific commercial product, process, or service by trade name, trademark, manufacture, or otherwise does not necessarily constitute or imply its endorsement, recommendation, or favoring by the United States Government or any agency thereof. The views and opinions of authors expressed herein do not necessarily state or reflect those of the United States government or any agency thereof.”

## PUBLIC ABSTRACT

Natural gas combustion turbines are rapidly becoming the primary technology of choice for generating electricity. At least half of the new generating capacity added in the US over the next twenty years will be combustion turbine systems. The Department of Energy has co-sponsored with Siemens Westinghouse, a program to maintain the technology lead in gas turbine systems. The very ambitious eight year program was designed to demonstrate a highly efficient and commercially acceptable power plant, with the ability to fire a wide range of fuels. The main goal of the Advanced Turbine Systems (ATS) Program was to develop ultra-high efficiency, environmentally superior and cost effective competitive gas turbine systems for base load application in utility, independent power producer and industrial markets. Performance targets were focused on natural gas as a fuel and included:

- System efficiency that exceeds 60% (lower heating value basis)
- Less than 10 ppmv NO<sub>x</sub> emissions without the use of post combustion controls
- Busbar electricity that are less than 10% of state of the art systems
- Reliability-Availability-Maintainability (RAM) equivalent to current systems
- Water consumption minimized to levels consistent with cost and efficiency goals
- Commercial systems by the year 2000

In a parallel effort, the program was to focus on adapting the ATS engine to coal-derived or biomass fuels.

In Phase 1 of the ATS Program, preliminary investigators on different gas turbine cycles demonstrated that net plant LHV based efficiency greater than 60% was achievable. In Phase 2 the more promising cycles were evaluated in greater detail and the closed-loop steam-cooled combined cycle was selected for development because it offered the best solution with least risk for achieving the ATS Program goals for plant efficiency, emissions, cost of electricity and RAM. Phase 2 also involved conceptual ATS engine and plant design and technology developments in aerodynamics, sealing, combustion, cooling, materials, coatings and casting development. The market potential for the ATS gas turbine in the 2000-2014 timeframe was assessed for combined cycle, simple cycle and integrated gasification combined cycle, for three engine sizes. The total ATS market potential was forecasted to exceed 93 GW.

Phase 3 and Phase 3 Extension involved further technology development, component testing and W501ATS engine detail design. The technology development efforts consisted of ultra low NO<sub>x</sub> combustion, catalytic combustion, sealing, heat transfer, advanced coating systems, advanced alloys, single crystal casting development and determining the effect of steam on turbine alloys. Included in this phase was full-load testing of the W501G engine at the McIntosh No. 5 site in Lakeland, Florida.

The major DOE/Siemens Westinghouse ATS Program accomplishments are listed below.

### TECHNOLOGY VERIFICATION

**Incorporated ATS technology into the Siemens Westinghouse gas turbine product line** - Technologies successfully developed in the ATS program were incorporated into the complete Siemens Westinghouse product line, including W501D, W501F, and W501G.

**W501G engine field testing to verify ATS technology** - An extensive test was carried out on the Prototype W501G engine at the City of Lakeland, Florida, power plant to verify the ATS technology incorporated in its design. These technologies included the first sixteen stages of the ATS compressor, stage three detail turbine blade cooling, stage four turbine shrouded and snubbed (a blade with an interlocking connector, a snubber, between blades similar to a tip shroud except occurring near mid-span) blade, advanced turbine airfoil bond coat/TBC coating system, brush seals in the turbine interstage locations, and abradable coatings on compressor and turbine stationary air seals to reduce blade tip clearances without incurring severe blade tip rubs. More than 1,200 sensors were installed to measure temperatures, pressures, flow angles, emissions, stresses, tip clearances and blade vibration characteristics.

**Twenty-stage ATS compressor design and full scale verification test** - The twenty-stage 30 to 1 pressure ratio ATS compressor was designed using the latest viscous analysis codes available at the time. A test facility was designed and constructed at the US Navy Base in Philadelphia. A full scale ATS compressor test was then tested in this facility to verify the compressor starting characteristics, performance and mechanical integrity.

**W501F viscous compressor field verification** - To improve the W501F, which is the main production engine in Siemens Westinghouse, the compressor was redesigned using viscous design methods developed under the ATS program for increased flow and efficiency using further advances in viscous design philosophy, such as end bends. This compressor design was verified by a field test at a customer site.

#### GAS TURBINE COMBUSTION

**Dry low NO<sub>x</sub> combustor development** - Development was carried out on several lean premixed dry low NO<sub>x</sub> combustors to ensure that low emissions can be achieved at ATS firing temperatures without combustion instabilities and flashback. The most successful concept is the Dry Low NO<sub>x</sub> (DLN) combustor, which consists of eight premixed swirler assemblies arranged around a diffusion/pilot nozzle/swirler assembly. Development tests were carried out in atmospheric, mid pressure, and high pressure test rigs, as well as in field engines.

**Test trials of catalytic combustor module** - In order to achieve single digit NO<sub>x</sub> emissions at ATS firing temperature without incurring combustion instabilities associated with very lean premixed flames, a catalytic pilot and a completely catalytic combustor are being developed. Tests were carried out to demonstrate catalyst performance characteristics over long periods of operation.

**Sub-scale demonstration of active combustion noise control** - An active combustion noise control system is being developed to allow safe lean premix combustor operation without resorting to catalytic components. Subscale tests were carried out on a system using a sensor located in the combustor, signal processor, actuator, and a control valve located in the fuel bypass line. Tests demonstrated a four-fold reduction in combustion dynamics.

**Non-intrusive laser-induced fluorescence probe development** - Controlling combustion dynamics in lean premix combustors requires very well mixed fuel/air mixtures. Poor mixing results in uneven flame temperatures, and hence combustion instabilities and high NO<sub>x</sub> in regions of high flame temperatures. A non-intrusive laser-induced fluorescence probe was

developed for measuring fuel/air concentrations and combustion product concentrations. This probe was used in unfired and fired tests.

#### ADVANCED SEALING & COOLING

**Advanced sealing development** - ATS engine performance and hot parts' mechanical integrity are detrimentally affected by cooling air or hot gas leaks. To reduce these leaks brush seals, rope seals, face seals, and abradable coatings were developed.

**Closed-loop steam cooling technology development** - One of the main contributors to the ATS engine performance is closed-loop steam cooling of turbine components. Designs were carried out for the first and second stage turbine closed-loop steam cooled stators and ring segments (air seals).

**Advanced Air Cooling Technology Development** - Tests were carried out to optimize turbine airfoil air cooling designs. These included multi-pass blade cooling, stator endwall cooling, third stage shrouded blade cooling, and effect on internal heat transfer coefficients of different turbulator shapes located in internal airfoil cooling passages.

#### ADVANCED MATERIALS & COATINGS

**Advanced bond coat/TBC system development** - Long life bond coat/TBC systems are required to ensure the mechanical integrity of turbine airfoils. This is especially important for closed-loop steam cooled designs, which do not have protection of film cooling used in current gas turbine cooling designs. To address this issue an advanced high temperature bond coat/TBC system capable of 24,000 hour operation was developed.

**Effect of steam on turbine alloy materials** - Rig tests were carried out to investigate the effect of cooling steam on turbine components. These tests included fouling, scaling, oxidation, and corrosion characteristics of several alloys used in turbine airfoils, transitions, and steam pipes. Based on the results steam purity criteria and internal surface coating requirements were defined.

**Weldable turbine vane alloy development** - A more weldable version of IN939 alloy was developed to allow welding cracks in new turbine vane castings to improve casting yields and cracks in service run parts to reduce life cycle costs.

**Single Crystal casting technology development for large land based turbines** - Higher operating gas temperatures in the ATS application and the requirement to minimize coolant flows to improve performance necessitate the use of Single Crystal (SC) turbine alloys. Casting development was carried out on thin wall first stage vanes, first stage blades, second stage blades, and third stage shrouded blades to demonstrate the feasibility of SC castings for use in large utility gas turbines.

# TABLE OF CONTENTS

<b>DISCLAIMER</b> .....	<b>I</b>
<b>PUBLIC ABSTRACT</b> .....	<b>II</b>
TECHNOLOGY VERIFICATION .....	ii
GAS TURBINE COMBUSTION .....	iii
ADVANCED SEALING & COOLING .....	iv
ADVANCED MATERIALS & COATINGS .....	iv
<b>LIST OF FIGURES</b> .....	<b>XIII</b>
<b>LIST OF TABLES</b> .....	<b>XVI</b>
<b>LIST OF ACRONYMS</b> .....	<b>XVII</b>
<b>1.0 TECHNICAL SUMMARY</b> .....	<b>1</b>
TECHNOLOGY VERIFICATION .....	2
GAS TURBINE COMBUSTION .....	2
ADVANCED SEALING & COOLING .....	3
ADVANCED MATERIALS & COATINGS .....	3
<b>2.0 TECHNICAL DISCUSSIONS</b> .....	<b>4</b>
2.1 PHASE 1 .....	4
2.1.1 <i>Introduction/ Background</i> .....	4
2.1.2 <i>Cycle Studies</i> .....	6
2.1.2.1 Intercooling .....	6
2.1.2.2 Recuperated.....	6
2.1.2.3 Intercooled, Recuperative Combined Cycle .....	6
2.1.2.4 Inlet Cooling/Steam Injection/Water Spray After Cooling .....	6
2.1.2.5 Continual Evaporative Cooling.....	7
2.1.2.6 Closed-Loop Cooling.....	7
2.1.2.7 Thermochemical Recuperation .....	8
2.1.2.8 Reheat .....	8
2.1.2.9 Reference Cycle .....	9
2.1.3 <i>Efficiency Enhancement</i> .....	9
2.1.4 <i>Emissions</i> .....	11
2.1.5 <i>Adaptability to Coal-Derived Fuels</i> .....	12
2.1.6 <i>Conclusions</i> .....	12
2.2 PHASE 2 / PHASE 2 EXTENSION.....	12
2.2.1 <i>Introduction</i> .....	12
2.2.2 <i>Task 1.0 - Project Plan</i> .....	13
2.2.2.1 Task 1.1 Develop Project Plan .....	13
2.2.2.2 Task 1.2 Program Management .....	14
2.2.3 <i>Task 2.0 Information Required for National Environmental Policy Act (NEPA)</i> .....	14
2.2.4 <i>Task 3.0 Selection of Natural Gas-Fired Advanced Turbine Systems</i> .....	15
2.2.4.1 Introduction.....	15
2.2.4.2 Discussion .....	16
2.2.4.3 Cycle Analysis .....	18
2.2.4.3.1 Baseline Cycle.....	18

2.2.4.3.2	Component Improvements	19
2.2.4.3.3	Steam Cycle Enhancements	20
2.2.4.3.4	Rotor Air Cooler Heat Utilization	20
2.2.4.3.5	Closed-Loop Steam Cooling	21
2.2.4.3.6	Increased Compressor Pressure Ratio	23
2.2.4.3.7	Increased Turbine Inlet Temperature	25
2.2.4.3.8	Compressor Intercooling	25
2.2.4.3.9	Recuperation	27
2.2.4.3.10	Intercooling with Recuperation	28
2.2.4.3.11	Reheat Combustion Turbine	29
2.2.4.3.12	Thermochemical Recuperation	30
2.2.4.3.13	Steam Injection	31
2.2.4.3.14	Evaluation of Candidate Systems	32
2.2.5	<i>Task 4.0 Conversion of an Advanced Natural Gas-Fueled Combustion Turbine to Coal-Based Fuel Application</i>	33
2.2.5.1	Introduction	33
2.2.5.2	Selection of Coal-Fired Plant Reference System	34
2.2.5.3	IGCC CFATS Description	34
2.2.5.4	Second-Generation PFBC CFATS Description	36
2.2.5.5	Performance and Emissions Estimates	37
2.2.5.6	Identification of Design Changes to GFATS	41
2.2.5.7	Conclusions	46
2.2.6	<i>Task 5.0 Advanced Turbine System Market Study</i>	47
2.2.6.1	Introduction	47
2.2.6.2	IGCC Analysis	52
2.2.6.3	Summary	53
2.2.7	<i>Task 6.0 System Definition and Analysis</i>	55
2.2.7.1	Introduction	55
2.2.7.2	Plant Configuration	56
2.2.7.2.1	Combustion Turbine	57
2.2.7.2.2	Heat Recovery Steam Generator	57
2.2.7.2.3	Fuel Gas Heater	57
2.2.7.2.4	Steam Piping	58
2.2.7.2.5	Steam Turbine	59
2.2.7.2.6	Generator-Exciter	59
2.2.7.2.7	Condenser/Cooling Tower	60
2.2.7.2.8	Site Arrangement	60
2.2.7.2.9	Generation Equipment Layout	60
2.2.7.3	ATS Engine Conceptual Design	60
2.2.7.3.1	Inlet	61
2.2.7.3.2	Compressor	61
2.2.7.3.3	Combustion System	62
2.2.7.3.4	Turbine	64
2.2.7.3.5	Secondary Flow System	65
2.2.7.3.6	Rotor System	66
2.2.7.3.7	Exhaust Diffuser	66
2.2.8	<i>Task 7.0 Integrated Program Plan</i>	66
2.2.8.1	R&D Plans for Critical Components/Barrier Issues	66
2.2.8.2	Full Scale GFATS Demonstration Plan	67
2.2.9	<i>Task 8.0 Design and Test of Critical Components</i>	67
2.2.9.1	Background	67

2.2.9.2 Technology Improvements .....	68
2.2.9.2.1 Turbine Improvements .....	69
2.2.9.2.2 Plant Improvements .....	69
2.2.9.3 Importance of Materials .....	71
2.2.9.3.1 General Material Requirements .....	71
2.2.9.3.2 Gas Turbine Disc Materials .....	72
2.2.9.3.3 Combustion System Materials .....	73
2.2.9.3.4 Gas Turbine Vane Materials .....	73
2.2.9.3.5 Turbine Blade Materials .....	74
2.2.9.3.5.1 Row 1 to 3 Blade Alloys .....	74
2.2.9.3.5.2 Row 4 Blade Alloys .....	76
2.2.9.4 Coatings for Hot Section Components .....	77
2.2.9.5 Combustion .....	78
2.2.9.6 Cooling .....	79
2.2.9.7 Mechanical Design .....	81
2.2.9.8 Leakage Control .....	81
2.2.9.9 Design and Test Results .....	81
2.2.9.9.1 Blade Cooling .....	81
2.2.9.9.1.1 Task 8.1 Effects of Blade Cooling Alternatives on Performance .....	82
2.2.9.9.1.2 Task 8.10 and 8.28 Stator Cooling .....	82
2.2.9.9.1.3 Task 8.12 Shrouded Blade Cooling Development .....	84
2.2.9.9.1.4 Tasks 8.14 and 8.31 Closed-Loop Steam Cooling - Row 1 Vane .....	84
2.2.9.9.1.5 Task 8.22 Serpentine Channel Cooling Tests .....	85
2.2.9.9.1.6 Task 8.38 Closed-Loop Steam Cooling (CLSC) Effects .....	88
2.2.9.9.2 Blade Materials .....	90
2.2.9.9.2.1 Tasks 8.5 and 8.33 Single Crystal Blade Material Development .....	90
2.2.9.9.2.1.1 Row 1 Blade Casting Results .....	91
2.2.9.9.2.1.2 Row 3 Blade Casting Results .....	91
2.2.9.9.2.1.3 Conclusions .....	91
2.2.9.9.2.2 Tasks 8.7 and 8.32 Ceramics .....	92
2.2.9.9.2.2.1 Selection of hot gas path components suitable for conversion to ceramics .....	93
2.2.9.9.2.2.2 Selection of the ceramic material .....	93
2.2.9.9.2.2.3 Manufacturing Feasibility .....	94
2.2.9.9.2.2.4 Preliminary Design Studies .....	94
2.2.9.9.2.3 Task 8.11 Directional Solidified Blade Material .....	95
2.2.9.9.2.4 Tasks 8.18 and 8.30 Thermal Barrier Coatings .....	96
2.2.9.9.2.4.1 Experimental Procedure .....	97
2.2.9.9.2.4.2 Results and Discussion .....	97
2.2.9.9.2.4.3 New Ceramics .....	100
2.2.9.9.2.4.4 Thermal Barrier Coating Field Tests .....	101
2.2.9.9.2.4.5 Test Results .....	102
2.2.9.9.2.4.6 Conclusions .....	102
2.2.9.9.2.5 Task 8.37 Forged Disc Materials .....	103
2.2.9.9.3 Tasks 8.3 and 8.13 Last Row Blade Development .....	104
2.2.9.9.3.1 Design Obstacles .....	104
2.2.9.9.3.2 Design Approach .....	106
2.2.9.9.3.3 Design Results .....	106
2.2.9.9.4 Task 8.15 Active Tip clearance Control .....	107
2.2.9.9.4.1 Conceptual Design .....	107
2.2.9.9.4.2 Test Results .....	107
2.2.9.9.5 Combustor Development .....	108

2.2.9.9.5.1	Catalytic Combustor .....	108
2.2.9.9.5.1.1	Initial Investigation .....	108
2.2.9.9.5.1.2	NO <sub>x</sub> Prediction .....	108
2.2.9.9.5.1.3	Preliminary Design .....	108
2.2.9.9.5.2	Task 8.16 Flow Dynamics and Visualization .....	109
2.2.9.9.5.3	Task 8.17 Combustor Noise.....	109
2.2.9.9.5.3.1	Stabilization System Description .....	109
2.2.9.9.5.3.2	Sub-Scale Combustor Test Section Design.....	111
2.2.9.9.5.3.3	Experiment Construction .....	113
2.2.9.9.5.3.4	Test Results .....	114
2.2.9.9.5.3.5	Conclusions.....	114
2.2.9.9.6	Tasks 8.23, 8.24 and 8.29 Seal Development .....	115
2.2.9.9.6.1	Preliminary Investigation.....	116
2.2.9.9.6.3	Focused Seal Development.....	118
2.2.9.9.7	Diagnostics Instrumentation .....	121
2.2.9.9.7.1	Tasks 8.20 and 8.36 Optical Diagnostics Probe.....	121
2.2.9.9.7.2	Task 8.26 Combustion Turbine Blade Vibration Monitor System .....	122
2.2.9.9.8	Tasks 8.8 and 8.21 Diffuser Extraction Study .....	123
2.2.9.9.8.1	Computational Study.....	124
2.2.9.9.8.2	Experimental Study.....	125
2.2.9.9.9	Task 8.25 High Efficiency Compressor Design.....	127
2.2.10	<i>Conclusions</i> .....	128
2.3	PHASE 3/ PHASE 3 EXTENSION.....	130
2.3.1	<i>Introduction</i> .....	130
2.3.2	<i>Task 1 NEPA Information</i> .....	131
2.3.3	<i>Task 2 ATS Engine Design</i> .....	131
2.3.4	<i>Task 3.0 Specification and Design of Power Plant Equipment</i> .....	134
2.3.5	<i>Task 4.0 Specification and Design of Balance of Plant Equipment</i> .....	136
2.3.6	<i>Task 5.0 Plant Performance Analysis</i> .....	137
2.3.7	<i>Task 6.0 Market Study</i> .....	137
2.3.8	<i>Task 7.0 and 12.6, Adaptation of ATS to Coal and Biomass Fuels</i> .....	137
2.3.8.1	<i>Introduction</i> .....	137
2.3.8.2	<i>ATS Turbine Adaptation to APFBC</i> .....	138
2.3.8.3	<i>ATS Turbine Adaptation to IGCC</i> .....	140
2.3.9	<i>Task 8.0 Integrated Program Plan</i> .....	141
2.3.10	<i>Tasks 9.0 and 12.0 Design, Test and Development of Critical Components</i> .....	144
2.3.10.1	<i>Cooling Development</i> .....	144
2.3.10.1.1	<i>Tasks 9.1 and 12.1.4 Closed-Loop Cooling Development/Vane Cascade Test</i> .....	144
2.3.10.1.1.1	<i>Introduction</i> .....	144
2.3.10.1.1.2	<i>Design of Rig Components</i> .....	145
2.3.10.1.1.3	<i>Instrumentation</i> .....	148
2.3.10.1.1.4	<i>Hardware Manufacture</i> .....	148
2.3.10.1.1.5	<i>Combustion Test Rig Commissioning</i> .....	149
2.3.10.1.1.6	<i>Conclusions</i> .....	149
2.3.10.1.2	<i>Task 9.19 Closed-Loop Cooling Internal Heat Transfer Tests</i> .....	149
2.3.10.1.2.1	<i>Introduction</i> .....	149
2.3.10.1.2.2	<i>Models Tested</i> .....	150
2.3.10.1.2.3	<i>Test Results</i> .....	150
2.3.10.1.2.4	<i>Conclusions</i> .....	150
2.3.10.1.3	<i>Task 12.1.9 Turbulator Model Tests</i> .....	150
2.3.10.1.3.1	<i>Introduction</i> .....	150

2.3.10.1.2.2 Test Results .....	150
2.3.10.2 Sealing Development .....	151
2.3.10.2.1 Task 9.3 Rotor Sealing Development .....	151
2.3.10.2.1.1 Introduction .....	151
2.3.10.2.1.2 Seal Design and Selection .....	152
2.3.10.2.1.3 Seal Validation Testing .....	154
2.3.10.2.1.4 Conclusion .....	154
2.3.10.2.2 Tasks 9.6 and 12.2.3 Advanced Sealing Development .....	155
2.3.10.2.2.1 Introduction .....	155
2.3.10.2.2.2 Development Program .....	156
2.3.10.2.2.3 Brush Seal Design .....	157
2.3.10.2.2.4 Tribological Testing .....	159
2.3.10.2.2.5 Subscale Seal Rig Testing .....	161
2.3.10.2.2.5.1 Static Leakage Flow .....	162
2.3.10.2.2.5.2 Dynamic Rig Testing .....	162
2.3.10.2.2.5.3 Transition Mouth Brush Seal .....	163
2.3.10.2.2.6 Full-Scale Hardware Design/Fabrication .....	163
2.3.10.2.2.7 Validation Testing .....	164
2.3.10.2.2.8 Conclusions .....	165
2.3.10.2.3 Task 9.17 Transition Mouth Seal Development .....	165
2.3.10.2.3.1 Introduction .....	165
2.3.10.2.3.2 Seal Design and Manufacture .....	166
2.3.10.2.4 Task 9.7 Active Tip Clearance Control/Abradable Coating Development .....	167
2.3.10.2.4.1 Introduction .....	167
2.3.10.2.4.2 Abradable Coating Development .....	167
2.3.10.2.4.3 Requirements .....	168
2.3.10.2.4.4 Compressor Abradable Coatings .....	169
2.3.10.2.4.4.1 Coating Selection .....	169
2.3.10.2.4.4.2 Erosion Testing .....	170
2.3.10.2.4.4.3 Abradability Testing .....	170
2.3.10.2.4.4.4 Coating Validation .....	171
2.3.10.2.4.5 Turbine Abradable Coatings/Tip Treatments .....	172
2.3.10.2.4.5.1 Turbine Blade Tip Treatment Development .....	173
2.3.10.2.4.6 Conclusions .....	174
2.3.10.3 Aerodynamic Development .....	175
2.3.10.3.1 Task 9.4 Compressor Aerodynamic Development .....	175
2.3.10.3.1.1 Introduction .....	175
2.3.10.3.1.2 Description of Experimental Facility .....	176
2.3.10.3.1.2.1 Compressor and Driver .....	176
2.3.10.3.1.2.2 Auxiliary Equipment .....	176
2.3.10.3.1.2.3 Control Room .....	178
2.3.10.3.1.2.4 Instrumentation .....	178
2.3.10.3.1.2.5 Data Acquisition System .....	179
2.3.10.3.1.2.6 Operation .....	179
2.3.10.3.1.3 Test Results .....	180
2.3.10.3.1.3.1 Aerodynamic .....	180
2.3.10.3.1.3.2 Mechanical .....	181
2.3.10.3.1.4 Conclusions .....	181
2.3.10.3.2 Tasks 9.5 and 12.1.5 Turbine Aerodynamic Development .....	181
2.3.10.3.2.1 Introduction .....	181
2.3.10.3.2.2 Test Facility and Test Rig .....	183

2.3.10.3.2.3	Experimental Procedure.....	184
2.3.10.3.2.4	Results and Discussion.....	185
2.3.10.3.2.5	Conclusions.....	186
2.3.10.3.3	Task 9.18 Rotor Cooling Air Compression/Diffusion Development.....	186
2.3.10.3.3.1	Introduction.....	186
2.3.10.3.3.2	System Design.....	187
2.3.10.3.3.3	Rig Design.....	187
2.3.10.3.3.4	Test Results.....	187
2.3.10.3.3.5	Conclusions.....	188
2.3.10.4	Tasks 9.8 and 12.2.1 Combustion System Development.....	188
2.3.10.4.1	Introduction.....	188
2.3.10.4.2	Piloted Ring Combustor.....	190
2.3.10.4.3	Active Control of Combustion Noise.....	191
2.3.10.4.4	Dry Low NO <sub>x</sub> Combustor Development.....	192
2.3.10.4.5	Conclusion.....	192
2.3.10.5	Materials Development.....	192
2.3.10.5.1	Task 9.9 Ceramic Ring Segment Development.....	192
2.3.10.5.1.1	Conceptual Design.....	193
2.3.10.5.1.2	Analyses.....	193
2.3.10.5.1.2.1	Heat Transfer and Thermal Stresses.....	193
2.3.10.5.1.2.2	Mechanical and Combined Stresses.....	193
2.3.10.5.1.2.3	Stress Summary and Comparison to Material Properties.....	193
2.3.10.5.1.3	Base Technology and Subelement Testing.....	193
2.3.10.5.1.3.1	Subelement Testing.....	193
2.3.10.5.1.3.2	Base Technology.....	194
2.3.10.5.1.4	Conclusions.....	194
2.3.10.5.2	Tasks 9.10 and 12.2.6 Advanced Coating Development.....	194
2.3.10.5.2.1	Introduction.....	194
2.3.10.5.2.2	The Complete Coatings Approach.....	196
2.3.10.5.2.3	Bond Coat Development.....	196
2.3.10.5.2.3.1	New Bond Coat Chemistries.....	196
2.3.10.5.2.3.2	Diffusion Barriers.....	196
2.3.10.5.2.3.3	Composite Bond Coat.....	197
2.3.10.5.2.3.4	Bond Coat Processes.....	197
2.3.10.5.2.4	New TBC Development.....	197
2.3.10.5.2.4.1	APS of New Ceramics.....	198
2.3.10.5.2.4.2	Lab Scale Evaluation.....	198
2.3.10.5.2.4.3	EB-PVD of New Ceramics.....	198
2.3.10.5.2.4.3	New TBC Concepts.....	198
2.3.10.5.2.5	High Heat Flux Rig Used in TBC Lifting Tests.....	199
2.3.10.5.2.6	NDE, Maintenance and Repair.....	200
2.3.10.5.2.6.1	Off-line monitoring.....	200
2.3.10.5.2.6.2	On-line monitoring.....	200
2.3.10.5.2.6.3	Patch repair.....	200
2.3.10.5.2.7	Manufacturing Issues.....	201
2.3.10.5.2.7.1	Masking.....	201
2.3.10.5.2.7.2	Coating Refurbishment On Surface Recrystallization Of Single Crystals.....	201
2.3.10.5.2.8	Conclusion.....	202
2.3.10.5.3	Tasks 9.11 and 12.3.5 Steam Effects on Materials.....	202
2.3.10.5.4	Task 9.12 DS Blade Development.....	203
2.3.10.5.5	Task 12.3.4 DS/CC Properties.....	203

2.3.10.5.5.1	Validation Of Component Material Properties .....	203
2.3.10.5.5.2	Effect Of Processing Heat Treatments.....	204
2.3.10.5.6	Task 12.3.11 LCF and TMF Properties of IN 939.....	204
2.3.10.5.7	Task 12.3.6 SC Casting Production Development .....	205
2.3.10.5.8	Task 12.3.15 Liquid Metal Cooling.....	205
2.3.10.5.9	<i>Task 12.3.2 Bonded Vane Development.....</i>	<i>205</i>
2.3.10.5.10	Tasks 9.14 and 12.3.8 Advanced Weldable Alloy Development .....	208
2.3.10.5.10.1	Background .....	208
2.3.10.5.10.2	Discussion .....	209
2.3.10.5.10.3	Conclusions.....	209
2.3.10.5.11	Task 12.3.9 Thermal Barriers Coating Life Prediction.....	209
2.3.10.5.12	Task 12.3.13 Back-Filled Honeycomb (BFH) Coating Development.....	210
2.3.10.5.12.1	BFH as a Thick Thermal Barrier Coating.....	210
2.3.10.5.12.2	BFH as an Abradable Coating .....	211
2.3.10.5.12.2.1	Engine Test of Baseline BFH Coated W501D5 Ring Segment .....	211
2.3.10.5.12.2.2	Modifications to Improve BFH Abradability .....	211
2.3.10.5.12.3	Summary - Technology Status of BFH Coating.....	212
2.3.10.5.13	Nondestructive Evaluation (NDE) of ATS Components.....	212
2.3.10.5.13.1	Introduction .....	212
2.3.10.5.13.1.1	Background.....	212
2.3.10.5.13.1.2	Program Needs for NDE.....	213
2.3.10.5.13.1.3	Summary.....	214
2.3.10.5.14	Task 9.16 Ni-Based Super Alloy Rotor Material Development .....	214
2.3.10.6	Mechanical Development .....	216
2.3.10.6.1	Tasks 9.2 and 12.2.4 Thin Wall Casting Development .....	216
2.3.10.6.1.1	Introduction .....	216
2.3.10.6.1.2	Casting Trials.....	217
2.3.10.6.2	Task 12.1.6 Blade Root Verification Test .....	217
2.3.10.6.3	Task 13.4.1 Closed-Loop Cooling Circuit Integrity and Vibratory Response.....	218
2.3.10.6.4	Task 12.4.3 Alternate Vane and Blade Design .....	219
2.3.10.7	Technology Verification .....	219
2.3.10.7.1	Task 14.1 Steam Cooled Component and Aerothermal Design Verification .....	219
2.3.10.7.1.1	Introduction.....	219
2.3.10.7.1.2	W501G Prototype Engine Tests.....	220
2.3.10.7.1.3	Summary .....	222
2.3.10.7.2	Task 14.2 Advanced Viscous Compressor Test Program.....	223
2.3.10.7.2.1	Introduction.....	223
2.3.10.7.2.2	Aerodynamic Design.....	223
2.3.10.7.2.2.1	Conceptual Design .....	223
2.3.10.7.2.2.2	The “Viscous” Method.....	224
2.3.10.7.2.2.3	Results and Discussion.....	224
2.3.10.7.2.3	Field Test.....	225
2.3.10.7.2.4	Test Results .....	226
2.3.10.7.3	Task 14.3 Catalytic Combustor Development .....	226
2.3.10.7.3.1	Accomplishments.....	227
2.3.10.7.3.2	Catalyst Development .....	228
2.3.10.7.3.3	Sub-Scale Module Testing.....	229
2.3.10.7.3.4	Development of the Full-Scale Catalytic Module.....	229
2.3.10.7.3.5	Combustion System Design .....	230
2.3.10.7.3.5	Summary .....	231
2.3.10	<i>Conclusions.....</i>	<i>231</i>

3.0	ATS TECHNOLOGY FLOWDOWN TO MATURE FRAMES .....	234
4.0	PUBLIC BENEFITS.....	235
5.0	OVERALL ATS PROGRAM CONCLUSIONS.....	237
<b>REFERENCES.....</b>		<b>240</b>

## LIST OF FIGURES

Figure 1	Gas Turbine Inlet Temperature Trend .....	5
Figure 2	Evolution of Large Siemens Westinghouse Gas Turbines.....	16
Figure 3	Selected ATS Cycle Configuration.....	18
Figure 4	High Temperature Engine Baseline Combined Cycle.....	19
Figure 5	Thermal Efficiency Variation with Cooling Leakage Air .....	22
Figure 6	Effect of Compressor Pressure Ratio on Thermal Efficiencies .....	24
Figure 7	Effect of Compressor Intercooling on Specific Output .....	25
Figure 8	Effect of Compressor Intercooling on Thermal Efficiencies .....	26
Figure 9	Intercooled, Aftercooled (Evaporative), Recuperative Combined Cycle .....	29
Figure 10	Thermochemical Recuperation Cycle with Steam Reforming .....	31
Figure 11	Coal-Fired Advanced Turbine System - IGCC .....	36
Figure 12	Coal-Fueled Advanced Turbine System - PFBC.....	37
Figure 13	Conceptual Dual Topping Combustor Arrangement .....	43
Figure 14	Topping Combustor Outlet to Turbine Inlet Gas Flow Concept.....	44
Figure 15	Topping-PFBC Process Schematic.....	45
Figure 16	Screening Methodology.....	48
Figure 17	ATS Cost Advantage.....	50
Figure 18	ATS & “G” Technology Market Penetration.....	51
Figure 19	Estimated Worldwide ATS Capacity Additions.....	52
Figure 20	Estimated ATS IGCC Market Penetration .....	53
Figure 21	Worldwide ATS Capacity Additions Summary .....	54
Figure 22	ATS Market Penetration by Frame Size.....	55
Figure 23	Cross Section of ATS Engine.....	61
Figure 24	Multi-annular Swirl Combustor .....	63
Figure 25	Conceptual Design of Shell/Spar Vane .....	65
Figure 27	Typical Vane Shroud Cooling Scheme.....	83
Figure 28	General Test Configuration .....	84
Figure 29	Stage 3 Blade Tip Shroud Cooling .....	86
Figure 30	Airfoil Cross Section of Blade.....	87
Figure 31	Typical Serpentine Cooled Blade .....	87
Figure 32	Issues: Steam Cooling Effects .....	88
Figure 33	Interactive Elements of the Program for Steam Chemistry .....	90
Figure 34	CMSX-4 SC R3 Blade Casting Process Flow Chart and Process Variables .....	92

Figure 35	Single Crystal Blade .....	92
Figure 37	Thermal Fatigue Life Evaluation.....	98
Figure 38	Comparison of Coating Performance and Oxidation.....	99
Figure 39	Spalled APS Coating.....	99
Figure 40	HMA with APS Bond Coat.....	100
Figure 41	New Ceramic with Improved Performance.....	101
Figure 42	Coated Ring Segments .....	103
Figure 43	EB PVD TBC.....	103
Figure 44	Row 1 Vane.....	103
Figure 45	Row 1 Blades .....	103
Figure 46	Comparison of Simulated Pressure Signal (dotted line) with Actual. ....	110
Figure 47	Combustion Fluctuation Response to Secondary Fuel Oscillations.....	111
Figure 48	High Pressure, Preheated Air Test Facility .....	112
Figure 49	Scaled Down Test Combustor.....	113
Figure 50	Frequency Spectra of Oscillations Before Active Stabilization.....	114
Figure 51	Measured Pressure Responses Before and After Active Cancellation. ....	115
Figure 52	Start-up Cycle for a Turbine Interstage Location.....	117
Figure 53	Uncoated Rotor Used in Test.....	118
Figure 54	Subscale Seal Design Methodology.....	119
Figure 55	High Speed Friction Test Rig Used in Tribological Testing .....	120
Figure 56	First Generation Optical Probe.....	122
Figure 57	Second Generation Optical Probe.....	122
Figure 58	Two Probe CT Blade Vibration Monitor.....	123
Figure 65	ATS Engine Cross-Section .....	132
Figure 66	ATS Plant Layout.....	135
Figure 67	Integrated Combustion/Hot Cascade Test Facility .....	146
Figure 68	Integrated Combustion/Hot Cascade Test Rig.....	147
Figure 69	Axial Flow Combustion Test Rig .....	147
Figure 70	ATS Combustion Test Rig.....	149
Figure 71	W501ATS Sealing Focus Areas.....	151
Figure 72	Standard Brush Design .....	158
Figure 73	Advanced Seal Design.....	158
Figure 74	Results from Turbine-Front Brush Seal Subscale Rig Testing.....	163
Figure 76	Compressor Test Facility.....	176
Figure 77	Schematic of the Ohio State University Gas Turbine Shock Tube Facility.....	183

Figure 78 Schematic Diagram of the Turbine Test Rig .....	184
Figure 79 Turbine Airfoil Geometries and Clocking Positions .....	184
Figure 82 Effects of Clocking at Different Radial Heights, Blade Two Clocking .....	185
Figure 86 NO <sub>x</sub> vs Secondary Flame Temperature .....	190
Figure 87 Schematic of Active Combustion Noise Control System .....	192
Segment Under Steady-State Conditions .....	193
Figure 93 Stress-Rupture Test Data for Nicalon/Alumina CMC.....	194
Figure 94 Comparison of Temperature Gradients between the ATS and W501G (and F) Engines.....	195
Figure 95 A Full Cycle Approach To Development Of Advanced Coatings Technology .....	202
Figure 101 W501G Engine .....	220
Figure 102 Advanced Technology Applied to W501G.....	220
Figure 103 W501G Prototype Test Instrumentation .....	221
Figure 104 Thermal Paint Test .....	222
Figure 105 Thermal Paint Test Results on First Stage Blade .....	222
Figure 106 Measured Transition Metal Temperatures .....	222
Figure 108 W501FD Compressor Third Stage Stator.....	225
Figure 109 ATS Catalytic Module Concept.....	227
Figure 111 Catalytic Combustor .....	231

## LIST OF TABLES

	Title	Page
Table 1	Estimated Cycle Performance .....	9
Table 2	CFATS Thermal Performance .....	39
Table 3	CFATS Emissions Performance .....	42
Table 4	Turbine Frame Size Preferences .....	49
Table 5	Overall Performance of ATS Plant .....	56
Table 6	HRSG Design Parameters .....	57
Table 7	Fuel Gas Heater Performance Data .....	58
Table 8	Steam Piping Design Parameters .....	59
Table 9	Steam Turbine Performance Parameters .....	59
Table 10	Condenser Performance Parameters .....	60
Table 11	ATS Component Development Projects .....	70
Table 12	Qualitative Evaluation of Available CMCs for Ring Segment Application .....	95
Table 13	TBC Tests in Progress .....	102
Table 15	ATS Advisory Board .....	143
Table 17	Summary of Catalytic Combustor Development in ATS Program .....	228

## LIST OF ACRONYMS

ACT	Asymmetric Crystal Topography
AEDC	Arnold Engineering Development Center
APFBC	Advanced Pressurized Fluidized – Bed Combustion
APS	Air Plasma Spray
ATS	Advanced Turbine Systems
BOP	Balance of Plant
BOT	Burner Outlet Temperature
BTU	British Thermal Unit
BFH	Back-Filled Honeycomb
BVM	Blade Vibration Monitoring
CA	Cobalt-based Bondcoat with Higher Aluminum Content
CBN	Cubic Boron Nitride
CC	Conventional Casting or Combined Cycle
CDA	Controlled Diffusion Airfoils
CFATS	Coal-Fueled Advanced Turbine System
CFD	Computational Fluid Dynamics
CLSC	Closed-Loop Steam Cooling
CMC	Ceramic Matrix Composites
CT	Combustion Turbine
CVD	Chemical Vapor Deposition
DAS	Data Acquisition System
DCA	Double Circular Arc
DCFT	Direct Coal-Fired Turbines
DLN	Dry Low NO <sub>x</sub>

DOE	Department of Energy
DS	Directionally Solidified
EB-PVD	Electron Beam Physical Vapor Deposition
EDM	Electro Discharge Machining
EGR	Exhaust Gas Recirculation
EPRI	Electric Power Research Institute
FE	Finite Element
FEA	Finite Element Analysis
FFT	Fast Fourier Transform
FGR	Flue Gas Recirculation
FSNL	Full Speed NO <sub>x</sub> Load
GFATS	Natural-Gas-Fired Advanced Turbine System
GT	Gas Turbine
HAT	Humid Air Turbine
HCF	High Cycle Fatigue
HIP	Hot Isostatic Pressing
HP	High Pressure
HRSG	Heat Recovery Steam Generator
HTC	Heat Transfer Coefficient
HVOF	High Velocity Oxy Fuel
ICRCC	Intercooled, Recuperative Combined Cycle
IGV	Inlet Guide Vane
IP	Intermediate Pressure
IR	Infrared
ISO	International Standards Organization
KRW	Kellog Rust Siemens Westinghouse

LCF	Low Cycle Fatigue
LHV	Lower Heating Value
LMC	Liquid Metal Cooling
LNG	Liquified Natural Gas
LP	Low Pressure
LPPS	Low Pressure Plasma Spray
MASB	Multi-annular Swirl Burner
MF	Magnification Factor
MHI	Mitsubishi Heavy Industries
MWM	Meandering Winding Magnetometer
NDE	Non-destructive Evaluation
NEPA	National Environmental Protection Act
NERC	National Electricity Reliability Council
NES	National Energy Strategy
NY	Nickel-based Bondcoat with Lower Yttrium Content
OGV	Outlet Guide Vane
ORNL	Oak Ridge National Laboratory
PC	Pack Cementation
PLC	Programmable Logic Controller
PRC	Piloted Ring Combustor
RAM	Reliability-Availability-Manufacturability
RFP	Request for Proposal
RIT	Rotor Inlet Temperature
SC	Single Crystal
SEM	Scanning Electron Microscope
SOW	Statement of Work

SPS	Shrouded Plasma Spray
STC	Science and Technology Center
TBC	Thermal Barrier Coatings
TCR	Thermochemical Recuperation
TGO	Thermally Grown Oxide
TLP	Transient Liquid Phase
TWI	Thermal Wave Imaging
UDI	Utility Data Institute
UHC	Unburned Hydrocarbons
VPS	Vapor Plasma Spray
WBS	Work Breakdown Structure
XRD	X-Ray Diffraction
YSZ	Yttria-Stabilized Zirconia

## 1.0 TECHNICAL SUMMARY

Natural gas combustion turbines are rapidly becoming the primary technology of choice for generating electricity. At least half of the new generating capacity added in the US over the next twenty years will be combustion turbine systems. The Department of Energy has co-sponsored with Siemens Westinghouse, a program to maintain the technology lead in gas turbine systems. The very ambitious eight year program was designed to demonstrate a highly efficient and commercially acceptable power plant, with the ability to fire a wide range of fuels. The main goal of the Advanced Turbine Systems (ATS) Program was to develop ultra-high efficiency, environmentally superior and cost effective competitive gas turbine systems for base load application utility, independent power producer and industrial markets. Performance targets were focused on natural gas as a fuel and included:

- System efficiency that exceeds 60% (lower heating value basis)
- Less than 10 ppmv NO<sub>x</sub> emissions without the use of post combustion controls
- Busbar electricity that are less than 10% of state of the art systems
- Reliability-Availability-Maintainability (RAM) equivalent to current systems
- Water consumption minimized to levels consistent with cost and efficiency goals
- Commercial systems by the year 2000

In a parallel effort, the program was to focus on adapting the ATS engine to coal-derived or biomass fuels.

During the ATS Program Phase 1 preliminary investigations of different gas turbine cycles demonstrated that net plant LHV based efficiency of greater than 60% as well as the other ATS program goals, were achievable. It was determined that cycle innovations, increased firing temperature, reduced cooling air usage, improved component efficiencies and improved material coating systems will all be needed to accomplish the ambitious goals.

In Phase 2, the more promising cycles were evaluated in greater detail and the closed-loop steam-cooled advanced combined cycle was selected for development because it offered the best solution with least risk for achieving the ATS Program goals of plant efficiency, emissions, cost of electricity and RAM. The cycles investigated included: combined cycle variants with different enhancements, including closed-loop cooling, recuperation, intercooling with recuperation, thermal recuperation and reheat. The market potential for the ATS gas turbine in the 2000-2014 timeframe was assessed for combined cycle, simple cycle and integrated gasification combined cycle, for three engine sizes. The total ATS market potential was forecasted to exceed 93GW. The combined cycle represents the greatest opportunity, because of its economic advantage. Each ATS product is expected to meet its maximum market penetration approximately 7 to 10 years after initial demonstration. An advanced 420 MW combined cycle, based on a 318 MW closed-looped steam-cooled gas turbine and a new advanced steam turbine/generator design, was selected. During Phase 2, conceptual ATS engine and plant designs were developed. To enhance the ATS gas turbine as well as plant efficiencies, the ATS gas turbine incorporated advanced materials, coatings, cooling concepts, sealing designs and 3D aerodynamic designs. Closed-loop steam cooling was employed in hot components for performance improvement and NO<sub>x</sub> reduction. To help in achieving ATS Program goals, technology development was started in aerodynamics, sealing, combustion, cooling, mechanical integrity, materials, coatings and single crystal airfoil casting. Investigation was carried out on the conversion of the ATS engine to coal derived fuel operation. Two coal-fueled power plant technologies

were selected for the coal fired ATS; air-blown integrated gasification combined cycle and second generation pressurized fluidized bed combustion.

Phase 3 and Phase 3 Extension involved further technology development, component testing and ATS engine detail design. The ATS engine design was based on the 20 stage compressor and closed-loop stream cooled turbine. The ATS plant design was an extension of the W501F reference plant with a single shaft concept. Integrated hot vane cascade/combustor test rig was designed and manufactured. The first two stages of the ATS turbine were rig tested to verify aerodynamic performance and efficiency benefits due to optimum airfoil "clocking." A novel concept was developed for compressing cooling air inside a closed-loop turbine rotor/blade system. Demonstrated feasibility of a CMC turbine blade tip air seal design. Determined material property data for several CC, DS and SC turbine alloys. Investigated feasibility of fabricating a SC turbine vane from smaller castings. Developed several nondestructive evaluation techniques for TBC quality monitoring and SC blade inspection.

The major DOE/Siemens Westinghouse ATS Program accomplishments are listed below.

### TECHNOLOGY VERIFICATION

**Incorporated ATS technology into the Siemens Westinghouse gas turbine product line** - Technologies successfully developed in the ATS program were incorporated into the complete Siemens Westinghouse product line, including W501D, W501F, and W501G.

**W501G engine field testing to verify ATS technology** - An extensive test was carried out on the Prototype W501G engine at the City of Lakeland, Florida, power plant to verify the ATS technology incorporated in its design. These technologies included the first sixteen stages of the ATS compressor, stage three turbine blade cooling, stage four turbine shrouded and snubbed blade, advanced turbine airfoil bond coat/TBC coating system, brush seals in the turbine interstage locations, and abradable coatings on compressor and turbine stationary air seals to reduce blade tip clearances without incurring severe blade tip rubs. More than 1,200 sensors were installed to measure temperatures, pressures, flow angles, emissions, stresses, tip clearances and blade vibration characteristics.

**Twenty-stage ATS compressor design and full scale verification test** - The twenty-stage 30 to 1 pressure ratio ATS compressor was designed using the latest viscous analysis codes available at the time. A test facility was designed and constructed at the US Navy Base in Philadelphia. A full scale ATS compressor test was then tested in this facility to verify the compressor starting characteristics, performance and mechanical integrity.

**W501F viscous compressor field verification** - To improve the W501F, which is the main production engine in Siemens Westinghouse, the compressor was redesigned using viscous design methods developed under the ATS program for increased flow and efficiency using further advances in viscous design philosophy, such as end bends. This compressor design was verified by a field test at a customer site.

### GAS TURBINE COMBUSTION

**Dry low NO<sub>x</sub> combustor development** - Development was carried out on several lean premixed dry low NO<sub>x</sub> combustors to ensure that low emissions can be achieved at ATS firing temperatures without combustion instabilities and flashback. The most successful concept is the Dry Low NO<sub>x</sub> (DLN) combustor, which consists of eight premixed swirler assemblies arranged around a diffusion/pilot nozzle/swirler assembly. Development tests were carried out in atmospheric, mid pressure, and high pressure test rigs, as well as in field engines.

**Test trials of catalytic combustor module** - In order to achieve single digit NO<sub>x</sub> emissions at ATS firing temperature without incurring combustion instabilities associated with very lean premixed flames, a catalytic pilot and a completely catalytic combustor are being developed. Tests were carried out to demonstrate catalyst performance characteristics over long periods of operation.

**Sub-scale demonstration of active combustion noise control** - An active combustion noise control system is being developed to allow safe lean premix combustor operation without resorting to catalytic components. Subscale tests were carried out on a system using a sensor located in the combustor, signal processor, actuator, and a control valve located in the fuel bypass line. Tests demonstrated a four-fold reduction in combustion dynamics.

**Non-intrusive laser-induced fluorescence probe development** - Controlling combustion dynamics in lean premix combustors requires very well mixed fuel/air mixtures. Poor mixing results in uneven flame temperatures, and hence in combustion instabilities and high NO<sub>x</sub> in regions of high flame temperatures. A non-intrusive laser-induced fluorescence probe was developed for measuring fuel/air concentrations and combustion product concentrations. This probe was used in unfired and fired tests.

#### ADVANCED SEALING & COOLING

**Advanced sealing development** - ATS engine performance and hot parts' mechanical integrity are detrimentally affected by cooling air or hot gas leaks. To reduce these leaks brush seals, rope seals, face seals, and abradable coatings were developed.

**Closed-loop steam cooling technology development** - One of the main contributors to the ATS engine performance is closed-loop steam cooling of turbine components. Designs were carried out for the first and second stage turbine closed-loop steam cooled stators and ring segments (air seals).

**Advanced air cooling technology development** - Tests were carried out to optimize turbine airfoil air cooling designs. These included multi-pass blade cooling, stator endwall cooling, third stage shrouded blade cooling, and effect on internal heat transfer coefficients of different turbulator shapes located in internal airfoil cooling passages.

#### ADVANCED MATERIALS & COATINGS

**Advanced bond coat/TBC system development** - Long life bond coat/TBC systems are required to ensure the mechanical integrity of turbine airfoils. This is especially important for closed-loop steam cooled designs, which do not have protection of film cooling used in current gas turbine cooling designs. To address this issue an advanced high temperature bond coat/TBC system capable of 24,000 hour operation was developed.

**Effect of steam on turbine alloy materials** - Rig tests were carried out to investigate the effect of cooling steam on turbine components. These tests included fouling, scaling, oxidation, and corrosion characteristics of several alloys used in turbine airfoils, transitions, and steam pipes. Based on the results, steam purity criteria and internal surface coating requirements were defined.

**Weldable turbine vane alloy development** - A more weldable version of IN939 alloy was developed to allow welding cracks in new turbine vane castings to improve casting yields and cracks in service run parts to reduce life cycle costs.

**Single Crystal casting technology development for large land based turbines** - Higher operating gas temperatures in the ATS application and the requirement to minimize coolant flows to improve performance necessitate the use of Single Crystal (SC) turbine alloys. Casting development was

carried out on thin wall first stage vanes, first stage blades, second stage blades, and third stage shrouded blades to demonstrate the feasibility of SC castings for use in large utility gas turbines.

## **2.0 TECHNICAL DISCUSSIONS**

### **2.1 Phase 1**

#### 2.1.1 Introduction/ Background

The National Energy Strategy (NES) called for a balanced program of greater energy efficiency, use of alternative fuels, and the environmentally responsible development of all U.S. energy resources. Consistent with the NES, a Department of Energy (DOE) program was created to develop Advanced Turbine Systems (ATS). The technical ATS requirements were based upon two workshops held in Greenville, SC that were sponsored by DOE and hosted by Clemson University (Bajura, Webb and Parsons, 1992). The objective of this 10-year program, managed jointly by DOE's Office of Fossil Energy and Office of Conservation and Renewable Energy, was to develop natural gas-fired base load power plants that will have cycle efficiencies greater than 60%, lower heating value (LHV), be environmentally superior to current technology, and also be cost competitive. The program was to include work to transfer advanced technology to the coal-and biomass-fueled systems being developed in other DOE programs (Webb, Parsons and Bajura, 1993).

The Advanced Turbine Systems program was structured into four elements:

- Innovative Cycle Studies
- Utility Advanced Turbine Systems
- Industrial Advanced Turbine Systems
- Technology Base

Within each program element there were several planned phases. The Innovative Cycle Studies element includes two phases:

- Program Definition/Planning Studies
- Concept Development

Phase 1 of the ATS Program consisted of program definition/planning studies of innovative cycles. The results of these studies demonstrated that natural gas-fired net plant efficiency (LHV based) greater than 60% could be achieved (Little, Bannister, and Wiant, 1993).

The gas turbine combined cycle, a synergistic combination of the Brayton and the Rankine cycles, was developed to increase overall cycle efficiency. Heat rejected by the higher temperature topping cycle is recovered in the lower temperature bottoming cycle to produce additional power from the energy initially released by the fuel. In the last 25 years combined cycle efficiency has

increased, primarily driven by the escalation in gas turbine inlet temperature shown in Figure 1.

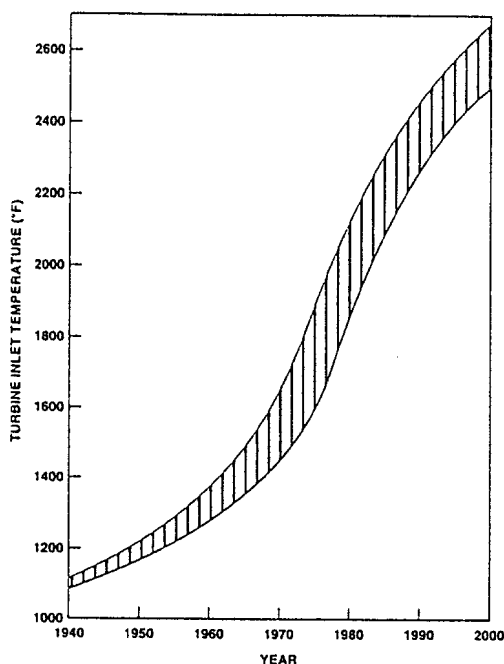


**Figure 1 Gas Turbine Inlet Temperature Trend**

In 1967, for example, a Siemens Westinghouse supercharged, evaporative cooled, W301 (1450°F [790°C] burner outlet temperature [BOT]) gas turbine, rated at 25 MW, was placed in operation. The hot turbine exhaust gases were used in a heavy fuel reheat boiler (1500 psi, 1000°F [10.3 MPa, 537°C]) which furnished steam to drive a 85 MW turbine. This West Texas Utilities, San Angelo Power Station held the distinction of achieving the highest operating efficiency in the U.S. for a number of years. In 1990 this plant, with over twenty-three years of successful operating experience, continued to demonstrate that good combined cycle efficiency over a broad load range can be obtained with a gas turbine combined with a heavy fuel reheat boiler.

By 1992, with a BOT of 2460°F (1350°C), and 2300°F (1260°C) rotor inlet temperature (RIT), ISO conditions, combined cycle efficiencies were in the range of 54% (LHV). To achieve this improvement in efficiency, the bottoming cycle has been fine-tuned to convert as much of the turbine's exhaust heat into electricity as possible.

In 1992, the ATS Program target of greater than 60% combined cycle efficiency by year 2000 seemed very optimistic. In Phase 1, innovative changes to the combined cycle were investigated to show how the efficiency target could be achieved. In this investigation the following cycles were studied: intercooled, recuperative, intercooled/recuperative/combined cycle (ICRCC), evaporative inlet air cooling, evaporative after cooler in ICRCC, continual evaporative cooling, closed-loop steam/air cooling, thermochemical recuperation, and reheat. In order to further enhance cycle efficiency the following were investigated: increased firing temperature, reduced cooling air requirement, use of pressure

gain combustion, increased component aerodynamic efficiencies, reduced clearances and reduced leakages.

## 2.1.2 Cycle Studies

### 2.1.2.1 Intercooling

Intercooling between compressor stages to reduce compression power (that increases shaft power) has long been a feature of centrifugal compressor installations. Thus, inclusion of intercooling by splitting the single axial compressor into a low pressure and a high pressure section was an obvious suggestion. Since high pressure compressor delivery temperature is greatly decreased with intercooling, additional benefits accrue to the cooling air system. The traditional rotor air cooler which supplies cooled air can be eliminated. To maintain the same cooled airfoil metal temperatures, less (uncooled) compressor delivery air can be used.

### 2.1.2.2 Recuperated

The lower compressor delivery temperature also leads logically into another idea, that of exhaust gas recuperation. Heat exchange between exhaust gas and compressor delivery air significantly reduces the quantity of fuel required to achieve a specified turbine inlet temperature. With intercooling, compressor delivery air temperature would be lower, thus there would be an even greater flow of exhaust energy back into the Brayton cycle through the recuperator. In the combined cycle configuration the effect of recuperation on efficiency is not quite as obvious because exhaust gases leave the cycle at a stack gas temperature which is typically 220°F (104°C) whether or not recuperation is employed. However, recuperation redirects exhaust energy from the bottoming, Rankine cycle, into the topping, Brayton cycle, thus as long as the Brayton cycle is more efficient than the Rankine cycle, recuperation should benefit cycle efficiency.

### 2.1.2.3 Intercooled, Recuperative Combined Cycle

Combining intercooling and recuperation in the intercooled, recuperative combined cycle (ICRCC), resulted in a significant increase in combined cycle efficiency. The turbomachinery for the ICRCC is directly coupled to form a single shaft operating at 3600 rpm. The high pressure compressor and gas turbine would be a two bearing rotor in a single housing. The low pressure compressor generator and steam turbine would have individual rotors in separate housings. The generator rotor would be double ended so that it could be driven from both ends. The steam and gas turbines would have their own thrust bearings to maintain proper axial position of the rotors relative to the stationary parts.

### 2.1.2.4 Inlet Cooling/Steam Injection/Water Spray After Cooling

Evaporative cooling of inlet air has long been a technique employed to increase gas turbine and combined cycle power when inlet air is hot and dry. Steam injection into compressor delivery air for power augmentation has been incorporated into many gas turbines over the years. Water spray evaporative intercooling was designed for the Japanese Advanced Reheat Gas Turbine pilot plant project, designated Moonlight. The Humid Air Turbine (HAT) cycle entirely

eliminates the steam turbine bottoming cycle, and instead uses recuperator exhaust energy to heat water for humidification of compressor delivery air.

One alternative considered was to incorporate an evaporative aftercooler into the basic ICRC. High pressure compressor delivery air is cooled as it evaporates preheated intercooler water, thus allowing more heat transfer from turbine exhaust gas into after cooler exit air through the recuperator. Gas turbine power increases considerably since additional mass (water vapor) is now available for expansion through the turbine while the compressor's mass flow has not changed. Bottoming cycle power decreases, but by only one-third of the gas turbine's power increase. However, gas turbine fuel consumption also increases because the additional water vapor flowing through the combustors has to be heated to turbine inlet temperature. The net effect on combined cycle efficiency is not clear, and conflicting results have been calculated, depending on cycle assumptions. Further study will be needed to clarify the potential for this type of humidification.

#### 2.1.2.5 Continual Evaporative Cooling

The ultimate form of intercooling is continual evaporative cooling of the compression process through the introduction of a fine water mist into each compressor stage. Preheated water droplets, about 5 microns in diameter, would possibly evaporate in each stage providing a continuous reduction in the heat of compression. Initial cycle calculations show that this concept may provide a significant boost to cycle efficiency. A preliminary analysis of this concept indicates a 25 to 30% reduction in the work of the compressor; a corresponding reduction in the temperature increase over the compressor; and, perhaps a reduction in the water used over a staged inter- and after-cooler process.

Continual or staged evaporation of water into the recuperator air stream is yet another idea investigated in this preliminary phase. Recuperator gas side exit temperature will be lowered by this technique leaving less energy for the lower efficiency bottoming cycle. Preliminary indications are that combined cycle efficiency will be enhanced by the additional transfer of exhaust energy into the topping cycle.

With evaporation of water into the open Brayton cycle, all the latent heat of vaporization which has been supplied by the cycle is rejected to atmosphere. Cycle efficiency can be raised by condensing a portion of the exhaust vapor in a condensing economizer, as long as the very low grade heat (<212°F [100°C]) is returned to the cycle. A Teflon coated condensing economizer, heating evaporation water from 59° to 200°F (15° to 93°C) by condensing and cooling the stack gases, would recover about 16% of the heat required to evaporate water into the gas turbine.

#### 2.1.2.6 Closed-Loop Cooling

Another innovation in the combined Brayton and Rankine cycles, which will provide increased cycle efficiency at constant RIT, is closed-loop steam cooling. Closed-loop steam cooling involves directing a portion of the dry steam raised in the heat recovery steam generator (HRSG) through the walls of stationary hot

end components, such as combustor baskets, transitions, and vanes, prior to expanding it through the steam turbine. The steam, which is superheated as it removes heat radiated and convected from the hot gas path, is supplied to the steam turbine.

By comparing steam turbine output with, and without, closed-loop steam cooling, it was found that additional power, equivalent to 35 to 40% of the heat absorbed by the steam in the gas turbine, would be generated. For Row 1 vane cooling alone, this could raise overall efficiency about 0.8 percentage points. Closed-loop steam cooling of stationary Rows 2 and 3 could provide another 0.5 percentage point, or more, in increased cycle efficiency, since in addition to the extra steam superheat, turbine exhaust temperature will increase significantly, thus enhancing the effectiveness of both the recuperator and the HRSG.

Because of the complexity introduced by closed-loop steam cooling and the potential for steam leaks, closed-loop air cooling was investigated next and selected for the Reference Cycle.

#### 2.1.2.7 Thermochemical Recuperation

Thermochemical recuperation of gas turbine exhaust energy was also considered. Here only the gas turbine would produce power (no longer a combined cycle) by burning reformed, recuperated fuel. Methane and sufficient steam in the presence of a catalyst, and at appropriate temperature, will reform into a low Btu fuel consisting of H<sub>2</sub> and CO. None of the latent heat of vaporization of steam generated in the HRSG is lost to the cycle, and so the potential exists for efficient exhaust energy recuperation. In current reforming technology, methane conversion efficiency is a function of pressure, temperature and excess steam/methane ratio (Khinkis, 1991).

At ATS turbine exhaust temperatures (1200° to 1400°F [649° to 760°C]) conversion efficiency ranges from 45 to 90%. The optimum cycle efficiency may exist when a portion of the reformed fuel is burned in direct burners to heat exhaust gas to greater than 1500°F (815°C) where methane reformation is most efficient. Alternately, the development of a low temperature catalyst (which could provide near 100% conversion in the 1200°F [649°C] range) could optimize the potential of chemical recuperation to enhance ATS efficiency. Several low temperature catalysts are reportedly under development, but evaluation will be required to verify claims.

The potential for this innovative cycle could not be discounted nor confirmed in Phase I of the ATS project. Its potential should be further investigated and refined by experimentation with catalyst and reformer structures. The possibility of incorporating a reformer system into a combined cycle should be explored. A trade-off study between capital and operating costs and plant cycle efficiencies would be required to assess the complete potential of this concept.

#### 2.1.2.8 Reheat

The final combined cycle studied was reheat, where the turbine is split to allow reheat after partial expansion.

### 2.1.2.9 Reference Cycle

The conclusion reached from the Phase I studies was that intercooling combined with exhaust recuperation and closed-loop air cooling was the best route to achieve the ATS Program efficiency target. This was designated as the Reference ATS Cycle. Table 1 summarizes the results of Phase 1 cycle studies.

**Table 1 Estimated Cycle Performance**

	Cycle Description	Cycle PR	Turbine Inlet Temp. °F (°C)	Cooling Flow Inlet Flow (%)	Cycle Efficiency (%) LHV
1	W501F, 1 Press Level HRSG	14.3	2460 (1350)	21.4	53.2
2	W501F, 3 Press Level HRSG	14.3	2460 (1350)	21.4	55.1
3	Increase Temp, 1 Press Level HRSG	14.3	2680 (1471)	24.0	54.5
4	Increase Temp, 3 Press Level HRSG	14.3	2680 (1471)	24.0	55.3
5	Increase Press and Temp, 1 Press Level HRSG	20.0	2680 (1471)	24.0	55.0
6	Increase Press and Temp, 3 Press Level HRSG	20.0	2680 (1471)	24.0	56.3
7	Ref. Cycle: I/C and A/C, Recuperation, 1 Press Level HRSG	20.0	2680 (1471)	19.6	57.1
8	Ref. + Continuous Compressor Cooling	20.0	2680 (1471)	19.6	60.3
9	Ref. + Closed Circuit Air Cooling of First Vane	20.0	2680 (1471)	9.6	61.5
10	Ref. + No Cooling	20.0	2680 (1471)	0.0	67.2
11	Ref. + Evaporative Recuperation	20.0	2680 (1471)	19.6	61.3
12	Chemical Recuperation (H <sub>2</sub> O/CH <sub>4</sub> = 3)	20.0	2680 (1471)	26.5	57.2
13	Chemical Recuperation (H <sub>2</sub> O/CH <sub>4</sub> = 6)	20.0	2680 (1471)	26.5	57.9
14	Turbine Reheat	64.0	2680 (1471)	21.6	53.4
15	Ref. + Cont. Compressor Cooling + Closed Circuit Air + Evaporative Recuperation	20.0	2680 (1471)	19.6	65.5

### 2.1.3 Efficiency Enhancement

Further enhancements to the ICRCC Cycle efficiency were considered, such as:

- increasing firing temperature
- reducing cooling air requirement
- employing pressure gain combustion
- increasing component aerodynamic efficiencies, and
- reducing clearances and leakages.

Increasing firing temperature from current (1992) levels was necessary for achieving the 60% efficiency target.

If the RIT increase on its own was considered, while holding metal temperatures in the hot gas path components constant through the use of additional quantities of cooling air, the increase in cycle efficiency would be quite small. Based on theoretical (Carnot) efficiency calculation, even without holding metal temperatures constant, for a 200°F (111°C) increase in RIT only 1.2 percentage points gain in cycle efficiency could be expected.

As RIT increased, the cooling air quantity required to hold metal temperature would also increase significantly. Reducing this cooling air requirement is an extremely effective method for increasing cycle efficiency, since more of the air which has absorbed work in the compressor can now be expanded through all stages of the turbine. Because exhaust temperature increases, heat transfer through the recuperator into the compressor air stream is enhanced, requiring less fuel/pound of air, and more heat is available to the bottoming cycle. At ATS conditions, each reduction in cooling air requirement of 1% of compressor inlet flow would increase cycle efficiency approximately 0.2 percentage points.

To obtain the maximum benefit of increased firing temperature, the amount of air used to cool turbine components must be minimized. This can be achieved by applying thermal barrier coatings (TBC) to turbine airfoil outside surfaces to reduce heat conduction from the hot gases into the cooled airfoil, and thus reduce the cooling air requirement.

To further reduce cooling air requirement, the currently used cooling schemes will have to be refined and new cooling designs incorporated.

One of the most promising of these is shell/spar construction. Shell/spar vanes and blades may be formed by bonding a thin nonporous airfoil shaped metal sheet (the shell) to an inner hollow cast support member (the spar), or by casting (Levari, Jeffries, and Cohn, 1984). Cooling air for the assembly is supplied from alternate cavities within the spar (the supply cavities). It flows along chordwise convection cooling channels between the spar and the shell and returns to the remaining spar cavities (the discharge cavities). The heated or spent cooling air is then routed from the discharge cavities to the main gas stream through exit holes in the shrouds or airfoil.

Cooling flow could also be reduced if higher temperature material/coating systems could be incorporated. Higher creep strength vane and blade alloys, which when processed to form directionally solidified (DS) or single crystal (SC) structures should offer temperature advantages of 75° to 200°F (42° to 111°C) over conventionally cast alloys. Hot corrosion/oxidation protection of these blades at the higher operating temperatures will be provided by advances in existing MCrAlY coatings. Development of these systems to allow implementation into the ATS is required.

Uncooled blade path components would obviously greatly increase advanced turbine system efficiency. Ceramics and ceramic composites will be considered during the ATS program for application in stationary components.

Another concept to consider that could raise plant cycle efficiency is pressure gain, pulse combustion. This is a process by which periodic reignition and combustion of a combustible mixture causes a time averaged steady inflow of

fresh air and fuel, and outflow of products of combustion. In essence, the combustor, in addition to combusting the fuel, pumps its own air. The advantage of this phenomena is that in the ATS environment the combustor can act as an additional compression device instead of a pressure loss component.

With a potential 5% pressure gain in the ATS from a pulse combustor (vs. 3 to 4% loss with conventional combustors) it is estimated that ATS efficiency should increase at least 1.2 percentage points by incorporation of a pulse combustor. NO<sub>x</sub> production from pulse combustors is inherently low because of the very short duration of the pulse (approximately 6 milliseconds at 80 Hz frequency), and the fact that thermal NO<sub>x</sub> is generated both as a function of temperature and time. With the requirement for dry, ultra-low NO<sub>x</sub>, CO and UHC emissions driving combustor development, the possible use of pulse combustion should be explored to establish emission levels for a larger scale combustor.

Within the ICRC configuration, improving the aerodynamic efficiencies of the compressors to reduce compression work, and the turbine to increase expansion work will enhance overall efficiency.

To improve turbine efficiency 3-dimensional, viscous, aerodynamic computations will be further refined using sophisticated aero engine procedures integrating through flow, blade-to-blade, boundary layer and 3-dimensional viscous calculations.

Configurations of all diffusers in the engine will be carefully designed to maximize efficiency and all pressure losses through ducting, piping, manifolding, and components such as inter (and after) coolers and recuperators, will be minimized to reduce compression work and maximize expansion potential.

ATS efficiency will be improved even further by reducing all clearances between stationary and rotating parts. Leakage has always been of concern in gas turbines and is even more important as the potential of the cycle is pushed to the limit. Blade tip clearances will be maintained as small as possible by careful control of casing circularity and temperature. Reactive clearance control to avoid transient rubs will be needed to hold these tight clearances.

Diaphragm/vane segment seal clearances will be minimized and leakage further reduced through the extensive use of abradable material or filed honeycomb structures in combination with knife edge seals. Innovative seals such as brush seals, which have had aero application, will be investigated.

#### 2.1.4 Emissions

The requirement for single digit NO<sub>x</sub> levels with CO and UHC less than 20 ppmvd each, to be achieved without any post-combustion emissions control devices, is a serious challenge which will require significant R&D effort. The premix, lean-burn combustion systems were receiving the focus of attention, and it was predicted that these will eventually reach the required emissions levels. An alternative which is gaining attractiveness is the use of a catalytic metal or a ceramic matrix reactor within the combustor.

Both of these systems will benefit from the higher (when compared to compressor delivery temperature in the W501F) air temperature entering from

the recuperator of the ATS. For catalytic combustion, the higher temperature air will enhance the reactivity threshold of the catalyst for natural gas fuel. In the case of the lean premixed combustor, the flammability range should be broadened, thus reducing pilot burner fuel. In both cases, no additional temperature rise will be needed across the combustor (compared to the base cycle) since both combustor outlet and combustor inlet temperatures increase in the ATS.

If large concentrations of moisture become part of the ATS, then combustor stability and CO production will have to be further developed, as these quantities of water vapor will far exceed past experience with steam injection.

#### 2.1.5 Adaptability to Coal-Derived Fuels

A key feature of the ICRCC, chosen as the reference natural gas-fired ATS, is the combustor shell design. The shell will not be structural, but will contain only pressurized compressor delivery and recuperator return air. The structural connection between high pressure compressor and turbine cylinders will be through radial-axial struts. This leaves the shell free to be reconfigured for compressor air take-off to the coal-fuel processing system and return from the recuperator.

The coal-fired system is an integrated system bleeding air from the compressor and returning a low heating value fuel to the gas turbine (Bannister, Newby and Diehl, 1992). The increase in volume flow to the turbine, compared to a natural gas-fired (dry) system, can usually be accommodated without turbine modifications. However, if large amounts of moisture are evaporated into the air stream in the natural gas-fired ATS, then by comparison, turbine flow would be reduced in the coal-fired case. To match compressor and turbine flows, compressor flow may be increased by the addition of inlet stages to the low pressure compressor, and/or by the use of variable compressor geometry.

#### 2.1.6 Conclusions

The feasibility of achieving 60% (LHV) efficiency in a natural gas-fired cycle within a 10-year time frame was established. Cycle innovations, increased firing temperature, reduced cooling air usage, improved component efficiencies and improved material/coating systems will all be needed to accomplish this ambitious goal. The resulting advanced turbine system will be environmentally superior, as well as adaptable to coal-derived fuel systems.

## 2.2 Phase 2 / Phase 2 Extension

### 2.2.1 Introduction

The objective of the ATS Program Phase 2 was to develop ultra-high efficiency, environmentally-superior, and cost-competitive gas turbine systems for base-load application in utility, independent power producer, and industrial markets. Specific performance targets have been set using natural gas as the primary fuel:

- System efficiency that will exceed 60% (lower heating value basis (LHV)) on natural gas for large-scale utility turbine systems; for industrial applications,

systems that will result in a 15% improvement in heat rate compared to currently available gas turbine systems.

- An environmentally superior system that will not require use of post-combustion emissions controls under full-load operating conditions.
- Busbar energy costs that are 10% less than current state-of-the-art turbine systems, while meeting the same environmental requirements.
- Fuel-flexible designs that will operate on natural gas but are also capable of being adapted to operate on coal, coal-derived, or biomass fuels.
- Reliability-Availability-Maintainability (RAM) that is equivalent to the current turbine systems.
- Water consumption minimized to levels consistent with cost and efficiency goals.
- Commercial systems that will enter the market in the year 2000.

Phase 2 tasks included project plan, documentation in accordance with NEPA for work performed under Task 8, natural-gas-fired advanced turbine system (GFATS), conversion to coal fueled advanced turbine system (CFATS), market study, system definition and analysis, integrated program plan and design, and test of critical components. The results of cycle studies are summarized in a technical paper by Briesch, et al. (1995), and the Phase 2 program in general in a technical paper by Diakunchak, et al. (1996).

### 2.2.2 Task 1.0 - Project Plan

The purpose of this task was to define the plan to accomplish the work as defined in the Request for Proposal (RFP) Statement of Work (SOW), Tasks 2 through 8.

#### 2.2.2.1 Task 1.1 Develop Project Plan

A project plan was developed describing how the Phase 2 SOW was to be accomplished as well as how the project was to be controlled to ensure all work was done in accordance with requirements as described in the Management Plan. The plan, the first submittal dated October 1, 1993, included a summary of the project, its objectives and the interrelationships among the major tasks to be performed in Phase 2. The project organization, how the project was to be managed, and the management systems used to control the project were identified. A Program Work Plan was developed as part of the project plan. The Program Work Plan presented the work breakdown structure and the SOW to the levels necessary to provide cost, schedule and technical control of the project. The technical approach to the SOW addressed a combination of innovative changes in the thermodynamic cycle, high temperature developments and gas turbine improvements, that together will achieve an ATS of greater than 60% cycle efficiency. Improvements were addressed in parallel to ensure that all system and engine changes and the conversion from natural gas to a coal-fueled system were all compatible. Barrier issues were identified along with their resolutions as the work progressed. The Program Work Plan described the technical approach, the task work, responsibilities, and deliverables for each task. Task work described the selection and conceptual design of the Gas Fired

Advanced Turbine System (GFATS) as well as identifying the parametric and trade-off studies to be done. RAM along with emissions and environmental compliance of the GFATS system were addressed in the work plan.

A revised program schedule was developed using project management software from which the program's performance was measured, reported and controlled. The schedule included major milestones and decision points. A cost plan was also prepared that established the basis for measurement of actual cost accumulation against planned costs and provides information for updating and forecasting budget requirements.

#### 2.2.2.2 Task 1.2 Program Management

The Program Manager and his subcontractor counterparts monitored project performance and cost to ensure compliance with the project objectives and adherence to cost estimates. The Program Manager was the primary interface with the customer. The subcontract lead personnel interfaced with the Deputy Program Manager on day-to-day matters pertaining to the contract.

As required, a technical paper was presented at the DOE Heat Engines Contractors' Review Meeting and at one other technical conference or symposium each year during the duration of this contract.

#### 2.2.3 Task 2.0 Information Required for National Environmental Policy Act (NEPA)

The purpose of this task was to supply DOE with the information required to prepare documentation in accordance with NEPA for the work performed under Task 8.

A topical report was prepared and submitted to DOE within 120 days after contract award. The report included the following:

A brief description of the project was provided which included project goals, a summary schedule, a summary of the development/test plans for Task 8, locations of tests that were conducted, along with a description of the facilities and equipment to be used in conducting the tests. A discussion was provided for the type and quantities of materials used: feedstocks, utilities, effluents, unrecovered material, and solid wastes.

For each proposed test site, current environment characteristics and any potential environmental impacts were developed and evaluated. Information on environmental impacts included data for minimum, maximum and average values and encompassed the following: air quality, water resources, land use, waste management, ecological impacts, socioeconomic impacts, archaeological, cultural and historical resources, noise, occupational safety and health and cumulative impacts.

In the topical report for each test site, all federal, state and local permits and licenses required for the project were explained. The explanation provided information on the permitting and licensing schedule and the status of each permit and license. Included in, or accompanying the explanation was discussion on the allowable releases of solid, liquid, and air pollutants under the respective permits and licenses. A list of all agencies and persons contacted to

collect information on the environmental, health and safety aspects of the project was provided. The list included the addresses and phone numbers of all contacts.

## 2.2.4 Task 3.0 Selection of Natural Gas-Fired Advanced Turbine Systems

### 2.2.4.1 Introduction

The objective of Task 3 was to analyze and evaluate different cycles for the natural gas-fired Advanced Turbine Systems (GFATS) in order to select one that would achieve all of the ATS Program goals. Detailed cycle performance, cost of electricity, and RAM analysis were executed to provide information on which the final selection of the GFATS cycle would be made. Innovative approaches and technological advances are required to achieve these challenging goals. Improvements in combustion, aerodynamic design, cooling design, mechanical design, leakage control, materials, and coating technologies are requisite. The ATS program goals are as follows:

- greater than 60% plant cycle efficiency (on LHV basis)
- <10 ppm NO<sub>x</sub> emissions than current commercial values
- cost of electricity 10% less than current values
- RAM results comparable with current combined cycle plants
- demonstration by year 2000

The ATS engine will be the next model in the series of large heavy duty gas turbines developed by Siemens Westinghouse. Siemens Westinghouse engineers have made significant contributions in advancing gas turbine technology, especially in the field of heavy duty engines used in industrial and electrical utility applications. Some of the innovations included single shaft two bearing design, cold end drive, axial exhaust, cooled turbine airfoils in an industrial engine, and tilting pad bearings. The improvement in gas turbine performance and mechanical efficiency was both evolutionary, where small improvements were made continuously, and revolutionary, where new designs were produced to achieve a large step change in engine output power and efficiency, as well as mechanical integrity and reliability. Figure 2 shows the evolution of large operating industrial and utility gas turbines developed by Siemens Westinghouse.

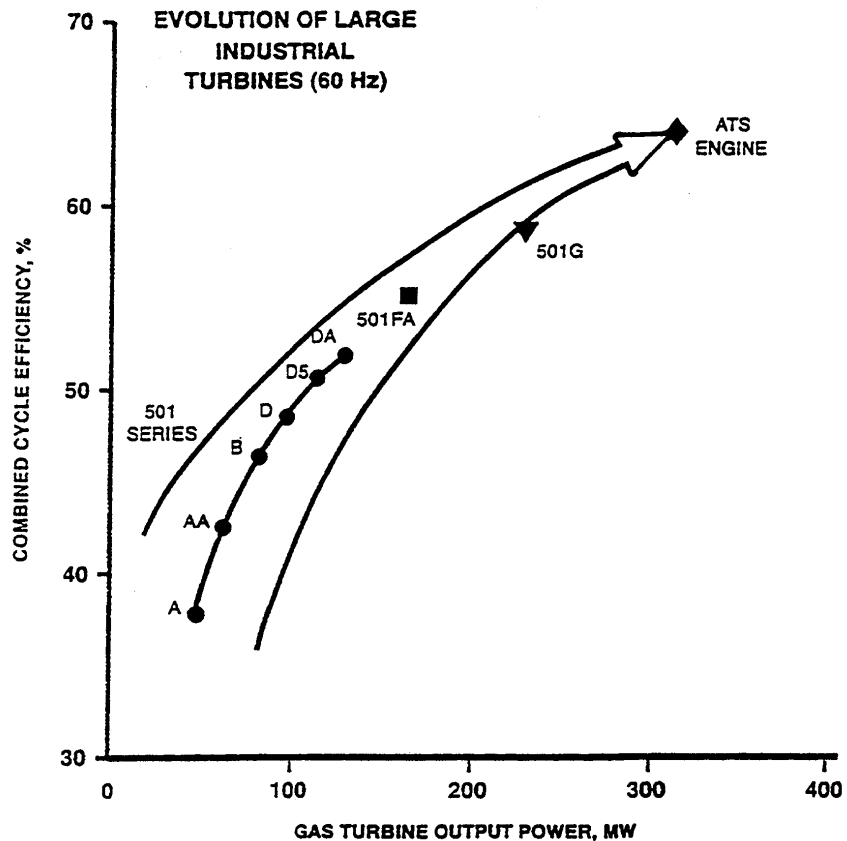


**Figure 2 Evolution of Large Siemens Westinghouse Gas Turbines**

#### 2.2.4.2 Discussion

Various cycles were considered and evaluated for the ATS Program on the basis of plant efficiency, emissions, cost of electricity, reliability-availability-maintainability (RAM), and program schedule requirements. The main cycle concepts investigated were the advanced combined cycle, intercooled, recuperated, reheat, and thermochemically recuperated cycles. The advanced combined cycle was selected for the ATS Program because it was considered to have the best potential for achieving all of the ATS Program goals by the year 2000.

Detailed cost and RAM analyses were carried out on six selected cycle configurations and compared to the W501F combined cycle. These comparisons determined whether or not the evaluated cycles met the performance requirements of the ATS program.

The various cycles evaluated had combustion turbine inlet temperatures ranging from 2450°F (1343°C) to greater than 2750°F (1510°C); pressure ratios of 18:1 to 48:1; and power outputs of 243 MW to 339 MW. The advanced combined cycle selected will exceed all the ATS requirements and has a net plant output of 452 MW.

Issues critical to the successful development of the advanced combined cycle plant were identified. The achievement of the ATS plant cycle efficiency and cost of electricity goals will require higher engine firing temperatures with minimized cooling of hot end components. This, in turn, will necessitate the selection and/or development of new alloys, materials, casting processes, and coatings for the ATS engine. To ensure success of this program, a concerted development effort and technological advancements will be mandatory in combustion, aerodynamic design, cooling design, mechanical design, leakage control, and materials/coating technologies. The plan was to pursue an advanced combined cycle plant with the following features:

- Advanced aero/heat transfer/materials technology
- Burner outlet temperature in excess of 2730°F (1499°C)
- Closed-loop steam cooling
- Single crystal and directionally solidified airfoils
- Improved thermal barrier and anti-corrosion coatings
- Ceramic ring segments
- Active tip clearance control
- Brush seals
- Reduced compressor dump/combustor loss
- Increased Row 4 blade exit area
- Reduced inlet and exhaust losses
- Fuel preheating
- All rotating turbine-generator power components on a single shaft
- Advanced steam turbine design technology
- 1800 psi/1050°F/1050°F (12.4 MPa/566°C/566°C) steam cycle

This advanced combined cycle power plant is designated as “ATS” throughout this report. Figure 3 shows the selected cycle.

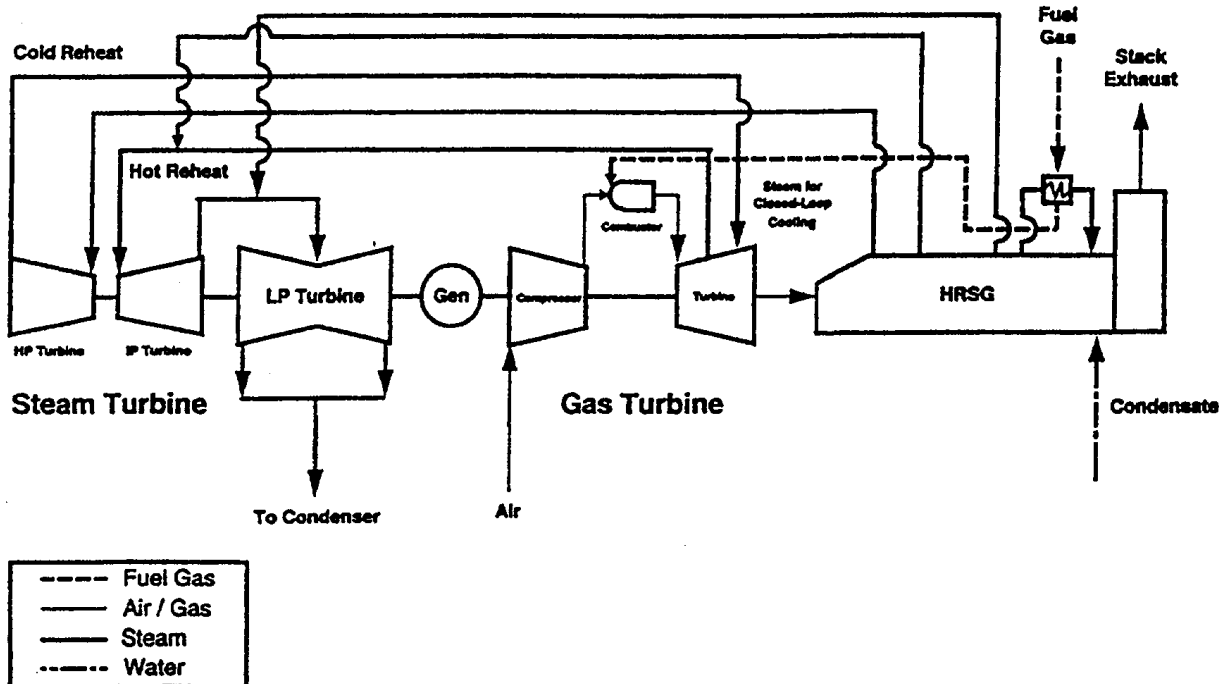


Figure 3 Selected ATS Cycle Configuration

### 2.2.4.3 Cycle Analysis

Today, current large natural gas-fired combined cycle power generation systems are capable of efficiency levels in excess of 56%. Within the ATS program, there was opportunity to re-evaluate cycle efficiencies using proven, established concepts, such as intercooling and recuperation, and newer concepts, such as thermochemical recuperation. In addition, efficiency enhancements within the ATS selected cycle are to be evaluated to determine the best approaches to raising overall thermal plant efficiencies to greater than a net 60% while adhering to the other ATS program goals. The concepts considered in these analyses were to be capable of demonstration within a three to four year time frame. From a baseline cycle definition, this report discusses how different concepts will affect the overall plant thermal efficiency. Our analysis indicates that a plant efficiency of greater than 60% is achievable.

#### 2.2.4.3.1 Baseline Cycle

In order to evaluate different technologies and concepts applicable to combined cycle power generation systems, a high temperature engine baseline combined cycle configuration first had to be developed to provide a basis for comparison of all the cycle concepts and technologies to be considered. For this purpose, a conventionally configured combustion turbine coupled with a three-pressure level reheat steam cycle (Figure 4) was modeled to provide a high temperature engine baseline combined cycle. The combustion turbine rotor inlet temperature (RIT) was set at 2600°F (1427°C) to approximate near-term temperature capabilities. The compressor pressure ratio was set at 18. High pressure steam conditions

entering the steam turbine were specified at 1450 psi (10 MPa) and 1000°F (538°C) and the hot reheat steam temperature was also set at 1000°F (538°C). Note that this configuration utilizes turbine rotor cooling air heat to produce additional low pressure steam in the steam cycle via a heat exchanger located in the heat recovery steam generator (HRSG). Also, the natural gas fuel is preheated by feedwater recirculation flow.

The ATS engine will be based on the proven technologies incorporated in the W501 frames. To meet the ATS program plant cycle efficiency and emission goals, however, will require advancements in several key gas turbine technologies: closed-loop steam cooling, catalytic combustor components and advanced coating systems. Additional enhancements include advanced aerodynamic and sealing design, active blade tip control, and materials and coatings with high-temperature capabilities.

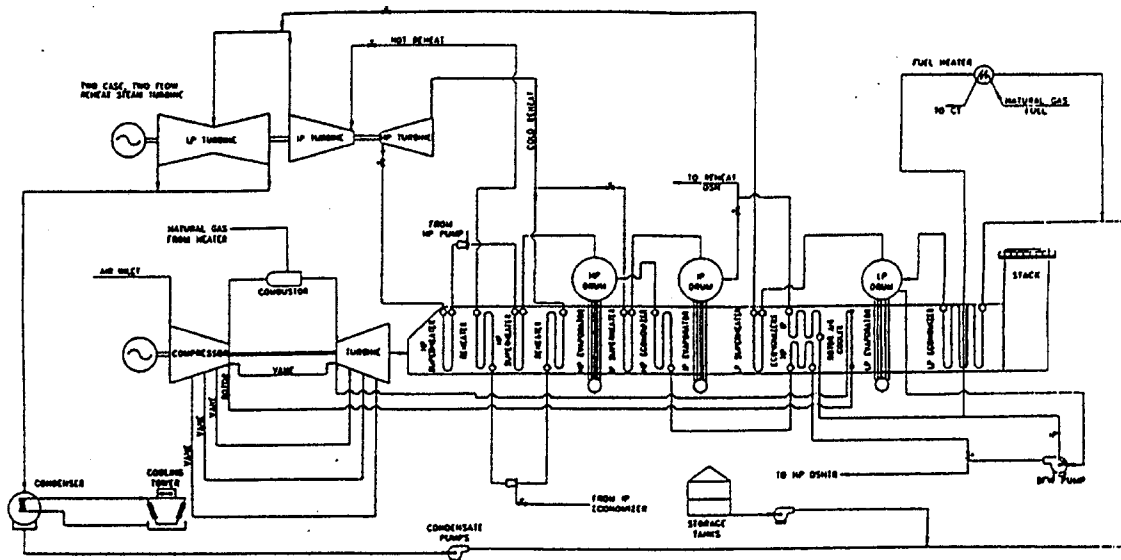


**Figure 4 High Temperature Engine Baseline Combined Cycle**

#### 2.2.4.3.2 Component Improvements

Incorporation of several component improvements, available through recent technological developments and advanced design techniques, into the power generation system of Figure 4 results in significant efficiency gains. The application of advanced design tools will enable the analysis and incorporation of design changes that will increase compressor and turbine efficiencies. Blade tip and seal leakages will be minimized to further enhance efficiency. Improved materials, including ceramic components, coatings, and cooling designs will be incorporated to reduce cooling requirements and improve cycle efficiency.

There are two generators in the high temperature baseline configuration. One of these is the combustion turbine generator, while the other is the steam turbine generator. Current generator designs are capable of higher efficiency than those chosen for the high temperature baseline cycle. While the combustion turbine generator of the high temperature baseline configuration is of sufficient size to cost effectively apply this technology, the steam turbine generator is not. By utilizing a single shaft arrangement, however, the smaller steam turbine

generator is eliminated and the remaining single generator may be designed at the higher efficiency.

When the component improvements listed above are all incorporated into the high temperature baseline cycle, the net plant thermal efficiency is increased by approximately 2 percentage points.

#### 2.2.4.3.3 Steam Cycle Enhancements

The basic reason for raising the steam pressure and temperature of the Rankine cycle is to improve the potential thermal efficiency. The first cycle variations investigated within this study were modifications to the high temperature baseline cycle in which the steam cycle was enhanced. Study results indicated that increasing either high pressure steam superheat temperature or reheat steam temperature by 50°F (28°C) results in an improvement in combined cycle thermal efficiency of 0.1 percentage point. Increasing high pressure steam pressure from 1450 psi to 1800 psi (10 MPa to 12.4 MPa) results in an increase in net plant thermal efficiency of 0.1 percentage point. A further increase in pressure to 2400 psi (16.5 MPa) yields only an additional 0.05 percentage point in thermal efficiency, while adding to the cost of the high pressure steam system. Also, since the steam turbine size is set by the exhaust energy of the combustion turbine, increasing steam pressure reduces the blade heights in the high pressure steam turbine. For 2400 psi (16.5 MPa) high pressure steam, the resulting blade heights are much smaller and less efficient than for the 1800 psi (12.4 MPa) steam. Therefore, the optimum steam cycle was determined to be at 1800 psi (12.4 MPa) with 1050°F (566°C) high pressure superheat steam and 1050°F (566°C) reheat steam (both 100°F [56°C] above the baseline cycle temperature). This resulted in a 0.5 percentage point increase in net plant thermal efficiency and also in a slight increase in output due to the increased efficiency of the steam cycle. The steam temperatures were limited to 1050°F (566°C) for this study due to steam turbine materials, reliability, and cost considerations. The steam temperature of 1050°F (566°C) plus a reasonable steam superheater approach  $\Delta T$  is determined by the combustion turbine exhaust temperature and this, in turn, set the baseline cycle pressure ratio.

#### 2.2.4.3.4 Rotor Air Cooler Heat Utilization

The W501F combustion turbine combined cycle provides two options for rotor air cooler heat utilization. The first option is an air-to-air cooler to cool the rotor cooling air after it exits the compressor and prior to its introduction into the rotor. The rotor air heat is rejected to the atmosphere via an air-to-air cooler. The other option is to cool the rotor air via an air-to-exhaust gas heat exchanger located in the HRSG upstream of the low pressure evaporator, as was done in the high temperature baseline cycle. With this configuration, the rotor air cooler heat is recovered by the steam cycle, which produces low pressure steam. This results in higher plant efficiency than that of the air-to-air cooler method, since the rotor air cooler heat is recovered by the low pressure steam system.

Another concept involves removing the HRSG rotor air cooler used in the high temperature baseline configuration and installing a rotor air cooler, which exchanges heat with the incoming natural gas fuel. This returns the rotor air heat back to the combustion turbine, which then requires less fuel to achieve the

desired rotor inlet temperature. Therefore, the rotor air heat is recovered at the combustion turbine efficiency (typically about 40%), which is much higher than the low pressure steam system efficiency. This is, therefore, a much more effective recovery of the heat than is obtained via low pressure steam production and results in an increase in net plant thermal efficiency of 0.4 percentage point over the high temperature baseline configuration.

#### 2.2.4.3.5 Closed-Loop Steam Cooling

Most current gas turbine engines utilize air to cool the turbine vanes and blades. This allows the turbine inlet temperature to be increased beyond the temperature at which the turbine material can be used without cooling, thus increasing the cycle efficiency and power output. However, the cooling air itself is a detriment to cycle efficiency in four ways. First, it is ejected from the turbine airfoils, thereby causing a disruption in the surrounding flow field. This increases the airfoils' irreversible pressure losses and results in a reduction in turbine efficiency. Secondly, since the cooling air is ejected from the airfoil into the gas path, the resulting mixing of the cooling air into the gas path results in irreversible pressure losses due to the non-ideal mixing of the streams, which have very different velocity vectors. The third loss mechanism is caused by the reduction in gas path temperature that accompanies the mixing of the cooling air into the gas path. This reduction in temperature reduces the work output of the turbine and, therefore, compromises cycle efficiency. Finally, the turbine cooling air must be pumped to pressures significantly higher than that of the gas path pressure at the location where it is injected. This is done to assure that the cooling flow rate will be sufficient during certain operating conditions where the ratio of coolant pressure to gas path pressure drops below its design level. While some of this pressure is recovered by the turbine, there are internal losses as the cooling air passes from the compressor to the turbine gas path. The additional pumping work required to raise the cooling air to the required pressure is the associated loss.

The effect of cooling air on cycle efficiency is shown in Figure 5. This figure shows the potential increase in combined cycle thermal efficiency for fractional reductions in cooling or leakage flows. In this figure, the lines labeled 'Fixed P/P' show the effect for fixed compressor pressure ratio (i.e., the turbine expander is increased in size to handle the additional flow resulting from the reduction in cooling or leakage) and the lines labeled 'Fixed Expander' show the effect for fixed expander size (the compressor pressure ratio is allowed to rise so that the additional flow caused by the reduction in cooling or leakage can be accommodated by a turbine of the original size). Note that, although turbine leakage generally carries a larger efficiency penalty than turbine cooling per given amount of flow, the fact that the amount of leakage flow is far less than the amount of cooling flow results in far less efficiency benefit from reducing turbine leakage flows a given fractional amount compared to reducing turbine cooling flows by the same fraction of their baseline value.

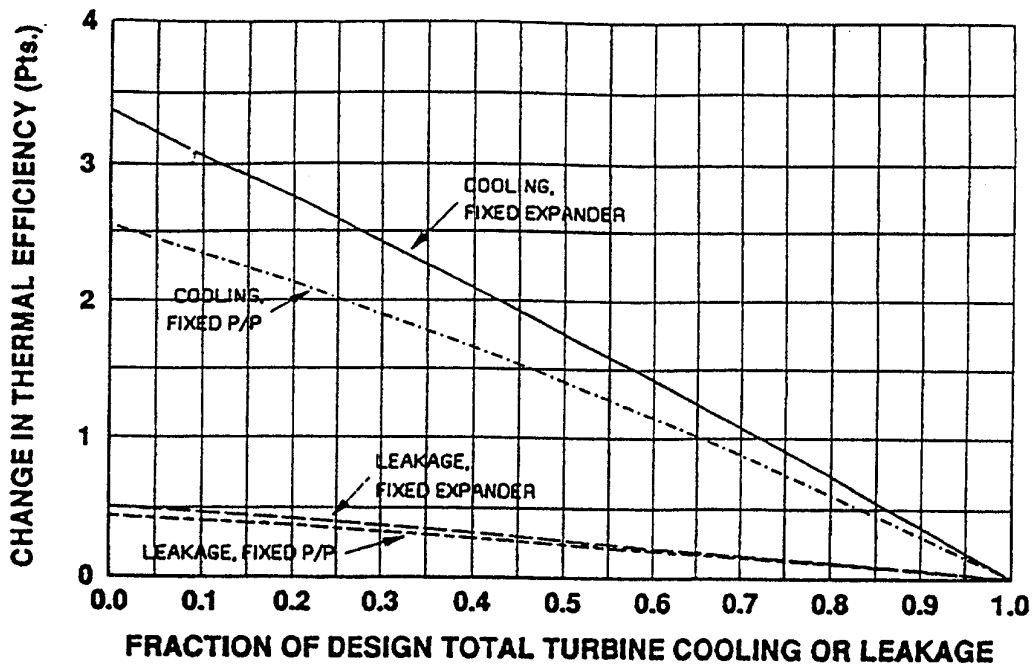


Figure 5 Thermal Efficiency Variation with Cooling Leakage Air

By using closed-loop steam cooling, the loss mechanisms described above can be largely eliminated, while still maintaining turbine material temperatures at acceptable levels. In combined cycles, the steam used for cooling the combustion turbine hot parts is usually taken from the steam bottoming cycle. This steam is then returned to the bottoming cycle after it has absorbed heat in the closed-loop steam cooling system. For an advanced bottoming steam cycle, closed-loop steam cooling would route cold reheat steam from the exit of the high pressure steam turbine to the combustion turbine vane casing and rotor. The steam is passed through passageways within the vane and rotor assemblies and through the vanes and rotors themselves, then collected and sent back to the steam cycle intermediate pressure steam turbine as hot reheat steam. This approach to turbine cooling relies solely on convective heat transfer. Since no steam or cooling fluid is ejected from the airfoils, aside from a small amount of steam leakage through the rotor seals, there is very little influence of the cooling steam on the airfoil flow fields, and hence minimal mixing losses. Also, the reduction in gas path temperature is minimized, since the convective heat flux across the airfoils is relatively small. Typically, first vane cooling air mixing reduces the gas path temperature approximately 100°F to 150°F (56°C to 83°C). For closed-loop steam cooling however, the reduction in gas path temperature is only about 10°F to 15°F (6°C to 8°C), or one tenth of the reduction of conventional cooling techniques. Application of closed-loop steam cooling to the baseline configuration yields a 2 percentage point increase in combined cycle efficiency.

Closed-loop steam cooling of the transitions, which is used on the ATS engine, will result in a small (about .05 percentage point) penalty in cycle efficiency due to heat extraction from the combustion gases.

However, both closed-loop exhaust gas cooling and impingement air cooling of the transitions will result in a higher loss in cycle efficiency. The closed-loop

exhaust gas cooling will be less efficient because of the work of compression. The impingement air cooling will be less efficient because of the higher combustor pressure loss requirement for this type of transition cooling scheme.

#### 2.2.4.3.6 Increased Compressor Pressure Ratio

Commercial aircraft gas turbine engines are designed with high overall pressure ratios, to maximize the simple cycle efficiency. For the ideal Brayton gas turbine cycle, the cycle efficiency is a function solely of the cycle pressure ratio and increases with cycle pressure ratio. In real cycles, the effect of non-ideal components causes the peak efficiency pressure ratio to decrease significantly from that of the Brayton cycle. Figure 6 shows the effect of compressor pressure ratio on simple cycle performance for a family of engines based on the high temperature combustion turbine of the baseline configuration. Also included in Figure 6 are the corresponding steam cycle and combined cycle efficiencies. Note that the simple cycle efficiency curve is relatively flat above a pressure ratio of approximately 40. This indicates that it is nearing the peak simple cycle efficiency. The steam cycle efficiency is seen to decrease with increasing combustion turbine pressure ratio. This is due to the reduction in combustion turbine exhaust temperature, which in turn reduces the maximum steam temperature and pressure and the steam's availability, and results in lower steam cycle efficiency. The effect of all of this on combined cycle efficiency is that it peaks around a pressure ratio of about 20, but remains approximately constant for a relatively large increase in compressor pressure ratio.

Reducing the compressor pressure ratio below the baseline value of 18 results in a significant decrease in combined cycle efficiency. This is due to the fact that, since the maximum steam temperature considered for this study was 1050°F (566°C), any decrease in pressure ratio below the baseline value of 18, where the maximum steam temperatures are reached, will increase the turbine exhaust temperature while maintaining the steam temperatures at 1050°F (566°C). This results in a much smaller increase in steam cycle efficiency than that obtainable by allowing the steam temperatures to rise with the turbine exhaust temperature. Figure 6 shows the significant reduction in the slope of the steam cycle efficiency line at this point, which causes the combined cycle efficiency decrease.

The maximum work output of the Brayton cycle occurs at a significantly lower value of pressure ratio than that for the peak efficiency. Figure 7, which includes intercooled cycle characteristics to be discussed later, shows the specific output of the cycles (solid lines). The simple cycle peak specific output occurs at a pressure ratio of approximately 18. Also, note that the steam cycle specific output is reduced as pressure ratio is increased, since there is less exhaust energy available to the steam cycle. The combined cycle specific output, which is merely the sum of the simple cycle and steam cycle specific outputs, decreases for increasing pressure ratio across the entire range shown.

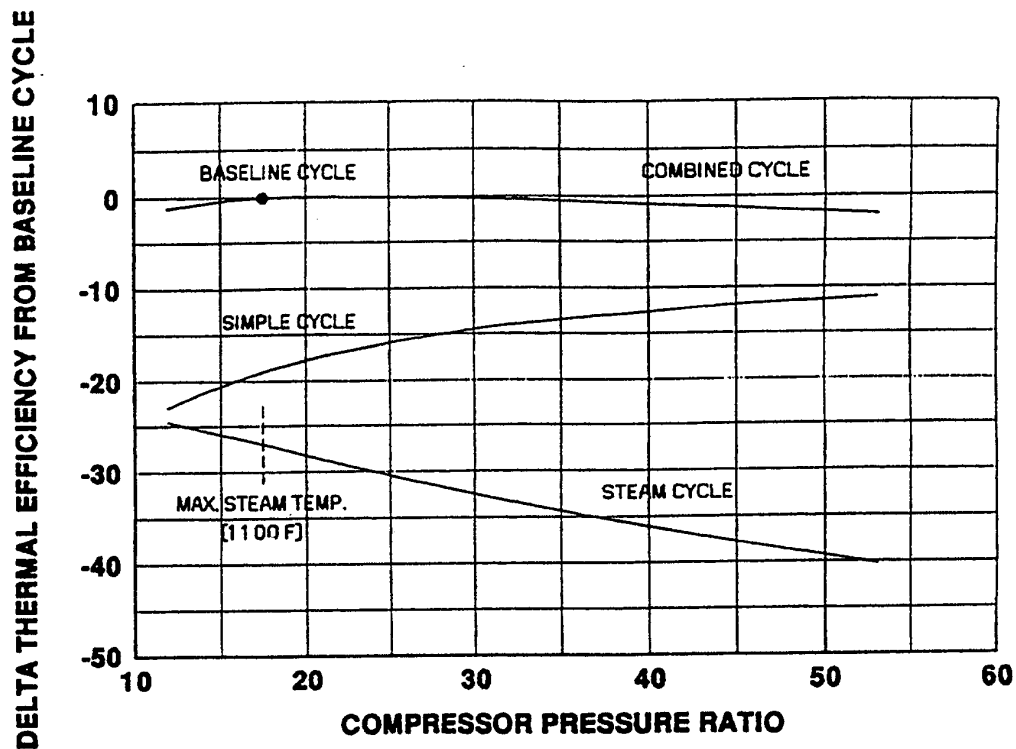


Figure 6 Effect of Compressor Pressure Ratio on Thermal Efficiencies

The optimum pressure ratio design point involves the selection of the lowest pressure ratio at which the peak combined cycle efficiency level is obtained. Selecting the design point in this manner allows both efficiency and output to be maximized and the cost of electricity to be minimized (the high temperature engine baseline cycle is designed in this fashion).

The results of the above analysis apply to air cooled combustion turbines. To determine the optimum pressure ratio for closed-loop steam cooled turbines, the effects of the closed-loop steam cooling must first be considered. Since the turbine gas path temperature is reduced less for closed-loop steam cooling than for air cooling, the combustion turbine exhaust temperature is higher for closed-loop steam cooled turbines than air cooled turbines operating at the same pressure ratio. Application of closed-loop steam cooling to the baseline configuration results in an increase in turbine exhaust temperature of approximately 100°F (56°C). Therefore, since Figure 6 indicates that cycle pressure ratio should be set so that turbine exhaust temperature is equal to the maximum steam temperature plus margin for the superheater approach, cycle pressure ratio must be increased to reduce the turbine exhaust temperature 100°F (56°C). In the baseline cycle, this corresponds to increasing cycle pressure ratio from 18 to 25. Note that the steam cycle will still have the same efficiency as the optimum steam cycle, but the combustion turbine simple cycle efficiency has been increased by approximately 3 percentage points (see Figure 6). This results in a further increase in combined cycle efficiency of 1.6 percentage points, bringing the total combined cycle efficiency increase due to application of closed-loop steam cooling to 3.6 percentage points.

### 2.2.4.3.7 Increased Turbine Inlet Temperature

Since thermal efficiency increases with increasing turbine inlet temperature, the potential benefits of increased turbine inlet temperature were investigated. The RIT for the high temperature engine baseline cycle was increased 300°F (167°C) to 2900°F (1593°C). This resulted in a cycle output increase of 10%, and combined cycle thermal efficiency increase of slightly more than 1 percentage point. The reason that the performance increase was relatively small for such a large increase in turbine rotor inlet temperature is that, since the cooling technology remained constant as the temperature was increased, large amounts of additional turbine cooling air were required to maintain turbine material operating temperatures at acceptable levels. This increase in cooling flow decreased cycle efficiency by the three mechanisms described earlier, and this significantly offsets the benefit of increasing the turbine rotor inlet temperature. Therefore, since efficiency and output would have been increased much more if turbine cooling was held at the same level as in the baseline cycle, increased turbine operating temperature must be accompanied by corresponding advancements in turbine cooling. However, even if cooling technology advancements were available to allow operation at much higher rotor inlet temperatures, the formation of NO<sub>x</sub> at these higher temperatures would result in unacceptable emissions characteristics.

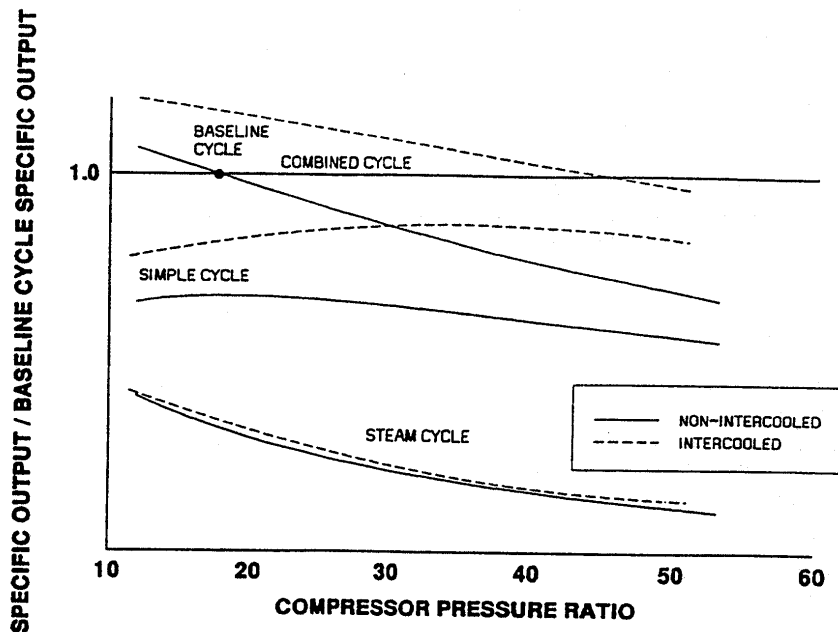


Figure 7 Effect of Compressor Intercooling on Specific Output

### 2.2.4.3.8 Compressor Intercooling

The typical arrangement for compressor intercooling involves removing the compressor air flow partway through the compressor temperature rise, sending it through an air-to-water heat exchanger, and then returning it to the compressor for further compression to combustor inlet pressure. The heat removed from the compressor air flow by the intercooler is rejected to the atmosphere, because, at the pressure ratios considered in this study, the heat is of too low a quality to be of use to the cycle.

Another intercooling concept is to spray water droplets into the compressor. As the air is compressed and increases in temperature, the water evaporates and absorbs heat. This results in a continuous cooling of the compressor. Note that for this concept the heat absorbed by the water is also rejected to the atmosphere, since this water is never condensed by the cycle but instead exhausted with the stack gases as low pressure steam.

Compressor intercooling reduces the compressor work, because it compresses the gas at a lower average temperature. Since the combustion and steam turbines produce approximately the same output as in the non-intercooled case, the overall cycle output is increased. However, since the compressor exit temperature is lowered, the amount of fuel that must be added to reach a given turbine inlet temperature is greater than that for the non-intercooled case. The ratio of the amount of compressor work saved to the amount of extra fuel energy added is about equal to the simple cycle efficiency. It can therefore be concluded that intercooling adds output at approximately the simple cycle efficiency. Since combined cycle efficiencies are significantly greater than simple cycle efficiencies it would be expected that the additional output at simple cycle efficiency would reduce the combined cycle net plant efficiency for the intercooled case. Figure 8 verifies this expectation and shows that this trend is the same for a wide range of cycle pressure ratios. Note that the simple cycle shows almost no change in efficiency for intercooling, which is expected since output is added at approximately the simple cycle efficiency.

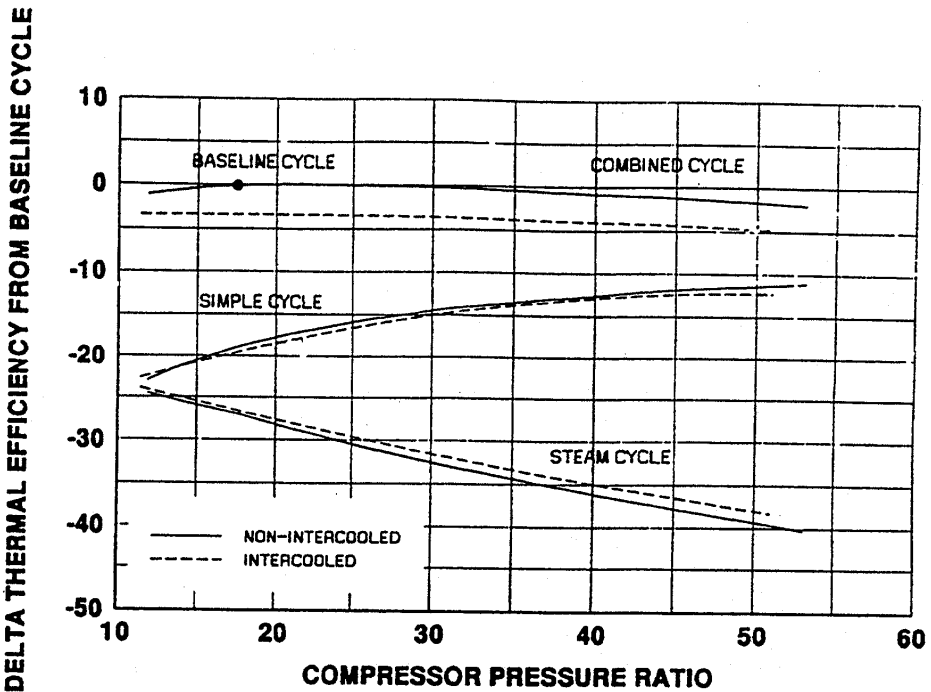


Figure 8 Effect of Compressor Intercooling on Thermal Efficiencies

Figure 7 shows the effect of intercooling on specific output. Since the compressor work requirement is reduced while the gas and steam turbine work outputs remain approximately the same as in the non-intercooled case, the net power output of both the simple and combined cycles is increased. Also, since the turbine exhaust temperature is increased slightly due to the aforementioned

exhaust gas composition effects, the steam cycle specific output is also increased slightly.

#### 2.2.4.3.9 Recuperation

In recuperative cycles, turbine exhaust heat is recovered and returned to the combustion turbine combustor, usually via a heat exchange between the turbine exhaust gases and the compressor exit air flow. The discharge from the compressor exit is piped to an exhaust gas-to-air heat exchanger located aft of the combustion turbine. It is then heated by the turbine exhaust and returned to the combustor. Since the resulting combustor air inlet temperature is increased above that of the non-recuperated cycle, less fuel is required to heat the air to a given turbine inlet temperature. Because the turbine work and the compressor work are approximately the same as in the non-recuperated cycle, the decrease in fuel flow results in an increase in thermal efficiency. This is especially true for the simple cycle, since the heat recovered by recuperation is rejected to the atmosphere in the non-recuperative case. For combined cycles the efficiency is also increased, because the combustion turbine recovers the recuperated heat at the simple cycle efficiency, which is larger than the 30 to 35% thermal efficiency of the bottoming steam cycle, which recovers this heat in the non-recuperated case.

Installation of a recuperation system on the baseline configuration results in an increase in thermal efficiency of 1 percentage point. The steam cycle in this recuperated cycle has a lower efficiency than the steam cycle in the baseline configuration, because the recuperator exit temperature is significantly lower than the turbine exhaust temperature. However, the effect of reduced steam cycle efficiency is smaller than the effect of recovering the recuperated heat at the combustion turbine efficiency.

Since the combustor inlet flow is smaller than the turbine exhaust flow (due to the removal of the turbine cooling air prior to combustion) and has a higher specific heat (due to the combustion of the fuel), the heat capacity of the turbine exhaust flow is somewhat higher than that for the burner inlet flow. This means that the recuperated cycle described above does not fully utilize the quantity of heat available in the turbine exhaust. By placing a steam superheater in parallel with the recuperator, the remainder of the available turbine exhaust heat can be recovered at its maximum quality. The maximum steam temperature can then be raised to that of the baseline cycle (1000°F [538°C]), and the cycle efficiency is increased by an additional 0.1 percentage point.

Since recuperative cycles return exhaust energy to the combustion turbine, less energy is available to the steam cycle, and the resulting steam turbine output is lower than that of the baseline configuration. However, the combustion turbine output is approximately the same as in the baseline cycle (minus losses in the recuperation system). This means that recuperative cycles carry a significant output penalty, with this penalty being proportional to the amount of recuperation performed.

#### 2.2.4.3.10 Intercooling with Recuperation

For a simple cycle, the combination of intercooling with recuperation eliminates the problem of the reduced combustor inlet temperature associated with intercooled cycles. The simple cycle then gets the benefit of the reduced compressor work and, at all but high pressure ratios, actually has a higher burner inlet temperature than the corresponding non-intercooled, non-recuperated cycle. This results in a dramatic increase in the simple cycle efficiency.

However, the bottoming cycle receives even less energy than in the recuperated cycle, since the recuperator removes much more heat from the turbine exhaust than in the recuperated, non-intercooled cycle. The additional heat removed corresponds to the heat rejected to the atmosphere by the intercooler. This means that we have merely displaced the lost energy of the intercooler by taking energy from the bottoming cycle. This is in addition to the energy already removed from the bottoming cycle in the non-intercooled, recuperative cycle. This results in a very low recuperator exit temperature, which in turn translates into a low generated steam pressure (low availability) and a low efficiency steam bottoming cycle. The result is that, while simple cycle efficiency can be increased to over 50%, the combined cycle efficiency is reduced for the entire useful range of compressor pressure ratios. For conventional air-to-water heat exchanger intercooling of the compressor, the combined cycle efficiency is reduced approximately 1.9 percentage points at the baseline cycle pressure ratio. For continuously cooled compressors utilizing water droplet spraying into the compressor, the combined cycle efficiency is reduced by 0.4 percentage point.

Since the continuously cooled compressor with recuperation is not far below the baseline level of combined cycle thermal efficiency, it is worth investigating further optimization of the steam cycle in this case. As mentioned earlier, steam may be superheated in parallel with the recuperator, yielding more efficient recovery of the heat available to the steam cycle. Utilizing this approach, along with a two pressure level steam cycle, results in an increase in net plant efficiency of 0.8 percentage point over the baseline efficiency level.

Another approach to optimizing the intercooled recuperative cycle is to place a saturator between the compressor exit and the recuperator entrance, as illustrated in the combined cycle shown in Figure 9. This saturator, also called an aftercooler, evaporates water into the compressor exit flow, resulting in a lower temperature, higher mass flow entering the recuperator. While this may be seen as a way to better balance the heat capacities of the hot and cold streams in the recuperator and thereby increase the amount of heat recuperated by the combustion turbine (in addition to the fact that the air flow is at lower temperature), it is important to realize that all of this additional recuperation is accomplished by the evaporation of water in the saturator. Since this water is never condensed by the cycle but instead is rejected through the stack as low pressure steam, the additional amount of energy recuperated is not recovered anywhere in the cycle. Furthermore, the recuperator exit temperature is reduced even farther than in the intercooled recuperative cycle, resulting in an even lower efficiency steam cycle.

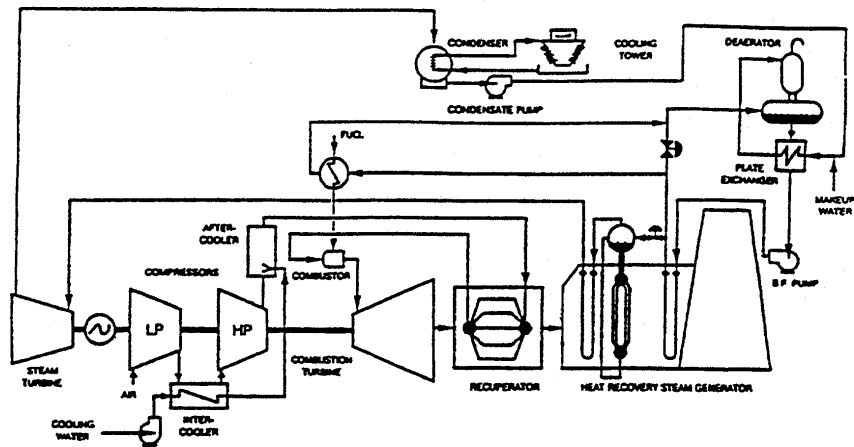


**Figure 9 Intercooled, Aftercooled (Evaporative), Recuperative Combined Cycle**

Finally, since the heat capacity of the cold side recuperator flow now closely matches that of the hot side flow, parallel steam superheat cannot be utilized to increase the steam cycle efficiency. The application of this concept to the baseline cycle results in a decrease in thermal efficiency of 2 percentage points.

#### 2.2.4.3.11 Reheat Combustion Turbine

Reheat combustion turbines utilize a two step combustion process in which the air is compressed, combusted, expanded in a turbine to some pressure significantly greater than ambient, combusted again in a second combustor, and finally expanded by a second turbine to near ambient pressure. For a fixed turbine rotor inlet temperature limit, the simple cycle efficiency is increased for a reheat combustion turbine compared to a non-reheat cycle operating at a pressure ratio corresponding to the second combustor's operating pressure. This is because the reheat cycle performs some of its combustion and expansion at a higher pressure ratio, which increases simple cycle efficiency (see section on increased compressor pressure ratio). From a purely thermodynamic standpoint, the average temperature at which heat is added is raised, thus raising the Carrot efficiency of the cycle. For combined cycles, the turbine exhaust temperature can be controlled by the selection of second turbine inlet temperature and expansion ratio. This in turn allows control over the efficiency of the steam bottoming cycle.

Another beneficial feature of reheat combustion turbine cycles is that they exhibit higher output for a fixed compressor flow rate and turbine inlet temperature than non-reheat cycles. This is due to the fact that they burn sequentially with an expansion between the combustors. This allows for the addition of more fuel (in the second combustor) without violation of the turbine rotor inlet temperature limit. Also, since this results in a higher fuel-to-air ratio than in non-reheat cycles, they burn closer to stoichiometry and exhaust lower concentrations of excess oxygen.

Applying combustion turbine reheat to the baseline cycle, with the second combustor operating at the exit pressure and temperature equal to those of the baseline cycle, results in nearly identical turbine exhaust temperatures and therefore the steam cycle of the combustion turbine reheat case is not

compromised and is identical to the steam cycle of the baseline cycle. However, the compressor pressure ratio has been increased to 36. This necessitates the addition of 6 compressor stages, and an additional combustor and turbine stage located upstream of the second combustor. The simple cycle efficiency is increased nearly 2 percentage points from the baseline simple cycle level. Since steam cycle efficiency remains at the level of that in the baseline cycle, the combined cycle efficiency is increased 1.3 percentage points.

An investigation was made into the application of intercooling and recuperation to reheat combustion turbine cycles with the same reduced efficiency results as for non-reheat combined cycles.

#### 2.2.4.3.12 Thermochemical Recuperation

In a thermochemical recuperation power plant, a portion of the stack exhaust (flue) gas is removed from the stack, compressed, mixed with natural gas fuel, heated with exhaust heat from the combustion turbine, and mixed with the compressor exit air as it enters the combustor. As the mixture of natural gas and flue gas is heated by the combustion turbine exhaust, an endothermic reaction occurs between the methane and the carbon dioxide and water in the flue gas. This reaction occurs in the presence of a nickel-based catalyst, and results in the production of hydrogen and carbon monoxide. For complete conversion of the methane, the effective fuel heating value is increased approximately 30%. Therefore, the natural gas / flue gas mixture absorbs heat thermally (as it is heated) and chemically (via the endothermic reaction), resulting in a larger potential recuperation of exhaust energy than could be obtained by conventional recuperation, which recovers energy by heat alone. In fact, with full conversion of the natural gas fuel to hydrogen and carbon monoxide, up to twice the energy recuperated by the standard recuperative cycle may be recovered.

The endothermic reaction described above is accelerated for low excess oxygen in the reacting mixture, low pressures, and high mass ratios of recirculated flue gases to methane. Therefore, in order to take full advantage of this concept, the engine is controlled by running the combustor at near stoichiometric fuel-to-air ratios (10% excess air at the combustor exit) and using flue gas recirculation to quench the combustion products down to the desired turbine inlet temperature. This maximizes flue gas recirculation and minimizes excess oxygen in the flue gas. For typical cycles utilizing this control philosophy, the resulting recirculation rate of flue gas is over 50% of turbine flow. This means that both the air compressor flow rate and stack exhaust flow rate are less than half that of conventional cycles with the same turbine size.

Another advantage of the thermochemical recuperation / flue gas recirculation (TCR/FGR) concept is that, because the fuel has a low adiabatic flame temperature, it contains a significant amount of hydrogen and operates with very low levels of excess oxygen in the exhaust, the resulting emissions of NO<sub>x</sub> and CO are much lower than those for conventional design power plants.

When applied to the baseline configuration, thermochemical recuperation yields a combined cycle thermal efficiency over 2 percentage points greater than that of the baseline cycle for several different TCR/FGR configurations. There are many possible cycle configurations, other than those described above, which can utilize

thermochemical recuperation. One of these, using steam reforming, is illustrated in Figure 10.

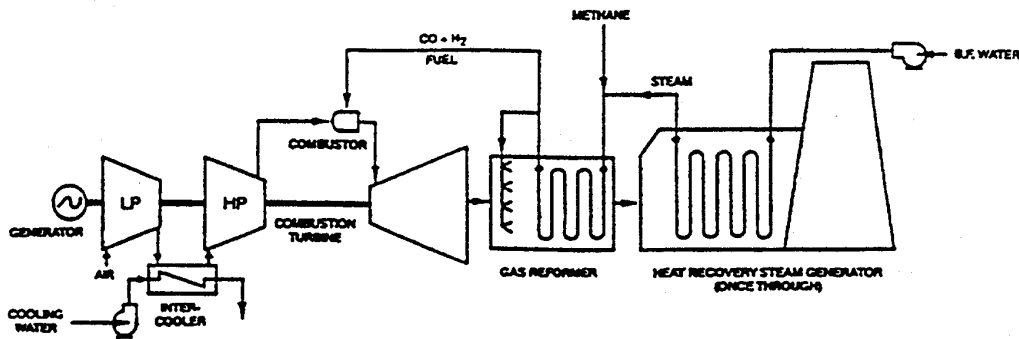


**Figure 10 Thermochemical Recuperation Cycle with Steam Reforming**

#### 2.2.4.3.13 Steam Injection

To apply steam injection to the baseline configuration, both the high pressure and low pressure steam systems are eliminated, leaving only the intermediate pressure steam system. The intermediate pressure superheated steam is then routed into the combustion turbine combustor inlet. Therefore, all steam turbines are eliminated, along with the condenser and the cooling tower. This results in a cycle which is significantly less expensive to build than the baseline cycle and it provides a means to reduce  $\text{NO}_x$  emissions via the large amount of steam injection. However, the cost associated with demineralization of the large cycle make up flow must also be considered.

For a given turbine flow area, the compressor flow size must be reduced significantly, due to the addition of a large amount of steam, which now must pass through the turbine in addition to the compressor exit air flow. Since the steam is generated with exhaust heat, which is not used in a simple combustion turbine cycle, this concept provides a significant portion of the combustor inlet gas flow with very little work requirement (a small amount of energy is needed to run the feedwater pumps which pump the water to the intermediate steam pressure). Therefore, from a simple cycle standpoint, the work of compression is much reduced due to the fact that some of the combustor inlet gas flow is compressed as a liquid. Also, the turbine output is increased significantly, since the average specific heat of the working fluid is increased considerably by the presence of the steam. The simple cycle efficiency and output are therefore increased by steam injection.

Compared to combined cycles, however, elimination of the high pressure steam system results in generation of more intermediate pressure steam, but this steam is at significantly lower availability due to its lower pressure. Also, since the low pressure steam system has been eliminated as well, the exhaust stack gas temperature is much higher, as is the associated heat loss. Finally, since the steam injected into the gas turbine is effectively throttled to its partial pressure upon mixing with the compressor exit air without doing any work, and is only expanded to its partial pressure in the exhaust stack (which is significantly higher than typical low pressure steam turbine exit pressure), the resulting steam

expansion ratio is much smaller than that of the conventional steam turbine cycle. These losses result in a reduction in combined cycle efficiency in the range of 5 to 8 percentage points. Net plant output, while much higher than the baseline configuration simple cycle output, is less than the combined cycle output.

#### 2.2.4.3.14 Evaluation of Candidate Systems

Seven natural gas-fired combustion turbine power plants were selected to be evaluated using Version 6 of the Electric Power Research Institute (EPRI) Technical Assessment Guide (TAG). A RAM analysis was also performed for each plant configuration.

Siemens Westinghouse, Gilbert/Commonwealth (G/C) and EPRI data bases were used to estimate the cost of advanced and commercially available systems. The EPRI TAG was then used to calculate the levelized Cost of Electricity (COE) for each plant. The levelized COE is a sum of five levelized components (i.e., carrying charges [a function of capital cost], fixed and variable operating and maintenance expense, variable operating and maintenance expense, cost of consumables, and fuel costs).

The following assumptions were made for all seven plant configurations:

##### **Location - Ohio River Valley**

Capital Cost Year Dollars - 1994 (January)

Delivered Cost of Natural Gas - \$3.00/MBtu

Land Area/Unit Cost - 12.5 acre (\$8,000/acre)

Project Book Life - 30 years

Project Tax Life - 20 years

Tax Depreciation Method - Reform

Property Tax Rate - 1.0%/year

Insurance Tax Rate - 1.0%/year

Federal Income Tax Rate - 34.0%

State Income Tax Rate - 6.0%

Weighted Cost of Capital - 10.8%

General Escalation - 4.0%/year

Fuel Price Escalation - 6.5%/year

For the seven natural gas-fired combustion turbine cycles evaluated, a capacity factor of 90% was assumed. The plant configuration designated ATS with a 25:1

pressure ratio was selected as the best economical choice that also has a plant RAM (92%) equivalent to today's commercial practice. (The combustion turbine RAM for ATS is 95% which again matches today's commercial practice.)

This ATS plant was compared against the Reference Plant (a combined cycle which uses a W501F combustion turbine), a new high temperature combustion turbine with a standard Rankine cycle, a new high temperature combustion turbine with an improved Rankine cycle, an ATS plant with a (35:1) pressure ratio, a recuperative cycle, and a reheat combustion turbine cycle. The calculated levelized COE for the selected ATS plant is 52.25 \$/MWh (5.23 cents/kWh) versus 60.36 \$/MWh for the Reference Plant, a 13.4% reduction in COE.

Evaluation showed that the ATS plant had the lowest COE. Comparisons were also made, separately, which showed how the capital and plant efficiency can vary and still maintain a 10% COE margin. For example, the capital cost for ATS could increase 13%, but the COE for ATS would still be 10%, less than the Reference Plant. For the recuperative cycle a 10% decrease in capital cost is required to lower the COE margin from 6.7% to 10.0%.

## 2.2.5 Task 4.0 Conversion of an Advanced Natural Gas-Fueled Combustion Turbine to Coal-Based Fuel Application

### 2.2.5.1 Introduction

Currently, development and demonstration programs are under way that are applying advanced, coal-fueled technologies for clean, effective power generation using the current generation of combustion turbines. Integrated gasification combined cycles (IGCC), pressurized fluidized bed combustion (PFBC), and second-generation PFBC are examples of advanced, coal-conversion technologies that will be demonstrated in the next 5 to 10 years.

Today's gas turbine systems feature high fuel-to-electricity efficiencies. Efficiencies, on a lower heating value (LHV) basis, for large natural-gas-fired combined-cycle systems for the utility market have been demonstrated at 54%. Cycle innovations, plus gas turbine design advancements will achieve LHV efficiencies greater than 60% for natural gas-fired utility machines. Within the United States, a 250-year coal reserve has been identified. Therefore, developing advanced systems that can use coal or biomass derived fuels are candidates to ensure that the United States will have cost-effective, and environmentally sound options for supplying post 2000 power generation needs.

A natural gas-fired advanced turbine system (GFATS) combined cycle reference system has been selected and described. This GFATS meets the established advanced turbine systems (ATS) program goals for power plant thermal performance (>60% LHV) and emissions ( $\text{NO}_x < 10$  ppmvd at 15% oxygen). This section discusses the conversion of GFATS to a coal-fueled advanced turbine system (CFATS). Two coal-based applications are described. Their development issues and emissions and performance levels are reviewed.

### 2.2.5.2 Selection of Coal-Fired Plant Reference System

A number of advanced, coal-fired power generation technologies have been under development that could be applied to the GFATS. These include a broad range of coal gasification technologies (fixed bed, fluid bed, and entrained bed), second-generation pressurized fluidized bed combustion (PFBC), and direct coal-fired turbines (DCFTs), and indirectly coal-fired, heated air turbines. Two advanced, coal-fueled technologies have been selected for consideration as CFATS: air-blown integrated gasification combined cycle (IGCC), with hot gas cleaning, based on the Kellogg, Rust, Westinghouse (KRW) fluidized bed gasifier; and second-generation PFBC.

The selection of a coal-fired reference system for the conversion of the GFATS to a CFATS has been made based on performance potential (high efficiency and low emissions), cost potential, and state of development. The air-blown IGCC technologies with hot gas cleaning, and second-generation PFBC appear to have the greatest thermal performance and cost potential based on published process evaluations and cost comparisons. Their respective status of development is categorized as early demonstration, which is suitable for the ATS program.

Air-blown IGCC with hot gas cleaning, and second-generation PFBC have outstanding environmental performance. The solid waste from these technologies without sorbent regeneration is higher than that from several other advanced technologies, but is lower than that from conventional, coal-fired power plants. Solid waste disposal, potential by-product uses and sorbent are development issues.

Air-blown, fluidized bed coal gasification processes with hot gas cleaning (e.g., the KRW gasifier [Sierra Pacific, Pinon Pine Project] and second-generation PFBC [Air Products, Four Rivers Energy Modernization Project]) are scheduled to be demonstrated in Clean Coal Technology Programs. Both of these technologies are considered for CFATS because they pose very similar conditions and constraints on the combustion turbine and are both involved in major demonstration programs that will lead to commercialization.

These selected technologies also provide greater challenges to the combustion turbine than other advanced technologies such as oxygen-blown gasification with cold gas cleaning, because: 1) air-blown, hot gas cleaning systems deliver a high-volumetric flow of low-Btu fuel gas to the combustion turbine at a high temperature, requiring large manifolding/combustion systems adapted to high-temperature duty; and, 2) hot gas cleaning produces fuel gas conditions with potentially higher contaminant contents than do low-temperature cleaning systems. Successful development of the selected CFATS implies that adaptation to the other coal-fueled and biomass technologies can be achieved.

### 2.2.5.3 IGCC CFATS Description

An IGCC, CFATS process flow diagram, illustrated in Figure 11, is representative of several types of air-blown, coal gasification plants with hot gas cleaning being developed in Clean Coal Projects, such as the Sierra Pacific, Pinon Pine Project (KRW fluid bed gasifier), the Tamco Power Partners, Tom Creek Project (Institute of Gas Technology fluid bed gasifier), and the Springfield Project (ABB Combustion Engineering entrained gasifier). Estimates of plant cycle

performance and emissions were made for a specific KRW fluid bed gasification process using process design information reported in a recent DOE study.

In the process diagram, coal and a sulfur sorbent, limestone or dolomite, are prepared (sized and dried) for feeding using conventional handling and preparation equipment. The coal and sorbent are pressurized and distributed to the fluid bed gasifier by a commercial feeding system in either dry or slurry form. The gasifier generates a low heating value fuel gas that has been partially desulfurized by the in-bed sorbent.

The fuel gas is pre-cleaned by conventional cyclones and the captured ash, char and sorbent particles are either recycled to the gasifier or removed for solid waste processing. The fuel gas is cooled by indirect, high-pressure steam heat exchanger, to a temperature of 800° to 1000°F (427°C to 538°C), as dictated by the zinc-based, sulfur removal process. After cooling, the fuel gas sulfur content is reduced to an acceptable level by a regenerative, zinc-based, fluid bed sulfur removal process. The sulfur removal process may either produce a sulfur by-product, or recycle the regenerator sulfur stream to the gasifier; or to solid waste processing. The desulfurized fuel gas then passes through a ceramic barrier filter for final particle removal before entering the combustor. Fuel gas particle content is limited to a total solids content and maximum particle size acceptable to the turbine expander, as well as to environmental standards.

Air provided by the turbine compressor burns the fuel gas and produces combustion products at the desired temperature. The combustor is a dry, low-NO<sub>x</sub> design that is closely integrated with the turbine. A portion of the turbine compressor air also is boosted in pressure for gasifier oxidant supply. The combusted fuel gas is expanded in the turbine, and steam is generated in the heat recovery steam generator (HRSG) for the steam bottoming cycle. A portion of the high-pressure, cold reheat steam is consumed in the gasifier, assisting the coal gasification reactions. High-pressure steam is also heated in the fuel gas cooler. The stack gas temperature exiting the HRSG is limited by the gas dew point for its prevailing acid-gas content.

Waste solids from the gasifier, the cyclones and the ceramic barrier filter are treated in a waste process facility to utilize the waste solids fuel content and sensible heat content, and to render the waste environmentally acceptable.

The coal gasification process chosen for study is the KRW process. It utilizes a bed of char and ash with limestone sorbent added for fuel gas desulfurization and volatile product cracking. The bed is fluidized by the air and steam required for carbon conversion and temperature adjustment. The ash is agglomerated to facilitate its removal. The fuel gas leaving the fluidized bed is cleaned hot. The possible cleaning steps include:

- absorption of residual H<sub>2</sub>S and alkalis (Na and K compounds carried in the gas) by solid sorbents
- reduction of the NH<sub>3</sub> content by catalytic decomposition
- removal of particulates by a filter

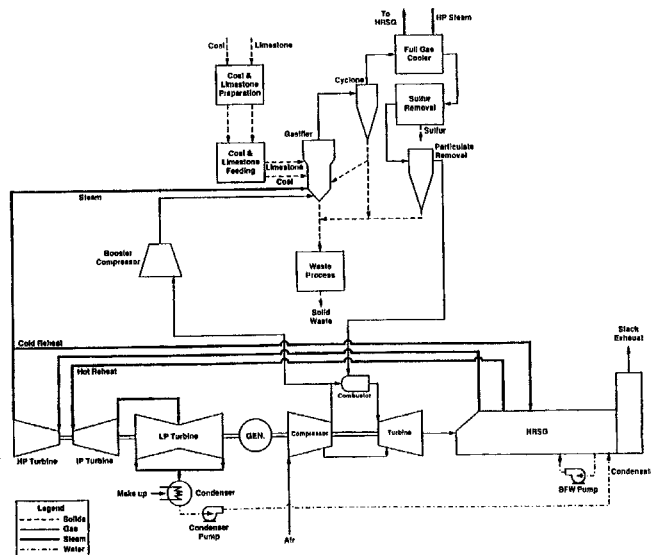


**Figure 11 Coal-Fired Advanced Turbine System - IGCC**

The temperature of the fuel gas between the gasifier and the turbine is lowered for cleaning and for delivery to the turbine at 1000°F (538°C). This reduction is accomplished either by a steam quench or preferably by heat interchange for best efficiency, with the steam and/or air fed to the gasifier.

The ash and sorbent solids removed from the bed are oxidized with air to recover their carbon content as heat and to convert the sulfided limestone based sorbent to a sulfate, suitable for disposal. The temperature of the process must be carefully controlled to prevent the release of sulfur from the sulfided sorbent as SO<sub>2</sub>. An alternative process carries out the oxidation of the ash and sorbent at pressure with the return of the hot gases to the gasifier. In this instance, the heat is efficiently recovered in fuel production, and the escape of SO<sub>2</sub> is effectively prevented.

#### 2.2.5.4 Second-Generation PFBC CFATS Description

The process flow diagram in Figure 12 illustrates the general second-generation PFBC configuration adapted for the CFATS. Specific plant performance and emissions estimates were prepared for the specific configuration of the technology.

In the process diagram, coal and a sulfur sorbent, limestone or dolomite, are prepared (sized and dried) for feeding using conventional handling/preparation equipment. The coal and limestone are pressurized and distributed to the carbonizer with a commercial feeding system in either dry or slurry form. The carbonizer generates a low heating value fuel gas that has been substantially desulfurized by the in-bed sorbent. The carbonizer differs from a gasifier in that it produces a large flow of char that must be burned separately. The carbonizer fuel gas acts as a topping fuel for the char combustor. Char drained from the carbonizer and captured by the cyclones and ceramic barrier filter is circulated to a fluidized bed combustor. In this combustor, char is burned, sulfur released

from the char is captured by the sorbent contained in the solids from the carbonizer, and steam is generated in the fluid bed heat exchanger.

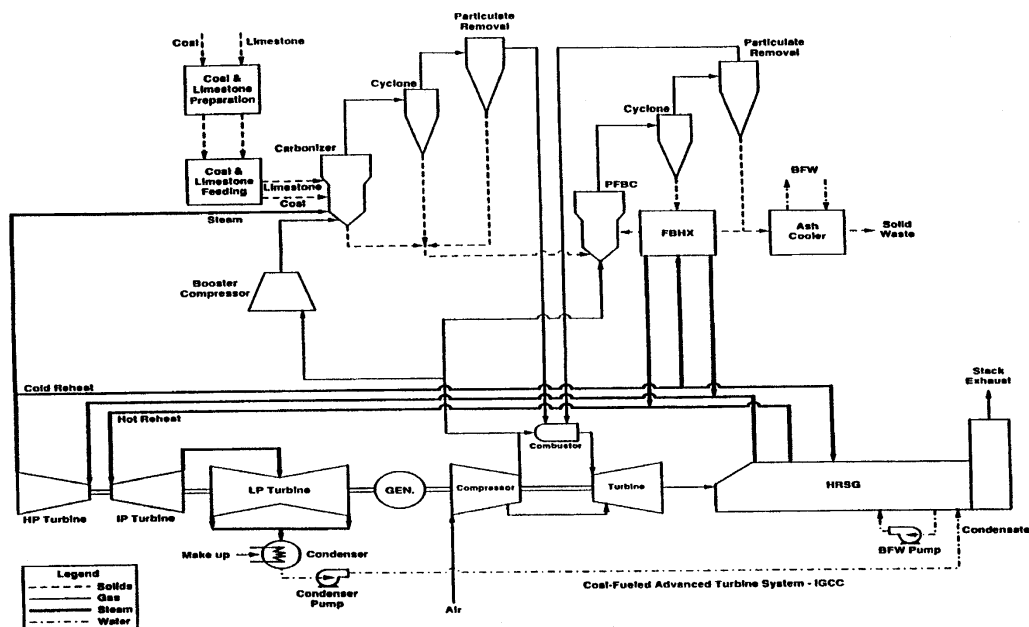


**Figure 12 Coal-Fueled Advanced Turbine System - PFBC**

The fuel gas and combustion gas streams are pre-cleaned by conventional cyclones. Neither the fuel gas or the combustion gas is cooled before final particle control is performed by ceramic barrier filters. Additional sulfur removal is not required. Particle penetration is limited to total content and particle sizes acceptable to the turbine expander. Alkali removal may be required from the fuel gas or vitiated air streams.

Vitiated air from the fluid bed combustor fires the fuel gas to a desired temperature of 2700°F (1482°C). The combustor is a dry, low-NO<sub>x</sub> design configured to utilize the hot fuel gas and the hot, vitiated air. A portion of the turbine compressor air is boosted in pressure for carbonizer oxidant supply. The fired fuel gas is expanded in the turbine, and steam is generated in the heat recovery steam generator for the steam bottoming cycle. A small portion of the high-pressure, cold reheat steam may be consumed in the carbonizer, preventing coking from occurring. The stack gas temperature in the HRSG is limited by the gas dew point at its prevailing acid-gas content.

Waste solids from the fluid bed combustor, the cyclones and the ceramic barrier filter are cooled to use waste solids sensible heat content. No treatment is required to render the waste environmentally acceptable.

#### 2.2.5.5 Performance and Emissions Estimates

The performance and emissions of the selected CFATS have been estimated by modifying the process designs used by Southern Company Services, and Foster Wheeler Corporation. Table 2 lists the power plant thermal performance for both the reference studies and the CFATS cases, along with the steam cycle

conditions and the combustion turbine conditions. The fluidized bed IGCC system presented in the reference study has the following unique features:

- The moist coal is dried and preheated at atmospheric pressure prior to feeding into the fluidized bed gasifier. Hot combustion product gases from a combined carbon burnup/sorbent sulfation operation are used in this process and exhausted to the stack.
- The coal feed and the char recycle streams are transported with cooled, cleaned, and compressed fuel product gases. The recycle fraction is not quantified in the flow sheet, but calculations indicate that between 30% and 45% of the fuel product is recycled for coal and other transport. The recycle stream also provides most of the water vapor, steam, required to moderate the operating temperature of the gasifier.
- The product fuel gas is cleaned --  $H_2S$ ,  $NH_3$ , Na, K, and Cl; and particulates-- and cooled to 1000°F (538°C) in preparation for recycle and for feed to the turbine. Fuel gas cooling is completed with heat exchange, generating steam and hot boiler feed water for the bottoming Rankine cycle, and of steam quench, enhancing the steam content of the product gas for recycle to the gasifier and feed to the turbine.

The air/coal ratio is 3.4 lb/lb (kg/kg). The steam/coal ratio estimated to be in the range 0.4 to 0.7 lb/lb (kg/kg). The Ca/S mol ratio for the sorbent feed is 3.0.

**Table 2 CFATS Thermal Performance**

	IGCC (KRW gasifier)	Second-Generation PFBC
REFERENCE STUDY		
Steam turbine conditions		
Temperature °F (°C)	1000 (538)	1000 (538)
Pressure, psig (MPa)	1600 (11)	2400 (16.5)
Combustion turbine conditions		
Combustor outlet temperature , °F (°C)	2350 (1288)	2800 (1538)
Expansion ratio	14	12
Stack gas temperature, °F (°C)	280 (138)	280 (138)
Plant net efficiency (LHV)	41.5	48.7
Gasifier cold gas efficiency (LHV)	72.1	--
CFATS PERFORMANCE		
	Modified Process*	
Turbine frame	ATS	ATS
Steam turbine conditions		
Temperature °F (°C)	1100 (593)	1100 (593)
Pressure, psig (MPa)	1800 (12.4)	1800 (12.4)
Combustion turbine conditions		
Combustor outlet temperature, °F (°C)	2700 (1482)	2700 (1482)
Expansion ratio	18	18
Stack gas temperature, °F (°C)	280 (138)	280 (138)
Plant net efficiency (LHV)	50-53	52-53
Gasifier cold gas efficiency (LHV)	86.8	--
Gasifier hot gas efficiency (LHV)	95.8	--

-----  
 \* Process was modified to incorporate coal drying, carbon burnup, and sorbent processing within the gasifier. Steam used for coal and char transport rather than recycle gas. Fuel gas cooling produced steam fed directly to the gasifier.

A modified fluidized bed coal gasification process has been proposed and evaluated for the CFATS, having these distinct features:

- The moist coal and recycle char are fed to the gasifier in superheated steam. No cooled, cleaned, compressed fuel gas is recycled.
- Burnup of carbon from the ash and sulfation of the spent sorbent are carried out with air at system pressure, the hot gases are routed to the gasifier.
- The product fuel gas is cleaned as previously, but cooling is accomplished in exchangers which provide superheated steam (and perhaps also heated air) for gasification. No steam is exported to the bottoming Rankine cycle.

The air/coal ratio is 3.0 lb/lb (kg/kg); the steam/coal ratio is 0.8 lb/lb (kg/kg) . The Ca/S mol ratio is 2. The gasification temperature is 1800°F (982°C), the product fuel gas temperature, 1000°F

(538°C). Material and energy balances have been carried out for this process based on the Illinois No. 6 coal feed selected for the reference study described above.

The fuel gas quantity and composition have been calculated for this modified fluidized bed coal gasification process. Both the hot and the cold gas efficiencies are significantly increased by the process modifications. Further increases in efficiency, to the extent practical in the design and operation of the plant, might be obtained by:

- increasing the temperature of the product fuel gas fed to the gas turbine;
- reducing the air/coal, steam/coal, and sorbent/coal ratios; and,
- increasing the pressure and reducing the temperature of the gasification process.

The overall performance of a CFATS plant in power generation has been estimated based on the modified fluidized bed coal gasification process described above and on the GFATS cycle selected for development. The selected GFATS cycle calculations have been used to define three work terms:

- compression of the air used in combustion, dilution, and gasification --assumed proportional to the mols of air;
- compression of the air used in turbine vane, blade, and rotor cooling --assumed proportional to the mols of hot gases entering the turbine;
- generation and expansion of steam in the bottoming Rankine cycle --assumed proportional to the mols of diluted combustion product gases times their specific heat times the temperature difference between inlet and outlet gases.

The gasification and combustion calculations for the gasification process described above have been used to determine the proportionality factors described above and in turn to estimate the work quantities associated with the compressor, expander turbine, and bottoming cycle of a CFATS plant from those of the GFATS. The work of the booster compressor for air feed to the gasifier from the turbine compressor has been calculated based on an assumed efficiency and inlet temperature. Mechanical, electrical, and windage losses and auxiliary power for the generation section have also been estimated from the GFATS study and auxiliary power for the gasifier and coal feed sections, from the reference study, previously cited.

The second-generation PFBC reference study was a recent evaluation of a commercial plant, using a high temperature gas turbine, performed by Foster Wheeler and Gilbert/Commonwealth Associates. A major modification to this study was a significant reduction in the turbine air cooling needs. The CFATS conditions result in significant performance improvements over the reference studies.

Environmental performance estimates are listed in Table 3 for the CFATS cases. Comparison is also made with conventional, coal-fired power plants and with conventional, natural gas-fired power plants in the table. The basis of reporting the emissions in this table is per unit of net power output, lb/hr/MWe (kg/hr/MWe), rather than the current per unit of fuel energy input, lb/MBtu (kg/kJ). A large improvement for the CFATS relative to representative commercial coal-fueled technology is shown in this table.

#### 2.2.5.6 Identification of Design Changes to GFATS

While the two coal-based power systems differ significantly in their major process conditions, power cycles, process designs and equipment arrangements, both pose a similar set of requirements on the fuel gas combustion and the combustion gas expansion equipment. Both require effective use of the turbine compressor air supply with minimal compressor modifications. With both, a hot low heating value fuel gas is generated that must be efficiently combusted, with acceptable NO<sub>x</sub> and CO emissions, producing the designated 2700°F (1482°C) combustor outlet temperature, uniformly distributed over the inlet of the turbine expander.

The GFATS consists of several functional components that must be modified for the CFATS: the air compressor, the combustor inlet fuel gas and oxidant gas manifolds, the flow controls, the combustor, the turbine inlet scroll, and the turbine expander. The GFATS compressor can be modified by standard techniques to provide the air requirements for the coal processing steps and for the low heating value fuel gas combustor. Some 20% to 30% of the air leaving the combustion turbine compressor must be boosted in pressure and ducted to the coal gasifier. Customarily, the booster compressor, with associated cooling and heat recovery exchangers, is a device independent of the combustion turbine. Low pressure loss takeoffs for gasification air, as well as for turbine cooling air, are required. Also, because higher combustion product flows and higher gas temperatures in the turbine result from replacing natural gas fuel by coal gas, slightly higher airflows may need to be extracted from the compressor for turbine cooling. This is a modification that can be accomplished by available engineering design and evaluation techniques.

**Table 3 CFATS Emissions Performance**

	Emissions, lb/hr/MW <sub>e</sub> (kg/hr/MW <sub>e</sub> )				
	NO <sub>x</sub>	SO <sub>2</sub>	CO <sub>2</sub>	Particulate	Solid Waste
<u>CFATS</u>					
IGCC (air-blown) <sup>a</sup>	1.4 (0.64)	0.64 (0.29)	1409 (639)	5.4 (2.5)	212.3 (96.3)
2nd-Gen. PFBC <sup>b</sup>	1.3 (0.59)	1.55 (0.7)	1366 (620)	5.2 (2.4)	190.2 (86.3)
<u>Conventional</u>					
AFBC <sup>c</sup>	2.8 (1.27)	4.45 (2.02)	1959 (889)	22.2 (10.1)	257.3 (116.7)
PC/FGD <sup>d</sup>	5.7 (2.59)	4.45 (2.02)	1959 (889)	22.2 (10.1)	244.6 (110.9)
Gas Simple-Cycle <sup>e</sup>	0.8 (0.36)	---	1061 (481)		
Gas Combined-Cycle <sup>e</sup>	0.7 (0.32)	---	843 (382)		

a: NO<sub>x</sub> 0.2 lb/MBtu (85.9 mg/MJ), sulfur removal 98%, Ca/S ratio 1.8, particulate 0.01 lb/MBtu (4.3 mg/MJ)

b: NO<sub>x</sub> 0.2 lb/MBtu (85.9 mg/MJ), sulfur removal 95%, Ca/S 1.8, particulate 0.01 lb/MBtu (4.3 mg/MJ)

c: NO<sub>x</sub> 0.3 lb/MBtu (129 mg/MJ), sulfur removal 90%, Ca/S 2.5, ESP particulate 0.03 lb/MBtu (12.9 mg/MJ)

d: NO<sub>x</sub>, 0.6 lb/MBtu ((259 mg/MJ), sulfur removal 90%, Ca/S 1.1, ESP particulate 0.03 lb/MBtu (112.9 MG-MJ) These represent current NSPS for coal-fired power plants.

e: Low-NO, burners with 25 ppmv NO, (at 15% oxygen)

The IGCC, low-Btu fuel gas can be efficiently burned by internal, rich-lean combustor baskets located within the turbine cylinder, much like the GFATS, but adapted to the high temperature fuel gas conditions. The flow of air to the gas turbine combustor is reduced by some 20% to 30% due to the airflow extracted for the coal gasification process; thus, there is less air available for combustor cooling. But the maximum stoichiometric, adiabatic flame temperature associated with coal gas is much lower than that with natural gas. Therefore, the reduction in the quantity of combustor cooling air may not be critical. The lower flame temperature will reduce the formation of thermal NO<sub>x</sub>, but is sufficiently high to limit the conversion of fuel-bound nitrogen to NO<sub>x</sub> in the rich zone. The volumetric flow rate of the coal gas is higher than that of the natural gas fuel by a factor from 6 to 9. The temperature of the coal gas is 1000°F (538°C); that of the natural gas, 670°F (354°C). The volumetric flow of the fuel is thus greatly increased, and redesign of the fuel nozzle and mixing arrangements is required. Flame stability in the combustor does not appear to be a problem because of the high H<sub>2</sub> content of the coal gas fuel. If this larger cylinder exceeds the maximum shipping dimensions, the engine would have to be shipped without the top half.

The second-generation PFBC combustor conditions may require that the multiple, internal combustor baskets of the GFATS be replaced by external combustor chambers, as shown in the illustration of Figure 13, due to the large size of the combustor chambers required. Two combustion chambers, each with eight combustor modules, would be located externally to the main engine cylinder, one on each side, as shown. Hot, low-Btu fuel gas, and combustion

vitiated air, would be distributed to these combustors uniformly to achieve the required combustion performance. The external combustion requires that an inlet scroll be designed, with an appropriate cooling scheme, to introduce the combustion gas into the turbine.

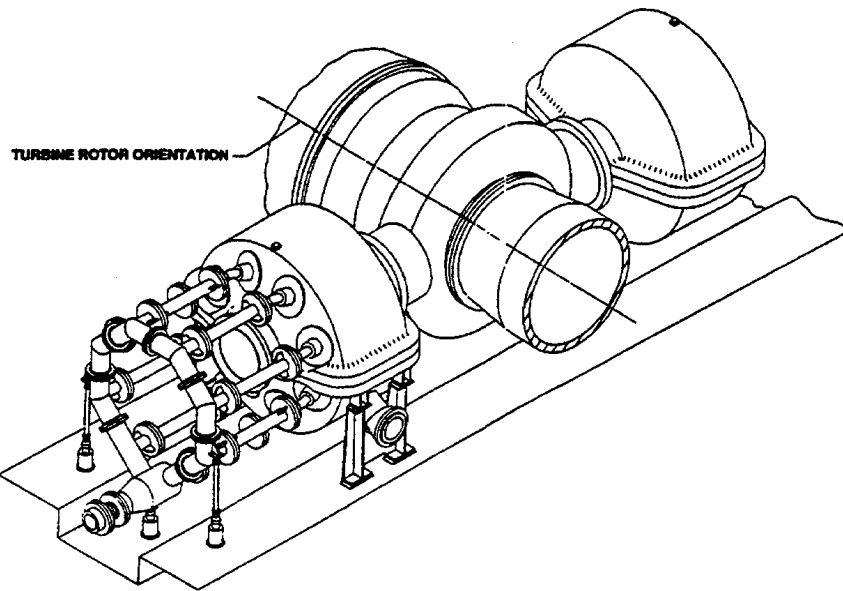


**Figure 13 Conceptual Dual Topping Combustor Arrangement**

The combustors must be designed with minimal structural cooling, to burn the low heating value fuel gas efficiently and with acceptable pressure drop, acceptable outlet temperature uniformity, acceptable metal surface temperatures, low CO, soot and unburned hydrocarbons, low conversion of fuel-bound nitrogen to NO<sub>x</sub>, acceptable turndown performance, and with multiple fuel capability.

The combustion turbine cylinder from the compressor discharge to the turbine inlet would require major design changes for the second-generation PFBC case. The casing inlet, manifold/inlet scroll and outlet arrangement would be modified from the GFATS to duct the combustion products by transition liners into a uniform annular flow, as is shown in Figure 14. Engineering analysis must be performed, considering heat transfer analysis, stress analysis, pressure drop analysis and computational fluid dynamic analysis. Engine thrusts must be reviewed and thrust bearings redesigned, if required. The combustion turbine bedplate mounting will also be substantially modified, in the second-generation PFBC case, from the GFATS. Similar considerations of the combustion turbine casing for the IGCC case must be made, but under much less challenging conditions. The substitution of coal gas from the KRW or the modified fluidized bed process for natural gas fuel increases the volumetric flow of the combustion product gases by some 13% to 24%, depending on specifics of gasifier operation. This flow increase and the higher specific heat of the coal gas combustion products, with their higher CO<sub>2</sub> content, increases both the work output from the turbine by 15% to 28% and the temperature of the expanding gases within the turbine -- by as much as 80°F (44.4°C) at the turbine exit. The blade design and blade cooling arrangements must be adequate to cover these increased loads and temperatures.

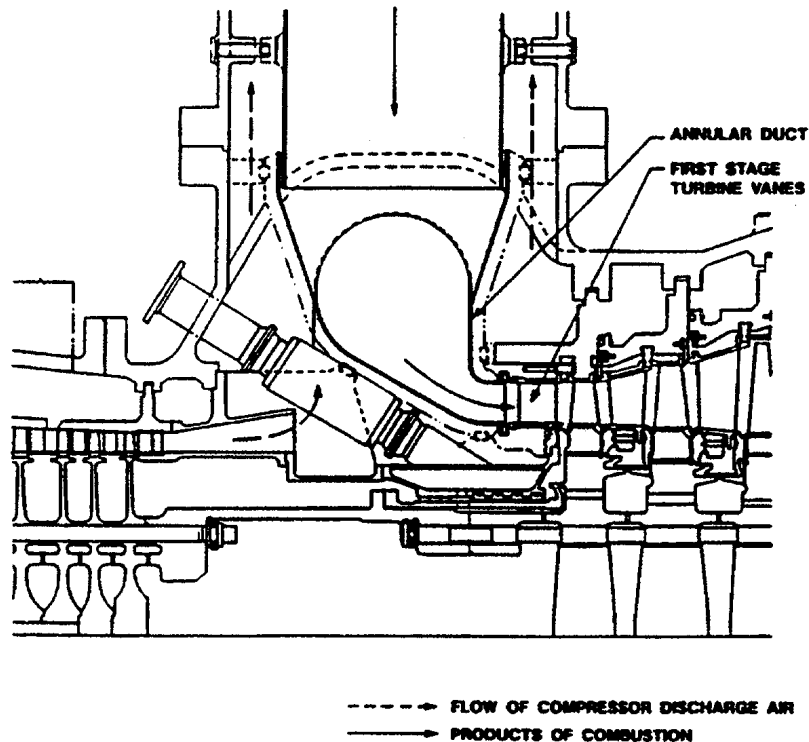


**Figure 14 Topping Combustor Outlet to Turbine Inlet Gas Flow Concept**

Special consideration must be given to the operation and control of the integrated coal gasification, hot gas cleaning, coal-fired advanced turbine system, CFATS. Operation includes startup, load follow, and shutdown -- planned and emergency. Control includes maintaining steady optimal operation. Startup of the plant will probably require special provisions for natural gas firing of the gas turbine(s) -- fuel nozzles and perhaps auxiliary combustors. Emergency shut down, for example on load loss, will require quick acting valves to isolate the gasification and gas cleaning systems from the turbine to prevent overspeed and blow back into the compressor.

Load follow and control of the turbine with its integrated coal gasification, hot gas cleaning fuel supply will require coordinated adjustment of the coal, air, and steam feed to the gasifier. A single fuel flow valve, customary for a natural gas fired turbine, is not adequate to provide load follow and to protect the turbine from excessive combustion temperatures. A fuel flow control may need to be omitted due to the high temperatures and flows involved. In this case the coal, air, and steam valves on the gasifier feeds will be required to provide both the turbine and gasifier control functions. Flow controls may be placed in differing positions in the CFATS plant, so that they may provide control over lower-temperature streams located upstream of the major coal processing steps. For example, in second-generation PFBC, vitiated air control to the combustor may be achieved by air control to the fluid bed combustor, providing valves that operate at commercially available temperatures. Similarly, over speed protection valves must be supplied for the CFATS that are placed in acceptable locations that may differ substantially from the those of the GFATS. Compressor air bypass, through the turbine startup burner, to the combustor may be used to cool

the expansion gas and promote turbine speed reduction, as is shown in Figure 15.

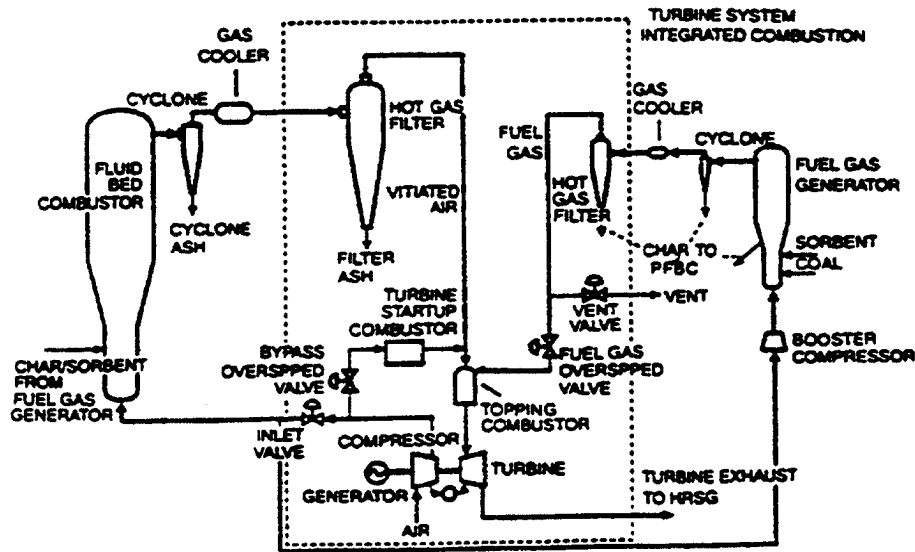


Figure 15 Topping-PFBC Process Schematic

The piping to and from the coal to fuel processing system must be designed to reduce and control thermal expansion stresses and pipe reactions on the turbine cylinder. The requirement for the use of by-pass valves to prevent turbine overspeed in the event of sudden load loss must be studied and the piping arrangement will be evaluated to minimize piping cycle flow pressure losses. The control system functions should be similar except where changes are required to account for the considerable larger fuel flow. The control concept must be reviewed to identify modifications. Many of the control issues are being evaluated within the current advanced, coal-fuel technology development programs and do not need to be considered in the ATS program.

The turbine airfoil geometry and casing sections themselves will not be substantially modified from the GFATS, although the Row 1 vane spacing must be increased to accommodate differences in flow between the GFATS and the CFATS, providing acceptable pressure reduction. The airfoil materials may also be substantially modified. The combustion products will contain vapor and solid/liquid contaminants that are known to induce turbine airfoil material corrosion: sodium, potassium, vanadium, lead, calcium, lithium, phosphorous, silica, chlorine, iron, copper, and nickel. These may reduce the life of key turbine components and increase system maintenance requirements. Not only must hot corrosion when selecting appropriate thermal barrier and corrosion resistant coatings, induced by deposition of slag-like particles and condensable vapors, be considered, but cold-end corrosion due to acidic mists, condensates and slurries must also be considered. The effectiveness of hot gas filters should make turbine airfoil erosion a secondary concern. Particle deposition may be more severe in the CFATS than in the current coal-fired turbine cases because of the higher firing temperature and resulting adherence of particles. Available on-line and off-line airfoil cleaning methods may need to be optimized for the CFATS. Specific turbine airfoil base materials and thermal barrier coatings will need to be

specified for the CFATS that are tolerant of the gas contaminants both during steady operation, during off-design conditions, turndown, startup and shutdown transients, as well as during off-line conditions.

It is expected that the material for the main cylinder, horizontal joint, and vertical flange bolting will be the same as used in the GFATS. The hot gas containment system in the second-generation PFBC case could present the most critical challenge for this design. This containment system represents a large area to maintain at acceptable metal temperatures, control leakages at the juncture to the turbine inlet, and minimize distortion to stay within acceptable limits. Materials would need to be the same as used in state-of-the-art combustion turbine combustors and transition pieces, or possibly even using new concepts, such as ceramics, in some areas.

The possible arrangement of the second-generation PFBC combustor system into two off-board combustor housings, as opposed to the conventional in line, on-board combustors of the GFATS will require a significant design effort. The extended surface of the hot gas flow path is much greater in area than would be the surface of the transition pieces in the GFATS. All of this surface must be cooled by compressor discharge air. The cooling required will be much more than can be achieved by surface convection, which has been the conventional way of cooling the transitions. Impingement cooling of ceramic tiles lining the interior of the extended hot gas flow path means a significant amount of compressor discharge air will by-pass the combustion process within the combustors, thereby reducing the amount of air available for the combustion process, cooling the combustor wall surface, and the profiling of combustion products for uniform turbine inlet temperature for the first row vanes. It is difficult in an off-board combustion system arrangement, to have any real final control of turbine inlet temperature profile, because of the lack of control of the mixing process in the large volume of space between the exit of the combustor and the inlet to the turbine

Critical structural problems exist that differ from those of the GFATS. Both stationary and rotational parts must consider short-term loading, fatigue, creep, and embrittlement failure mechanisms. These considerations especially must be made for the combustors (primarily thermal fatigue due to overheating and shocking), and the turbine discs, blades, and nozzle vanes. The critical structural problem in the CFATS is thermal stress and distortion caused by temperature differences between the compressor and combustor legs and the mating leg from the turbine cylinder. Also, a similar problem exists for the hot gas duct containment cylinder, and inlet scroll that guides the hot gases into the turbine inlet. An extensive finite element heat transfer analysis will be required to redesign the cylinders, flanging, and the interior hot gas flow system to insure that stress and distortion limits are met.

#### 2.2.5.7 Conclusions

Two coal-fueled power plant technologies were selected to represent the CFATS -- air-blown, fluidized bed gasification using hot gas cleaning, and second-generation PFBC. Both of these concepts are currently being demonstrated in major Clean Coal Technology Programs, and both have high performance and improved emissions control potential in the CFATS.

Both of these CFATS cases require gas turbine combustors which cleanly burn hot, low heating value coal derived fuel gas and turbine expanders which operate effectively on combustion products of gases cleaned at high temperature. The cases differ in the fraction of air removed from the turbine casing for coal processing and in the location of the turbine combustors -- internal or external to the casing. The IGCC case can utilize rich-lean, low-Btu fuel gas combustion baskets located within the combustion turbine cylinder. The second-generation PFBC case may require the use of external combustors due to the large size of the combustor chambers required by the use of hot, depleted air from the PFBC unit.

Major development areas directly relating to the conversion to the CFATS, in addition to those areas already identified in current coal-fueled technology development programs, are:

- low heating value, low-emission, fuel gas combustor design,
- combustor outlet manifolding and turbine inlet scroll design,
- turbine corrosion deposition; and materials selection.

The technology developed under the GFATS program will be transferred to the CFATS, as applicable. With GFATS cycle efficiencies greater than 60% (LHV), it should be possible to obtain CFATS cycle efficiencies in the range of 52% to 54%.

## 2.2.6 Task 5.0 Advanced Turbine System Market Study

### 2.2.6.1 Introduction

The market potential for the Advanced Turbine System (ATS) gas turbine was assessed using analytical screening curves, product introduction life cycle curves, market demand forecasts by world region, and appropriate fuel cost scenarios. The markets for the ATS in simple cycle, combined cycle and integrated gasification combined cycle (IGCC) application were separately evaluated. Three unit sizes were postulated and economic and market comparisons performed with respect to "G" and "F" technology. In the context of this report, it is to be recognized that ATS "technology" is first being introduced and demonstrated in what are referred to as "G" machines to demonstrate technical feasibility. In this respect the overall DOE ATS program benefits comprise the current and future success of both the "G" and the "ATS". Under Siemens Westinghouse direction and using Siemens Westinghouse defined gas turbine cost, maintenance and performance data, a subcontractor performed the analysis. Regular review and interaction by Siemens Westinghouse occurred throughout the effort.

Worldwide power generation capacity additions are expected to exceed 100 GW per year in the forecast period, led by Asia/Pacific.

The ATS will compete for a portion of projected natural gas, oil and coal additions, which represent more than 70% of the total market. The simple cycle and combined cycle technical market potential was estimated by screening out segments which will not be accessible to ATS technology (see Figure 16). Markets inaccessible to the ATS are:

- Markets for fuel other than natural gas and distillate oil.
- Small regional markets unable to absorb large capacity increments.
- Markets traditionally served by small gas turbines (e.g. small cogeneration).
- Gas and oil markets served by non-GT technologies (e.g. oil-fired steam turbines, reciprocating engines, fuel cells).

A similar screening analysis was conducted for coal markets.

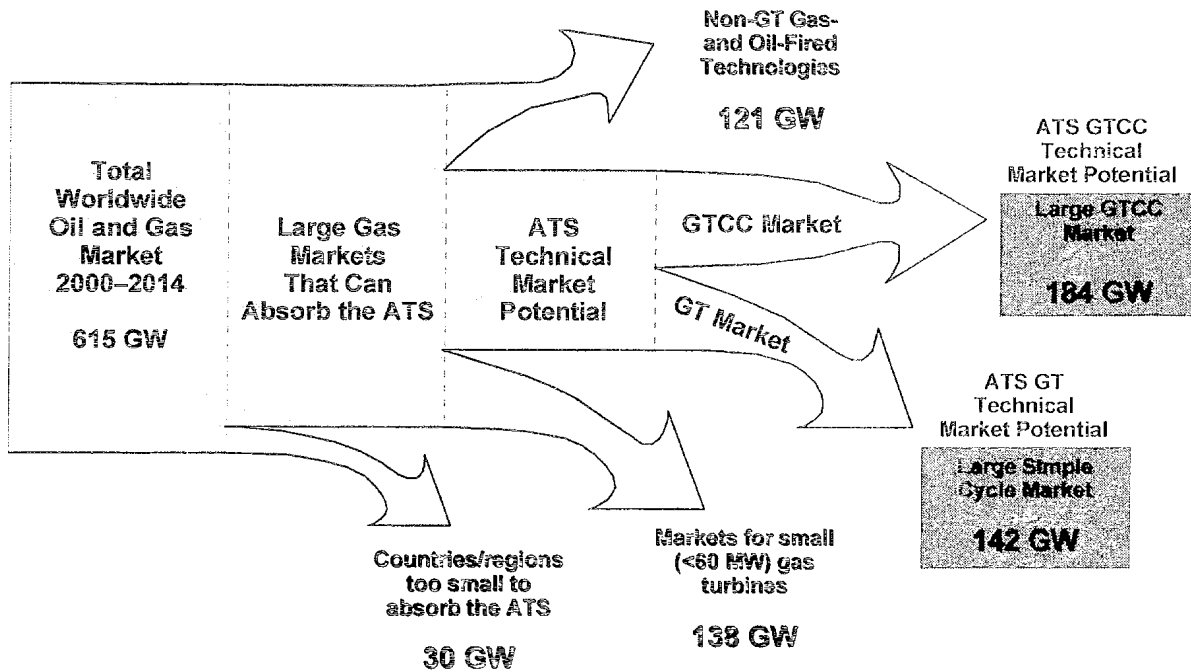


**Figure 16 Screening Methodology**

Relative size categories used in the study vary by frame technology, line frequency and project classification, as shown below:

	<u>Small</u>	<u>Medium</u>	<u>Large</u>
ATS 50 Hz	170-240 MW	240-285 MW	>285 MW
ATS 60Hz	100-150 MW	170-235 MW	>235 MW
Combined cycle	<300 MW	300-500 MW	>500 MW

The market potential of each GT frame size was estimated by examining project and frame size preferences worldwide.

Historical gas turbine sales data, National Electricity Reliability Council (NERC) forecasts and Utility Data Institute (UDI) forecasts were used to assess the likely size distribution of gas turbine projects for different countries and regions. The result was four different market types representing key regional differences.

The same data sources were used to make an assessment of the relative attractiveness of the different GT frame sizes for a given project size. For example, historical data indicates that large GTCC projects have typically made use of the largest available frame size. This distribution was assumed to be the same for each market type.

From these two analyses, the technical market potential of each ATS and "G" frame size (as a percent of the total technical market potential) was calculated.

This was supplemented by information obtained during contractor conducted interviews and by contractor estimates of future trends.

The following Table 4 summarizes the results.

**Table 4 Turbine Frame Size Preferences**

<b>Market Type</b>	<b>Example Characteristics (GTCC)</b>	<b>Example Countries/Regions</b>
<b>USA Type</b>	<ul style="list-style-type: none"> <li>• Few large projects (&gt;500 MW)</li> <li>• Focus on small to medium sized projects (100-500 MW)</li> <li>• Modest load growth</li> </ul>	<ul style="list-style-type: none"> <li>• North America</li> <li>• Western Europe</li> </ul>
<b>Large Gas-Fired Projects</b>	<ul style="list-style-type: none"> <li>• Large GTCC projects predominate (&gt;500 MW)</li> <li>• LNG importing regions</li> <li>• High load growth</li> </ul>	<ul style="list-style-type: none"> <li>• Japan</li> <li>• India</li> <li>• Thailand</li> <li>• South Korea</li> </ul>
<b>Small/Medium Gas-Fired Projects</b>	<ul style="list-style-type: none"> <li>• Few large projects (&gt;500 MW)</li> <li>• Smaller gas markets</li> <li>• Lack of gas infrastructure</li> </ul>	<ul style="list-style-type: none"> <li>• South America</li> <li>• Bangladesh</li> <li>• Pakistan</li> <li>• FSU</li> </ul>
<b>Middle East/Africa</b>	<ul style="list-style-type: none"> <li>• Trend towards larger projects (&gt;500-600 MW)</li> <li>• Ample gas supplies</li> <li>• Shift from simple to combined cycle plants continues</li> </ul>	<ul style="list-style-type: none"> <li>• Saudi Arabia</li> <li>• Syria</li> <li>• Iran</li> </ul>

Cost of Electricity comparisons are shown in Figure 17.

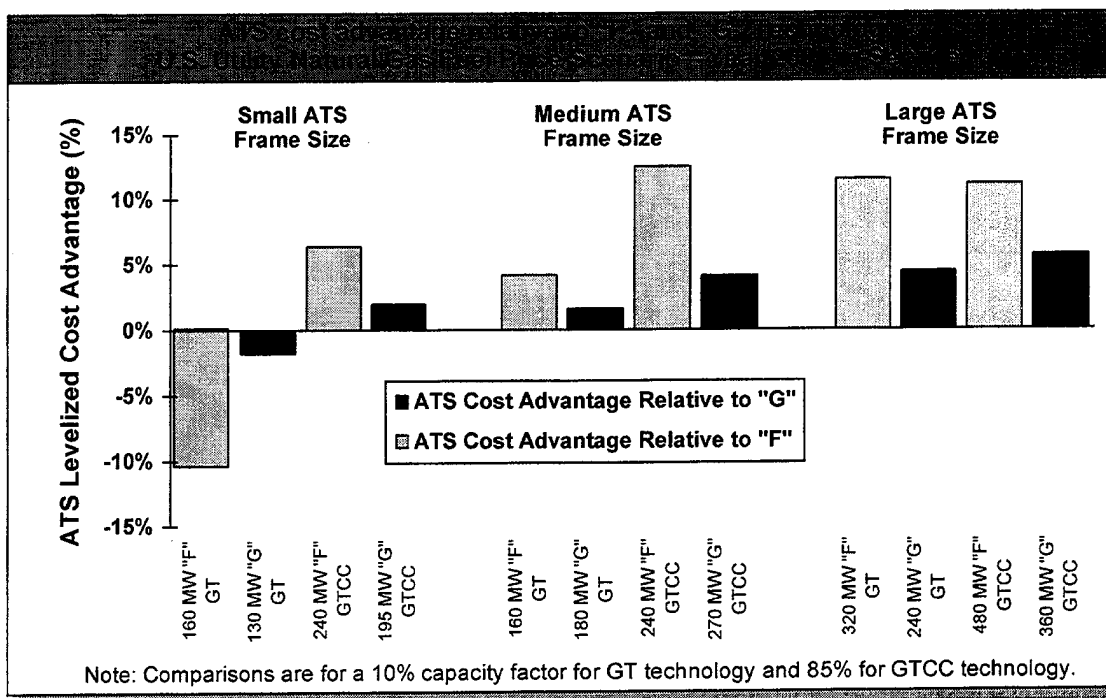


**Figure 17 ATS Cost Advantage**

The medium and large ATS frame sizes have the greatest cost advantage over both "F" and "G" technology; the small ATS frame size is less competitive.

Under the model assumptions, the medium and large ATS GTCC configurations, operating at an 85% capacity factor, are expected to have levelized electricity costs which are 4-6% lower than those of competing "G" GTCC technology, and more than 10% lower than the "F" GTCC. The small ATS GTCC is 1-5% lower in cost than the small "G" GTCC and 5-10% lower in cost than the "F" GTCC.

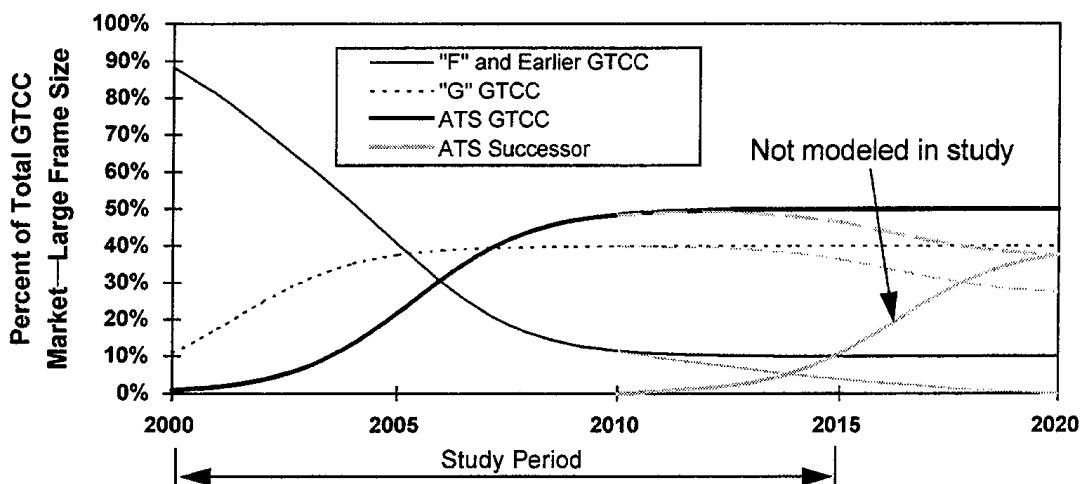
In simple cycle (10% capacity factor), the large ATS frame size enjoys a 10% cost advantage over a comparably sized plant based on "F" technology, and a 4-5% advantage over the "G" simple cycle.

The cost advantage for the medium frame size ATS GT simple cycle is only 1-2% relative to the medium frame size "G" GT and -1% to 5% relative to the "F" GT. Neither the small frame size ATS GT nor "G" GT appears competitive with the "F" simple cycle, with levelized costs 7-20% higher in peaking applications (5-10% capacity factor).

The total ATS and "G" market sizes were assumed to be functions of both ultimate market share and the rate of market penetration. For the ATS products with a 10% or greater cost advantage over "F" technology, an ultimate market penetration of 50% is expected. Where the ATS has a smaller economic advantage, a lower ultimate market share was assumed. Because of its earlier introduction the "G" will be farther along its market penetration curve when the ATS is introduced. Thus, within the forecast period of 2000-2014, the total market for "G" technology is comparable to that of the ATS, even though the

ultimate penetration of the ATS is assumed to be higher. The maximum market penetration for the ATS and "G" are expected to occur at different times. The market for "F" and previous technology makes up the remainder of the market.

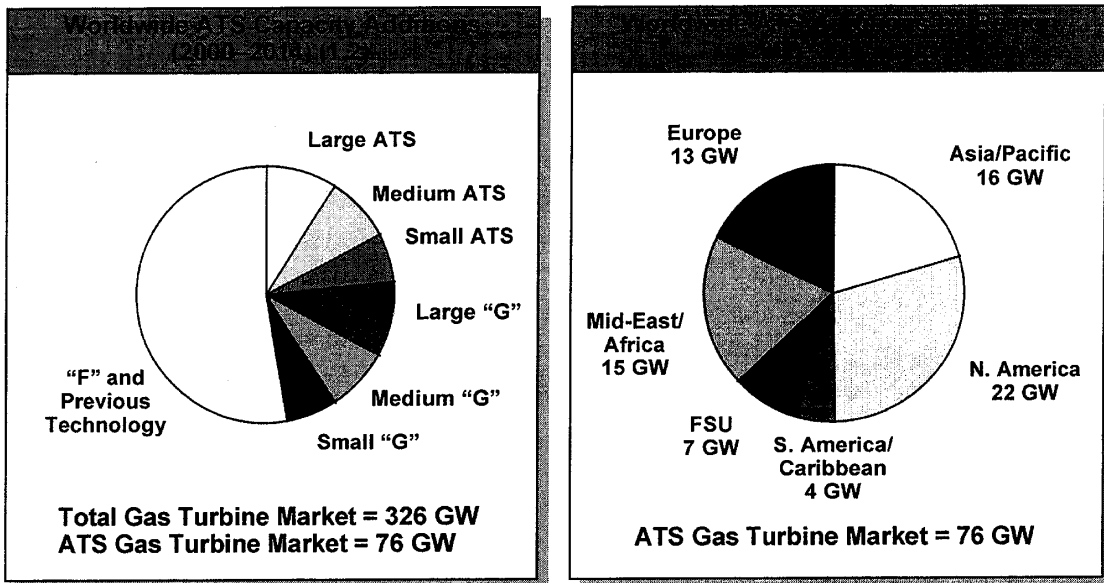
Figure 18 depicts the market dynamics and penetration.



	Estimated Maximum Market Penetration by Frame Size					
	"G" Technology			ATS Technology		
	Large	Medium	Small	Large	Medium	Small
Simple Cycle	40%	25%	10%	50%	35%	10%
Combined Cycle	40%	40%	25%	50%	50%	35%
IGCC	40%	N/A	N/A	50%	N/A	N/A

**Figure 18     ATS & "G" Technology Market Penetration**

In the baseline forecast the total ATS market potential exceeds 75,000 MW in the 2000-2014 time frame. Including the "G" as part of the ATS technology program, the market is about 155,000 MW, corresponding to half the market (see Figure 19).



- (1) Includes simple and combined cycle applications for both oil and gas. GTCC capacity is total plant capacity.
- (2) All ATS products are assumed to exist simultaneously.

**Figure 19 Estimated Worldwide ATS Capacity Additions**

Relative to "F" technology, the ATS will have a 10% or greater cost advantage in large baseload GTCC applications and a 5-10% cost advantage in medium to large peaking applications, making it a highly competitive alternative to "F" technology. Given the study's assumptions, the smallest ATS frame size does not appear to be competitive with existing "F" technology in simple cycle peaking applications due to the lower projected capital cost of the "F" GT.

North America and Asia/Pacific appear to be the most attractive geographic regions. North America will rely on gas turbines for the majority of new capacity additions in the forecast period. Asia/Pacific is expected to experience rapid growth in power generation capacity in the forecast period.

Based on the assumptions regarding size class segmentation and market penetration, the large and medium ATS frame sizes achieve the highest market shares, with the small ATS being slightly less attractive. In a sensitivity case it was concluded that the U. S. market for larger power projects may increase as a result of deregulation.

Circumstances leading to increased natural gas-based power generation could increase the demand for the ATS by up to 20,000 MW in the forecast period, and would likely favor the largest ATS frame size.

#### 2.2.6.2 IGCC Analysis

The baseline ATS IGCC forecast of 27 units (over 9 years) reflects the assumption that roughly 15% of new coal additions in the forecast period will be IGCC using F, G, or ATS technology. It is also assumed ATS technology will not be available until 2005.

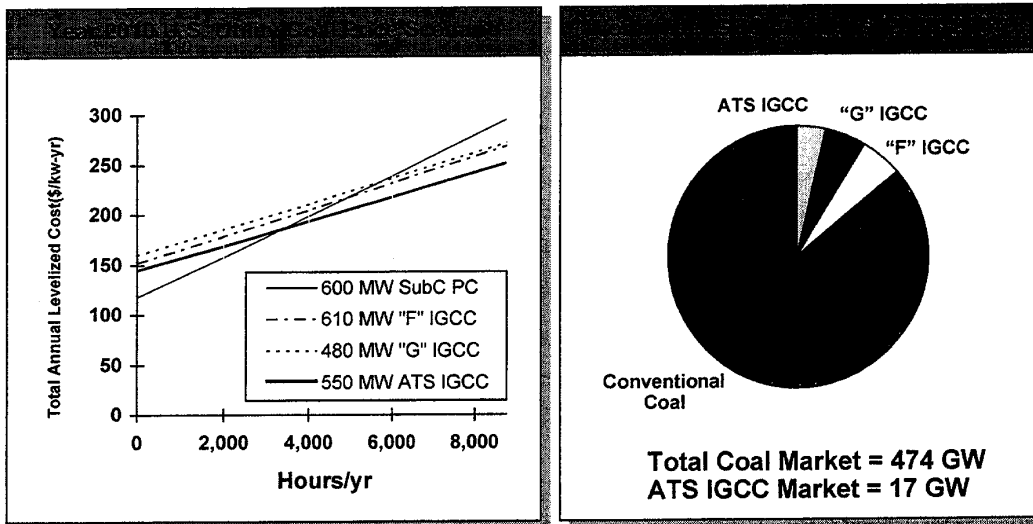


**Figure 20 Estimated ATS IGCC Market Penetration**

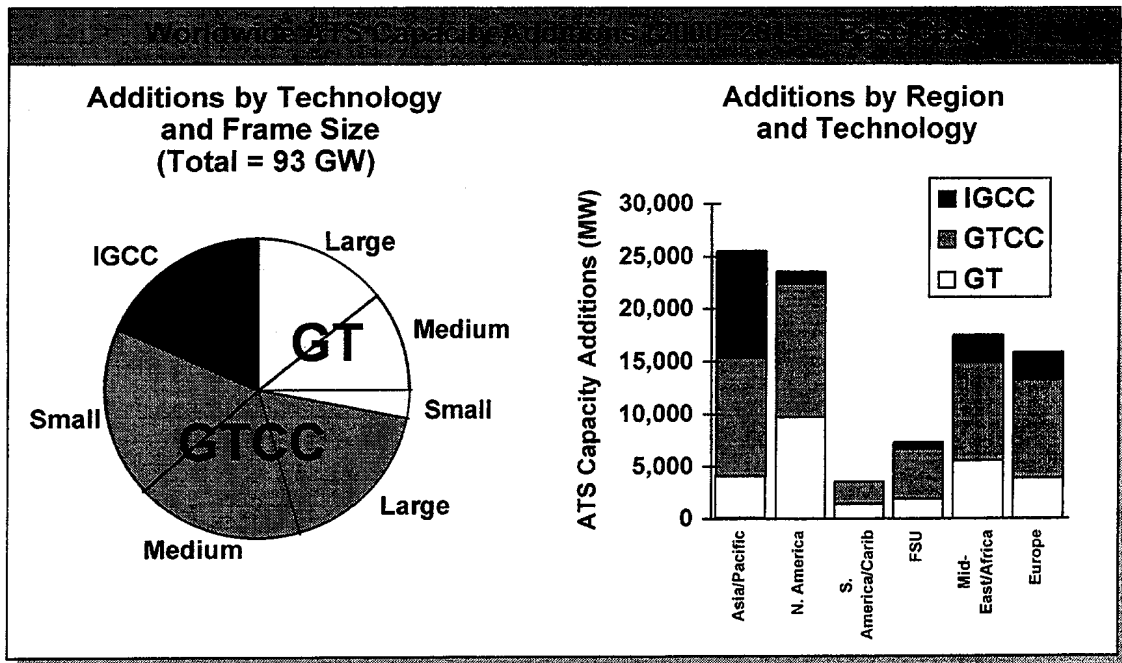
The ATS IGCC appears to become the lowest cost technology in most regions above capacity factors of 65-75%. In order for the cost advantage to become significant, capacity factors of 85-95% will be required (see Figure 20).

Total ATS IGCC market potential is limited in the forecast period by the assumption that it will not be commercially available until 2005. Nevertheless, the maximum market penetration of the ATS is higher than that of the "G" IGCC due to more favorable economics.

The 50 Hz IGCC markets are likely to develop earlier and ultimately become the largest market segment for the ATS IGCC. In an optimistic scenario, demand for the ATS grows by 50% to a total of 40 units, driven by increased market share.

### 2.2.6.3 Summary

In the baseline forecast the total ATS market potential exceeds 93 GW in the 2000-2014 time frame (see Figure 21).



Note: Values represent total plant capacity. All Frame Sizes are assumed to exist simultaneously.

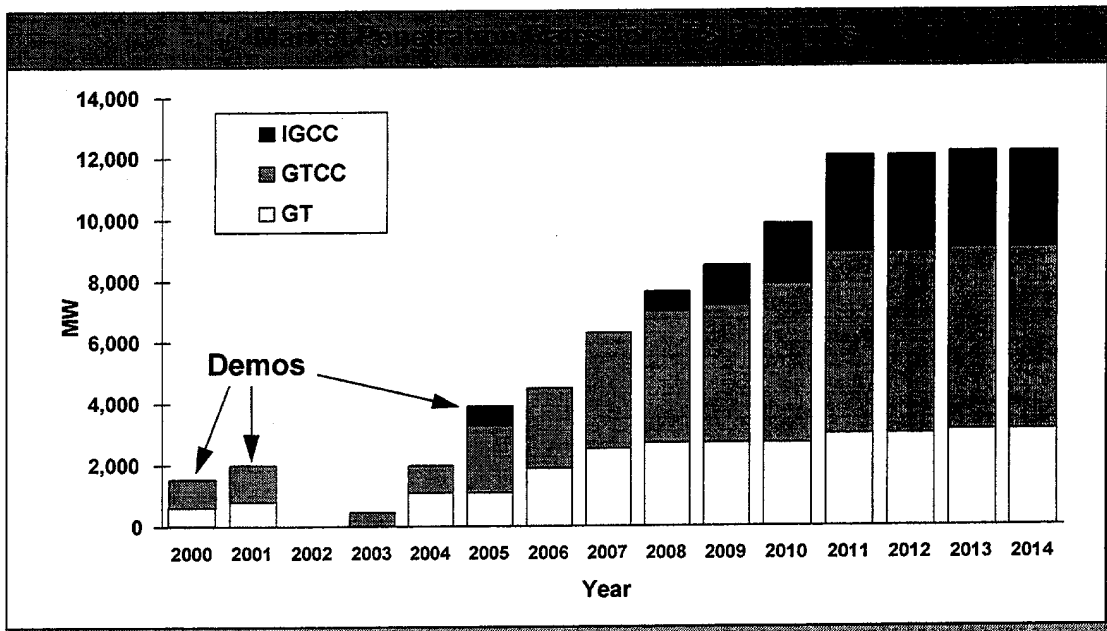
**Figure 21 Worldwide ATS Capacity Additions Summary**

The GTCC market represents the greatest opportunity for the ATS, in part because this is the application in which the ATS will likely have the greatest economic advantage. All three ATS frame sizes appear equally attractive, but uncertainties due to deregulation and the rate of infrastructure development in some regions may change this "base case" result.

In the simple cycle market, the largest potential opportunity is for the smallest frame size, but because of more attractive economics, the larger frame sizes are more likely to capture a substantial market share.

Although the total coal market is substantial, the ATS IGCC market is limited by the assumption that it does not become available until late in the forecast time period (i.e., in 2005). The greatest opportunity for IGCC technology may be beyond the year 2015.

Following one or two years of successful demonstration, the ATS market is expected to follow a typical S-shaped penetration curve (see Figure 22).



Note: All three frame sizes are assumed to exist simultaneously, each with its own demonstration projects.

**Figure 22 ATS Market Penetration by Frame Size**

The combined market for ATS-based technology could reach 12 GW per year by the end of the forecast period, representing roughly a 10% market share relative to the total global power market.

Each ATS product is expected to achieve its maximum market penetration approximately 7-10 years after initial demonstration. The ATS IGCC is expected to follow a similar penetration curve to the ATS GT and GTCC, but it will reach its ultimate market share at the end of the forecast period due to its later introduction. The ATS IGCC market is also limited by the assumed growth and size of IGCC markets in general, which limits the technical potential to a portion of the total coal market.

Finally, a comparison of the study's overall market forecast was made against both published studies and Siemens Westinghouse's internal model. Siemens Westinghouse's analysis of future overall power generation demand, the baseline forecast used by the subcontractor may be conservative. Based on combinations of higher overall power demand, coupled with a higher proportion of that demand being met by gas turbine based capacity, the volume for ATS and "G" could range higher.

## 2.2.7 Task 6.0 System Definition and Analysis

### 2.2.7.1 Introduction

A conceptual design for critical and noncritical components of the gas fired combustion turbine system was completed. The conceptual design included specifications for the flange to flange gas turbine, power plant components, and balance of plant equipment. The ATS engine used in the conceptual design is an

advanced 300 MW class combustion turbine incorporating many design features and technologies required to achieve ATS Program goals.

Design features of power plant equipment and balance of plant equipment are described. Performance parameters for these components are explained. A site arrangement and electrical single line diagrams were drafted for the conceptual plant.

ATS advanced features include design refinements in the compressor, inlet casing and scroll, combustion system, airfoil cooling, secondary flow systems, rotor and exhaust diffuser. These improved features, integrated with prudent selection of power plant and balance of plant equipment, have provided the conceptual design of a system that meets or exceeds ATS program emissions, performance, reliability-availability-maintainability, and cost goals.

### 2.2.7.2 Plant Configuration

The Advanced Turbine Systems plant conceptual design and layout is based on a recently completed combined cycle plant design. This state of the art 240 MW W501F Reference Plant incorporates flexible proven design features that minimize design changes usually required to tailor the plant to site specific constraints. The power trains of both plants include one combustion turbine and one multi-pressure steam turbine. The 240 MW Reference Plant is a multishaft design. The ATS Plant utilizes a single shaft design with a common generator between the combustion turbine and steam turbine. Both plants are fueled by natural gas and utilize mechanical draft cooling towers. The ATS plant generates considerably more power at a higher efficiency than the 240 MW Reference Plant, mainly because of the increased power and efficiency of the ATS combustion turbine and the higher throttle pressure and reheat temperatures of the steam turbine.

Overall performance parameters for the ATS plant are given in Table 5 at ISO (59°F [15°C], 14.696 psia [101.3 kPa] & 60% relative humidity) conditions.

**Table 5 Overall Performance of ATS Plant**

<b>Performance Parameters</b>	<b>ATS Plant</b>
Approximate Combustion Turbine Power	290,000 kW(e)
Approximate Steam Turbine Power	130,000 kW(e)
Approximate Plant Output	420,000 kW(e)
Net Plant Efficiency, LHV	>60%
Fuel Type	Natural Gas
Cooling Tower	Forced Draft
Combustion Turbine Inlet Air Flow	1,196 lb/sec (542 kg/sec)
Approximate Rotor Turbine Inlet Temperature	2700°F (1482°C)
Turbine Exhaust Temperature	1130°F (610°C)

### 2.2.7.2.1 Combustion Turbine

The combustion turbine of the ATS plant is larger and more efficient than the W501F model used in the 240 MW Reference Plant because of its advanced aerodynamic cooling and mechanical design, higher mass flow and firing temperature, and pressure ratio. The gas fuel is preheated, using recovered low-grade heat from the heat recovery steam generator (HRSG). Turbine airfoils are steam-cooled, using higher-grade heat recovered in the bottoming cycle. Additional details of the ATS combustion turbine are given in Section 2.2.7.3. Key combustion turbine parameters of the ATS turbine are shown in Table 5.

### 2.2.7.2.2 Heat Recovery Steam Generator

The HRSG for the ATS plant is a natural circulation, triple pressure unit with vacuum deaeration. The HRSG configuration allows the addition of duct firing at a later date. Customer requirements often dictate the need for additional steam that duct firing can provide. The duct firing option has the same performance level as the HRSG without the duct firing option in the unfired operational mode. The HRSG will operate over the entire operating range of the combustion turbine. Materials are commercial grade commonly used in boilers today. Design criteria are conventional engineering practice, applying ASME Pressure Vessel Code design guidelines. Key design parameters are given in Table 6.

**Table 6 HRSG Design Parameters**

<b>Performance Parameters</b>	<b>Value</b>
Turbine Exhaust Temperature	1130°F (610°C)
CT Exhaust Gas Flow	1,196 lb/sec (542 kg/sec)
Number HRSG Pressures	3
Deaerator Type	Vacuum
Approximate HRSG Duty	1,050 MBtu/hr (1.136 x 10 <sup>6</sup> kJ/hr)
HRSG Exhaust Temperature	207.9°F (97.7°C)

### 2.2.7.2.3 Fuel Gas Heater

Natural gas entering the ATS plant is heated to 800°F (427°C) before entering the combustion turbine. This fuel pre-heating is done in two stages: heating with feedwater and heating with CT exhaust. The thermal performance data for the fuel gas heater is tabulated in Table 7.

**Table 7 Fuel Gas Heater Performance Data**

<b>HEATING FLUID</b>	<b>Feedwater</b>	<b>HRSG Gas</b>
Approximate methane flow	1.21 x 10 <sup>5</sup> lb/hr (5.49 x 10 <sup>4</sup> kg/h)	1.21 x 10 <sup>5</sup> lb/hr (5.49 x 10 <sup>4</sup> kg/h)
Methane inlet temp	59°F (15°C)	204.3°F (95.7°C)
Methane exit temp	204.3°F (95.7°C)	800°F (427°C)
Methane pressure	500 psia (3.44 MPa)	500 psia (3.44 MPa)
Approximate Water/gas flow	7.5 x 10 <sup>4</sup> lb/h (3.4 x 10 <sup>4</sup> kg/h)	4.5 x 10 <sup>6</sup> lb/h (2.04 x 10 <sup>6</sup> kg/h)
Water/gas inlet temp	271.8°F (133°C)	941.2°F (505°C)
Water/gas exit temp	147.4°F (64°C)	903°F (484°C)
Water/gas pressure	800 psia (5.52 MPa)	15 psia (0.1 MPa)
Heat duty (Q)	9.3 MBtu/h	47.5 MBtu/h
Mean Temp Diff. (MTD)	77.5°F (43°C)	349°F (194°C)
Approximate Conductance (UA)	1.2 x 10 <sup>5</sup> Btu/hr- °F (2.28 x 10 <sup>5</sup> kJ/h - °C)	1.36 x 10 <sup>5</sup> Btu/hr- °F (2.58 x 10 <sup>5</sup> kJ/h - °C)

#### 2.2.7.2.4 Steam Piping

The main steam piping transfers high-pressure throttle steam from the superheater to the HP turbine inlet. The exhaust from the HP turbine is combined with slightly superheated IP steam from the HRSG, reheated in the steam-cooled stators of the ATS combustion turbine, then piped to the inlet of the IP steam turbine. Low-pressure steam piping carries induction steam from the LP superheater to the IP/LP crossover piping.

Piping design, size selection and wall thickness is based upon ASME B31.1. Pipe sizing remains the same, regardless of duct firing option. Only the wall thickness varies. This philosophy keeps the piping layout and hanger design constant.

The design parameters for the steam piping are listed in Table 8.

**Table 8 Steam Piping Design Parameters**

Line Identifier	Main Steam	Cold Reheat	IP Induction	Hot Reheat	LP Induction
From	HP Superheater	HP Steam Turbine	IP Superheater	ATS Cooled Stators	LP Superheater
To	HP Steam Turbine	ATS Cooled Stators	ATS Cooled Stators	IP Steam Turbine	IP/LP Crossover
Line Size	16 inches (406.4 mm)	20 inches (508 mm)	6 inches (152.4 mm)	24 inches (609.6 mm)	14 inches (355.6 mm)
Wall Thickness	1.75 inches (44.5 mm)	0.75 inches (19.1 mm)	0.375 inches (9.5 mm)	0.875 inches (22.2 mm)	0.375 inches (9.5 mm)
Flow	615,967 lb/hr (299,397 kg/h)	610,707 lb/hr (277,023 kg/h)	55,543 lb/hr (25,194 kg/h)	666,250 lb/hr (302,205 kg/h)	67,032 lb/hr (30,405 kg/h)

#### 2.2.7.2.5 Steam Turbine

The steam turbine cycle for the ATS plant utilizes a single reheat cycle. The steam turbine exhaust flow of the ATS plant necessitates the use of a double-flow LP exhaust. Operational design parameters include up to 50 starts per year and 8000 hours per year base load operation. Table 9 shows the primary steam turbine performance parameters.

**Table 9 Steam Turbine Performance Parameters**

Performance Parameters	Value
Approximate S/T Power	130,000 kW(e)
Approximate S/T Throttle Flow	616,000 lb/hr (279,412 kg/hr)
Approximate S/T Throttle Temperature	1050 °F (566°C)
Approximate S/T Throttle Pressure	1,800 psig (12.4 MPa)
S/T Exhaust Flow Type	Double Flow
Number Reheat Passes	1

#### 2.2.7.2.6 Generator-Exciter

The combustion turbine and steam turbine are on a single shaft. Both turbines share a common hydrogen cooled generator. Generator design will be conventional design. Dimensions for the generator are:

- length of generator and exciter is 611 inches (15.52 m), with a width of 174 inches (4.42 m)
- height above foundation is 137 inches (3.5 m)
- depth below foundation is 40 inches (1.02 m)

### 2.2.7.2.7 Condenser/Cooling Tower

The ATS plant steam turbine requires a double flow back end. For design convenience, a side entry saddlebag condenser was modeled rather than a conventional vertical type. The saddlebag condenser imposes a lower height and shorter overall length requirement on the building. A tabular listing of performance parameters for the condenser and cooling tower is shown in Table 10.

**Table 10 Condenser Performance Parameters**

<b>Performance Parameters</b>	<b>ATS Plant</b>
S/T Exhaust Flow Type	Double Flow
Condenser Duty	700.4 MBtu/hr (739 x 10 <sup>6</sup> kJ/hr)
Cooling Tower Type	Mechanical Draft
Cooling Tower Cells at Design	8 Cells

### 2.2.7.2.8 Site Arrangement

The arrangement of generation equipment and peripheral equipment needed at the plant site is shown in the Site Arrangement drawing. Peripheral balance-of-plant equipment includes:

- An 8-cell cooling tower
- A 1.8-million-gallon (6.81 x 10<sup>6</sup> liter) (3-day supply) fuel storage tank
- A 1.5-million-gallon (5.68 x 10<sup>6</sup> liter) (3-day supply) condensate storage tank
- A 1.5-million-gallon (5.68 x 10<sup>6</sup> liter) (3-day supply) demineralized water storage tank
- Provisions for other optional equipment

The footprint of the plant measures 828 ft. by 682 ft. (252.4 m by 208 m). The ATS Plant layout is also shown in the Site Isometric drawing.

### 2.2.7.2.9 Generation Equipment Layout

The layout of the generation equipment reflects the single-shaft arrangement of the HRSG, combustion turbine, generator, and steam turbine. The low-pressure steam turbine is flanked by twin side-entry saddlebag condensers.

### 2.2.7.3 ATS Engine Conceptual Design

A conceptual design was carried out to define the preliminary configuration of the ATS engine (see Figure 23). The ATS engine is an advanced 300 MW class design incorporating many proven design features used in previous Siemens Westinghouse gas turbines and new design features and technologies required to achieve the ATS Program goals. The compressor design philosophy is based on that used in the advanced W501G compressor. The combustion system uses

16 combustors of lean-premixed multistage design. Closed-loop steam cooling is used to cool the combustors and transitions. The four-stage turbine design is an extension of the advanced W501G turbine design, employing 3D design philosophy and advanced viscous analysis codes. To further enhance ATS plant efficiency, the turbine airfoils are closed-loop cooled.

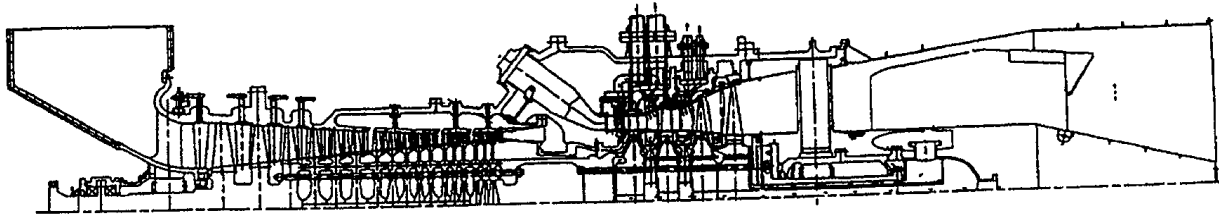


**Figure 23 Cross Section of ATS Engine**

#### 2.2.7.3.1 Inlet

The compressor inlet is through side entry. The inlet casing, incorporating the front engine supports, is the scroll bellmouth type. The bellmouth surface profile is generated with the aid of a 3D viscous code to ensure optimum surface velocity distributions, and hence minimum inlet losses. The flow path surfaces of the inlet casing, which is a nodular iron casting, are coated with a ceramic coating to provide a smooth surface finish and, and therefore, further reduce the inlet losses and improve the velocity profile into the compressor.

#### 2.2.7.3.2 Compressor

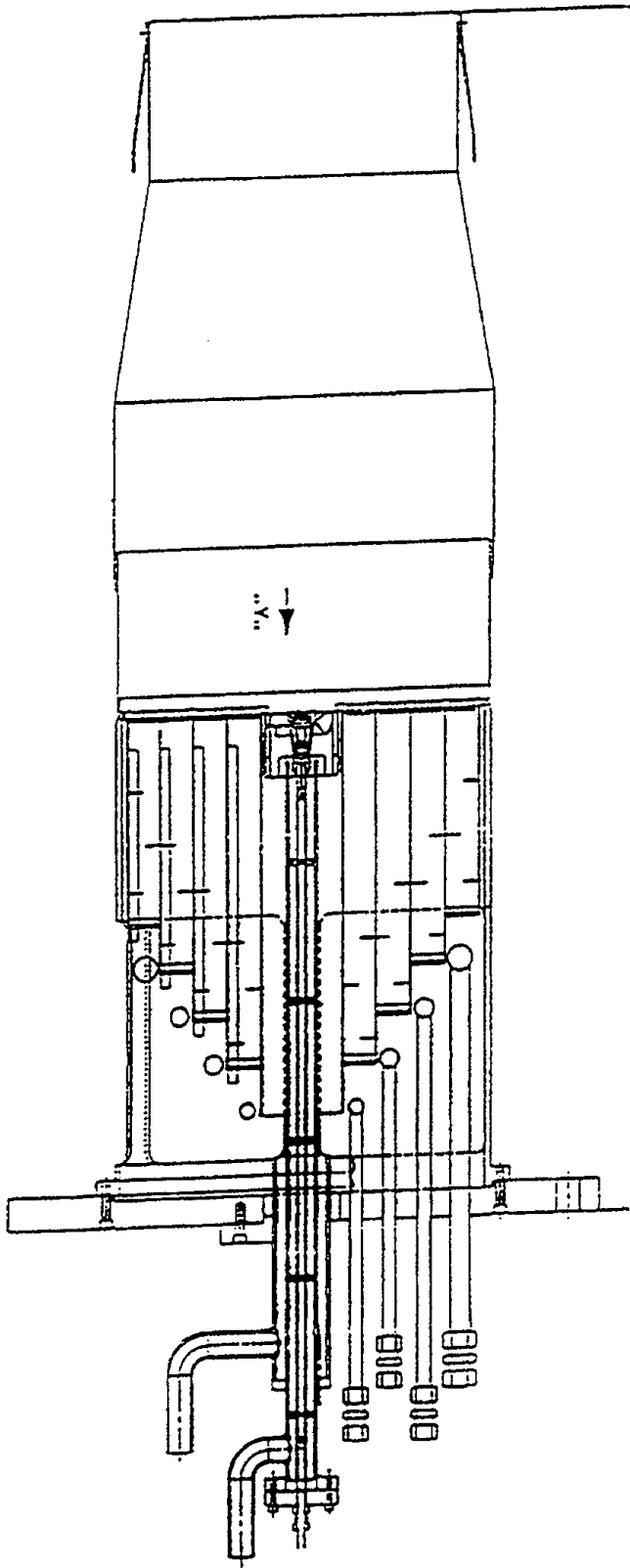
The ATS compressor design pressure ratio is 25:1. The design philosophy is based on that used in the advanced W501G compressor, but with additional design enhancements such as the incorporation of brush seals to minimize leakage under the stator shrouds. Advanced aerodynamic design tools and controlled diffusion design process are employed in order to minimize loss and maximize airfoil loading. In addition, airfoil thickness is reduced to the minimum allowable from mechanical considerations to reduce diffusion and shock losses. Abradable coatings are applied to the outer shroud to minimize blade tip clearances. As a result of the 25:1 pressure ratio, variable stators are incorporated in the front stages to improve starting and part-load operation.

The front- and middle-stage compressor discs are made of conventional material forgings. Due to the increased compressor exit air temperature in the ATS application Ni-based alloy disc material is used in the back stages. The compressor rotor is joined to the turbine rotor through a torque tube. The front part of the compressor cylinder, which is horizontally split (as are all the other engine cylinders), is made of cast steel. Blade rings, which are intermediate cylinders, are used in the back end to minimize eccentricity and hence blade tip clearances. The blade rings are made of 2-1/2% Cr-1% Mo low alloy steel. The compressor blades, which are attached to the discs by a dove tail root design, are made of 17-4 PH and 12% Cr steels. The stators are made of similar material as the blades and all, except for the variable stators, are fabricated into diaphragms.

### 2.2.7.3.3 Combustion System

The combustion system incorporates 16 can-annular combustors of lean-premixed multistage design with catalytic components as necessary to meet emissions requirements and ensure good stability. Figure 24 shows the multi-annular swirl ultra low NO<sub>x</sub> combustor, which is one of the candidate combustors for the ATS engine. To obtain less than 10 ppmvd NO<sub>x</sub> emissions, nearly all of the compressor delivery air must be premixed with the fuel. Therefore, closed-loop steam cooling is used to cool the combustors and transitions, which duct the hot combustion gases into the turbine. The cooling stream is supplied and extracted through manifolds located on the stage 1 and 2 turbine blade ring.

Conventional Ni-based sheet materials are used in the manufacture of the combustors and transitions.



VIEW ON "A"

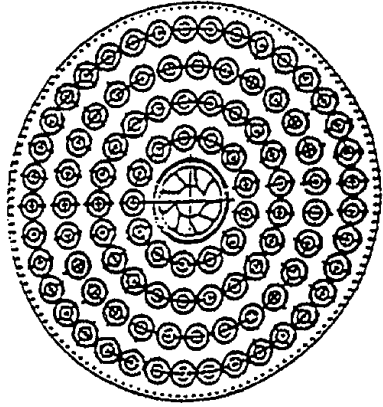


Figure 24 Multi-annular Swirl Combustor

#### 2.2.7.3.4 Turbine

The ATS turbine is an extension of the advanced four-stage turbine designed for the W501G engine. The W501G turbine efficiency was increased over that of W501F by applying 3D design philosophy and advanced viscous analysis codes. The airfoil loadings were increased above previous levels to optimize airfoil efficiency while minimizing airfoil solidity. The reduced airfoil solidity resulted in reduced cooling requirements and enhanced plant efficiency. The ATS turbine design incorporates the following additional enhancements: closed-loop cooling of vanes and blades, blade tip clearance control on the first two stages, and airfoil clocking (optimum circumferential alignment of airfoils in downstream stage with respect to those in the upstream stage).

To improve plant efficiency closed-loop steam cooling (CLSC) is used to cool some turbine airfoils. The heat capacity of steam is almost double that of air. Less steam than air is thus required to cool the turbine components. The major benefit of CLSC is the elimination of cooling air ejection into the flow path. This results in an increase in gas temperatures downstream of the first-stage vane and hence an increase in gas energy level during the expansion process. A secondary benefit is the elimination of mixing losses associated with cooling air ejection into the gas path. The combination of the above effects results in a significant increase in ATS plant efficiency. In addition, the NO<sub>x</sub> emissions are reduced because more air is available for lean-premix combustor at the same burner outlet temperature.

Achieving acceptable blade metal temperatures in a closed-loop cooling design is a challenge due to the absence of cooling air film to shield the turbine airfoil and shroud wall, and no shower-head or trailing edge ejection to provide enhanced cooling in the critical leading and trailing edge regions. To produce an optimized closed-loop cooling design, the following approaches are utilized: (1) airfoil aerodynamic design tailored to provide minimum gas side heat transfer coefficients, (2) minimum coolant inlet temperature, (3) thermal barrier coating applied on airfoil and end wall surfaces to reduce heat input, (4) maximized cold side surface area, (5) turbulators to enhance cold side heat transfer coefficients, and (6) minimum outside wall thickness to reduce wall temperature gradients and hence the internal heat transfer coefficients required to cool the airfoil.

The shell/spar cooling concept will be considered for cooling stage 1 vanes and blades (see Figure 25). This concept consists of a cast airfoil-shaped support structure (spar) around which a thin sheet of superalloy (shell) is diffusion bonded. The outside surface of the spar incorporates chordwise grooves that form small, closely spaced cooling channels under the shell. Thus, the shell/spar configuration achieves the desired qualities of a thin outside wall and a favorable cold-to-hot surface area ratio. The airfoil spar contains three cavities: the fore and aft cavities supply the cooling steam, and the midcavity discharges the spent cooling steam. Cooling channels extend in a chordwise direction from a supply cavity to the discharge cavity. Holes drilled through the spar connect the cooling channels with the cavities. The trailing edge is cooled by spanwise holes.

Recent advances in casting technology have produced cooling configurations with thin outside walls and internal cooling passages suitable for CLSC. To increase cold-side heat transfer, turbulence promoters can be incorporated in the

cooling channels. The peripheral radial cooling hole concept will also be evaluated.

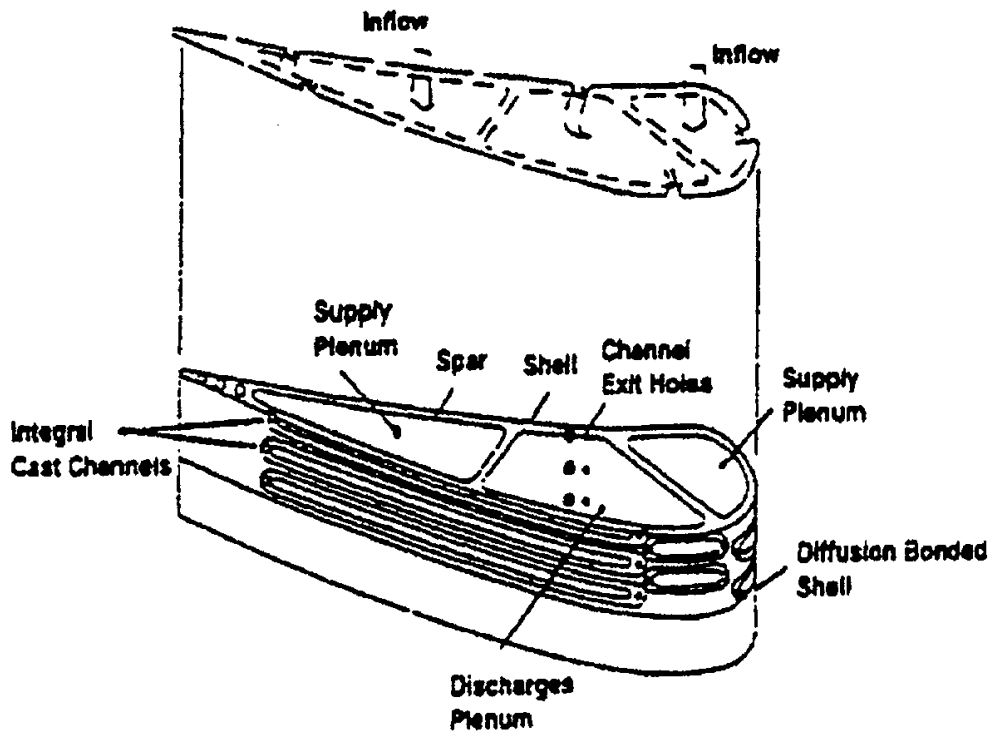


**Figure 25 Conceptual Design of Shell/Spar Vane**

The heat load on stage 2 vanes will permit steam-impingement-cooled castings to be used. Impingement cooling will be applied to the airfoil fore and aft cavities, with convection cooling via spent stream return flow in the midcavity. Heat load on the stage 2 blade will also permit a conventional serpentine cooling design. The stage 3 vane will use a serpentine cooling design. Stage 4 airfoils will be uncooled.

#### 2.2.7.3.5 Secondary Flow System

The engine secondary flow system consists of air and steam flows. These two fluids are isolated from each other and supplied to the proper locations with minimum leakage. Airflow from the compressor exit passes through the torque tube seals and cools the front face of the Row 1 turbine disc. This air is then cascaded through the rotating rotor to the stage 2 interstage region to prevent entry of hot gas in front of and behind the stage 2 vane. Air leakage is reduced by using brush seals in the critical sealing areas.

Cooling steam is supplied to the stationary parts through pipes passing through the turbine cylinder and into a circular manifold. Reheated steam is returned through a similar manifold/piping system. Pipes are connected to the manifolds by flanges with piston ring seals, which seal tightly and accommodate thermal growth. The system is designed to provide parallel cooling steam flow to stage 1, 2, and 3 vanes.

The steam flow system for the rotating blades consists of an inlet manifold at the turbine end of the rotor shaft; a rotating axial annular passage inside the rotor shaft that conducts steam from the manifold area to the discs; a series of holes and slots in the rotor discs to supply steam from the rotating passage to the roots of the cooled blades; another series of holes and slots in the discs to carry the reheated steam from the blades to a hole in the center of the rotor discs; and finally, a steam exhaust from this center bore into a plenum at the rotor stub end.

#### 2.2.7.3.6 Rotor System

The turbine rotor is constructed from a series of individual turbine discs, spacer discs, and a stub shaft attached by a single set of spindle bolts and weldments. The turbine discs are of conventional design, except for a rotor bore used as a steam passage and the additional downstream blade groove sealing hardware. Ni-based components are used, as required, to cater to the exhaust steam temperature.

#### 2.2.7.3.7 Exhaust Diffuser

The ATS engine has an axial exhaust diffuser similar to that used in previous Siemens Westinghouse designs. It consists of the exhaust cylinder and an exhaust manifold. The exhaust cylinder carries the hot end journal bearing, which is contained in the front part of the inner tailcone. This portion of the tailcone is supported by tangential or radial struts. This strut system allows for thermal expansion without changing the bearing centerline location. The struts are protected from the hot gases by airfoil type shielding. The exhaust manifold has two access ports for lube oil, seal air, and steam piping. One of the ports has provision for accessing the hot end bearing. The materials used in the exhaust are Ni-based sheet metal.

### 2.2.8 Task 7.0 Integrated Program Plan

The Integrated Program Plan described the research and development program that, when completed, will lead to the commercialization of an ATS system meeting program goals.

#### 2.2.8.1 R&D Plans for Critical Components/Barrier Issues

In order to achieve higher operating temperatures ( $\geq 2650^{\circ}\text{F}$  [ $\geq 1454^{\circ}\text{C}$ ]) in gas turbines, advancements in materials capabilities need to be developed. Siemens Westinghouse has several material development programs in place and has identified, in addition to these, thermal barrier and corrosion resistant coatings, and ceramics as critical developments needed to make significant advancements in operating temperatures.

Critical components/technologies and barrier issues were identified after the analyses of Task 3 had been performed and trade-off studies conducted for both the potential cycle and high temperature developments. Selected R&D programs were developed for each of these components/technologies and barrier issues. The R&D plans described all the work necessary to develop and prove that the hardware, equipment, material and/or system was capable of operating at the design conditions of the proposed ATS. The schedule and costs associated with each of these programs were developed as well. Preliminary test plans for each

of the development programs were included. The detailed test plans for each program were prepared as part of Task 8. A discussion of schedule risk and risk abatement with respect to the projected success of each program was presented.

#### 2.2.8.2 Full Scale GFATS Demonstration Plan

An Integrated Program Plan was prepared by Siemens Westinghouse. The Plan described all the work necessary to take the selected ATS from conceptual design to commercialization by the year 2000. Included in the plan was all the research, development and demonstrations needed to accomplish programs goals. The integrated plan consisted of a series of plans, as follows:

- R&D plans for critical components and barrier issues,
- Detailed design/specification plans for the gas turbine, power plant and balance of plant equipment.
- Manufacturing/procurement plan for the gas turbine, power plant and balance of plant equipment.
- Overall demonstration plant A&E design plan that included mechanical, civil and structural, and electrical design as well as balance of plant and overall plant controls.
- Site selection/permitting/financing plan.
- Plant construction plan.
- Start-up and test plan.
- Commercial demonstration plan which included analysis of operating costs and verification of plant hardware condition at first inspection interval.

A comprehensive schedule was prepared, along with the associated costs for all activities necessary for full scale demonstration and verification of program goals.

### 2.2.9 Task 8.0 Design and Test of Critical Components

#### 2.2.9.1 Background

New technologies must be developed and existing technologies extrapolated beyond the state-of-the-art in order to achieve the challenging ATS Program performance and emissions goals. A considerable improvement in gas turbine engine performance is necessary to achieve the required plant efficiency level. The engine performance enhancement requires improvements in firing temperature, aerodynamic design, cooling design, and in sealing. All of the above need technological development and innovation. In this section, the component development required to make ATS a reality is discussed. It is known that higher firing temperature operation necessitates developments in technologies related to improved materials, such as directionally solidified and single crystal airfoils, improved coatings, such as TBC, improved

corrosion/oxidation protection coatings, and improved or novel cooling schemes. Technological developments are needed in the flow visualization, optical diagnostics, combustion noise, and catalytic combustion fields to reduce combustion emissions at the higher firing temperatures required for the ATS engine. An active blade tip clearance control system and brush seal technology will be incorporated in the appropriate locations in the compressor and the turbine to improve the turbine efficiency. A brief review of the state-of-the-art is presented. This is followed by a discussion of results from the individual component development projects completed in Task 8 of the ATS Phase 2 program.

A strategy was developed to achieve the ATS Program plant cycle efficiency target of greater than 60%. The foundation of this strategy is based on the advanced combined cycle concept, which incorporates an advanced engine design, as well as improvements in the bottoming cycle and the generator. The selection of this cycle was based on performance criteria, including overall plant efficiency, cost of electricity, practicability, reliability-availability-maintainability, and the time frame of the ATS Program. Some of the options considered in the ATS cycle evaluation, such as recuperation, reheat, and thermochemical recuperation, had potentially higher plant cycle efficiency, compared to the advanced combined cycle concept. However, they were not selected for further development due to a low ranking in one of the performance criteria.

The primary contributor to achieving the ATS Program objectives is an advanced gas turbine design, with the enhanced bottoming cycle and high efficiency generator playing a minor role. The new components and technologies developed in this program have advanced the state-of-the-art for gas turbine design to a new plateau. There is also a synergism with gas turbine designs in other applications, such that benefits derived from the ATS Program can enhance the performance of gas turbines designed for use in aero, marine, pipeline and industrial applications.

#### 2.2.9.2 Technology Improvements

When the ATS project started, the current Siemens Westinghouse production engine, the W501F, represented the latest step change in engine performance. The output power is 160 MW. The simple cycle efficiency is about 36%. In a combined cycle application, the efficiency exceeds 54%. This performance level was achieved by increasing firing temperature approximately 200°F (111°C) over the previous commercial engine design, advanced aerodynamic design of both the compressor and the turbine, enhanced cooling design of hot end components, and improved materials.

In 1994, Siemens Westinghouse introduced its latest engine model, the W501G. The W501G possesses an output power of about 230 MW and a net combined cycle efficiency of about 58%. The large improvement in efficiency results from an additional 250°F (139°C) increase in firing temperature and advancements in aerodynamic design, cooling design, and hot end materials.

The ATS engine will represent a larger step in the development cycle than previous improvements. Additional simultaneous advances in aerodynamic design, heat transfer, and materials technologies are necessary to achieve the

required improvement in efficiency of greater than 60%. The following improvements were targeted to ensure the efficiency goal was achieved:

#### 2.2.9.2.1 Turbine Improvements

- Advanced aero/heat transfer/materials technology
- Burner outlet temperature (BOT) > 2730°F (1499°C)
- Closed-loop steam cooling
- Single crystal and directionally solidified airfoils
- Improved thermal barrier and anti-corrosion coatings
- Ceramic ring segments
- Active tip clearance control
- Brush seals
- Reduced compressor dump/combustor loss
- Increased Row 4 blade exit area

#### 2.2.9.2.2 Plant Improvements

- Reduced inlet/exhaust losses
- Fuel preheating
- Single shaft: Combustion Turbine - Generator - Steam Turbine
- Advanced steam turbine design technology
- 1800 psi (12.4 MPa), 1050°F/1050°F (566°C/566°C) steam cycle

State-of-the-art aerodynamic, heat transfer and materials technologies are deployed in the design of the ATS engine. The burner outlet temperature is between 2730°F and 2800°F (1499°C and 1538°C). This temperature range allows a high cycle efficiency, but is still low enough to attain emissions goals. Catalytically enhanced combustor components have been employed to attain low NO<sub>x</sub> emissions at the high burner outlet temperatures.

Closed-loop steam cooling will be employed on hot end components (i.e., transitions, Rows 1 to 3 vanes, Rows 1 and 2 blades, and some of the blade rings) to optimize plant cycle efficiency. Single crystal casting technology is deployed on Rows 1 to 3 blades and directionally solidified casting technology on Row 1 vane. Improved or advanced alloys are used in these castings. Improved thermal barrier and anti corrosion/oxidation coatings are applied to the turbine airfoils to allow long term operation at surface metal temperatures approaching 1800°F (982°C).

Active tip clearance control was developed for Rows 1 and 2 turbine blades, to reduce blade tip leakage losses. Better blade tip control improves efficiency and significantly reduces turbine performance deterioration with increasing operating time. Blade tip clearance is held to smaller gaps because of fewer tip rubs, reducing losses. Brush seals are installed in the appropriate locations in the turbine and compressor to reduce leakage, as well as hot gas ingestion into turbine disc cavities.

Design changes initiated by flow tests on a model of a combustion cylinder and the elimination of showerhead cooling on turbine airfoils can reduce compressor exit dump losses and the combustor pressure losses significantly. Row 4 turbine exit area will be increased by about 12% compared to that of the latest design to reduce the turbine exhaust diffuser losses.

Improvements were made in the plant design to attain the overall efficiency objective. Inlet and exhaust systems were designed to minimize duct losses without incurring excessive costs. Fuel preheating was employed to recover exhaust heat. The single shaft concept was used, with the gas turbine, the generator and the steam turbine connected together. A high efficiency generator will be designed specifically for the ATS plant. Advanced aerodynamic design technology is applied to the steam turbine design to optimize its efficiency. A three-pressure level steam cycle, with 1800 psi (12.4 MPa) and 1050°F (566°C) high pressure steam and 1050°F (566°C) reheat steam, is employed.

The estimated ATS plant cycle efficiency will be greater than 60% with the planned improvements in the gas turbine and plant design. An extensive development effort in all of the major gas turbine technologies is required to achieve this efficiency level. These projects are grouped under the following main headings: combustion, cooling, mechanical design, leakage control, diagnostics and materials/coatings. Listed in Table 11, these projects were started in Phase 2 to support the design and test of critical ATS components. Some of the projects were completed in Phase 2, while others were carried forward into Phase 3 of the ATS program. A foundation explaining current technology of materials, coatings, combustion, cooling, mechanical design and leakage is presented before proceeding to a discussion about each of the component development projects.

**Table 11    ATS Component Development Projects**

TECHNOLOGY	PROJECTS
I    Combustion	Flow Visualization Combustion Noise Investigation Catalytic Combustion
II    Cooling	Airfoil/Shroud Cooling Integral Shroud Cooling Serpentine Channel Cooling Closed-loop Steam Cooling
III    Mechanical Design	Last Row Turbine Blade Diffuser Design High Efficiency Compressor
IV    Leakage Control	Active Tip Clearance Control Brush Seals

V	Materials/Coatings	Directionally Solidified Castings Single Crystal Castings Thermal Barrier Coatings Ceramic Components
VI	Diagnostics	Blade Vibration Monitor Optical Diagnostics Probe

### 2.2.9.3 Importance of Materials

Materials and related manufacturing technologies play a critical role in achieving the efficiency goals of the ATS program. Theoretically, there are two approaches to increase the turbine efficiency. In the first approach, the efficiency can be increased partly by improving cooling technology, thus using less cooling air to achieve the same amount of temperature reduction required to maintain the component temperatures within the capability of the materials. However, increasing cooling efficiency alone is not sufficient. The second approach is to utilize materials that have higher temperature capabilities, so that components can operate reliably at higher temperatures with reduced cooling air usage. It is only by the contribution of improved cooling technology and advanced materials combined that maximum efficiency increase can be realized. Materials with higher temperature capabilities and advanced cooling provisions will be key contributors toward meeting the ATS efficiency goals.

The high performance of the W501G engine can claim part of its heritage from the ATS program. Specifically, the W501G engine incorporates:

- Thermal barrier coatings with improved reliability
- Directionally solidified airfoils
- Enhanced airfoil cooling design
- Reduced leakage (brush seals)

#### 2.2.9.3.1 General Material Requirements

Hot section components for land based turbines typically require materials with superior mechanical properties and good corrosion/oxidation resistance at elevated temperatures. Conventional Ni- and Co-based superalloys, which are extensively used in the current land based turbines, were considered. In addition, the protection of hot section components by oxidation/corrosion resistant coatings and thermal barrier coatings (TBC) has become a necessity.

Advanced materials, such as single crystal (SC) and directionally solidified (DS) alloys, which have been developed for aeroderivative engines with proven service experience, were evaluated for large land-based turbine applications. Furthermore, the higher firing temperature of ATS warrants the evaluation of emerging materials, such as ceramic materials and intermetallic materials for future ATS plants. These materials have emerged from their development stage to become viable engineering materials ready to be evaluated for implementation in land-based turbines. Understandably, the development risk associated with these relatively new materials will be higher than that of the metallic alternatives.

But, the potential benefits offered by these emerging materials in efficiency improvement and emission reduction are commensurably compelling. Therefore, in the future, advantage will be taken of the high temperature capabilities of these two emerging materials and they will be evaluated for implementation in the ATS turbine. More detailed analysis and the rationale for the material selection for the major components are discussed in the following paragraphs.

#### 2.2.9.3.2 Gas Turbine Disc Materials

Turbine disc materials are critical, because they are subjected to high centrifugal stresses resulting from the load applied by the blades which are attached to the rim. The requirements for the disc materials include strength, ductility, toughness, resistance to embrittlement, and resistance to corrosion.

High strength, low alloy steels are common for disc applications in the land based turbine industry, although nickel-based superalloys, such as IN-706, have been used by some manufacturers in recent turbine designs. High strength, low alloy steel discs are used in the turbine section of the W501F turbine, which has a rotor inlet temperature of about 2300°F (1260°C) through the use of the cooling air to minimize in-service temper embrittlement and to assure long-term reliability of these discs.

Superalloys have superior strength at elevated temperatures compared to low alloy steels. Therefore, they can be used at higher service temperatures with reduced or eliminated cooling air, thus allowing improved turbine efficiency. Candidate disc materials under consideration are Discalloy (an iron-based superalloy similar to A286), IN-901, IN-706, IN-718, Waspalloy, and Udimet 729. The last three materials are difficult to forge in large discs, using state-of-the-art forging and melting technologies, without producing segregation and/or casting defects. Such characteristics would adversely affect the reliability and service life of the discs. In the 1970s, Siemens Westinghouse evaluated Discalloy, IN-901, and IN-706 alloys for disc applications. Large forgings could be made with these alloys. Discalloy is less expensive compared to the latter two alloys, since it is an iron-based alloy, whereas IN-901 and IN-706 are nickel-based alloys. Large Discalloy discs have been implemented successfully in the Siemens Westinghouse W101, W191, and W301 gas turbines, and accumulating extensive field experience. During the mid-1980's, Siemens Westinghouse in collaboration with a forging supplier, successfully produced a full size IN-706 rotor forging for the EPRI sponsored Superconducting Generator Program. Welding and machining techniques for IN 706 were also developed in this program for the fabrication of the large rotor assembly.

Low alloy steels will be considered for ATS turbine discs because of their low cost and extensive design and manufacturing experience developed in the past decades. However, with the increased RIT in the ATS, there is a strong possibility that the disc temperature may increase to a level which would exceed the strength capability of low alloy steels. In that case, superalloys will be needed in order to meet the more demanding ATS disc design requirement. Upon the completion of a detailed design analysis, a superalloy material will be selected, design data generated and forging and other necessary manufacturing processes developed.

### 2.2.9.3.3 Combustion System Materials

The combustion system components include baskets and transitions. Inside a combustor basket, fuel and air are mixed and burned to produce hot gases. The hot gases are then directed through a transition section, then onward to the first stage vanes. Baskets and transitions are subjected to low stresses due to their static condition. The key material requirements for these components are creep strength, LCF strength, corrosion/oxidation resistance, thermal fatigue resistance and ease of fabrication.

Sheet metal Ni- and Co-based alloys are the most common choice of materials for these applications by turbine manufacturers. These alloys include Hastelloy X, IN-617, Hayne 230, Nimonic 75, Nimonic 86 and Haynes 188. Siemens Westinghouse has satisfactory experience using Ni-based superalloys in the baskets and transitions. However, with the recent increase in firing temperatures in the latest turbine models, the use of TBC coatings has become mandatory to avoid distress due to excessive steady-state and transient temperatures. For the ATS combustor basket and transition applications, the current Ni-based alloys with corrosion/oxidation coatings and TBC coating are considered as the baseline design.

However, combustors and transitions appear to be ideal for ceramic application because of its chemical stability at high temperatures. Modern monolithic ceramic materials provide higher strength, better creep resistance and far better reliability than those of a few years ago. The addition of high strength continuous ceramic fibers woven into a two or three dimensional preform in a ceramic matrix makes the composite system even tougher and more strain tolerant than monolithic ceramics. These ceramic matrix composites (CMCs) are already in use in military aircraft engines as afterburner flame holders and exhaust nozzles. Experience gained through the development of these components has resulted in the improvement of materials, design and manufacturing methods.

The use of ceramic materials can benefit future ATS design in two important areas-increasing efficiency through less cooling medium usage, and reducing NO<sub>x</sub> emissions due to more uniform combustor temperature distributions. Therefore, the design of combustors and transitions with ceramic materials was pursued as a more favorable option, although the risk will be higher than that of the metallic counterpart. A design of ATS ring segments with ceramic matrix composites was undertaken. A two layer ceramic laminate was evaluated, having an outer structural layer and an inner, thermally insulating layer. The experience gained from the development of the ring segments serves as a stepping-stone toward the design of the larger and more complex ceramic combustors and transitions.

### 2.2.9.3.4 Gas Turbine Vane Materials

Turbine vanes primarily serve the function of directing the flow of hot gasses towards rotating blades. The design requirements imposed on the vanes are not as stringent as on the rotating blades due to their static nature. However, the vanes are subjected to gas temperatures higher than the rotating blades in the same row. Therefore, resistance to corrosion/oxidation, creep, low cycle fatigue

(LCF) and thermal fatigue are the most desired properties for vane alloys. Weldability, both for fabrication and repair, is also an important factor.

The land based turbine vanes are typically made of Ni-based or Co-based alloys using a conventional casting process (CC). The use of DS or SC vanes has not been introduced in land based turbines to date. In general, Co-based alloys exhibit superior weldability and hot corrosion resistance due to their higher Cr contents. Siemens Westinghouse has been using Co-based alloys, such as X-45, since the mid-1960s, and has switched to a Siemens Westinghouse patented alloy, ECY-768, since the 1970s. ECY-768 is a Co-Cr-Ni-W alloy, which exhibits significantly higher creep strength than X-45. Co-based alloys, such as ECY-768, in combination with more efficient cooling schemes and the use of oxidation/corrosion coatings and thermal barrier coatings, were considered for the ATS vane application.

In addition to the Co-based alloys, Ni-based alloys were considered. Ni-based alloys, in general, are inferior to Co-based alloys in hot corrosion resistance and they are more difficult to weld. However, Ni-based alloys have stronger creep strength than Co-based alloys in the CC condition. Furthermore, Ni-based alloys can be cast in the DS condition, which typically shows 5 to 8 times improvement in LCF life and also an increase in creep temperature capability as compared to the corresponding alloys in the CC condition. Co-based alloys are not used in the DS condition. IN-939 and IN-738 alloys, which contain high Cr for corrosion resistance and are widely used by European turbine manufacturers, were considered for use in these vanes. CM247LC in DS condition were also be considered. Due to the higher firing temperatures of the ATS, the hotter stages, Rows 1 and 2 for example, may require the creep and LCF strengths of the DS Ni-based alloys. These alloys can be cast in the DS condition to further enhance the creep and LCF properties of the vanes, if needed. All vanes will be coated with corrosion/oxidation resistant coatings and thermal barrier coatings because of the high temperature environment.

The selection of vane material will depend on the cooling scheme and the corresponding stress and temperature requirements of each individual row of vanes. Preliminary design analysis appears to favor Ni-base alloys which contain high Cr, such as IN 939, due to their high strength and desirable corrosion resistance. However, its chemistry may need to be modified in a later development program to enhance its weldability for the ATS vane application.

#### 2.2.9.3.5 Turbine Blade Materials

Based on the latest design stress analysis, Ni-based superalloys are considered to be the primary candidate for Rows 1 to 3 blades. The Row 4 blades, which are expected to be subjected to higher fatigue and creep stresses, may require intermetallic materials. The analysis and rationale are presented below:

##### 2.2.9.3.5.1 Row 1 to 3 Blade Alloys

Turbine blades of modern land based turbines are primarily made of Ni-based superalloys, such as IN-738 castings (cast by conventional casting process) and Udimet 520 forgings. These alloys are typically limited to the blade application up to 1650°F or 1700°F (899°C or 927°C) metal temperature range due to creep.

Materials with higher temperature capability are needed for the ATS. Reducing cooling air to increase efficiency requires that the blades operate at higher temperatures. Within the time frame of development of the ATS engine, the most viable candidate materials are high strength Ni-based alloys, and alloys which can be cast with DS and SC casting processes, in combination with oxidation/corrosion resistant coatings and thermal barrier coatings.

The need for high temperature blading alloys has long been recognized. Work on developing corrosion resistant DS and SC Ni-based alloys for turbine blade applications has been ongoing. In these development alloys, Cr content is maintained at a significantly higher level than that of current aeroderivative SC and DS alloys to promote corrosion resistance, which is more a concern for land based turbines than for aero engines. Preliminary test data from the DS blade development indicates that these new DS alloys offer a substantial temperature advantage over conventionally cast equiaxed IN-738. Castability studies of these alloys are in progress. The new DS alloys were expected to have better corrosion resistance than the current commercial aeroderivative Ni-based blade alloys due to their higher Cr contents, but it is not certain that the creep strength would meet the ATS design requirements.

CMSX-4 SC alloy and CM247LC DS alloy have been used extensively for airfoil applications in aero engines and small industrial gas turbines. These alloys were selected for ATS blade development. CMSX-4 is a second generation single crystal superalloy containing 3% rhenium (Re). CM247LC is a derivative of the MAR-M-247 alloy, specially designed for aeroderivative DS turbine blades and vanes. These materials offer excellent creep strength, long-term stability and castability (for small airfoils), and represent the most advanced SC and DS alloys commercially available to date. CM247LC in the DS condition and CMSX-4 in the SC condition offer approximately 90°F (50°C) and 150°F (83°C) temperature advantages, respectively, at typical operating stress levels, as compared to the current land based blade material IN-738 in the conventional casting condition.

The industrial experience with both CM247LC DS and CMSX-4 SC alloys to date has been limited to relatively small airfoils primarily for aircraft engines or small industrial turbines. The castability of these alloys and their applicability to large size blades used in industrial power generation turbines have yet to be verified, because of concerns about grain structure control, chemical segregation and property uniformity. A castability study of CMSX-4 SC blades using W501F blade design as a prototype was carried out with a leading casting supplier. A similar castability study will be needed for the CM247LC vanes and blades. If the results of the castability studies are favorable, further work, such as heat treatment and hot isostatic pressing (HIP) process optimization, design property data, corrosion/oxidation characterization and coating compatibility, is required.

The merit of CC alloys can never be ignored due to easier castability and lower cost, even with the temperature advantages offered by the DS and SC alloys. CM247LC (CC) were evaluated for applications in the latter stages, where temperatures are lower and DS properties may not be needed. CM247LC, the low carbon version of the MAR-M-247 alloy, in the CC condition, has been used for airfoils and discs in the aeroderivative engines. Although it was originally developed for the DS processing, the lower carbon content plus other alloy modifications are also beneficial to the castability and mechanical properties of

the CC castings. Therefore, CM247LC is selected for the blade CC casting because its creep rupture strength is superior to that of the CC casting alloys used in the land based turbines. However, further development effort is required. Whether the alloy can be cast in large size land based blades with intricate cooling schemes and shroud overhangs has yet to be demonstrated.

Two approaches were used in selecting the best blade materials. The first approach had taken advantage of the existing successful experience in the aeroderivative alloys, CM247LC (in both CC and DS conditions) and CMSX-4 (SC) alloy. The second approach evaluated Siemens Westinghouse SC and DS developmental alloys for the ATS turbine applications. The CMSX-4 SC alloy offers the greatest temperature advantage, but the cost will be the highest because of the high reject rate normally associated with the SC process. The CM247LC alloy with CC processing offers the lowest cost option, but the relatively lower creep strength most likely will limit the use of this alloy to the latter turbine stages. Understandably, the CM247LC DS alloys offer a middle ground between the SC and CC options in terms of temperature capability and cost. The blades must be protected with corrosion/oxidation resistant coatings and TBC coatings since they will be subjected to a high temperature environment. The final selection of alloys and casting processes will depend on the temperature and stress requirements corresponding to the cooling scheme of each stage. By making the CC, DS and SC options available for ATS blade design, and tailoring the cooling scheme for each individual row of blades, an optimization between component cost and system efficiency can be achieved.

#### 2.2.9.3.5.2 Row 4 Blade Alloys

The ATS engine Row 4 blades will operate at a higher temperature than those in the W501F and W501G engines. In addition, the ATS engine will employ larger/longer Row 4 blades in order to minimize exhaust loss and improve efficiency. Since the blade operating stress is proportional to its length, this results in highly stressed blades. The combination of high temperature and stress therefore requires a material which exhibits higher creep and fatigue strengths than the current IN-738 material. Other conventional Ni-based superalloys, such as CM247 may not meet the creep and fatigue strength requirement either. CM247 in the CC condition offers about 50°F (28°C) advantage in creep resistance and 15% higher HCF strength as compared to IN-738. CM247 in the DS condition does not improve the HCF strength over the CC condition. Therefore, it is necessary to develop a new material for the subject application.

Intermetallic materials offer a high strength to weight ratio which make them very attractive for high temperature rotating component application. These materials have not found industrial applications, because the first available materials suffered from low ductility. However, in the last decade, significant advancements have been made in understanding these materials and overcoming the brittleness problem. Today, a number of intermetallic compositions have emerged. Among them, Ti-Al and Ni-Al intermetallics appear to be promising and are considered for the ATS Row 4 blade application.

#### 2.2.9.4 Coatings for Hot Section Components

The Co- ad Ni-based alloys used in the hot section components have less than desirable corrosion/oxidation resistance in the turbine environment. The reason for this is that they are primarily designed for high temperature strength, and the chemistries required for strength and corrosion/oxidation resistance are not the same. Therefore, protective surface coatings are essential for reliable and durable performance of hot gas path components. Coatings used for land based hot section components fall into the categories of corrosion/oxidation resistant and thermal barrier. As the name implies, the former is applied for corrosion and oxidation protection, while the latter is used to reduce the heat transfer between the gas stream and the substrate of the coated component.

The corrosion/oxidation resistant coatings used in the land based turbines are of two types: diffusion and overlay coatings. Diffusion type coatings include various aluminides and slurry coatings. These coatings are applied by a pack cementation process (PC) or by a chemical vapor deposition (CVD) process. In diffusion type coatings, final coating composition depends strongly on the substrate chemistry. Overlay coatings are applied to component surfaces by electron beam physical vapor deposition (EB-PVD), thermal spray techniques such as low pressure plasma spray or vapor plasma spray (LPPS or VPS), high velocity oxy fuel (HVOF) spray, or air plasma spray (APS) processes. Substrate chemistries do not have significant influence on the final compositions of overlay coatings.

Land based turbine manufacturers have been using aluminide type diffusion coatings and MCrAlY (Where M can be Ni, Co, Fe or a combination thereof) type overlay coatings on the hot section components since the 1970s. The only differences in the use of these coatings are the selection of minor alloying additions and the methods of application. The use of an efficient cooling scheme permitted the use of MCrAlY coatings to about 1650°F (899°C) surface metal temperature with a service life of about 24,000 hours. A development program directed toward advanced corrosion/oxidation resistant coatings was instituted to further improve the temperature capability of these coatings. Promising compositions were identified to meet a set of target properties. These compositions were evaluated in laboratory cyclic corrosion tests and burner rig tests. The best available MCrAlY coating was selected for ATS application in terms of temperature capability and long-term durability

TBC is used to lower the temperatures at the substrate as well as the MCrAlY coating. The most commonly used TBC in land based turbines is yttria-stabilized zirconia (YSZ). The YSZ coating can provide a temperature gradient greater than 100°F (56°C) for a .010 inch (0.25 mm) thickness, in typical operating conditions. Siemens Westinghouse developed a YSZ coating under a DOE program in the 1970s, and this system, applied predominantly with an APS process, is still used in current turbines. With the advancement of the EB-PVD process, it is possible to reduce the coating thickness variation, minimize cooling hole blockage, and especially improve the coating surface finish. But other characteristics, such as foreign object damage and erosion resistance, have yet to be evaluated in comparison with the APS TBC. Field testing on blades which are coated with both the APS and EB-PVD processes were conducted. The

results from this engine test, discussed later in this section, provided a better understanding about both the process capability and field performance.

Field experience indicated that present MCrAlY coatings typically used by the turbine manufacturing industry may not provide reliable long term protection for substrate materials at the target firing temperature of the ATS engine. Since a reliable coating system is critical to the success of meeting the ATS goal, a three-prong approach to improve the coating reliability was undertaken.

The first approach was to develop an advanced bond coat and TBC system that is capable of operating at a 1800°F (982°C) metal temperature for 24,000 hours. Siemens Westinghouse has been developing a corrosion-resistant bond coat with an 1800°F (982°C) capability. Tests at 1850°F (1010°C) in a Na<sub>2</sub>SO<sub>4</sub> environment have demonstrated the superior environmental resistance of this bond coat as compared to CoNiCrAlY (RT122). A series of TBC stabilizers (e.g., Sc<sub>2</sub>O<sub>3</sub>) were identified. These materials featured new ceramic compositions and structural modifications aimed at improving the thermal stability, corrosion resistance and spalling resistance of TBC.

The second approach was to perform field and laboratory testing to estimate the reliability of current coating systems. Field testing of coated components has been ongoing for several years. The reliability of TBC coatings applied by air plasma and electron beam from physical vapor deposition (EB-PVD), on IN-738 rotating blades, were tested. Field testing to date has been carried out in units with relatively lower firing temperatures. Field testing in a unit with a firing temperature closer to that of the ATS was next considered. This additional testing was to confirm the long term TBC stability, and bond coat interaction with CMSX-4 and CM247 blade substrates, which contain lower Cr than IN-738. Additional lab testing to determine the effects of phase change, fatigue, creep and corrosion on TBC spalling were also pursued.

The third approach was to develop a computer based life prediction model with the ability to predict cycles to failure for bond coat and TBC. A life prediction model for uncoated cast airfoil alloy was developed. This model can be extended or modified to include coating systems. A reliable life prediction model for complex coated components can provide a systematic understanding and control of coating degradation and contribute to the more reliable application of coatings.

#### 2.2.9.5 Combustion

Combustion is one of the critical areas requiring significant development efforts because of the higher firing temperatures and the strict emissions requirements for the ATS engine. The following combustion development programs were undertaken to achieve ATS objectives: combustor flow visualization, combustion optical diagnostics probe development, combustion instability/noise investigation, and catalytic combustion components development.

Air flows inside the combustor cylinder and into the combustor baskets are very complicated. These flows have a pronounced effect on pressure losses that directly translates into lower engine performance. The combustion process is directly influenced by the flow distribution inside the combustor baskets.

Combustor basket flow patterns are especially critical in dry ultra low NO<sub>x</sub> lean premix combustors. These combustors rely upon the uniform fuel/air ratios, within a very narrow tolerance band, for low NO<sub>x</sub> production and operational flame stability. Flow tests were carried out on plastic models of the ultra low NO<sub>x</sub> baskets in the single can rig and the sector rig. Flow visualization and detail flow mapping tests were performed. Hot wire anemometry, as well as conventional measurement techniques were employed.

Flow mapping and flow visualization tests were performed on a half-scale plastic model of the W501F combustor cylinder at Clemson University. Higher order flow effects inside the combustor cylinder were investigated. Detail information on pressure, velocities and flow angles inside combustor cylinder, and especially around the combustor baskets, were obtained. The effect of struts, cooling air bleed port, cooling air return pipes, diffuser exit swirl, modulation of the by-pass valve, flow shields around the combustor baskets, top hat length, ultra low NO<sub>x</sub> basket, and curved compressor exit diffuser were investigated. In addition to studying and optimizing the flow around the combustor baskets, efforts to optimize the performance of the compressor exit diffuser and reduce the diffuser exit dump loss were undertaken.

Optical diagnostics allow measurement of pertinent parameters, such as the composition and concentration of combustion products, in addition to velocities and flow angles, without disturbing the main flow. An optical diagnostic probe was developed to aid in combustion system optimization. Rig and engine tests, using the optical diagnostic probe, were conducted.

High firing temperatures are required to achieve the very challenging performance goals of the ATS program. The higher firing temperature promotes NO<sub>x</sub> generation, making attainment of NO<sub>x</sub> emissions goals more difficult. Lean premix combustion systems are required. The very lean combustion requirements, along with its inherent flame instability, increases combustion generated noise. The combustion induced noise results in vibration problems in the combustion system as well as in the downstream components. A program to develop the theoretical background on combustion instabilities, carry out experiments to aid in the understanding of the problem, develop a generalized analysis procedure, and develop stability criteria for a particular combustor basket is a requisite part of developing a low NO<sub>x</sub> combustor for the ATS program.

NO<sub>x</sub> production rises with increasing flame temperature. Catalytically enhanced combustion will play an important role in achieving ultra low NO<sub>x</sub> emissions at firing temperatures in the range of 2500°F (1371°C) and higher. The catalyst allows ultra lean premix (fuel and air) combustion without flame instability and flame outs. A development program was carried out to gain theoretical understanding of catalytic combustion, to design a catalytic combustion system and to start development of a practical catalytic combustor. Combustor baskets with catalytic components can provide the key to attaining low NO<sub>x</sub> emissions.

#### 2.2.9.6 Cooling

The development of new cooling technologies is of paramount importance to the success of the ATS Program. The increased firing temperature will require

cooling of components which previously did not need cooling. Parts already cooled require more cooling to maintain acceptable material behavior. Closed-loop steam cooling is used on many of the hot end components because of the resulting large increase in plant cycle efficiency. However, film cooling tests were also performed in the event closed-loop steam cooling does not provide adequate cooling on some components, such as the trailing edge regions of the Row 1 vane.

The airfoil end walls or shrouds present a cooling design challenge even at current firing temperatures. Model tests were completed to optimize the cooling design of vane shrouds. Even with closed-loop steam cooling, sections of the Row 1 vane may have to be film cooled. The same model tests can be used to optimize vane section surface film cooling design.

Row 3 turbine blade will incorporate an integral interlocked tip shroud, as used on the W501F and W501G engines, to improve performance and reduce blade vibratory stresses. The tip shroud and the very large blade height may make it very difficult to develop the SC casting process in time for the first ATS engine. As a contingency, the blade will be designed with cooling to maintain the blade metal temperature at an acceptable level. It will be especially difficult to cool the tip shroud. Alternative cooling designs and manufacturing processes were evaluated. A blade casting development program for the selected design was undertaken.

Multi-pass serpentine cooling schemes are required to achieve the blade metal temperatures acceptable for the blade material. Plastic model tests were completed on the selected serpentine channel cooling schemes to verify and optimize the design prior to incorporation into the engine. Two models were tested: one model simulating the multi-pass mid chord region of the blade, and the second model representing the trailing edge portion of the blade. Tests were carried out at different cooling air flow rates. The internal heat transfer coefficients and pressure losses were measured.

One modification that results in the greatest improvement in the ATS plant cycle efficiency is the closed-loop steam cooling system. The heat capacity of steam is about 1.3 times that of air. Therefore, less steam is required to cool the hot end components than air. Closed-loop steam cooling negates the surface ejection of the cooling air and hence, the mixing losses. An improvement in stage efficiency is noted. Elimination of Row 1 vane cooling air ejection into the main stream results in an increase in Row 1 turbine blade inlet temperature and the turbine exhaust temperature for the same burner outlet temperature. A combination of the above effects will increase the ATS plant efficiency significantly. There are several challenges that must be overcome before a successful closed-loop steam cooling systems is developed. These include maintaining acceptable airfoil surface metal temperatures without outside film cooling, high wall temperature gradients, effect of steam on metal components over long periods of time, bringing steam to and out of rotating components, leakages, and cold start before steam from the downstream HRSG is available.

### 2.2.9.7 Mechanical Design

The last row turbine blade is another component requiring a substantial development effort. The annulus area of the last row turbine blade must be as large as possible to minimize exhaust losses. This results in a long, highly stressed, last row blade. This blade incorporates an integral interlocked tip shroud to avoid excessive vibratory stresses. There is a possibility that two blade natural frequencies may occur between adjacent harmonics in this type of a blade design. These two frequencies can become coupled, and the resulting vibratory stresses can cause blade failure. Three tasks must be completed to design a durable last row blade. The initial task consists of a preliminary investigation, which will cover a review of the design rules for last row turbine blades, the reevaluation of advantages/disadvantages of interlocked shroud versus free standing last row blades, and the evaluation of the effect of stimuli and damping on last row blade vibratory stresses. The next task requires the evaluation of alternative blade and shroud designs, including part span shrouds, and a blade casting development program on the selected design. Finally, a vibration test of the last row blade is required to verify the design. The Blade Vibration Monitoring (BVM) technique, developed by Siemens Westinghouse, is employed to measure vibration characteristics of individual blades during engine operation.

### 2.2.9.8 Leakage Control

Turbine blade tip clearance has a pronounced effect on the performance of highly loaded front stage blades. Stage efficiency may decrease by up to 2% for each 1% tip clearance increase (based on blade height). For a four-stage turbine, overall turbine efficiency decreases about 1/2% for the same 1% increase in tip clearance. Even if the initial cold blade tip clearances are set at minimum values, during transients, such as rapid starts and emergency shutdowns, the blade tips are ground off. This results in increased hot running blade tip clearances, which get progressively worse with time. An active tip clearance control system was developed to solve this problem. The system maintains large tip clearances on start-up and reduces clearances to a minimum acceptable value when the engine has attained steady state operating conditions. This can be accomplished by cooling, at appropriate times, the blade ring holding the ring segments located above the rotating blade tips. A conceptual design of an active tip clearance control system was completed. Field tests on a host engine are required to verify the viability of the concept.

Brush seals can be incorporated in the appropriate locations in the turbine and compressor to reduce air leakage, as well as hot gas ingestion into the turbine disc cavities. This results in an improvement of engine efficiency as well as mechanical integrity of the turbine components. The incorporation of an effective, reliable, and long-lasting brush seal system into a heavy duty industrial combustion turbine requires development.

### 2.2.9.9 Design and Test Results

#### 2.2.9.9.1 Blade Cooling

Development of cooling technology for hot gas path components is critical to the success of the ATS design. Closed-loop steam cooling is used in some hot

components to provide an increase in cycle efficiency. Airfoil end walls or shrouds need more cooling than previous designs because of higher firing temperatures. Multipass serpentine cooling schemes are used to maintain blade metal temperatures below acceptable limits for the blade material. Impurities in steam could possibly clog cooling passages, causing overheating. These problems were investigated concurrently. Results from each program are explained below.

#### 2.2.9.9.1.1 Task 8.1 Effects of Blade Cooling Alternatives on Performance

Conventional gas turbine airfoils now use air extracted from the compressor as the coolant in a system involving internal impingement and passage convection cooling, along with film cooling of the airfoil surfaces. With increased firing temperatures, more cooling air is required, above and beyond the 20 percent that is currently used. A substantial improvement in engine performance is possible if the cooling air is reduced, or closed-loop steam cooling is employed.

An automated performance calculation system was developed to assess the effects of different cooling media and cooling schemes on cycle performance. The effects of heat transfer, energy balance, mixing losses and expansion work was integrated into the computations.

#### 2.2.9.9.1.2 Task 8.10 and 8.28 Stator Cooling

Heat transfer data on the hot side surfaces of combustion turbine stators is required for design purposes. The surfaces of primary interest were the shroud surfaces, however, airfoil film cooling effects were also investigated. A scale model of the stator sections was constructed. Laboratory flow tests of the model provided heat transfer data used for stator cooling design.

The model stator employed a thermochromic liquid crystal technique which produced both convection heat transfer coefficient distributions and film effectiveness distributions. Figure 27 illustrates a typical vane shroud cooling scheme. Figure 28 shows a plan view of the general test configuration.

The test program was sequenced to produce the individual effects of each of the many elements which influence hot side heat transfer. A test plan was developed for collecting the required data.

The test program included:

- Basic configuration with no gas path surface interruptions or film effects
- Boundary layer sensitivity
- Reynolds number sensitivity
- Surface discontinuities from combustor transition seals, shroud edges, etc.
- Film effectiveness from transition seal film hole array
- Film effectiveness produced by leakage between circumferential gaps between adjacent shrouds

- Film effectiveness of airfoil film holes on airfoils
- Film effectiveness of airfoil film holes on shrouds
- Film effectiveness of several shroud film hole arrays

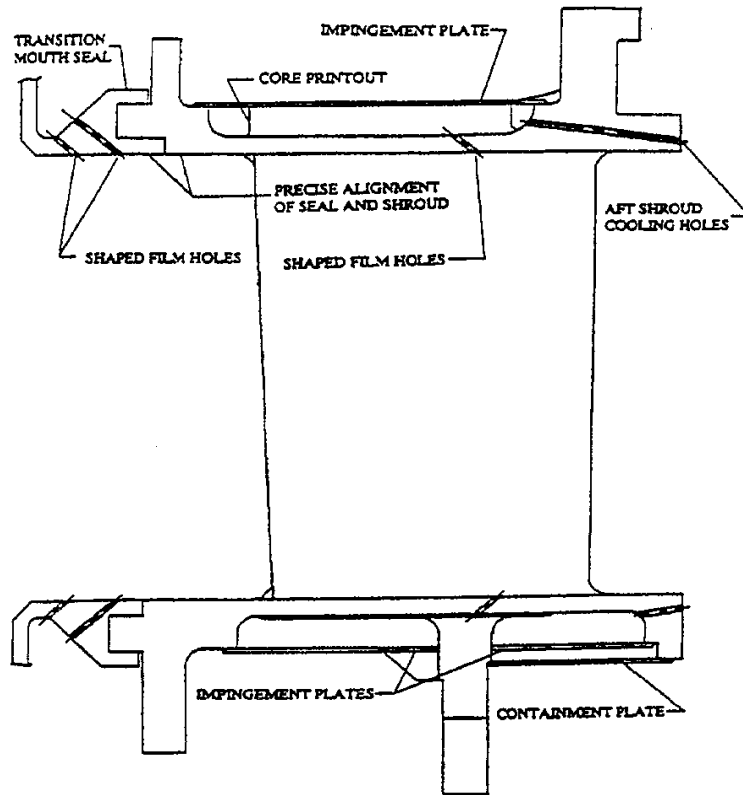
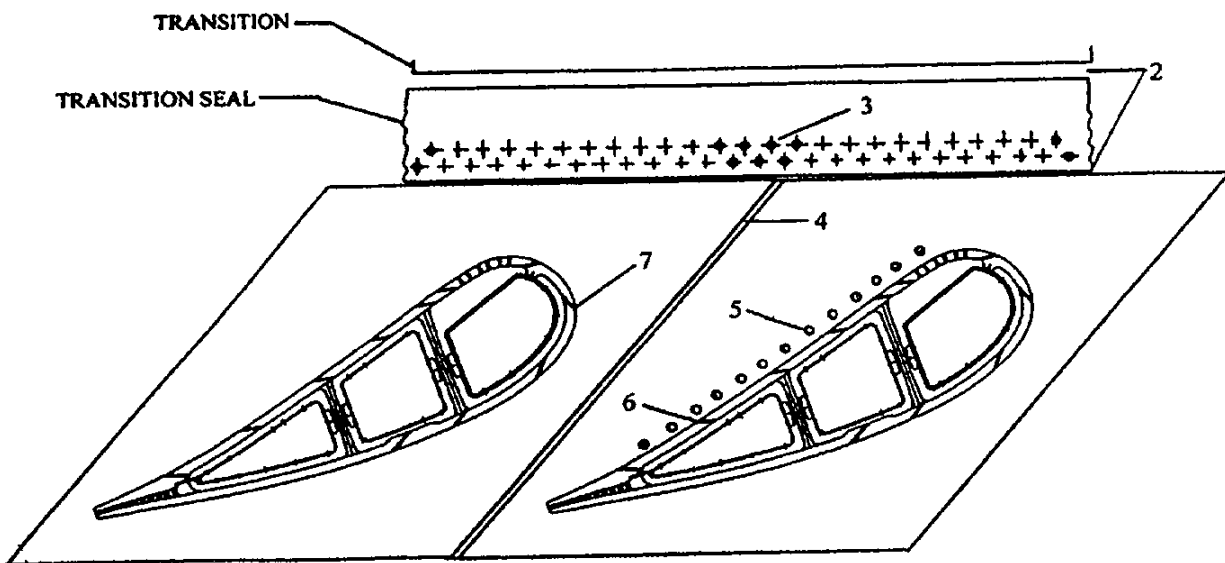


Figure 27 Typical Vane Shroud Cooling Scheme



## Figure 28 General Test Configuration

### 2.2.9.9.1.3 Task 8.12 Shrouded Blade Cooling Development

The stage 3 turbine blade must meet a unique combination of requirements. Exceptional performance, mechanical and thermal goals must be attained simultaneously. Cooling of the tip shroud is a design challenge because the blade is long and thin. Three cooling options were considered:

- Cool the tip shroud with spent airfoil cooling air
- Provide a separate cooling air passage through the airfoil to the tip
- Inject cooling air toward the tip shroud from the stationary outer diameter of the blade path

The last option was rejected early in the program. Severe performance penalties suffered from excessive use of coolant in this option. Alternatively, the first option produced the minimum impact on performance, but would have limited cooling capacity.

The second option, shown in Figure 29, was selected because of its versatility and reliability. The airfoil cooling scheme consists of a cast blade with two (2) cored cooling passages extending from the bottom of the root to the blade. Airfoil cooling is provided by electrochemically machined holes extending from the tip into the two cored cooling passages. Most of the coolant flow through the blade to the tip shroud is provided by a separate large round hole extending the entire length of the blade. The tip shroud cooling scheme consists of holes drilled through the shroud to mate with the large cored hole in the blade. The use of a large diameter round hole located between the airfoil cooling passages prevents overheating of the coolant during the traverse to the tip shroud.

The thermal analysis results of the cooled tip shroud indicated that cooling scheme met temperature limit criteria. Comparison of the running temperature distribution and the allowable temperature distribution necessary to meet blade creep life requirements indicated that the creep life requirement has been met. A conceptual design for cooling of the tip shroud has been completed.

Although the mechanical and thermal constraints for the blade and shroud have been satisfied in the conceptual design, manufacturing the hardware may alter the final design. The next phases of the ATS program will focus on the final design and the ability to manufacture these components cost effectively.

### 2.2.9.9.1.4 Tasks 8.14 and 8.31 Closed-Loop Steam Cooling - Row 1 Vane

For closed-loop cooling to be successful, the following are required:

- Thermal barrier coatings with high surface temperature and high bond coat temperature capability, along with high temperature gradient capability must be available
- High capacity coolants and/or low coolant supply temperature must be used

- Minimal airfoil wall thickness to reduce required coolant heat transfer coefficients and improve fatigue life is required
- Enhanced cold side heat transfer characteristics for higher effective coolant heat transfer coefficients through increased surface area, i.e., turbulators, and localized impingement must be examined

Three primary closed-loop cooling schemes have been analyzed for use on the Row 1 vane airfoil. These are: (1) peripherally placed spanwise radial hole design, (2) thin-wall chordwise channel design, and (3) radial flow thin-wall pedestal bank array. The chordwise channel design scheme has been selected for the following reasons:

- cooling geometry is highly configurable, which is important to allow use with multiple coolant types
- excellent cold side heat transfer characteristics
- demonstrated manufacturability

The trailing edge is an area of particular concern due to limited area, high external heat transfer coefficients, and concentrated heat loading due to cylindrical geometry. Several cooling schemes were considered for the trailing edge, with two particular techniques emphasized; a chordwise wrap-around channel design, and a midspan fed spanwise radial hole design. The former, the chordwise channel design, has been selected for various reasons, but primarily due to high pressure losses associated with the latter.

A peripherally fed, inward flowing pin-fin/pedestal array has been chosen for the Row 1 vane shrouds. This scheme utilizes impingement cooling at the shroud outer edges where the external thermal boundary conditions are severe. It takes advantage of the natural reduction in flow area from the shroud periphery to the vane to passively increase the coolant heat transfer coefficient. This compensates for the increase in coolant temperature through the pedestal array.

Detailed designs have been generated for both the airfoil and shroud. A concurrent engineering design philosophy, with continuous input and feedback from mechanical, aerodynamic, performance, and manufacturing disciplines, has been followed. Subsequent work will be continued toward the manufacture of this component.

#### 2.2.9.9.1.5 Task 8.22 Serpentine Channel Cooling Tests

Complex multipass serpentine cooling schemes were developed to maintain low blade metal temperatures. Plastic models were constructed to determine the feasibility of the concepts prior to incorporating them into the blade design. Two models were tested, each representing different regions of the blade. The models were painted with thermochromic paint for thermal mapping.

The models were tested in a flow chamber. Heat transfer and pressure loss data were created from the flow tests. This data was used to optimize serpentine blade cooling design. The data revealed several specific areas of concern:

- Serpentine reverse turns
- Thermal and flow benefits of turbulators in reverse turns
- Local effects within the passages as affected by:
  - aspect ratio
  - film cooling holes
  - film cooling flow rate

A hidden line view of a typical serpentine cooled blade is shown in Figure 30. An airfoil cross section of the blade is shown in Figure 31. The blade cooling system consists of three (3) circuits: 1) a single pass leading edge circuit, 2) a triple pass mid circuit, and 3) a single pass trailing edge circuit. It was decided to conduct test programs on the mid and trailing edge circuits. The mid circuit would provide the reverse turn and basic film hole data, and the trailing edge circuit would provide the high aspect ratio data.

Preliminary conclusions from these tests indicate that serpentine cooled blade design will not provide adequate cooling for Row 1 turbine blading. The most likely candidate for using the serpentine cooling scheme would be Row 2 blades.

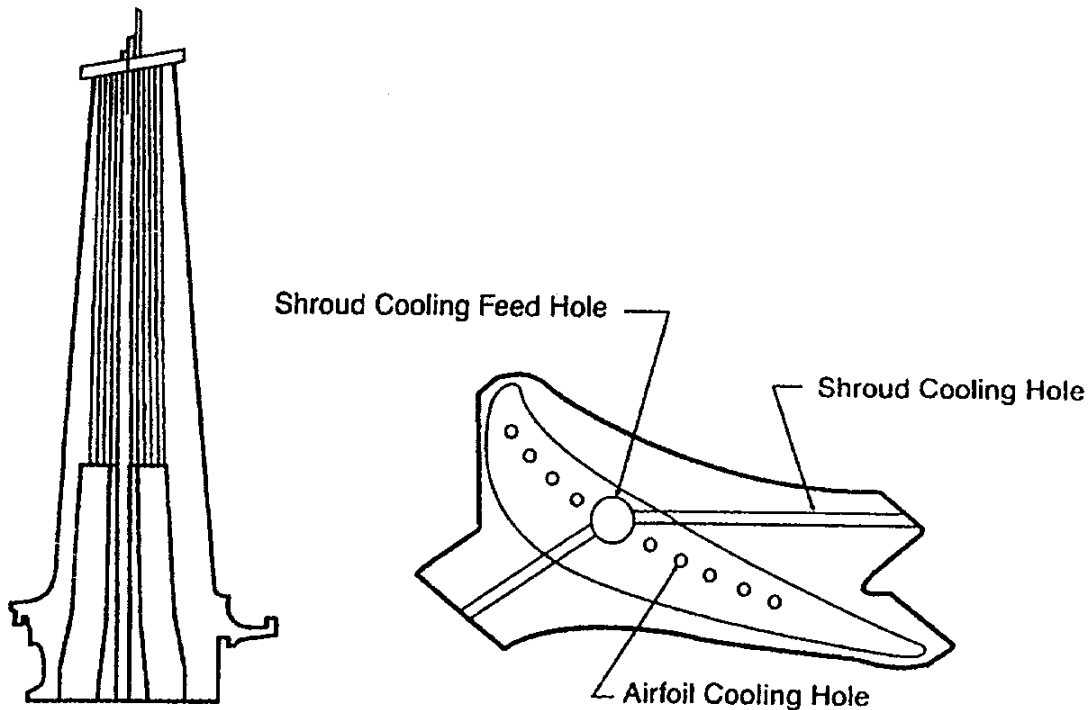


**Figure 29 Stage 3 Blade Tip Shroud Cooling**

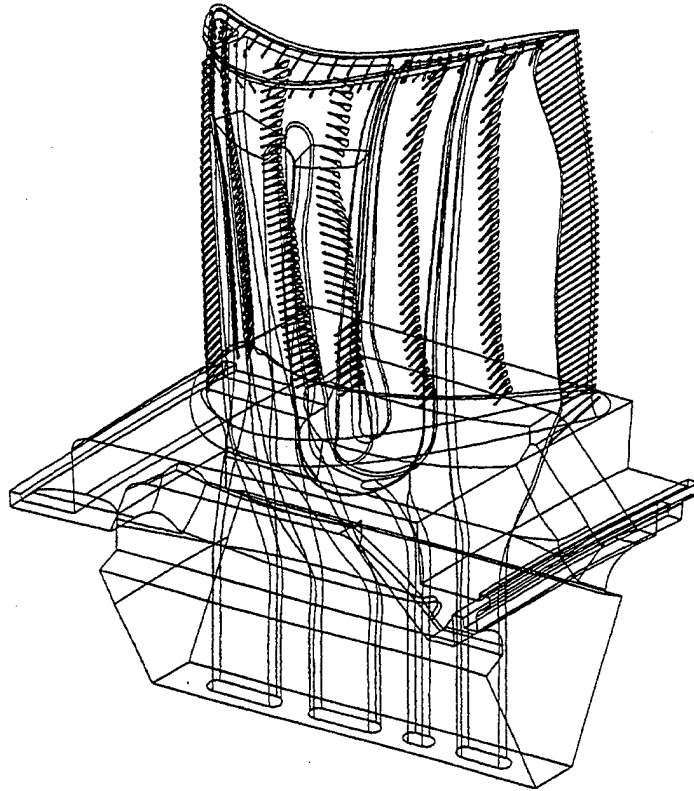


**Figure 30 Airfoil Cross Section of Blade**

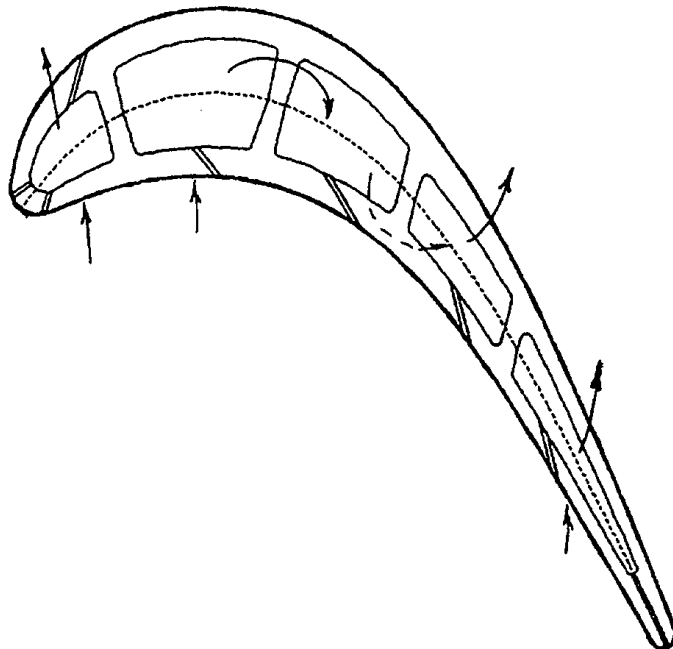


**Figure 31 Typical Serpentine Cooled Blade**

#### 2.2.9.9.1.6 Task 8.38 Closed-Loop Steam Cooling (CLSC) Effects

As steam passes through cooling passages, impurities in steam can deposit at various locations within the system. Corrosion can erode critical thin walls, causing steam leaks in rotating components. Potential deposition and corrosion of materials could lead to lower reliability (See Figure 32).

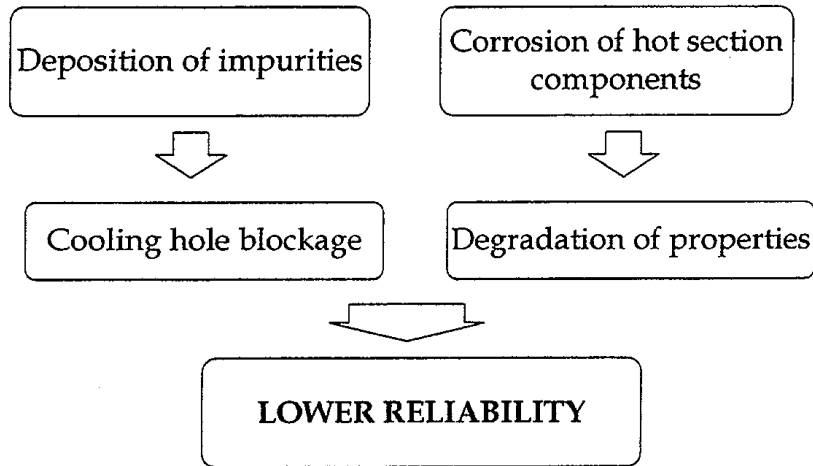


**Figure 32 Issues: Steam Cooling Effects**

An understanding of the corrosion/deposition mechanisms must be acquired. The consequences of corrosion and deposition in steam cooling circuit must be known. A test plan was developed to gain this understanding. Elements of the test plan included:

- Development of a steam chemistry model which will predict the type and quantities of impurities as a function of temperature and pressure
- Evaluation of the effects of steam chemistry on deposition and corrosion of materials

Testing was completed in subsequent phase. Portions of the testing hardware have been constructed. Details of the test plan are explained below.

A solubility model of common dissolved solids will be developed to predict deposition. The purpose of the steam chemistry model is to predict types and concentration of impurities along the cooling passages. Model verification requires lab testing with simulated impurities and cooling passages. A closed loop model with controlled pressure, temperature and quality will provide the ability to simulate almost any operational environment likely to be encountered. The first set of tests will be aggressive, i.e. higher level of steam impurities than would normally be expected.

The following tasks were identified for the proposed program:

- Define design parameters of the steam cooling system
- Review of impurities and corrosion data

- Identify potential corrosive and occlusive compounds
- Define the preliminary test environments
- Evaluate the solubility and stability of expected compounds
- Develop a steam chemistry model
- Define steam chemistry requirements
- Perform deposition/corrosion tests
- Evaluate test results
- Report

Design conditions of CLSC system have been obtained. A list of impurities that could lead to deposition/corrosion was generated. These impurities were classified into three categories (high, medium and low priority), based upon their potential for deposition/corrosion. The solubility of impurities as a function of temperature and pressure were correlated. Thermodynamic stability of likely impurities has been reviewed. All common contaminants are stable in the CLSC range of conditions. The scope of a dynamic deposition model has been prepared.

Facilities have been selected for performing tests. The test rig design has been completed. Test specimen design for the deposition/corrosion study has been completed. Materials have been procured for the deposition/corrosion tests. All the components for test rig manufacture have been procured.

Preliminary steam chemistry requirements will be obtained based on the steam chemistry model. Five deposition/corrosion tests are planned for subsequent work in Phase 3. The first test will be performed with high levels of impurities to evaluate deposition. Following evaluation of the first test results, subsequent tests will be performed with appropriate levels of impurities. The level of impurities used for testing will depend upon predictions made by the steam chemistry model, the CLSC system design and materials selections. The final steam chemistry recommendations will be determined, as depicted in Figure 33.

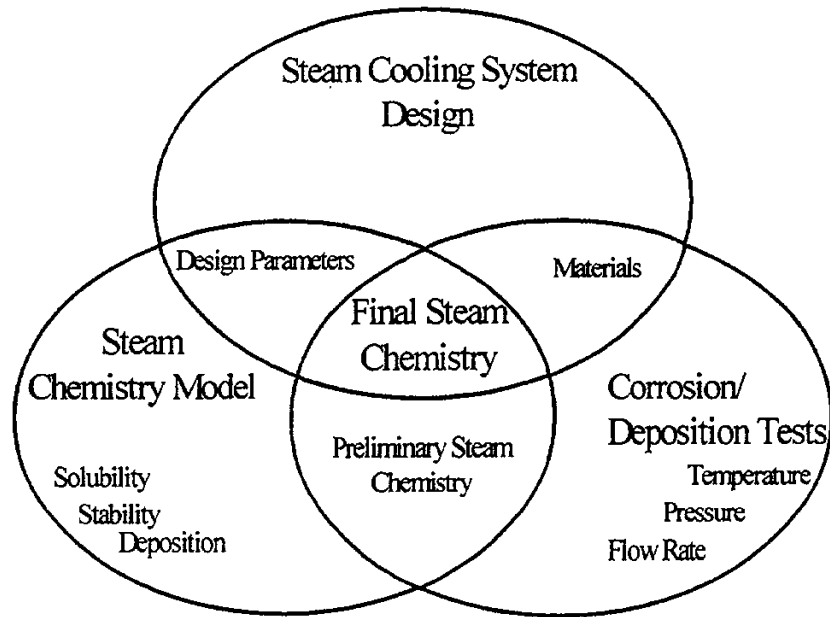


**Figure 33 Interactive Elements of the Program for Steam Chemistry**

#### 2.2.9.9.2 Blade Materials

The latest stress design information indicates DS and SC nickel based alloys potentially offer the best tradeoffs in performance and manufacturability for ATS blades. Row 4 blades may require some intermetallic elements for better fatigue and creep stress performance. Design data for these materials must be generated for a thorough evaluation of these materials at ATS conditions. Laboratory testing of specimens provided much of this data.

##### 2.2.9.9.2.1 Tasks 8.5 and 8.33 Single Crystal Blade Material Development

CMSX-4, a second generation Re containing SC alloy, was selected for the large ATS SC blade development because of its mechanical strength and its castability demonstrated in small aircraft engine blades. The castability of CMSX-4 alloy in large land-based SC turbine blades has not been attempted to date. Two large W501F blade designs, Row 1 and Row 3, were used in the casting trials to evaluate its castability. The Row 1 and Row 3 blades are currently made of conventionally cast superalloy in the equiaxed grain condition. The Row 1 blades are shorter and thicker (approximately 12 in. [305 mm] long with a weight of 18 lb. [8.16 kg]), whereas the Row 3 blades are longer and thinner (approximately 18 in. [457 mm] long with a weight of 14 lb [6.35 kg]). Both blades have internal cooling cores.

The experimental procedure included the fabrication of mold assemblies and casting trials. The patterns used in the evaluation were those used for the production of the equiaxed version of the blades. Core bodies were specially manufactured from high temperature ceramics in order to sustain the high temperature SC processing. Each mold assembly contained multiple blades. During casting trials, various gating configurations, blade orientations, shell procedures, and casting parameters were evaluated in order to achieve optimum

casting quality. Figure 34 outlines the SC casting process and the key variables that were considered.

#### 2.2.9.9.2.1.1 Row 1 Blade Casting Results

A series of four sets of Row 1 blades were cast. Freckles and chains of equiaxed grains were found to be present in all the experimental blades. The freckling appeared to be more severe at the root areas and less prominent at the airfoil areas. Some freckles at the root and airfoil caused the initiation and growth of secondary grains. It was concluded that the current process was not capable of achieving acceptable SC Row 1 blade casting. Further development efforts are required to produce blades in the size and configuration similar to the Row 1 blade.

#### 2.2.9.9.2.1.2 Row 3 Blade Casting Results

A series of five sets of Row 3 blades were cast with varying parameters. SC blades of different qualities were produced. One cored blade and one solid blade (cast without a core) with the best quality were selected for further NDE inspection. Figure 35 shows one of the SC blades in contrast with a conventionally cast blade. The blades were processed through the same visual, fluorescent penetrant, and radiographic inspections required for the conventionally cast Row 3 blades. The blades passed all inspections. The cored blade was also evaluated by ultrasonic instrumentation for core retention and wall thickness. Results indicated acceptable wall thickness and excellent core retention.

The grain structure was evaluated based on generally accepted industrial standards for single crystal components. Primary grain orientation, low angle boundaries and striation properties from one small sliver grain were examined by visual and X-ray diffraction methods. All grain properties were within the acceptable ranges. Slight freckles were found in the root area, but were removable by a subsequent machining operation.

#### 2.2.9.9.2.1.3 Conclusions

The results from this castability study have demonstrated that large SC blades of Row 3 configuration can be cast in CMSX-4 single crystal. Further process optimization will be needed to achieve acceptable product yield. For the Row 1 blade configuration, which is thicker and heavier than Row 3, further casting development is required to obtain acceptable blade quality.

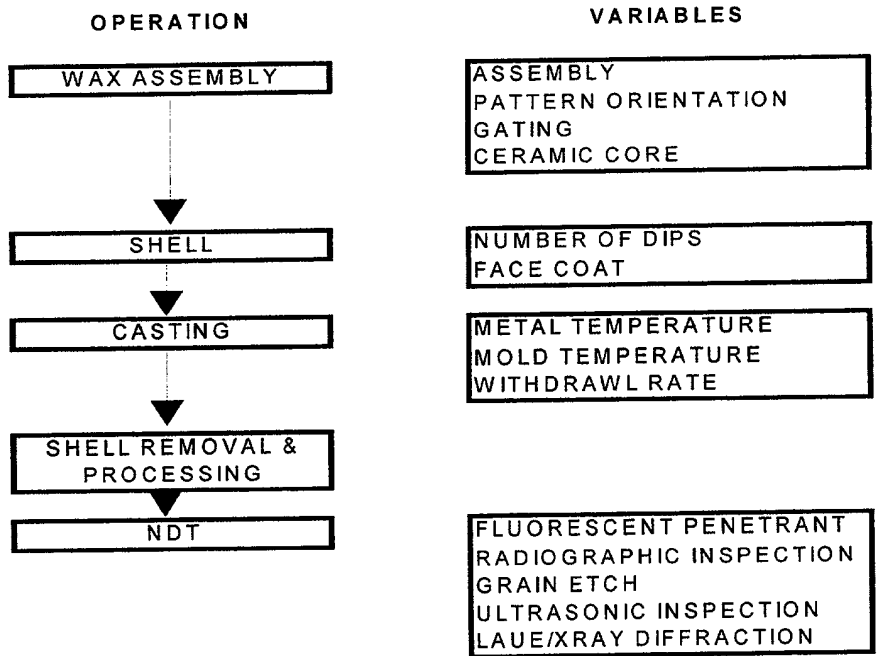


Figure 34 CMSX-4 SC R3 Blade Casting Process Flow Chart and Process Variables

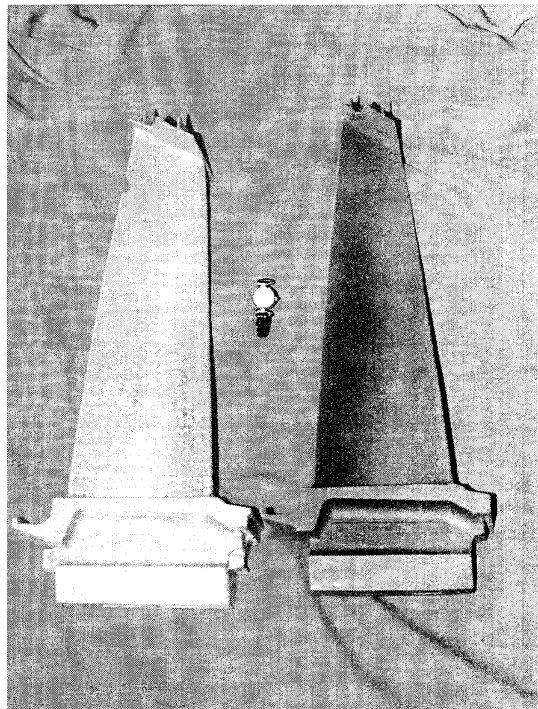


Figure 35 Single Crystal Blade

A single crystal W501F R3 blade (right) in contrast with a conventionally cast equiaxed blade (left) is shown. A wristwatch is centered between the blades for size comparison.

#### 2.2.9.9.2.2 Tasks 8.7 and 8.32 Ceramics

The use of ceramic materials in the ATS engine offers potential performance benefits. Ceramics are capable of withstanding higher temperatures than those

represented by today's metallic superalloys. Higher temperatures translate into higher thermal efficiencies. An estimated 15% to 20% of the total inlet airflow in a land based combustion turbine is diverted to cooling hot section metallic components. Ceramic components may alleviate the need for much of this cooling air. The selection process for identifying parts suitable for ceramic conversion progressed as follows:

1. Selection of candidate hot gas path components
2. Selection of the ceramic material
3. Manufacturing feasibility in association with a material supplier
4. Preliminary design studies on the selected component

#### 2.2.9.9.2.2.1 Selection of hot gas path components suitable for conversion to ceramics

The hot gas path components in combustion turbines exposed to the highest temperatures reside in or near the combustion zone:

- Combustor
- Transition
- Stationary ring segment
- Vane
- Blade

Each of these components use cooling air in different amounts to maintain temperatures below specified values. While detailed analyses are required to accurately predict the benefits in cooling air savings, engineering judgment indicates that the above order represents components with increasing potential for performance improvement through the use of ceramic materials. Vane and blade materials must survive very challenging operating conditions in a combustion turbine environment that is too demanding for the ceramic materials available today. The thermo-mechanical fatigue conditions, the cyclic stress patterns and attachment technologies warrant that these two components not be given serious considerations at this time. The stationary ring segment is considered to be the best choice for ceramic conversion because of its relatively smaller and simpler size, ceramic manufacturing experience with similar components, and a moderate amount of performance benefit to be expected. Combustor and transition components need the benefit of lower manufacturing costs before being considered for conversion to ceramics.

#### 2.2.9.9.2.2.2 Selection of the ceramic material

Monolithic ceramics can perform at considerably higher temperatures than can advanced metallic alloys, however, they are brittle. This brittleness precludes using this material in locations where the part is subjected to shock loads, high stress or vibration. Another class of ceramics, called continuous fiber reinforced ceramic matrix composites or simply ceramic matrix composites (CMCs), have

evolved in recent years as a possible material for high temperature, moderate stress level applications in combustion turbines. CMCs comprise of ceramic fibers with fiber-matrix interface coating intricately connected to a ceramic matrix by proprietary processes. Several of today's available CMCs were considered and evaluated these against the required and desired properties. Results of this evaluation are shown in Table 12.

Based on this evaluation, the selected material for the first application of CMCs in the ATS engine is Nicalon® Alumina which is silicon carbide (SiC) fibers in an alumina ( $Al_2O_3$ ) matrix manufactured by a proprietary process by DuPont Lanxide Composites (DLC) Inc. Nicalon Alumina CMC is suitable for use at temperatures up to 2100°F (1149°C) in low stress applications.

For more demanding applications such as vane or blade, this CMC (non-oxide/non-oxide) is not considered to be a good candidate. Rather, oxide/oxide CMCs are considered to be best suited for higher temperature, higher strength applications. While industry research is progressing to develop good oxide/oxide CMCs, none is currently available for combustion turbine component application. They need considerable development before being seriously considered for combustion turbines.

#### 2.2.9.9.2.2.3 Manufacturing Feasibility

Siemens Westinghouse has worked with DLC to better understand the capabilities and limitations of the DIMOX process which DLC uses to make Nicalon Alumina components. The most important manufacturing constraints for component shape are (1) composite preforming and tooling requirements; and (2) the DIMOX growth process limitations. Requirements for bend radii, T-sections, flanges, section thickness, tolerances, surface finish and machining have been identified and published for the benefit of the CMC component designer.

#### 2.2.9.9.2.2.4 Preliminary Design Studies

Initial design studies considered both ring segments and combustors for ATS because of limited benefit expected from a CMC combustor. After completing a cost benefit analysis, it was decided that only the ring segment design should be studied in detail. In its simplest form, the ring segment structural CMC substrate is a plate with a slight curvature; bonded to it is a ceramic abrasion layer. The abrasion layer serves two purposes: one is to provide thermal insulation to the CMC and second is to provide an abrasion surface for the blade tip to rub against the ring segment.

Several design concepts were evaluated. Creating an acceptable design, that limits the thermal and mechanical loading stresses to the maximum allowable, has proven to be a major challenge. CMC mechanical properties and low thermal conductivity restrict the design options available. A parametric evaluation of two CMC materials with different compositions and properties was completed. This provided an understanding of what properties (mechanical strength, thermophysical properties etc.) are important in the CMC and how they affect the component design. Further detailed design work will proceed in later phases of the ATS project.

**Table 12 Qualitative Evaluation of Available CMCs for Ring Segment Application**

Requirement	Nicalon/ Alumina	Nicalon/ SiC-CVI	SCS-6/ Silcomp	Enhanced SiC/SiC	SCS-6/ Si3N4
Short Term Database	✓	✓		✓	✓
Intermed Term Properties (<1000 hrs)	✓	✓		✓	✓
Long Term Properties (ca.10,000 hrs)	In process				
Abradable Layer	✓				
Bonding Method	✓				
Bondability	✓			✓	
Experience Base	✓	✓	✓	✓	✓
Commercial Supplier	✓	✓		✓	✓
Defined Process	✓	✓			✓
Improvement Potential	✓	✓	✓	✓	✓
Availability	✓	✓		✓	✓
Inert to Metals	?				?
Corrosion Resistant	?				?

Desirable Property	Nicalon/ Alumina	Nicalon/ SiC-CV1	SCS-6/ Silcomp	Enhanced SiC/SiC	SCS-6/ Si3N4
High Conductivity			✓	✓	✓
High Matrix Cracking Strength			✓		✓
Low Elastic Modulus	✓			✓	
Strain Tolerance	✓			✓	
Notch Insensitivity	✓			✓	
Machinability	✓	✓	?	✓	?
Machining Database	✓	✓		✓	
No External Coating Req'd	✓		?	?	
Manufacturability	✓	✓		✓	
Low Cost	✓	✓		✓	
Creep Resistance					✓
Surface Engineering	✓	?	?	?	?
Oxidative Stability	✓		✓	✓	

**2.2.9.9.2.3 Task 8.11 Directional Solidified Blade Material**

Preliminary test results from earlier work indicate that DS alloys offer a substantial temperature advantage over conventionally cast equiaxed IN-738 currently used in turbine blading. Material property data is required to analyze the feasibility of DS blading. Material properties, including tensile, LCF/HCF and creep rupture data must be generated for blade and vane designs. Specifically the following efforts were included to establish a comprehensive data base for design with DS materials.

- Evaluating the effects of alloy chemistry (CM247LC vs. Mar-M-002)
- Including conventionally cast materials as baseline for comparison with DS materials

- Evaluating the effects of DS casting withdrawal rate.
- Generating long term creep rupture data.
- Characterizing oxidation behavior of base metals.
- Evaluating the effects of coating on mechanical properties.
- Verifying test data generated from cast slabs by destructive testing of cast blades.

A partial set of material properties for directionally solidified CM247LC and Mar-M-002 has been generated. This data included:

- Long-term creep rupture with some specimens exceeding 10,000 hours of testing time.
- Strain controlled LCF tests and stress controlled HCF tests were performed at selected design temperatures. The effects of orientation on the fatigue properties were included in the tests.
- CM247LC material was tested at 1750°F (954°C) and 1850°F (1010°C) in a burner rig up to 1000 hours and oxidation rate was determined by metallographic examination of the test specimens.
- DS slabs cast with three different withdrawal rates have been received. The slabs have been heat treated and machining of test specimens is in progress.
- Two W501 Row 1 blades have been successfully cast, heat treated and NDE inspected; and machining of specimens is in progress. Two Mar-M-002 Row 1 blades were ordered for future testing.

Material properties for continuous cast CM247LC were generated, including:

- Tensile, HCF and LCF testing has been completed
- Creep rupture testing is proceeding

Additional material property generation was continued in Phase 3.

#### 2.2.9.9.2.4 Tasks 8.18 and 8.30 Thermal Barrier Coatings

The application of uniform and durable TBC on the turbine airfoil and end wall surface is critical to the design of closed-loop cooling systems. The protection provided by the cooling air film, in previous blade/vane/ring segment designs, is no longer available. The thermal barrier provided by the TBC will be important in maintaining low surface metal temperatures in the ATS engine, without the need for high rates of internal cooling.

Ceramic TBC must be capable of operating a minimum of 24,000 hours. Various ceramic coatings were evaluated, using innovative bond coats and deposition

methods. Field tests of a select set of coatings were made in various Siemens Westinghouse combustion turbines.

The performance of several bond coats were evaluated for use in the ATS combustion turbine. Air plasma sprayed (APS) and electron beam physical vapor deposition (EB-PVD) applied 8% yttria stabilized zirconia thermal barrier coatings to the bond coats. The life-limiting failure mode in both air plasma sprayed and electron beam - physical vapor deposition coating systems is the oxidation of the bond coat. The coating life is related to the growth rate and morphology of the thermally grown oxide.

A systems approach to improving coating performance must also consider the ceramic thermal barrier. The use of 8% yttria stabilized zirconia has demonstrated performance in the aerospace industry. It has many desirable properties, thermal stability at high temperature, high thermal expansion and low thermal conductivity. The life-limiting failure mechanism remains oxidation of the bond coat. It can be argued that improvements in the ceramic TBC performance under these circumstances are of secondary importance. The influence of ceramic TBC properties on coating durability will increase, as bond coat developments provide increased oxidation resistance. Further development of ceramic TBC will be limited by bond coat materials.

#### 2.2.9.9.2.4.1 Experimental Procedure

Three nickel base superalloys were selected as substrate materials for the evaluation of several commercial TBC systems. Each of these alloys received a conventional bond coat. Coatings were deposited onto 0.315 in. (8 mm) diameter rods, approximately 4.75 in. (12 cm) in length. The coated rods were sectioned into 1.0 in. (2.5 cm) test pieces.

Coating performance was based on the time to failure in furnace tests. Furnace exposure tests were conducted at 2100°F (1149°C). Samples were cooled to room temperature in static air once every 24 hours. Samples were removed from the test at prescribed intervals for metallographic inspection. At least three specimens for each system were tested to failure. Coating failure was defined as significant spallation of the coating.

Metallographic sections were prepared for each sample. The test pins were cross sectioned, mounted using epoxy vacuum infiltration techniques, polished and ground. The oxide thickness, morphology and chemistry were examined using scanning electron microscopy and wavelength dispersive spectroscopy. Oxidation rates were determined from oxide thickness measurements.

#### 2.2.9.9.2.4.2 Results and Discussion

The relative performance of each trial system is shown graphically in Figure 37. As expected, failure of the coating system is directly related to the oxidation of the bond coat. The growth of the oxide during service exposure introduces stresses into the system, which result in spallation of the coating. The thermal stresses, associated with heating and cooling from ambient to operating temperatures, introduce additional degradation. Creep of the bond coat, bond coat mechanical properties and TBC compliance will certainly contribute to the

overall stress state of the system. The critical life-limiting factor remains oxidation of the bond coat.

The oxidation rate is dictated by the capacity of the bond coat to form an impermeable, adherent alumina oxide scale. Diffusion of elements from the substrate influences the ability of the coating to form a protective oxide scale.

The oxide growth rate, as determined by measurements of oxide thickness, are presented in Figure 38 for each of the TBC systems. If the substrate played no role in determining the oxidation rate of the bond coat, then the three systems should have nominally equivalent life as measured by hours to failure. These systems, with the same bond coat have measurably different oxidation rates. The performance of the coating system on substrate IN-939 illustrates the axiom that having the highest oxidation rate has the lowest life.

### Thermal Fatigue Life of Bond Coat Candidate Materials Oxidation Exposure

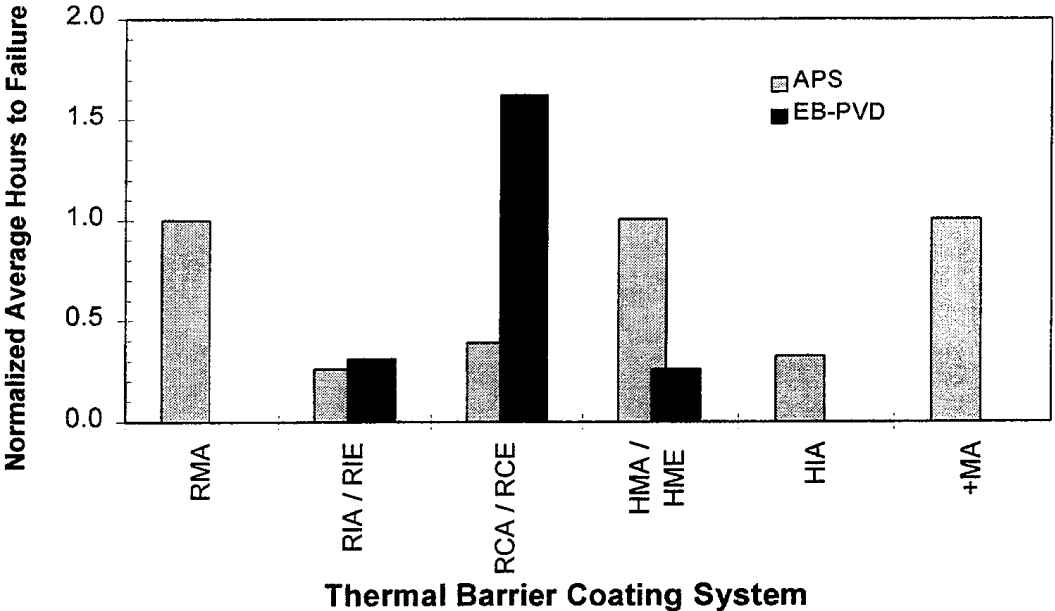


**Figure 37 Thermal Fatigue Life Evaluation**

Performance of each of the TBC systems evaluated as determined by furnace evaluations at 2100° (1149°C), samples were cycled to room temperature once every 24 hours.

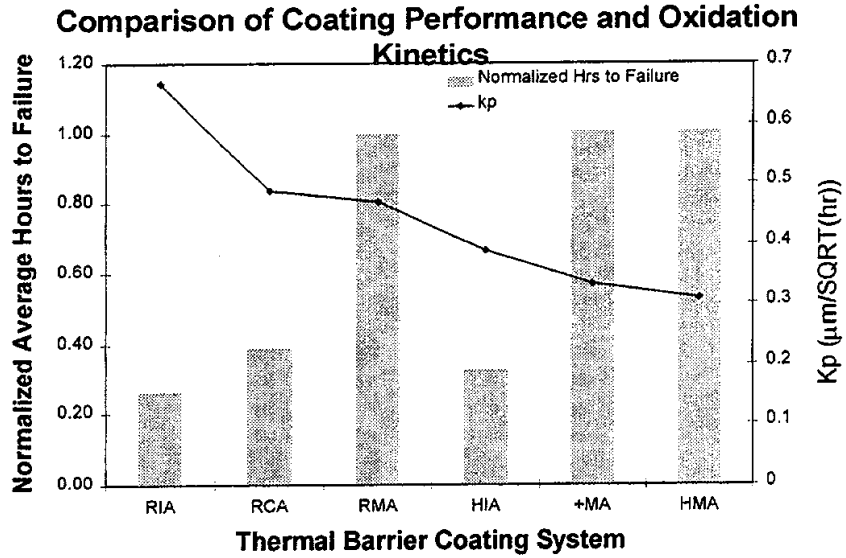


**Figure 38 Comparison of Coating Performance and Oxidation**  
 A comparison of oxidation rate,  $K_p$ , versus time to failure for the APS coating systems. The oxidation rates were determined from oxide thickness measurements.

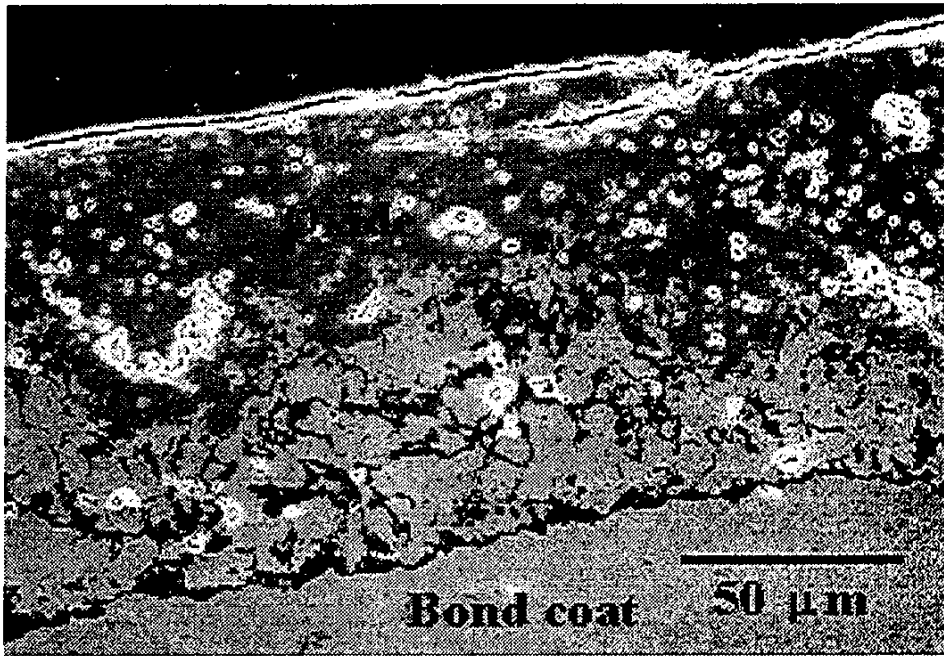


**Figure 39 Spalled APS Coating**  
 Characteristic oxide formed on RIA with APS coating

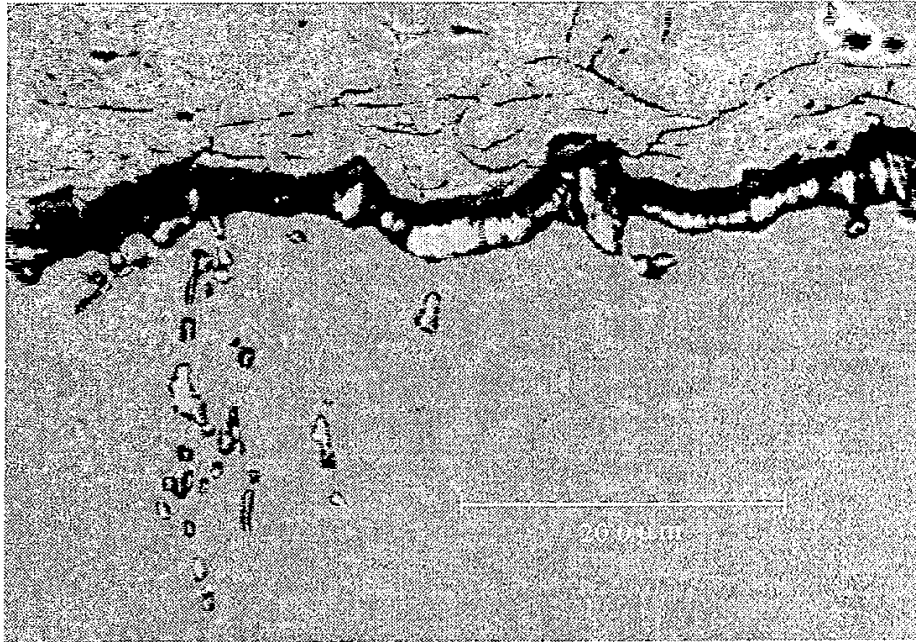


**Figure 40 HMA with APS Bond Coat.**

A significant number of hafnia pegs combined with insufficient surface roughness reduced the performance of this coating system.

The furnace tests revealed that substrate chemistry influences oxide formation and morphology. Figure 39 shows a specimen that experienced the longest life. The oxide formed on this system is characterized by an adherent, pure alumina layer. The micrograph in Figure 40 shows a specimen that developed a thin alumina scale with large amounts of hafnia. The hafnium diffused into the alumina scale and compromised the protective capacity of the scale.

#### 2.2.9.9.2.4.3 New Ceramics

Several new ceramic compositions have been selected for evaluation. These ceramics were selected based on the potential to reduce thermal conductivity, or their increased thermal stability. One system, a scandia stabilized zirconia, has exhibited improved life over that of the standard 8% YSZ when evaluated on the same bond coat and substrate materials (see Figure 41). As oxidation resistance of the bond coat increases the impact of the ceramic TBC system life will increase. The use of scandia stabilized zirconia may provide a means of increasing TBC system life.

Scandia Stabilized Zirconia has Superior Performance to Baseline Zirconia Coating  
1150°C Dynamic Oxidation Exposure

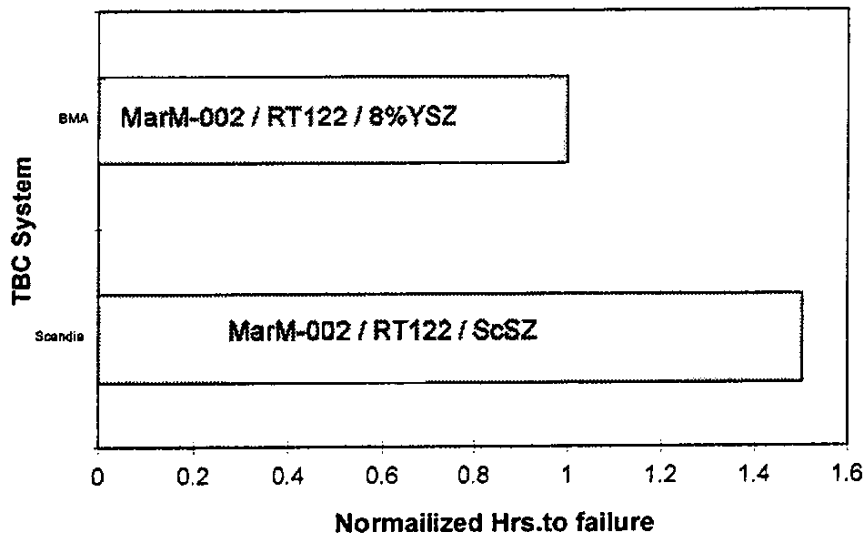


**Figure 41 New Ceramic with Improved Performance**  
Relative comparison of Scandia stabilized zirconia and conventional 8% YSZ TBC

#### 2.2.9.9.2.4.4 Thermal Barrier Coating Field Tests

Siemens Westinghouse has been field testing coated components for several years. Results from the TBC field test program provided information on the longevity and effectiveness of different coating systems. The tests were designed to compare coating longevity and effectiveness of air plasma sprayed and physical vapor deposition (PVD) TBC.

Tests on ring segments and blades with different coatings were initiated. These tests were carried out in W501D5 engines, and periodic inspection of these components were made visually. In addition to the tests, service performance monitoring of TBC coated W501D5 transitions, Row 1 vanes and Row 1 blades, has continued.

#### Test Plan

Twelve W01D5 Stage 1 turbine blades were coated and installed for long term field testing. Three coating configurations, of four blades each, were placed into service for field testing:

- 4 - blades with MCrALY bond coat and APS TBC
- 4 - blades with MCrALY bond coat and EB-PVD TBC
- 4 - blades with MCrALY bond coat only

Visual inspection of these blades was completed. Eight Row 1, W501F blades have been placed in service. Field testing of TBC coated W501D5 ring segments is also underway. After 8000 hours of operation, a limited visual inspection of the ring segments was made.

Table 13 describes components, component alloys and coatings that were included in the test sequence. Tests in Table 13 were conducted jointly with customers of W501D5 units. Additional ongoing tests in other Siemens Westinghouse frames with Row 1 blades and vanes along with coated transitions are in progress. In the later tests, the substrate material was varied to verify bond coat strength.

**Table 13 TBC Tests in Progress**

Component	Component alloy	Coating
Row 1 blades	U520	BC 1
	U520	BC 1
	U520	BC2
	U520	BC3
	U520	BC3
	U520	BC3
	U520	BC1
Row 1 Ring segments	CM247 (CC)	BC1
	IN738 (CC)	BC1
	SAS4 (DS)	BC1
	CM247 (CC)	BC3
	IN738 (CC)	BC3
	CM247 (CC)	BC1
	IN738 (CC)	BC1
	CM247 (CC)	BC1
	IN738 (CC)	BC1
	X-45 (CC)	BC1

#### 2.2.9.9.2.4.5 Test Results

Ring segments were visually inspected (see Figure 42) after about 8000 hours. Only one segment, coated with CoNiCrAlY + EB-PVD TBC, exhibited coating flaking at a corner (see Figure 43). The ring segments will be destructively inspected after 16,000 hours.

The transitions, Row 1 vanes and Row 1 blades were visually inspected. Photos of these parts are shown in Figures 44 and 45. Service hours are indicated in each figure caption.

#### 2.2.9.9.2.4.6 Conclusions

Results from the ring segment tests were encouraging, however, further testing was required. One out of 6 ring segments with EB-PVD TBC exhibited modest corner flaking in about 8,000 hours of operation. All the remaining coated segments had coating intact.

The transition inspections were favorable. TBC coating on the inner side of transitions extended the transition life significantly, and eliminated distortion.

Positive results from the coatings on blades and vanes are promising. APS TBC on Row 1 vanes extended the normal refurbishment interval. EB-PVD TBC on Row 1 blades was intact after 16,000 hours.

It is important to note that the tests were performed on commercial combustion turbines, not the ATS. The ATS will employ higher hot gas part temperatures and the performance of the coatings may not be the same. Additional testing on ATS engines are required before deployment into the commercial market.

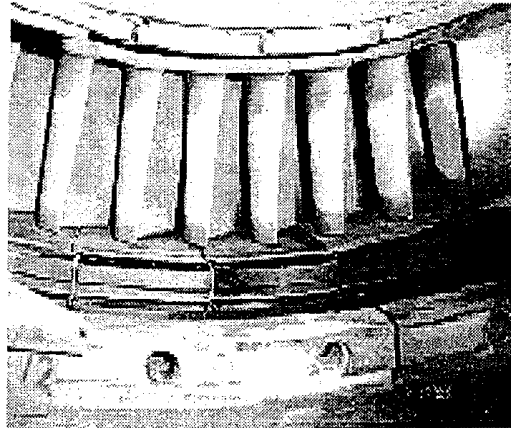


**Figure 42 Coated Ring Segments**  
General appearance, no coating loss (~8000 hours)



**Figure 43 EB PVD TBC**  
Some loss (~8000 hours)

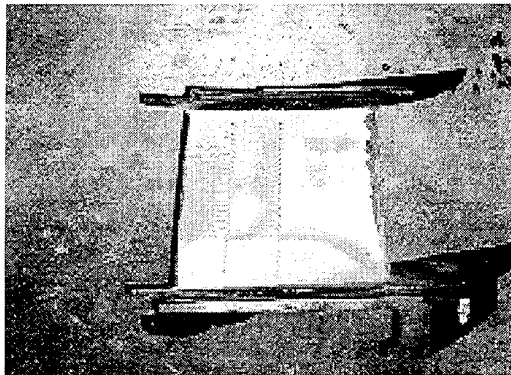


**Figure 44 Row 1 Vane**  
After 16,000 hours.

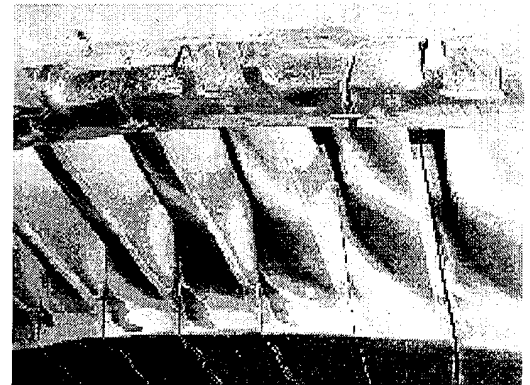


**Figure 45 Row 1 Blades**  
After 16,000 hours

#### 2.2.9.9.2.5 Task 8.37 Forged Disc Materials

New materials for production of high temperature discs and shaft components in the ATS Engine are required. Commercially available forgings in sizes needed for the ATS engine components are very limited. Developing and qualifying at least one supplier of high temperature disc and shaft components would proceed after identification of potential material suppliers.

Temperature and stress data for the various components of the turbine rotor were collected. The data revealed that turbine discs will be exposed to

temperatures and stresses above allowable levels for alloy steels. A review of the materials available for extended high temperature service was conducted using the design requirements as the basis. Materials from several different alloy systems were evaluated with regard to mechanical properties, availability, processing capabilities and cost. Results from the review identified IN-706 as the alloy that could meet design requirements.

Suppliers of IN-706 alloy were identified. Discussions with suppliers concluded that IN-706 discs could be produced in sizes large enough for the ATS engine. A specification for IN-706 discs was developed after meeting suppliers of the material.

A specimen of an IN-706 disc forging was obtained from both suppliers. A test plan was developed for measuring various material properties. Two suppliers of large Inconel 706 discs allows flexibility in material sourcing. An additional benefit of testing forgings from two different suppliers is that the data obtained will help identify the variance in properties from supplier to supplier and heat to heat. Sectioning and machining has proceeded on schedule. Material property testing is in progress and will be completed in Phase 3.

#### 2.2.9.9.3 Tasks 8.3 and 8.13 Last Row Blade Development

##### 2.2.9.9.3.1 Design Obstacles

The annulus area of the last Row blade must be as large as possible to achieve minimum exhaust losses. As blades become longer and more highly stressed, design methods become more precise and sophisticated to meet the demand for more efficient blades. Mechanically over-designed blades to compensate for imprecise design/calculation methodology are not acceptable.

The design of a long turbine blade is determined by thermodynamic efficiency and mechanical adequacy. The airfoil must be designed to have the optimum inlet angles and geometry to efficiently convert thermal energy into useful shaft torque. Mechanical materials properties, such as creep deformation and resistance to high-cycle fatigue (HCF) failures, must be evaluated.

A primary concern in blade design is the resistance of the material to high-cycle fatigue failure from time-dependent stresses. The primary excitation forces on a turbine blade are aerodynamic and can be either synchronous or nonsynchronous. The nonsynchronous forces are a result of turbine transients and the influence of combustors. The synchronous forces arise because the blade is rotating through a circumferentially non-uniform field which is fixed in space. This produces harmonic blade excitation forces which have frequencies which are integer harmonics of the turbine spindle rotational frequency. The magnitude of the vibratory excitation tends to be larger for the lower harmonics. Consequently, it is usually impractical to design long turbine blades strong enough to withstand resonance within the lower multiples of running speed. The lower modes are tuned to have their natural frequencies fall approximately halfway between the multiples of running speed. This will minimize the occurrence of high magnitude vibrations. Higher blade modes and complicated mode shapes make tuning impractical because manufacturing tolerances and material variability effect yields. The blades must be designed with sufficient

strength so that potential vibratory stresses will not exceed the fatigue strength of the blade.

Historically, long combustion turbine blades were designed for reliability by extrapolating previous successful designs. Blade strength was evaluated on the basis of steady stresses, since vibratory stresses could not be determined. The acceptability of a design was determined by evaluating design indices, which were compared with allowable values. The historical design index for HCF is the Magnification Factor (MF). MF is the ratio of local fatigue strength to the gas bending stress. This has been an adequate index for design of blades of similar construction. It does not explicitly consider the effects of damping or tuning.

The high cycle fatigue analysis and successful design of turbine blades requires a thorough knowledge of vibratory stresses and blade fatigue strength. Vibration stress is a function of frequency, mode shape, unsteady loading and damping. In recent years, technology has advanced to the point where 3-D finite element analysis is fast and efficient enough to be used as an effective design tool. Determination of vibratory stress is now a practical calculation procedure.

Testing methods have also improved. Verification and technology development testing on full-size turbines has provided important information on blade unsteady loads and blade damping. Numerous fatigue tests have been performed to determine the fatigue strengths of blading alloys at various temperatures and environments.

The stimulus method for estimating an index for HCF was selected. In this method, a design upper bound turbine vibratory force level, the "turbine stimulus", is defined. Stimulus is the ratio of unsteady loading to steady loading, at a given harmonic. The use of such an index implies that unsteady blade stress is approximately proportional to the turbine end loading. Vibratory stresses resulting from the upper bound force level are compared with the minimum material fatigue strength to determine a factor of safety (strength/stress). This approach considers damping and the modal characteristics of the blade in the calculation. The upper bound force levels, used in the design to ensure a minimum of 100,000 hour life, are deduced from the turbine tests. Another way of estimating turbine stimulus is through an analysis of field experience of existing designs. The excitation force level can be estimated from a knowledge of failure location, fatigue strength and the steady loading on the blade. The turbines stimulus level must be equal to or greater than the level required to produce a failure, for those cases where failures have occurred.

Having established a rational method for evaluating the vibratory stresses in blades, it becomes possible to examine the benefits of various types of construction for a given application. Selecting the optimum configuration also requires consideration of the processes involved in manufacturing. An iteration process between acceptable mechanical design and manufacturability continues until a safe practical blade is found.

#### 2.2.9.9.3.2 Design Approach

The objective of this effort was to develop an optimized last row blade with acceptable reliability and improved performance. Rational HCF design rules for combustion turbine blades are established in the process.

The available test data for interlocked blade damping and vibratory force levels was collected and reviewed. A design value for damping and turbine upper bound turbine vibratory force (stimulus) was proposed. Failure stimulus (safety factor) calculations for interlocked combustion turbine blade designs with operating experience were completed. This verification step was necessary to validate the proposed values against operating experience. Less successful designs failed the proposed criteria and were rejected.

#### 2.2.9.9.3.3 Design Results

Conceptual designs were performed for freestanding and interlocked blades with and without midspan snubbers. The reliability, efficiency, manufacturability and ease of assembly of each design concept was evaluated. An interlocked blades design was selected over the freestanding blade because of higher damping and better strength-to-weight ratio. The higher damping manifests lower vibratory stresses due to both forced and self-excited (flutter) vibration. The smaller physical size results in lower rotor stresses.

The final selected design was an interlocked blade with midspan snubber. This was the first known application of a midspan snubber to a cast combustion turbine blade. Midspan snubbers are widely used on steam turbine blades, which are generally longer than combustion turbine blades. The midspan snubber becomes more advantageous as blades become longer. A disadvantage for the snubber is the loss in performance from the snubber obstruction in the flow-path. An interesting factor was revealed during the design process. The airfoil can be better aerodynamically optimized with the snubber than without, which tends to offset the snubber loss. In fact, for the geometries considered in the evaluation, the midspan snubber design had overall better performance than the unsnubbed design.

Since this was the first application of a snubber to a cast turbine blade, manufacturability was a concern. Casting trials were performed using a similar existing airfoil and a mocked-up snubber to determine if the snubber design was feasible. The casing experiments were a success and, consequently, the design was completed.

The manufacture of the die patterns, tooling and gauges have been completed. A representative sample of Row 4 blades in the final design configuration has been manufactured. These blades have been dimensionally and metallurgically examined to determine if the manufacturing process is qualified to produce acceptable blades. It took several trial castings before a metallurgically acceptable blade was produced. Casting trials were successful and a manufacturing process was developed. The manufacturer has been qualified.

#### 2.2.9.9.4 Task 8.15 Active Tip clearance Control

Turbine blade tip clearance has a pronounced effect on the highly loaded front stages of the turbine. As a rule of thumb, each 1% tip clearance increase is accompanied with a decrease in stage efficiency of 2%. The ideal active tip clearance control system would maintain large tip clearances during startup, then decrease the clearance to minimum values when the turbine has achieved steady state operation.

##### 2.2.9.9.4.1 Conceptual Design

A conceptual design of a thermally actuated tip clearance control system was completed. The design consisted of an outer ring, which supports the high temperature segments that define the outer gas path around the rotating blades. The limiting point in setting tip clearance occurs at startup, when the maximum clearance is needed to prevent tip rubs. Before engine start-up had commenced, the ring was to be heated by an external steam supply, thereby expanding and increasing tip clearance. Heating the ring would effectively increase the tip clearance during the short lived start-up transient. Once the engine reached steady state the external steam supply could be removed. A limitation to this approach is evident. An external boiler is required to create steam before the engine came on line and before steam was available through the HSRG. The complexity of the steam heating manifold was further complicated by the obstruction of closed loop cooled vanes.

In addition to the actuating system development, testing of ceramic abrasion resistant coating was completed. These coatings are on the order of 0.050 inch (1.27 mm) thick. They provide: (1) thermal insulation for the mating, stationary ring segment to minimize required cooling air flow, and (2) a surface for the rotating blade tips to rub against without excessive wear. Such coatings have been under development for over 15 years by aero gas turbine engine manufacturers and their vendors. They are used in several production aero engines.

##### 2.2.9.9.4.2 Test Results

A coating vendor was selected to coat W501D engine Row 1 turbine ring segments for field testing. These pieces were installed in a W501D5 engine and tip clearance measurements were recorded for future comparison.

The vendor also coated and shock tested two test pieces. Testing was performed on a cyclic thermal rig capable of simulating engine heat flux levels. Test results demonstrated that the coating exceeded the vendor's coating specification shock resistance.

In addition to shock testing, the vendor completed abrasion testing of samples with their coating applied. The test determined wear characteristics of coatings and blade tips with simulated incursion rates and temperatures. Test results indicated that with the low incursion rates encountered in large industrial gas turbines, blade tip treatments would be beneficial in keeping blade tip wear within acceptable limits. Only a few blades in a given stage would need to be treated in order to minimize wear of all blades. Tip treatments would be unnecessary for designs where little rubbing would be expected.

## 2.2.9.9.5 Combustor Development

### 2.2.9.9.5.1 Catalytic Combustor

Catalytic combustion must play an important role in achieving ultra-low NO<sub>x</sub> emissions at advanced firing temperatures, especially in light of the exponential increase in NO<sub>x</sub> production with higher firing temperatures. A program to develop the theoretical background on combustion instabilities, carry out experiments to aid in the understanding of the problem, develop a generalized analysis procedure, and develop stability criteria for a particular combustor basket is a requisite part of developing a low NO<sub>x</sub> combustor for the ATS program.

#### 2.2.9.9.5.1.1 Initial Investigation

An investigation regarding the application of catalytic combustion to advanced ultra-low NO<sub>x</sub> combustors was initiated. Initial efforts focused on the relationship between catalyst effect and recirculation, flow turndown and durability. Catalyst light-off temperature for lean-premixed methane mixtures is typically greater than the compressor discharge temperature. Therefore, the combustor design must incorporate a method to raise the inlet gas temperature (such as exhaust gas recirculation [EGR]), raise the monolith surface temperature, decrease the catalyst light-off temperature (by enhancing fuel reactivity), or use an integrated combination of these approaches. Based on the ATS combustor conditions and geometry, the feasibility of several different integrated combustor designs was considered.

A combustor design using EGR was determined feasible by recirculating about 20% exhaust gas from 50% to 100% of base load. Several concepts were considered to extend the catalytic combustor operating range below 50% load. These included multiple pilots, variable EGR, heating the catalyst substrate and enhancing the fuel quality. One promising approach was to pre-react part of the fuel in a fuel-rich catalytic reactor to produce a highly reactive warmer effluent gas similar to syntheses gas production from methane.

#### 2.2.9.9.5.1.2 NO<sub>x</sub> Prediction

A computer program was written to predict NO<sub>x</sub> formation for a plug flow catalytic reactor with a downstream stabilization region. Various methane and NO<sub>x</sub> reaction mechanisms were examined for use in the model. The required reactor code modifications to predict emissions from a catalytic combustor with exhaust gas recirculation were investigated.

#### 2.2.9.9.5.1.3 Preliminary Design

Preliminary designs of several catalytic combustors were completed. In one concept, called the Multiple Catalyst Swirl Stabilized Burner (MCSSB), a catalytic pilot was integrated into the catalytic combustor. The pilot flame aids in stabilizing the premixed fuel/air mixture partially reacted in the catalytic reactor section. Two catalytic upper stages were envisioned to provide wider turndown. A second concept, the Advanced Catalytic Combustor, incorporated a catalytic reactor(s) into the pilot, to eliminate the diffusion flame fuel flow at higher load

conditions. In another design approach, a fuel pre-activator design was examined to eliminate EGR as a requirement.

Conceptual designs were completed and drawings were produced for the Multiple Catalyst Swirl Stabilized Burner (MCSSB) and Advanced Catalytic Combustor with integrated catalytic pilot and EGR.

#### 2.2.9.9.5.2 Task 8.16 Flow Dynamics and Visualization

Two and three-dimensional Fluent CFD modeling of two EGR concepts were completed. The computational and combustor venturi geometries were the same, however, the complex combustor swirler geometry was not modeled. Overall the 6° conical diffuser was predicted to do better than the elliptical diffuser design for both static pressure loss and mass of combustor gas recirculated. Static pressure losses were about one third less for the conical diffuser design.

Two EGR designs were provided for construction of the appropriate plastic model. Model construction required additions to an existing multi-swirl flow rig for atmospheric rig testing. Flow visualization tests were carried out on one model of the EGR combustor. The required flow area for 10% exhaust gas recirculation was established.

#### 2.2.9.9.5.3 Task 8.17 Combustor Noise

The combustor is one of the primary sources of noise in a power plant. The very lean premix combustion necessary to achieve ultra-low- NO<sub>x</sub> emissions compounds the noise problem. Very lean premix increases the likelihood of combustion instabilities with resultant noise and high vibratory stresses in the combustion system components and in the turbine blading. The objective of combustion stabilization is to extend the range of equivalence ratios over which low-emission combustion can occur without instabilities. Specific goals for the fulfillment of this objective included:

- the development of an active combustion stabilization control system in collaboration with Georgia Tech
- the design, assembly, and installation of a sub-scale combustion stabilization test section at the Siemens Westinghouse Science and Technology Center to provide an evaluation platform for the stabilization control system
- a successful sub-scale demonstration of the active stabilization of gas-fuel, lean-premix combustion at turbine operating conditions using the control system and test section developed in this program.

##### 2.2.9.9.5.3.1 Stabilization System Description

The concept of Georgia Tech's noise control system is to damp out combustion oscillations by modulating a secondary flow of fuel that is injected in close proximity to the flame. This system incorporates the following features in control technology:

- state observer software that can ascertain the frequency content of pressure or luminosity transducer signals within a few cycles of combustion oscillation; and
- a magnetostrictively actuated fuel flow modulator than can respond to control signal frequencies approaching 1 kHz.

Results from the observer software are illustrated in Figure 46. The figure is a reconstruction of an unstable-combustion pressure signal generated from output of the state-observer software. The solid line is the original time-history recording from a full scale, single-combustor test during a period of instability; the dashed line is the reconstructed version. The observer software has been integrated into a controller module for the control evaluation tests. Analog control signals generated by this module are amplified and input directly to the secondary fuel flow modulator. By driving the modulator with continuously updated signals of appropriate magnitude and phase, the controller introduces additional components of volume velocity fluctuation of the combustion gases such that the burning-rate oscillations are canceled.

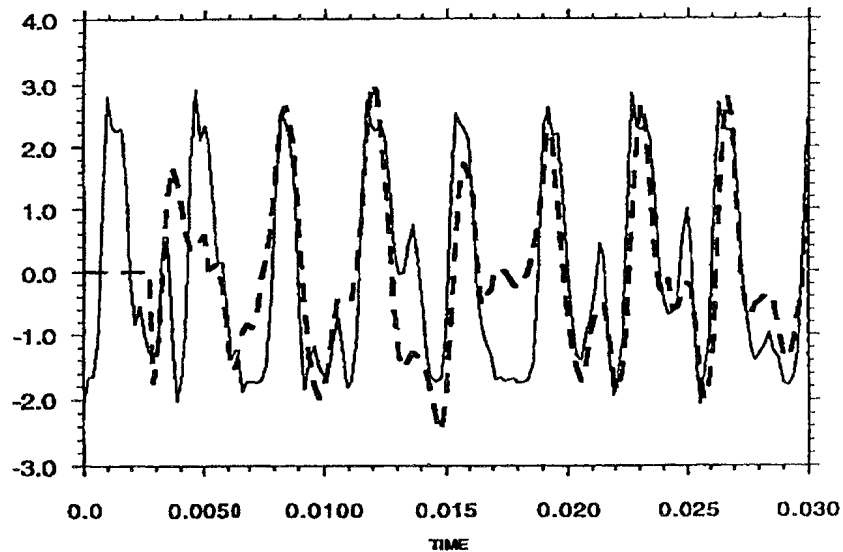


**Figure 46 Comparison of Simulated Pressure Signal (dotted line) with Actual.**

The fuel flow modulator furnished for the stabilization control evaluation is a scaled-up version of a prototype modulator that was used previously to demonstrate combustion controllability. Figure 47 shows measured combustion responses to fuel flow modulations imposed in test runs on a subscale, gas-fired, rocket engine. The top two graphs are time histories of luminosity signal from open loop control test runs at two different frequencies. The bottom two graphs are their corresponding frequency spectra. The throughput flow requirement for the present demonstration, 0.0013 lb/s ( $5.9 \times 10^{-4}$  kg/s) of natural gas at full flow, is substantially greater than that of the prototype modulator.

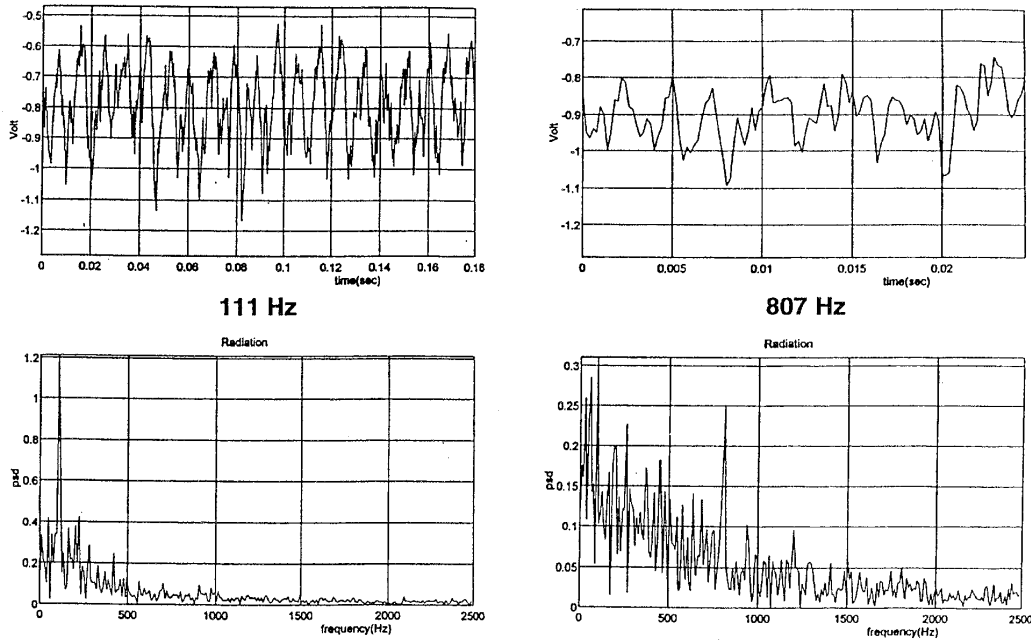


**Figure 47 Combustion Fluctuation Response to Secondary Fuel Oscillations. The oscillations were intentionally generated by the flow modulator over a wide frequency range**

#### 2.2.9.9.5.3.2 Sub-Scale Combustor Test Section Design

The primary subscale combustor requirements which were to be met in designing the test section included:

- main combustion to occur in a lean, premixed, single-stage natural gas flame with fuel gas introduced through a single primary fuel manifold and nozzle assembly;
- modulated secondary fuel flows for combustion stabilization to be introduced through a separate manifold and nozzle assembly;
- central disc for flame anchoring with integral igniter; and
- maximum total fuel flow rate of 0.013 lb/s ( $5.90 \times 10^{-3}$  kg/s).

The test section has been intentionally designed to have acoustically coupled combustion instabilities at full-flow conditions. As seen in Figure 48, the test section includes an inlet air vessel that acoustically isolates the combustor from the upstream compressed-air supply system; a spray cooler plenum isolates it from the exhaust system. Installation of the test section in the Siemens Westinghouse STC high-pressure, preheated-air test facility enables stabilization testing at gas-turbine operating conditions.

The test combustor, Figure 49, resembles a simplified version of a Siemens Westinghouse engine combustor having dimensions that are scaled down about 10-fold radially but having axial dimensions to keep the acoustic frequencies representative of full-scale combustors. Modulated flow of secondary fuel is

injected at the slot between the flame holder and its thermal barrier in the stabilization test combustor. A fuel/air premix swirler was added at the premix primary fuel nozzle location upon the suggestion of DOE-NETL. A  $ZrO_2$ -coated, secondary-fuel-cooled thermal barrier precludes erosion of the flame holder. A mounting platform, not shown in the figure, is provided for the mounting of the Georgia Tech fuel modulator on the OD surface of the pressure vessel.

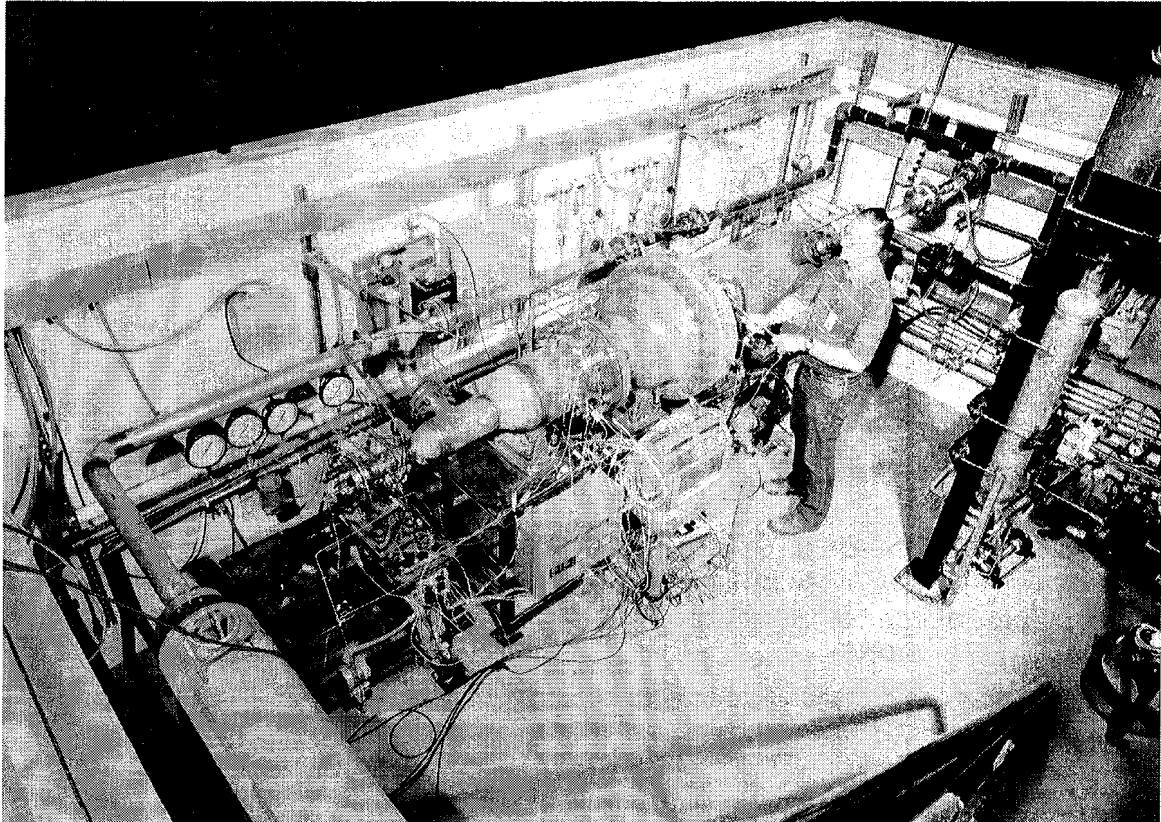


**Figure 48 High Pressure, Preheated Air Test Facility**

The portion of the vessel to the immediate right of the inlet air flange (center of far wall) acoustically isolates the combustor from the air supply system. The spray cooler plenum on the right isolates it from the exhaust system.

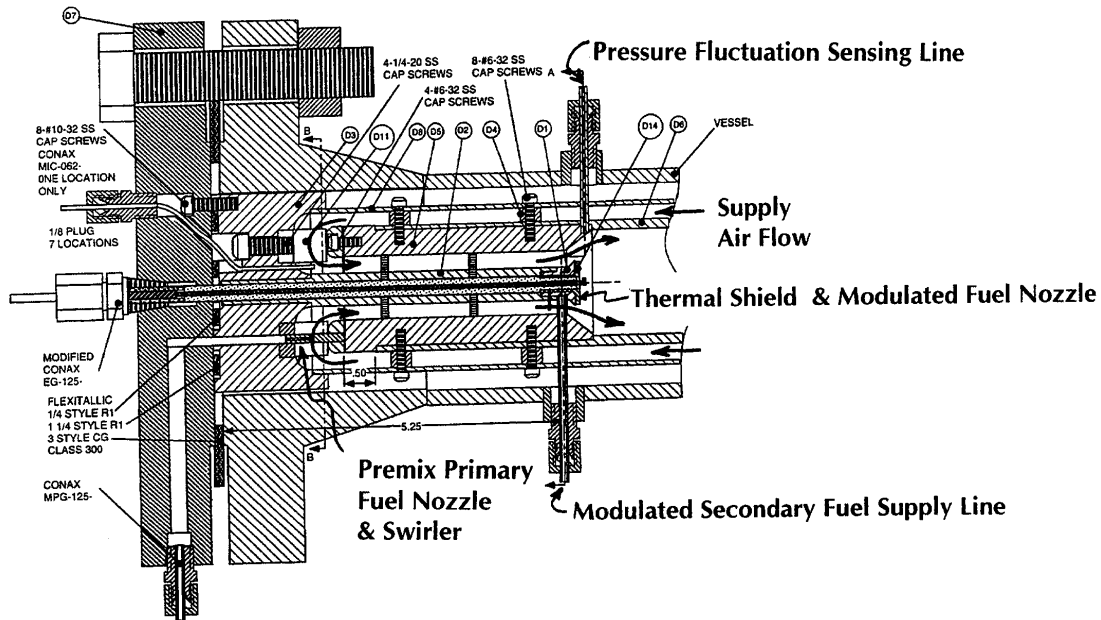


**Figure 49 Scaled Down Test Combustor**

#### 2.2.9.9.5.3.3 Experiment Construction

Georgia Tech investigators designed and fabricated a new, larger modulator to accommodate the needs of this program. Some minor design revisions to reduce back-transmission of combustor pressure oscillations to its internal components were completed after initial testing. Open-loop combustion tests in a sub-scale, gas-fired rocket engine verified that the enlarged modulator provided the necessary flow modulation amplitudes over the desired frequency range (frequencies up to nearly 1 kHz).

Software and electronics for the state observer and control algorithms were assembled into a stand-alone controller module. The module and fuel modulator were shipped to the Science & Technology Center for integration into the sub-scale combustion test setup.

Several design iterations were completed to resolve issues of safety, access, ignition and flame anchoring, and accommodation of high temperatures. The assembled components were instrumented for steady and fluctuating pressures, temperatures, and flow rates. Features were added for mechanically interfacing the fuel modulator to the combustor.

Procedures were established for lighting off the combustor and ramping up to full-power conditions in a manner that was compatible with the operation of the test facility's safety system. Changes made to the test combustor to enable lightoff at higher mass flows and stronger modulation of the combustion rate included:

- relocation of the secondary fuel nozzle to the slot between the flameholder and the thermal shield and

- enlargement of the premix primary fuel nozzle orifices to reduce the fuel flow resistance.

#### 2.2.9.9.5.3.4 Test Results

Variations in overall mixture ratio and main/secondary fuel flow split were introduced so that the operating regions of combustion instability could be mapped out. Instabilities such as shown in the Figure 50 waterfall plot were observed. The waterfall plot shows the frequency spectra of the test section prior to the installation of the active stabilization system. Instabilities were observed at about 220 and 530 Hz at 150 psi (1.034 MPa), 720°F (382.2°C) and 0.007 lb/sec (0.0032 kg/sec) inlet air flow.

The active cancellation of lean-premix combustion instabilities under combustion turbine operating pressures, temperatures and flow velocities was successfully demonstrated at reduced scale as illustrated in Figure 51. Future efforts to improve control effectiveness will include optimization of actuator location, scale up of combustor/actuator and more extensive system characterization.

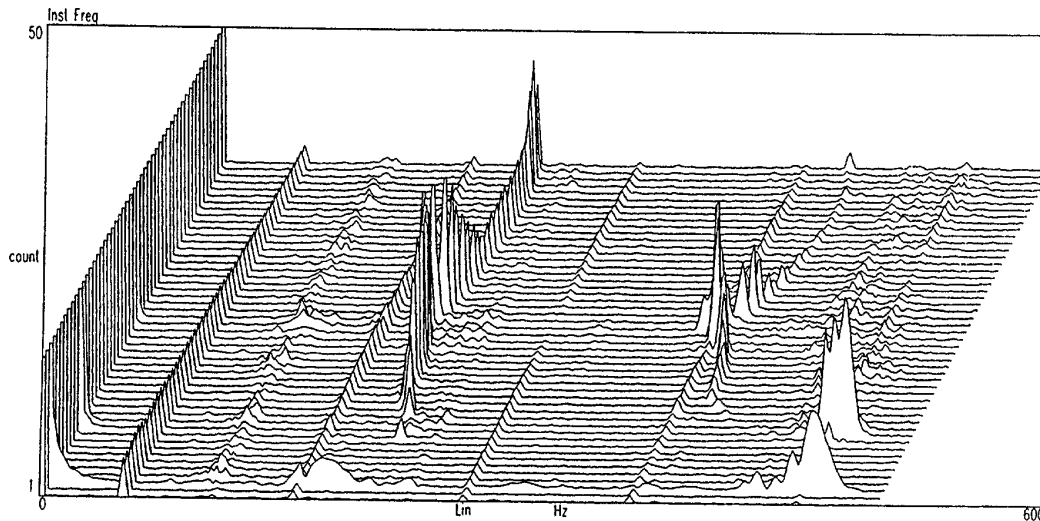


**Figure 50 Frequency Spectra of Oscillations Before Active Stabilization**

#### 2.2.9.9.5.3.5 Conclusions

This effort on active combustion stabilization has increased the viability of advanced ultra-low NO<sub>x</sub> gas-turbine power generation by demonstrating a control approach that:

- enables operation at leaner fuel/air ratios and lower NO<sub>x</sub> emission levels than otherwise possible;
- increases engine component life by reducing damaging pressure oscillations; and
- may reduce far field sound pressure levels, allowing attainment of noise guarantee

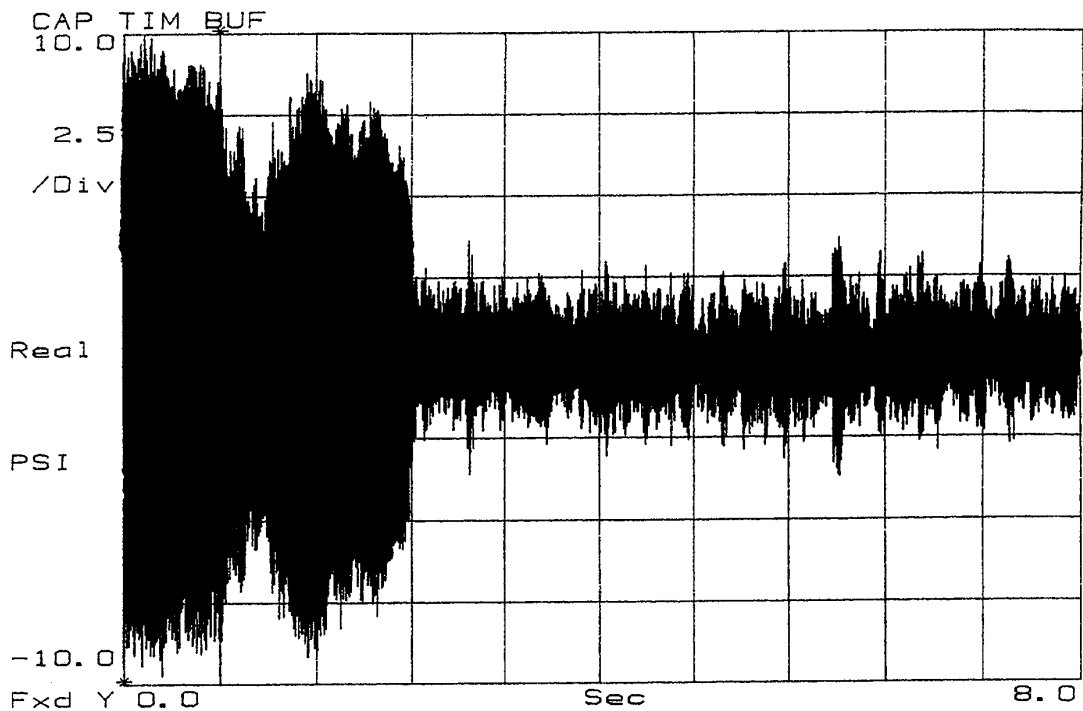


**Figure 51 Measured Pressure Responses Before and After Active Cancellation.**  
Four fold reduction in pressure oscillations occurred within 0.1 seconds.

#### 2.2.9.9.6 Tasks 8.23, 8.24 and 8.29 Seal Development

Over the last decade, research and development of brush seals has flourished in response to potential uses and leakage superiority of brush seals over conventional labyrinth seals in aero gas turbines. Brush seals can be installed wherever labyrinth seals are currently located in a gas turbine, with significant leakage reduction. Applying brush seals to industrial combustion turbines is attractive because the engines run primarily at constant speed where the seals do not encounter radial clearance excursions with the mating rotating surface and have significantly fewer transient closure cycles than aero engines.

The ATS Phase 2 advanced air sealing development effort focused on applying brush seals in the ATS combustion turbine engine.

Design requirements for applying brush seals in combustion turbines include:

- Good durability to accommodate handling, field installation and operation,
- Being segmented because combustion turbines have a horizontal split casing,
- Run against uncoated rotors because of cost and manufacturing issues associated with large combustion turbine rotors,
- Good sealing even after wear from repeated start-up cycles.

The program examined brush seals for large combustion turbines that could significantly reduce leakage flows while meeting design, life, durability, and cost requirements. The development effort consisted of:

- A preliminary investigation to look at the benefits, potential locations, feasibility of running against uncoated surfaces, and validation required in applying brush seals to combustion turbines
- A focused development effort for one selected engine location. Focused efforts for other engine locations are the subject of subsequent tasks.

The seal effort included:

- A concept study
- Tribology testing
- Fabrication of rig hardware
- Rig testing of candidate brush seals

#### 2.2.9.9.6.1 Preliminary Investigation

The first task done in the preliminary investigation was a cost/benefit analysis of replacing labyrinth seals with brush seals at various locations. Locations considered included the turbine interstage seal and rim, the compressor diaphragm seals, and the turbine front seal. Representative results showed that reduced leakage from incorporating brush seals would improve plant efficiency by one-sixth to one-fourth of a point depending upon location. Further, the reduced leakage also increases system power output.

A second task was to determine the start-up and steady-state operating conditions for the various seal locations. This task is ongoing as the ATS engine is being designed. Transient variations of seal inlet pressure, pressure drop, air temperature, speed and closure were determined from engine start-up conditions and finite-element analyses. Figure 52 shows transient trends of engine speed and seal closure for the turbine interstage.

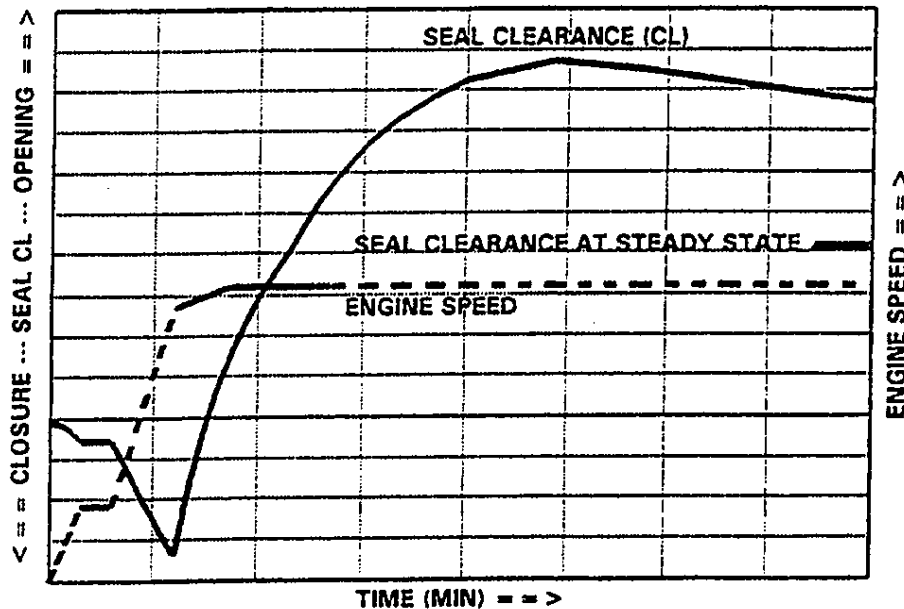


**Figure 52 Start-up Cycle for a Turbine Interstage Location**

A brush seal operating with the start-up closure characteristic in Figure 52 will initially wear line-to-line at steady-state. Each time a start cycle is incurred, cumulative bristle wear occurs as a result of the interference. Because of the relatively short duration of the start-up cycle, many start cycles are required before a brush seal would wear line-to-line at the maximum closure point. But even after such wear, the leakage rate will still be less than with labyrinth seals because the bristle tip clearance will be less than labyrinth seal operating clearances.

A third task in the preliminary investigation was to conduct preliminary tests to determine the feasibility of running brush seals against uncoated rotors. In the preliminary tests, the turbine interstage seal location was chosen to model engine operating conditions and geometry. Two dynamic, subscale tests were run at ambient temperature: one where the rotor was offset repeatedly for many cycles to model the interstage seal conditions during engine start-up, and the other was with a constant interference equal to the maximum interstage closure level. Both tests were run with rotors made of a material having a composition, surface roughness, and hardness matching Siemens Westinghouse turbine rotors. The seals tested had similar stiffness, bristle pack thickness, backplate gap, etc. as would be expected for a full-size brush seal.

Figure 53 is a photograph of one of the turbine rotors tested. A polished wear track can be seen on the outer diameter where the seal bristles ran against the surface. Leakage, wear, and surface characterization results demonstrated that a brush/uncoated rotor surface seal configuration could have a service life approaching that required for heavy duty gas turbines. Based on these preliminary tests, the focused brush seal development tasks were initiated.

A fourth task in the preliminary investigation was to determine possible validation tests. A search was made of available host Siemens Westinghouse combustion turbines. The W501F and W501G engines were selected for the validation tests.

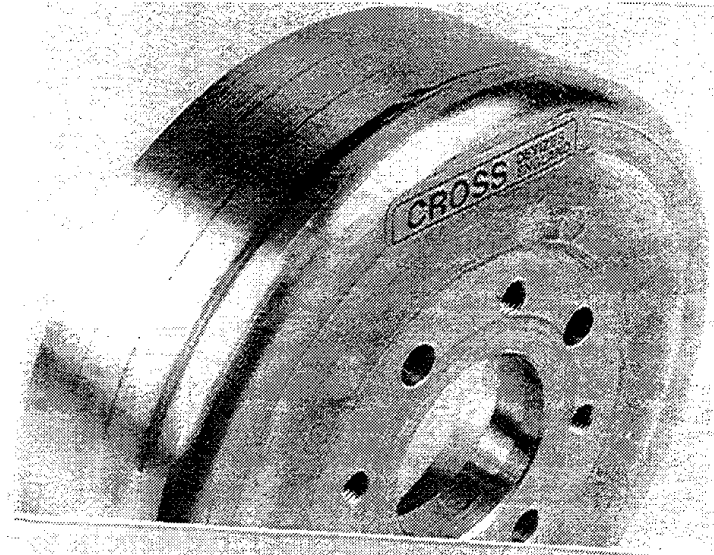


**Figure 53 Uncoated Rotor Used in Test**  
Note polished bristle wear track.

#### 2.2.9.9.6.3 Focused Seal Development

The initial development for these ATS activities was for brush seals to be incorporated into the turbine. This location was chosen because of its higher potential benefit to plant performance.

The focused development addressed the technical challenges of sealing in the given location, i.e., running a brush seal against an uncoated rotor, and design optimization for negotiating transient radial closure while still achieving minimal leakage at steady state. The development consisted of three separate efforts:

- Design of seals to meet the operational requirements,
- Tribological study in which various bristle alloys are run against current and future rotor materials, and
- Extensive subscale rig testing to assess performance of selected design configurations.

The overall objective of the design effort was to identify and include features to accommodate the transient closures, subsequently evaluated during the subscale testing effort. A specific objective was to estimate the transient variation of interference, surface speed, and pressure drop that can be accommodated by these designs. This was also evaluated later during subscale testing. Engine operating conditions were taken from the preliminary investigation. The materials selected for the subscale rotor were identical to the engine rotor materials for the selected location. This is important from the standpoint of reproducing the engine tribological environment. The bristle alloy selected for the seal designs is in accordance with tribological test results. A chart depicting the design methodology being used in design selection is given in Figure 54.

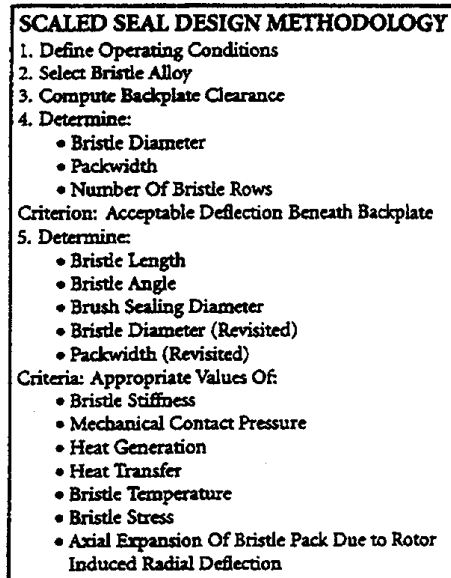


**Figure 54 Subscale Seal Design Methodology**

Seal design operating interference was selected in order to obtain a minimum steady-state clearance (i.e., leakage rate) after the cumulative wear of many starts (i.e., several hundred cycles). A large initial interference could result in excessive heat generation, high temperature, and rapid wear. Conversely, a low initial interference would yield a clearance larger than necessary at steady state, hence higher leakage.

The tribological testing was done using a high speed friction test rig (Figure 55). Miniature brush seals were run against uncoated rotors in the absence of a pressure drop to quantify friction and wear behavior under aggressive conditions. Tribopair combinations of five different bristle alloys and two rotor materials were tested. Each tribopair was first tested under cyclic conditions. After ten cycles, each tribopair was then tested for one hour at constant speed and temperature. Rotors were tested with two different surface roughness values to determine the effect of roughness on frictional heating and wear of the bristle alloys.

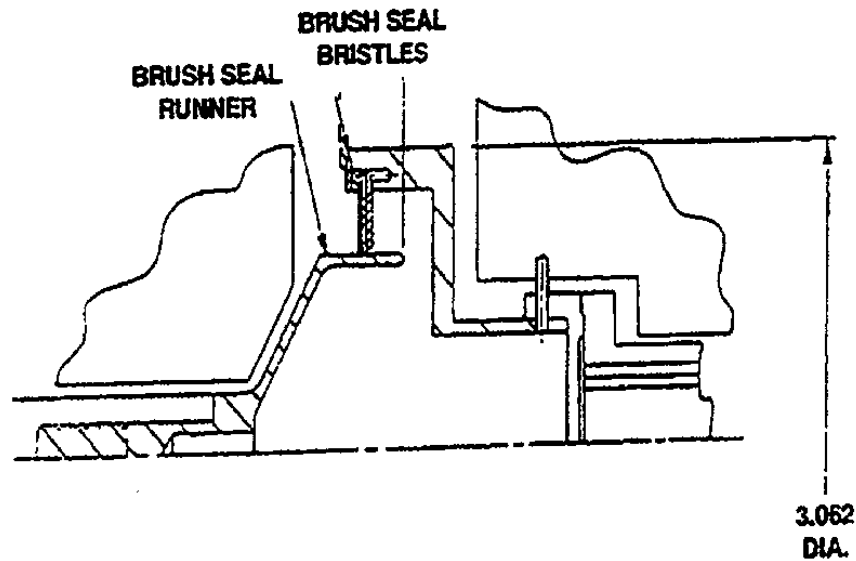


**Figure 55 High Speed Friction Test Rig Used in Tribological Testing**

Approximately forty different tribopair tests were conducted. Bristle wear and frictional heating results confirmed the feasibility of running against uncoated rotors, indicated the best bristle allows to run against the two rotor materials, and quantified a maximum desired rotor surface roughness.

In the subscale rig tests, one-fourth size brush seals were tested under the severe cyclic conditions representative of an actual engine turbine location. The important cyclic conditions modeled were pressure drop, air inlet temperature, surface speed, and interference (both decreasing and increasing closure). Cyclic interference was simulated by a prescribed variation of axial location on a stepped rotor with an intervening cone and speed. Prior to commencing cyclic tests, the seal was run dynamically at room temperature and viewed with a borescope from the upstream and downstream sides. During cyclic testing, seal leakage characteristics were determined every 50 cycles or so, and the seal was periodically removed to measure bristle and rotor wear. High magnification photographs were taken of the rotor surface and seal to define the tribological surface conditions. A special eccentric rotor test was also conducted with a rotor having an offset center to model whirl at engine rotor critical speeds.

Seals were tested for hundreds of cycles until the bristles wore line-to-line at the maximum interference point in the cycle. The expected seal leakage increase with wear was quantified under the simulated engine conditions. Measured flow characteristic data are directly applicable to engine conditions to define the flow savings over conventional labyrinth seals versus the number of start-up cycles. The data indicated the relative merits of the seal designs. The separate eccentric rotor tests showed how brush seals respond and wear when the engine rotor whirls as it passes through critical speeds.

These ATS activities were very successful and showed the feasibility and benefit of implementing brush seals in the turbine interstages. Results were used to define the best brush seal configuration for turbine interstage engine validation

testing and guide seal selection for the compressor diaphragm, turbine rim and turbine front seal in ATS.

#### 2.2.9.9.7 Diagnostics Instrumentation

New materials and turbine design require diagnostic instruments to measure the performance of critical parameters. These instruments were critical to optimizing combustor and blade design. Two developments from previous ATS work were continued.

The first development involved an optical diagnostics probe to observe the dynamics of combustor basket internals. The new combustors must be tested to verify performance. A means to monitor flow and composition undisturbed is necessary to obtain in site maps of flow/composition gradients. Understanding the dynamics of the combustor internals enables the designer to locate localized sources of NO<sub>x</sub> generation. Design optimization can proceed with this knowledge.

The second development involved a turbine blade vibration monitor. Modifications to engine cylinders, combustors, transitions and blade rings change the flow and thermal characteristics in unpredictable patterns. The blades must tolerate many different forces in adverse conditions. Vibration monitoring is used extensively to gauge the health of rotating machinery before a catastrophic event occurs. Field testing of the first ATS installation requires blade vibration monitoring for performance verification.

##### 2.2.9.9.7.1 Tasks 8.20 and 8.36 Optical Diagnostics Probe

The optical diagnostics probe was developed to allow measurement of important parameters inside combustor baskets without disturbing the main flow. This probe is instrumental in designing and developing combustor baskets. In site mapping of fuel/air mixing aids in optimizing flow patterns that reduce harmful emissions.

A non-intrusive optical diagnostics probe, using laser induced fluorescence technique, was developed (see Figure 56). The probe was designed, fabricated and tested in a small scale test rig. The probe was tested successfully at ambient temperature and atmospheric pressure, as well as at elevated temperature and up to 10 atmospheres. Limitations in cylinder accessibility and probe reach became apparent. A second generation probe (see Figure 57) was designed to overcome these limitations. The new probe was approximately twice as long as the original probe. The modified probe incorporated a new metal mirror, a target collection lens, and a thermocouple located at the tip to measure probe tip temperature. Provision was made for water cooling. The probe was calibrated at high temperature and pressure. Testing proceeded at atmospheric pressure and high temperature. Good results were obtained in both fired and unfired tests. The next series of tests will be on the K-point type combustor, that has a complete set of CFD analyses solutions for comparison with the test results.

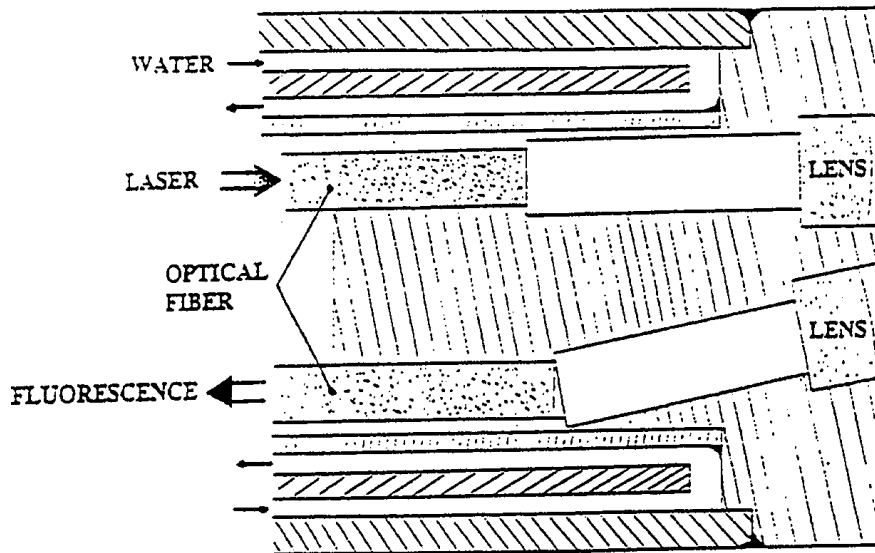


Figure 56 First Generation Optical Probe

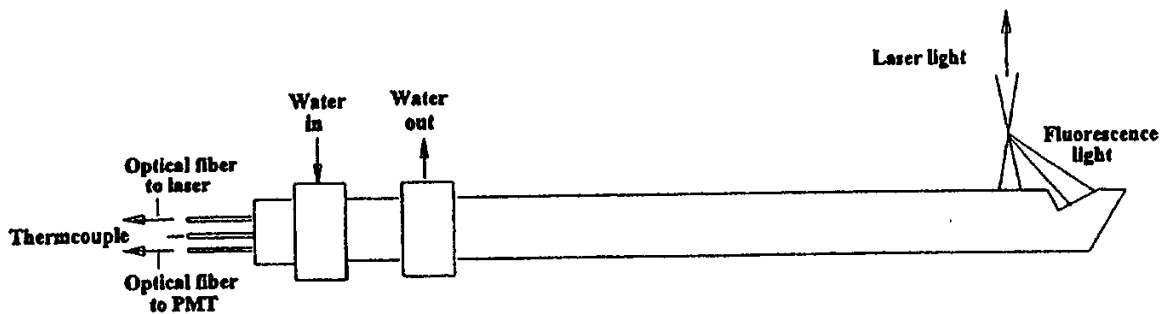


Figure 57 Second Generation Optical Probe

#### 2.2.9.9.7.2 Task 8.26 Combustion Turbine Blade Vibration Monitor System

Current methods used to verify turbine blade stresses in the field rely upon instrument strain gauges placed on several blades in the row. This method of testing is limited since: (1) strain gauges tend to fail after short periods of time, and, (2) only a small portion of the blades can be instrumented simultaneously, due to cost constraints. Siemens Westinghouse developed a BVM system for steam turbine application because of these limitations. The monitor incorporates eddy current or magnetic proximity probes that detect blade tip deflection. Blade stresses are derived from the deflection measurements.

Based upon the success of the steam turbine BVM, Siemens Westinghouse has pursued the development of a BVM system for use in high temperature combustion turbine applications. Combustion turbines run at much higher temperatures than steam turbines. An infrared (IR) sensor and a 2-probe sapphire lens IR system was developed to overcome the potential overheating conditions. The combustion turbine BVM was installed in one unit at a customer

site in the Fall of 1994. The 2-probe system has a limitation that allows monitoring at nonmultiple running speed frequencies ("nonsynchronous") only. Based upon the subsequent success of the 2-probe system, a 16-probe BVM IR system was developed and installed into a unit in the Spring of 1995.

Two systems were developed for field testing at a customer site. A 2-probe system was initially developed to verify the design basis. After the design basis was field proven, an improved model was conceived. A 16-probe system was subsequently developed with necessary modifications. The BVM consists of a set of IR probes mounted through the blade ring. The probes are directed to view the top of Row 4 turbine blade shrouds (Figure 58). IR sensors detect changes in emissivity. The 2-probe system is limited to determining nonsynchronous (non-multiple of running speed) frequencies while the 16-probe system can obtain synchronous and nonsynchronous frequencies.

All work, including field testing, has been completed. Turbine blade frequencies and vibratory stresses have been verified against known stress levels. Instrument software and reporting functions have been refined. The sixteen probe version of the BVM is ready for its intended function when ATS becomes operational.

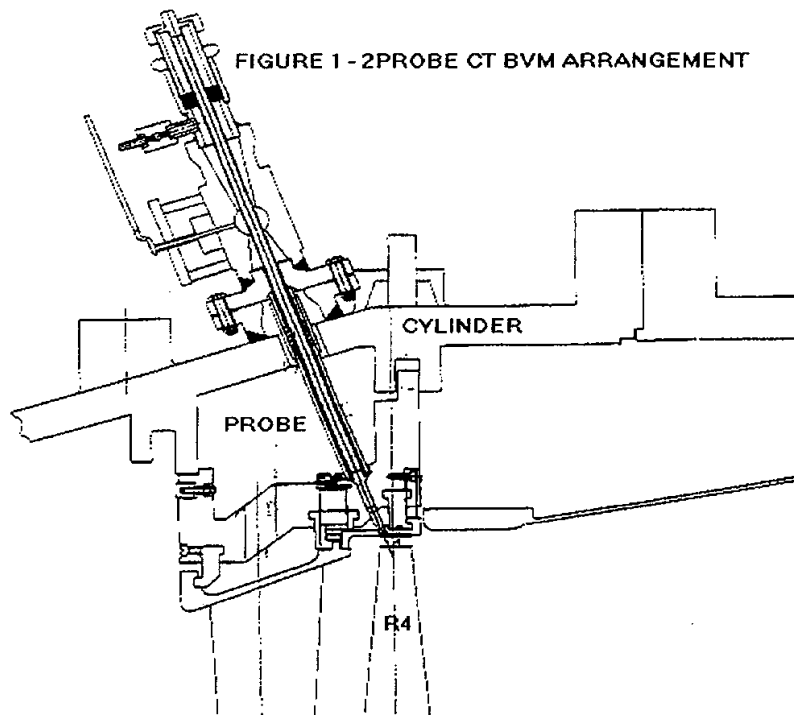


**Figure 58 Two Probe CT Blade Vibration Monitor**

#### 2.2.9.9.8 Tasks 8.8 and 8.21 Diffuser Extraction Study

The flow structure within the diffuser/combustor section of an advanced Siemens Westinghouse gas turbine has been studied. This study was conducted to provide information which can be used to minimize pressure losses, optimize air flow uniformity into the combustors and evaluate the effect of air extraction for

advanced integrated gasification combined cycle (IGCC) applications. The work was performed in several stages:

- Computational study was made to provide direction for the experimental portions of the study
- Experimental studies were performed to determine the flow characteristics of a baseline case with no air extraction and
- Experimental studies were performed to evaluate the effect of air extraction through a single port on the wall of the combustion shell

The results of this study are being applied to development of the pre-diffuser/combustion shell of an ATS combustion turbine.

#### 2.2.9.9.8.1 Computational Study

The diffuser/combustor section includes components from the exit of the compressor to the inlet of the turbine. The turbine utilizes a can-annular arrangement with 16 combustors. The major components consist of the turbine casing, the annular pre-diffuser, the dump diffuser, the combustor "top-hat" and the combustor/transition assembly. A solid model of the diffuser/combustor section of the turbine under consideration was constructed. Except for the rotor cooling pipes, the geometry is periodic every 1/16th (22.5°) in the circumferential direction (one combustor/transition assembly). Within the 1/16th sector, a plane of symmetry runs through the middle of the combustor/transition assembly. Thus, a 1/32nd sector was modeled to direct the experimental effort and provide information that would not have been obtainable through computational means.

These results show that the majority of the flow exiting the pre-diffuser passes between the combustor-transition assemblies into the upper portion of the dump diffuser. Only a small amount of air flows through the lower section of the dump diffuser. Hence, air enters the combustor top-hats preferentially from the upper dump diffuser. This air then flows through the annular passage between the top-hat and the combustor liner; past the cross-flame tubes and into the combustor. Velocity profiles in the annular passage were integrated across the annular gap and the mass flow distribution was determined.

This mass flow distribution is somewhat redistributed by the time the flow reaches the cross-flame tubes; however, a mass flow deficit is formed in the wake of the cross-flame tubes. This deficit is still evident at the inlet to the combustor, resulting in an apparent high degree of non-uniformity into the combustor. This result was not borne out by the experimental portion of the program and may have been a result of the outlet pressure boundary condition which was applied at the combustor inlet. A more appropriate location for this boundary condition may have been the outlet of the transition. However, as will be shown later, the experimental phase of the program did corroborate the preferential mass flow distribution toward the top half of the top-hat.

#### 2.2.9.9.8.2 Experimental Study

A 48% scale, 360° model of the diffuser-combustor section was fabricated to study the flow structure and losses in the diffuser-combustor section. The experiments were performed under cold flow conditions and then scaled to actual machine conditions through the use of a conventional flow parameter. A scaled down model of the Siemens Westinghouse DLN Multi-Nozzle combustor (Figure 62) was fabricated to analyze the air mass flow distribution into the combustor. The remaining 15 combustors were simulated using cylinders containing orifice plates that were sized to yield the same effective area as the scaled combustor.

Static pressure was measured at regular intervals along the inner and outer surfaces of the annular pre-diffuser and the pressure recovery coefficient was defined as

$$C_p = \frac{2(P_S - P_{S,in})}{\rho_{in} U_{in}^2} = \frac{(P_S - P_{S,in})}{h_{dyn}}$$

where;

$P_S$  - Local Static Pressure

$P_{S,in}$  - Static Pressure at the Inlet to the Pre-Diffuser

$\rho_{in}$  - Air Density at the Inlet to the Pre-Diffuser

$U_{in}$  - Air Velocity at the Inlet of the Pre-Diffuser

$C_p$  - Static Pressure Recovery Coefficient

$h_{dyn}$  - Dynamic Head at the Inlet of the Pre-Diffuser

It represents the fraction of the dynamic head into the pre-diffuser that is recovered as static pressure. Figure 64 shows the variation of the pressure recovery coefficient from the inlet to the exit of the pre-diffuser along three different planes in the circumferential direction. Ideally, the pressure recovery coefficient can reach unity if the flow was decelerated to zero velocity in a reversible process.

The benchmark value is based on studies of optimum diffuser geometries. The close agreement between the values measured for the pre-diffuser and the benchmark value indicates that the pre-diffuser is very efficient at recovering static pressure. Based on this finding, the ATS pre-diffuser design will be based on the current pre-diffuser design.

A number of measurements were performed to determine the velocity field at various locations throughout the combustion shell in order to characterize the performance of the dump diffuser. The experimental data confirms the CFD results that showed the majority of the flow passing through the top section of the dump diffuser with the lower section of the dump diffuser containing low velocity,

recirculation zones. Measurements in the annular gap between the combustor liner and the top-hat also confirm the CFD result which showed air entering the top-hat preferentially from the top section of the dump diffuser. Air flow then partially redistributes around the top-hat as the flow moves toward the combustor inlet. The large flow deficit regions behind the cross-flame tubes, which were predicted by CFD, were not evident in the experimental measurements.

The effect of 5 and 20% air extraction through a single port in the side of the combustion shell was studied for use in rotor cooling and IGCC applications. Based on results of this study, some important conclusions have been made regarding air extraction.

Air extraction of 5% (typical of rotor cooling needs) does not seem to significantly affect the flow field in the combustion shell, pressure drop or air mass flow distribution into the combustor. On the other hand, 20% air extraction (typical of IGCC application needs) through a single port has a significant effect on the flow patterns within the combustion shell. Perhaps the most significant manifestation of this effect can be seen in the mass flow distribution into the combustors. One of the main nozzles in the scaled down combustor was fitted with a hot-wire probe such that the tip was just upstream of the swirler inlet. The mounting technique allowed it to be rotated within a main swirler such that the average velocity into each main swirler (eight main swirlers per combustor) could be determined. The swirler located at  $0^\circ$  is furthest away from the machine centerline and  $180^\circ$  is closest to the machine centerline. All sets of data show the trend of preferential mass flow through the upper half of the combustor (since air flows preferentially into the upper half of the top-hat). The difference between the cooling pipe increases the flow into the combustor.

The flow structure within an advanced Siemens Westinghouse gas turbine was studied using a computational fluid dynamics model and a 48% scale experimental model. The major findings of this study were

- The current annular pre-diffuser design at the exit of the compressor performs very well and will be incorporated into the ATS design,
- Air flow is unable to make the sharp turn at pre-diffuser exit required to flow into the lower dump diffuser and most of the air flows into the upper dump diffuser,
- Air flows preferentially into the upper half of the top-hat and hence, into the top of the combustor.
- Five percent air extraction through a single port on the combustion shell does not significantly affect flow characteristics within the combustion shell, and
- Twenty percent air extraction through a single port on the combustion shell significantly affects flow characteristics within the combustion shell and should be avoided.

#### 2.2.9.9.9 Task 8.25 High Efficiency Compressor Design

Siemens Westinghouse's ATS engine is based upon a single shaft combustion turbine operating at an optimized pressure ratio. The pressure ratio was selected to maintain optimum exhaust temperature. All components must operate at optimum levels to achieve the target overall ATS efficiency of 60%. The compressor designs used in previous models had to be modified for increased efficiency.

The development of the ATS compressor has been accomplished in two steps:

- Advanced aeroengine aerodynamic and mechanical design tools were used to develop the blading 19:1 pressure ratio compressor, and
- Using the first 13 stages from the 19:1 compressor design, slightly modifying the blading in stages 14 through 16, and adding 4 additional stages (16 through 20).

The first step was completed and is explained below. The second step was completed in Phase 3.

Step one in the high efficiency compressor design was carried out using the following process:

- Meanline aerodynamic models were created for a series of compressors with gas path geometries varying from constant outer diameters, through gooseneck, to a W501F clone. Stage aerodynamics were optimized under each configuration, and results were compared in terms of efficiency, surge margin and risk.
- Further refinement of design point aerodynamics was made until each stage was operating near its maximum efficiency.
- Off-design prediction of compressor performance to verify that operating extremes would not result in major problems.
- CDA (controlled diffusion) airfoil shapes were designed along flow surfaces to maximize efficiency. Leading and trailing edge minimum radii were imposed to maintain reliability. Maximum thickness was set through repeated iterations to achieve rigorous frequency and stress requirements. Optimization of each stage was driven by minimizing thickness (lowers profile losses) against acceptable mechanical properties (i.e., stress, vibration, speed, etc.).
- Hot running clearances were calculated considering transient differential thermal growths, centrifugal stretching and all mechanical and build tolerances.
- Three dimensional viscous analyses were performed on each row during the design process to check on aerodynamics, and to produce surface pressure distributions for mapping directly onto the airfoil for mechanical analysis.

The analysis system was verified against the known characteristics of the W501F compressor. It was found that the model predicted mass flow and efficiency within a tolerance band acceptable for design purposes.

The results of analysis at off design conditions prompted changes in the axial chords in the initial stages to allow for better hot weather, under frequency operation. Analyses were conducted at the extremes of cold and hot weather, near 25% surge margin. Compressor operation was stable for a temperature range of -40° to 122°F (-40°C to 50°C) and under frequency condition at 57 Hz.

## 2.2.10 Conclusions

Different power extraction cycles were evaluated for their potential to achieve the ATS performance targets. Various thermodynamic cycles, including thermochemical recuperation, compressor intercooling, and reheat were considered, but eliminated from consideration, in general, due to these technologies not being able to support the ATS program schedule. An advanced 420 MW combined cycle with an ATS combustion turbine and new steam turbine/generator was selected to meet the ATS Program targets.

The advanced combined cycle differs from state of the art combined cycle in many aspects. The firing temperature is 250°F (139°C) higher than current production models, yielding some improvement in efficiency. To further enhance plant efficiency, the ATS combustion turbine incorporates advanced materials, coatings, cooling concepts, sealing designs and 3D aerodynamic designs. Closed-loop steam cooling is employed in hot end components for both performance improvement and NO<sub>x</sub> reduction.

To achieve the emissions targets, an ultra lean premix combustor is employed.

To ensure that ATS Program goals are achieved, the following design improvements were investigated:

- Cooling concepts, including closed-loop steam cooling
- Sealing, including brush seals
- Active tip clearance control
- Combustion system, including catalytic combustion
- Diffuser extraction (combustion cylinder flow investigation)
- Optical diagnostics
- Blade vibration monitor system
- Advanced metal alloys, including SC and DS
- Thermal barrier and anti-corrosion coatings
- Ceramic/CMC materials

- Effects of steam on turbine materials
- High efficiency compressor design
- Increased Row 4 blade exit area for reduced exhaust diffuser loss.

In addition to the ATS hardware development, specifications for the remaining plant equipment were written during the Phase 2 program. A site arrangement and electrical one-line diagrams were drafted for the conceptual natural gas-fired ATS plant. The plant design incorporates proven flexible design features that minimize design changes usually required to tailor a plant to site constraints.

The combustion turbine exhaust gases will pass through a three pressure level heat recovery steam generator before exhausting out the stack. The steam system is a triple pressure unit with vacuum deaeration that allows the addition of duct firing at a later date. Materials are commercial grade commonly used in today's boilers.

The steam turbine utilizes a single reheat cycle. Steam exhaust flow necessitates the use of a double-flow LP exhaust. The combustion turbine, steam turbine and generator are on a single shaft. Both turbines share a common hydrogen cooled generator.

Two coal-fueled power plant technologies were selected to power the CFATS: ATS air-blown, integrated gasification combined cycle and second generation pressurized fluidized bed combustion. Both concepts are being demonstrated in major Clean Coal Technology Programs. The coal-fired ATS plants rely upon gas turbine combustors, which burn hot, low BTU coal derived fuel gas, and turbine expanders that operate effectively on combustion products cleaned at high temperatures. The difference between the two coal technologies in their adaptation to ATS is the fraction of air removed from the turbine case for coal processing and the location of the combustors. Additional development work required to retrofit ATS to coal fuels will include the design of a low-BTU, low emission, fuel gas combustor; combustor outlet manifold and turbine inlet scroll; designs to mitigate corrosion/deposition; and material selection. Preliminary calculations show that coal fired ATS plants can achieve efficiencies in the range of 52 to 54%.

The market potential for the ATS gas turbine, in the 2000-2014 time frame, was assessed using analytical screening curves, product life cycle curves, market demand forecasts by world region, and appropriate fuel cost scenarios. The markets for the ATS in simple combined cycle and integrated gasification combined cycle applications were separately evaluated. Three ATS engine sizes were assumed and market comparisons were performed with respect to W501F and W501G frames. The total ATS market potential was predicted to exceed 93 GW in the forecast period. The combined cycle market represents the greatest opportunity for the ATS, because it will have the greatest economic advantage. The smallest ATS frame, 100 -150 MW, will be most attractive for the simple cycle market. After market introduction, ATS is expected to follow a typical S-shaped market penetration. The combined market for ATS-based technology could reach 12 GW per year by the year 2014, representing roughly 10% market share relative to the total global market. Each ATS product is expected to

achieve maximum market penetration approximately 7 to 10 years after initial demonstration. The ATS IGCC is expected to follow a similar penetration curve, but will reach ultimate market share at the end of the forecast period due to its later introduction.

To support the work within Phase 2, a description of the environmental, safety, and health information was provided by each subcontractor to enable DOE to prepare the appropriate documentation for the project. This information included a brief description of the project, a discussion of the environmental characteristics of all sites and any potential environmental impact from the project, a discussion of the impact from the seven criteria pollutants in the Clean Air Act, impact to surface and ground water, a description of the use of land for the project, a site waste management plan, noise generation, information regarding archaeological, cultural, and historical resources that maybe effected and plans to protect worker safety and health.

## **2.3 Phase 3/ Phase 3 Extension**

### **2.3.1 Introduction**

The Phase 3 scope included completion of research and development activities commenced in Phase 2 and development of the hardware specifications. The follow on Phase 4 activities were to consist of manufacturing, constructing and testing of a full-scale natural gas fired ATS Plant. Due to a cut back in funding, Phase 4 was not activated. It was replaced by Phase 3 Extension, which consisted mainly of continuing Phase 3 activities. Originally, a full speed no load (FSNL) ATS engine test was planned for Phase 3 Extension. FSNL test was not carried out due to ATS Program redirection. Emphasis was placed on technology development and completing W501G engine development. W501G was the platform to be used in demonstrating and validating the different technologies developed in the ATS Program. With enhancements, such as closed-loop steam cooling and ceramic components, W501G was to evolve into the ATS engine, which would achieve the 60% efficiency goal. In addition, there was a downflow of ATS technology into older as well as current production engines, such as W501D5A and W501F. Introduction of these technologies, such as advanced aerodynamic design, sealing and coating systems, as well as DLN combustion systems, would result in an immediate public benefit of reduced energy consumption and emissions, prior to the actual ATS engine introduction.

The Phase 3 activities described in this section, included:

- ATS engine design
- Plant, auxiliaries and BOP specification
- Study on the conversion of gas fired ATS to coal/biomass fuel
- Research in cooling, sealing, aerodynamics, combustion materials, and mechanical development
- W501G validation testing

- Advanced viscous compressor design verification testing

### 2.3.2 Task 1 NEPA Information

In the original ATS Program plan the Phase 3 objective was to complete the research and development program and hardware specification for the conceptual design completed in Phase 2. Phase 4 was to consist of manufacturing, constructing, and testing a full-scale natural gas fired ATS plant. However, congressional budget constraints impacted Phase 4 activities. In response to a DOE request, a Phase 3 Extension with a reduced Phase 4 scope was proposed. This reduced scope included construction of a dedicated ATS engine test facility at Siemens Westinghouse's existing Turbine Generator Plant at Charlotte, North Carolina, and carrying out the initial "No-load" demonstration testing of the ATS engine. A "Task 1.0 NEPA Information Report" was produced to demonstrate that this "no-load" testing would not cause significant impacts to the environment. Because of financial constraints and program redirection, the "no-load" test was abandoned.

### 2.3.3 Task 2 ATS Engine Design

The purpose of this task was to design all the critical ATS engine components and to produce the required manufacturing drawings. The ATS engine design specification was prepared and in conjunction with the Siemens Westinghouse Design Criteria Manual used as the basis for the detail engine design. To ensure that this engine would achieve its performance, emissions and mechanical integrity goals, the latest state-of-the-art aerodynamic, combustion/emissions, secondary airflow, heat transfer, mechanical and vibration analysis computer codes were employed. Figure 65 shows the ATS engine cross-section.

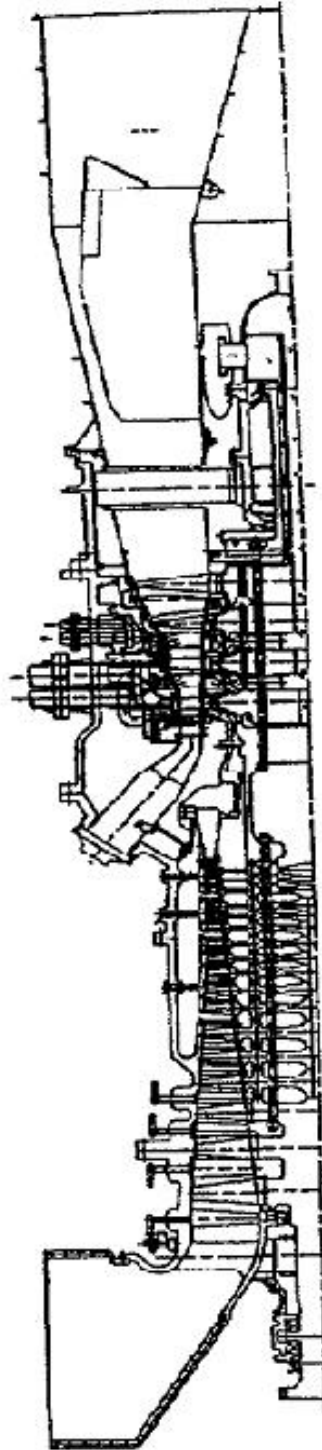


**Figure 65 ATS Engine Cross-Section**

The ATS Engine design concept was based on a mix of well proven Siemens Westinghouse design features with innovative, performance enhancing advanced technology. The 60% combined cycle efficiency had to be met while maintaining structural integrity and engine reliability. A risk analysis of ATS engine design had identified where the highest probability and consequences of risk exist. Mitigation plans to counter any identified risk have been initiated.

The 20 stage ATS compressor design philosophy was based on that used for the advanced W501G compressor, but with additional enhancements. The W501G compressor was a new aerodynamic design using reduced number of stages, controlled diffusion airfoils, and reduced airfoil thickness. An optimization study conducted on the W501G compressor showed that 16 individually optimized stages will maximize efficiency for the 19:1 pressure ratio design. Continuing the gas path and stage optimization for an additional 4 stages would result in the higher pressure ratio ATS compressor design. To produce the final ATS design, the inlet casing had to be modified as required, and the necessary design effort associated with additional variable stators in the ATS compressor was included. The required modifications to the last stages of the W501G compressor and the design of the additional rear stages were carried out. This effort included aerodynamic and mechanical flow path design, disc(s) design and compressor exit diffuser design.

The compressor rotor was constructed from an integral inlet shaft forging, which contained the first two rotating stages and the generator coupling, and 18 individual discs, machined from low alloy steel and Ni base alloy forgings. The axial disc(s) and shaft assembly were held together with 12 IN-718 compressor thru bolts. The engine torque was transmitted through use of special radially aligned IN-718 shear pins and friction between adjacent compressor disc faces. The shear pin concept has been fully proven on the W501G engine design. The first 13 compressor disc(s) and compressor blades were identical to the W501G compressor, which was designed during the ATS Phase 2, while the remaining 7 stages are unique to ATS. Nickel based alloys were used in the rear stages of compressor discs, compressor blades and compressor diaphragms in order to provide adequate parts life.

The final ATS combustor basket and transition design were to be completed in the combustion system development program. This task included the design effort related to the complete layout of the combustion system, transition duct support, transition outlet seals, igniters, fuel piping, closed-loop cooling piping, top hat covers, and miscellaneous details.

The four stage ATS turbine was an extension of the advanced W501G turbine design. The design was based on 3-D design philosophy and advanced viscous analysis codes. The airfoil loadings were optimized to enhance aerodynamic performance while minimizing airfoil solidity. The reduced solidity resulted in reduced cooling requirements and increased efficiency. To further enhance plant efficiency, the following features were included: turbine airfoil closed-loop cooling, active blade tip clearance control on the first two stages, improved rotor sealing, and optimum circumferential alignment of airfoils (which is also referred to as clocking). The turbine flow path design was covered in this task. Included in this design effort were the blade ring assembly components, interstage seal housings, turbine discs, torque tube seal housing, and rotor cooling piping.

The first two stages of turbine vanes were closed-loop steam cooled and the first two stages of turbine blades were closed-looped air cooled. The third stage vane and the third stage blade, which incorporated a “locked” tip shroud, were air cooled. The fourth stage was uncooled. The fourth stage had a “locked” tip shroud and a mid-span snubber to reduce its vibratory response and hence vibratory stresses. SC, DS, and CC alloys, as well as advanced bondcoat/TBC systems were employed on the turbine airfoils, as required, to achieve the performance, service life and cost targets. Thin wall castings were used on the first stage vanes and blades to aid in the cooling design of the closed-loop systems and insure that the mechanical design criteria would be met.

Considerable design effort was devoted to the steam cooling system and secondary air system design. Challenges were overcome in piping and manifolding the coolant steam into the engine, to the transitions, and the first two stages of vanes, and then returning the spent steam to the bottoming cycle. Special attention was paid to the flexible couplings on the steam piping connections to ensure minimum leakage as well as durability. The secondary air system design goal was to provide adequate cooling air to the air cooled components with minimum of unwanted leakages. This applied especially to the closed-loop air cooled components.

The turbine rotor design consisted of four bolted alloy steel discs with nickel based side plates for containing and guiding the cooling air to the individual blade rows. The cylinder and blade ring design followed the Siemens Westinghouse practice except for the use of higher grade steel and thicker walls in some locations. These modifications were necessitated by the higher temperatures and pressures, as well as presence of steam in the ATS engine. The exhaust diffuser and manifold design also followed the Siemens Westinghouse practice and was optimized for aerodynamic performance.

#### 2.3.4 Task 3.0 Specification and Design of Power Plant Equipment

The ATS Plant will be based on the advanced combined cycle. The ATS Plant utilizes a single shaft design concept which incorporates a gas turbine on one end of the generator and a steam turbine on the other. The gas turbine is coupled to the generator in the typical manner. However, the steam turbine is coupled to the generator through a self-shifting, and self-synchronizing clutch which is connected to the generator’s collector shaft.

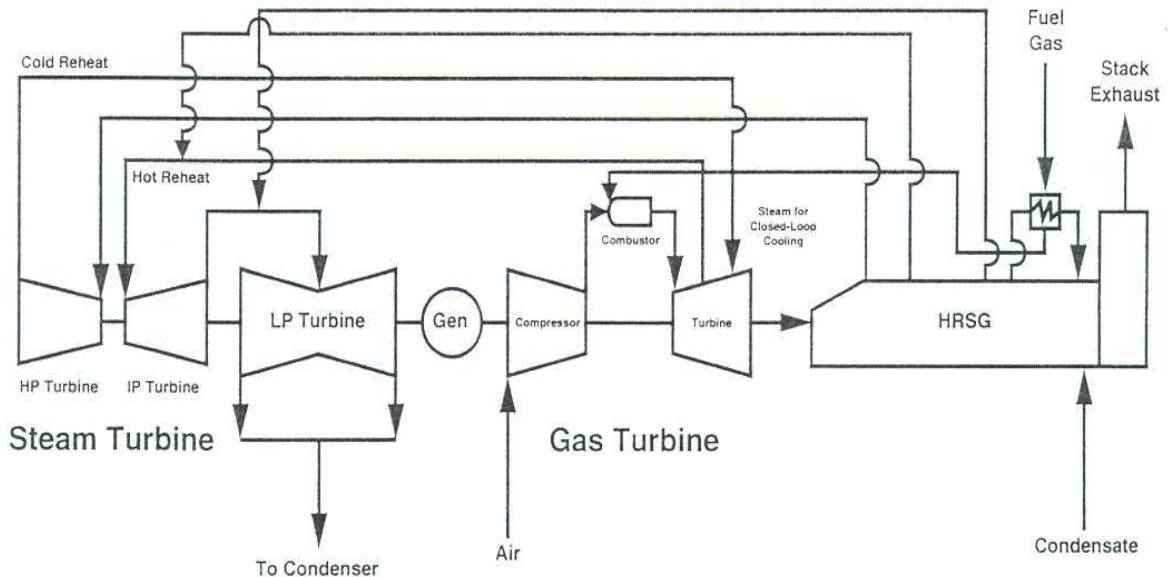


**Figure 66 ATS Plant Layout**

The gas turbine exhaust gases will pass through the three-pressure level heat recovery steam generator (HRSG) before being exhausted through the stack. The two case, multi-stage, single-flow reheat, axial exhaust, condensing steam turbine employs advanced 3-D aerodynamic design methods. High performance bowed impulse and reaction blades are used on the high pressure and intermediate pressure turbines, respectively. Optimized reaction blading is used on the low pressure turbine which includes 42 inch (1.07 m) long last stage rotating blades. The high pressure steam turbine exhaust steam is utilized to cool the transitions and the first two stages of turbine vanes. The reheated steam is returned to the steam cycle for reheat and induction into the intermediate pressure steam turbine. The two-pole, 60 Hz, hydrogen inner-cooled generator design absorbs the combined gas turbine and steam turbine power output. The generator operates with static excitation and supports static starting of the gas turbine. To achieve high efficiency, several design enhancements, such as reduced windage and core losses and improved insulation, were incorporated.

The ATS conceptual design was based on the 240 MW Reference Plant developed by Siemens Westinghouse for its W501F product. This design incorporated flexible proven design features that minimized design changes usually required for customizing the plant to local conditions. The 240 MW Reference Plant used multiple separate shafts and separate generators. After a considerable investigation, a single shaft approach was selected for the ATS Plant in order to optimize efficiency and minimize plant cost. The ATS design specified a single shaft for both the combustion turbine and the steam turbine and a single large generator coupled to the same shaft and located between the turbines.

The objectives of this task included preliminary design and specifications of the support systems auxiliary equipment required for the combustion turbine operation. This auxiliary equipment was designed to provide the plant operator with a complete optimized safe operating system.

The auxiliaries design emphasized modular construction to facilitate and assembly. Shop fabrication was specified to minimize field assembly. Where possible, complete packages were to be assembled, piped and wired in the factory, such that only interconnections would be required at the site. Pipe racks would be used to eliminate the need for extensive field pipe fabrication during construction.

Preliminary design and specification was carried out in the following auxiliary systems:

- Inlet system, consisting of the filter assembly, inlet duct and silencer, which is required for combustion turbine operation and ensuring that acceptable acoustical levels emanate from the combustion turbine inlet.
- Compressor water wash system.
- Mechanical package, including lube oil system and reservoir for the combustion turbine and generator, and instrument air system and pressure switch and gauge cabinet.
- Control system, including the following subsystems: combustion turbine, combustion turbine auxiliaries, generator auxiliaries, steam turbine, steam turbine auxiliaries, closed-loop steam and air supply, single shaft clutch control and combustion turbine start.
- Fuel control system, for both gas and oil fuels.
- Fuel preheat system to enhance engine performance. Fuel preheating will be done in two stages: heating the natural gas supply using a standard fuel gas heater (using plant feedwater) and then heating the fuel in the HRSG superheater section before entering the combustion turbine.
- Generator design specification.

#### 2.3.5 Task 4.0 Specification and Design of Balance of Plant Equipment

Objectives of this task were to initiate design and develop specification for the balance-of-plant equipment.

Preliminary steam turbine design was carried out for the three pressure level advanced ATS steam turbine, which is comprised of high pressure, and intermediate/low pressure sections.

Preliminary specification was produced for the Heat Recovery Steam Generator (HRSG). The HRSG will be a triple pressure design without integral deaeration (deaeration to be accomplished by separate vacuum deaeration). The HRSG will be horizontal with natural circulation and will supply main steam to the cycle at

1800 psia/1050°F (12.4 MPa/566°C), intermediate pressure steam at 560 psia (3.86 MPa), and low pressure steam at 70 psia (0.48 MPa). Other ATS plant systems investigated were electrical equipment, controls, mechanical systems, and other miscellaneous equipment such as condenser, cooling tower, circulating water pumps, boiler feed water pumps, control valves, and water treatment system.

### 2.3.6 Task 5.0 Plant Performance Analysis

The purpose of this task was to ensure that the ATS plant performance objectives would be achieved.

Throughout the ATS Program the CC plant efficiency and output power were estimated using in-house proprietary performance codes and the commercially available GATE Cycle. The input used in this estimation was the detail aerodynamic performance of the different gas turbine engine components, steam turbine, generator, HRSG and BOP equipment. The output was the net, LHV based CC plant performance. As the detail design progressed and new aerodynamic performance for the different components was generated, the plant performance was updated continually. The final results showed that the 400 MW class ATS Plant would achieve its 60% efficiency goal.

Quantitative analyses were carried out on risks associated with the identified key technical barriers to the success of the ATS Program. The analyses followed a rigorous structured five step process used in the aero engine industry. These analyses were performed on the ATS engine, individual engine and test rig components and critical tests. For all risks identified as having a high likelihood of occurrence and high resulting consequence, if they did occur, mitigation plans were developed and in many cases carried out to reduce the risks or eliminate them.

### 2.3.7 Task 6.0 Market Study

The ATS Market Study was covered in Section 2.2.6 in Phase 2.

### 2.3.8 Task 7.0 and 12.6, Adaptation of ATS to Coal and Biomass Fuels

#### 2.3.8.1 Introduction

The ATS gas turbine has been designed to fire natural gas as its primary fuel. It may be important to be able to adapt the ATS to the utilization of less costly, solid fuels, such as coal and biomass, in the future. Coal-fueled, Integrated Gasification Combined-Cycle power generation (IGCC) is a newly commercialized power generation technology that is expected to become a major technology for power generation in the future. A renewable fuel, biomass is also expected to become a significant contributor to smaller-scale IGCC power generation in the future in some locations of the world. Another advanced power generation technology closely related to IGCC is Advanced Pressurized Fluidized-Bed Combustion (APFBC). APFBC has been under development for several years and is in the early stages of commercial demonstration in Japan. This section focuses on the application of the ATS gas turbine to coal-fueled APFBC and IGCC power generation. The potential performances of these power plants are estimated, and those ATS turbine modifications needed to integrate

with them are discussed. This section also briefly considers biomass adaptations.

Fuel gas quality guidelines for the ATS gas turbine in APFBC and IGCC application have been based on specifications in place for the W501F gas turbine. The gas quality specifications are stringent, but they are achievable in IGCC applications using current gas cleaning technologies. Gas cleaning is more challenging for APFBC than for IGCC applications.

The natural gas-fired ATS turbine can be adapted to coal and biomass fuels to produce electricity with high power plant efficiencies and acceptable power plant emissions. The IGCC configuration evaluated in this report, consisting of an oxygen-blown, entrained gasifier using coal fuel gas cleaning and partial air-side integration, represents a state-of-the-art, conservative approach that has achieved commercial status. The APFBC configurations evaluated in this report, consisting of an air-blown carbonizer and a pressurized fluidized-bed combustor (PFBC) burning the carbonizer char product, and using high-temperature gas cleaning (limestone desulfurization and ceramic hot gas filters), represents a developmental, higher risk approach, specifically focused on high thermal efficiency.

The less mature APFBC technology provides several challenges to the ATS turbine. The thermal efficiency of the APFBC power plant is estimated to be far superior to any other coal-fired power plant technology, including IGCC, but plant reliability and availability would be expected to be less than for IGCC. The APFBC plant emissions are expected to be only slightly better than current, commercial coal-fired power plant technologies. The fuel gas and vitiated air streams supplied to the turbine are at high-temperature and high flow rate conditions that make integration much more difficult than in an IGCC plant. ATS turbine design modifications in the areas of the combustors, the compressor, the expander and the power island controls are extensive and must be coupled with development testing. The APFBC fuel gas and vitiated air streams are subject to possible contaminant levels (particulate and alkali metal vapor) that might exceed the ATS fuel contaminant specifications. The APFBC coal processing system itself needs extensive development and demonstration activities to reach a status where reliable power plant operation might be expected.

#### 2.3.8.2 ATS Turbine Adaptation to APFBC

The estimated performance results show that the APFBC-ATS net power is more than 30% greater than the net power output from a natural gas-fired ATS gas turbine power plant. The APFBC-ATS power plant efficiency is in excess of 52% (LHV) and is greater than the efficiency of any other coal-fueled power plant technology. While the selected APFBC operating conditions provide the potential for very high power plant efficiency, these conditions are difficult for the ATS turbine to adapt to, and the power plant is characterized by technology feasibility issues and potential availability and reliability concerns.

The estimated composition of the APFBC carbonizer fuel gas delivered to the ATS combustors is acceptable for gas turbine combustion, but it has a lower heating value than established turbine fuels. The large flow of very hot (1578°F, 859°C), low heating value fuel gas, and the larger flow of very hot oxidant from a

source external from the turbine are significant differences from the established natural gas combustor conditions.

The Siemens Westinghouse Multi-Annular Swirl Burner (MASB) has been developed as the topping combustor for the APFBC application. The major consideration in the design of the topping combustor is to provide a reliable combustor that will achieve acceptable NO<sub>x</sub> emissions when burning hot, low heating-value fuel gas containing fuel-bound nitrogen with hot, vitiated air. The MASB has been subscale model on natural gas and fuel gas has proven successful. Initial testing of the full scale MASB on natural gas was successful, and the MASB has demonstrated robustness by operating over a wide range of conditions that might otherwise seriously damage a more traditional combustor.

Unlike the ATS, the APFBC plant has the potential for particulate and alkali metal vapor contaminants in the gas turbine expansion gas, especially at the selected operating conditions. Estimated ATS turbine erosion results indicate that small particle penetration (0.5 ppmw) into the turbine expansion gas can be tolerated, with the predicted time before reblading being greater than that expected for normal blade life. Medium penetration (5 ppmw) reduces the APFBC reblading interval to 13,000 hours. Turbine deposition in the ATS turbine is a potentially more severe problem than erosion, although it may only require periodic water washing to recover. ATS turbine deposition with small particle penetration (0.5 ppmw) into the turbine expansion gas is significant, with the predicted time interval before airfoil washing being 1,500 – 13,000 hours, depending on the nature of the particulate. Medium penetration (5 ppmw) reduces the APFBC-ATS washing interval to 150 – 2,000 hours.

The APFBC-ATS power plant emissions in this study are particulate matter, SO<sub>2</sub>, NO<sub>x</sub>, CO, unburned hydrocarbons (UHC), CO<sub>2</sub>, and solid waste. Particulate emissions from the plant are very low, having satisfied the turbine erosion and deposition criteria. The SO<sub>2</sub> emission is controlled by limestone-based sulfur removal in the carbonizer and fluidized bed combustion, and levels of removal up to about 98% should be achievable. While the MASB is capable of very limited NO<sub>x</sub> generation from fuel gases (thermal NO<sub>x</sub> and fuel nitrogen), the vitiated air issued from the APFBC will have relatively high NO<sub>x</sub> content that will not be reduced in the MASB. Therefore, overall plant NO<sub>x</sub> emissions will be relatively high. CO and UHC will meet expected local emissions standards for gas turbines. The CO<sub>2</sub> emission from the plant per unit of electric output will be low relative to other coal-fueled power plant technologies due to the APFBC plant's high efficiency. Plant solid waste will consist of ash, and reacted limestone waste and will increase in amount as the sulfur removal efficiency is increased.

Required modifications to the ATS fuel system, turbine casing, shaft, and controls represent design development issues that can be addressed using current engineering methods, but must still be demonstrated through prototypic testing. The extent of ATS turbine modifications needed to accommodate the APFBC conditions is represented by the large increase in the mass and volumetric flows of the very hot fuel gas, the large flow of externally-supplied, hot vitiated air, the large increase in the ATS turbine mass flow, and the large ATS compressor air extraction requirement.

The combustion turbine cylinder from the compressor discharge to the turbine inlet will require major design changes for APFBC. The casing inlet, manifold/inlet scroll and outlet arrangement would be modified from the gas fired ATS (GFATS) to duct the combustion products by transition liners into a uniform annular flow. Engineering analysis must be performed, considering heat transfer analysis, stress analysis, pressure drop analysis and computational fluid dynamic analysis. Engine shaft thrusts must be reviewed and thrust bearings redesigned, if required. The combustion turbine bedplate mounting will also be substantially modified in the APFBC case.

Special consideration must be given to the operation and control of the APFBC-ATS plant with hot gas cleaning. Operation includes start-up, load follow, and shutdown – planned and emergency.

### 2.3.8.3 ATS Turbine Adaptation to IGCC

The IGCC-ATS power plant efficiency is estimated to be about 13 percentage-points lower than the natural gas-fired ATS combined-cycle power plant efficiency. The net power output for the IGCC-ATS power plant is about 4% higher than the net power output of the natural gas-fired ATS combined-cycle power plant. The ATS turbine flow is much more balanced with this IGCC process configuration than the ATS turbine flow for the APFBC power plant configuration. The IGCC power plant efficiency is lower than the APFBC power plant efficiency because the IGC gasifier is oxygen-blown, and because a conventional low-temperature process cleans the fuel gas.

The IGCC conditions are much easier to integrate with the ATS turbine than are the APFBC conditions. The IGCC fuel gas combustors can be diffusion flame type combustors that are sized for the high flow of diluted fuel gas, with which Siemens Westinghouse Power Generation has previous IGCC gas turbine integration experience. In general, IGCC fuel gas combustor baskets can be inserted into the ATS turbine without modifying the turbine casing.

Estimated ATS turbine erosion results indicate that small particle penetration in the IGCC fuel gas (0.5 ppmw) can be tolerated, with the predicted time before reblading being greater than that expected for normal blade life. Medium particulate penetration (5 ppmw) in the IGCC fuel gas is expected to result in reblading intervals comparable to natural gas reblading intervals. ATS turbine deposition is a potentially more severe problem than erosion, although deposition may only require periodic water wash to recover. ATS turbine deposition with small particle penetration (0.5 ppmw) into the turbine IGCC fuel gas is not very significant, with the predicted time before airfoil washing being 16,000 – 40,000 hours, depending on the nature of the particulate. Medium penetration (5 ppmw) reduces the IGC-ATS washing interval to 1,600 – 13,000 hours.

For the IGC-ATS plant, the stack gas NO<sub>x</sub> content is estimated to be 35 ppmv, equivalent to about 0.43 mg/kJ (0.093 lb/MBtu). While the IGCC plant is capable of much lower SO<sub>x</sub> emissions, only about 92% sulfur capture is required to achieve an emission of 0.42 mg/kJ (0.09 lb/MBtu). The IGCC-ATS plant performance and cost are sensitive to the plant sulfur removal efficiency and benefit by less stringent sulfur removal levels. IGCC plant particulate emissions are limited by the turbine fuel gas particulate requirement, which is assumed to

be 0.5 ppmw particulate for the ATS gas turbine. This results in a particulate emission much lower than other coal-fired power plant technologies. The IGCC plant generates no solid waste, assuming markets can be identified for its slag and sulfur by-products.

The degree of integration between the combustion turbine and gasification island will determine the design changes required for combustion turbine casing. Casing design changes are impacted by the amount of air extraction required for air separation unit or gasifier operation. In any case, the combustion turbine casing design for IGCC is subject to much less challenging conditions than for the APFBC design.

### 2.3.9 Task 8.0 Integrated Program Plan

The Integrated Program Plan was developed for the Phase 3 work as described in report on "Integrated Program Plan Task 8," dated August 8, 1996, and issued to the U.S. Department of Energy. Siemens Westinghouse has identified nine basic tasks that cover all the key elements of this phase of the ATS program. The tenth task handles program management functions. The ATS Organization was put in place to define the program structure and identify the team members who have primary responsibility for each of the main tasks.

Siemens Westinghouse has aligned a program organization and work breakdown structure so that there is a clear assignment of individual accountability and responsibility for each task and each deliverable. The lines of communication among the people working on related tasks will be open. The assigned leaders of the various tasks will be accountable for the successful completion of the work, and will be responsible for keeping the program manager informed about progress and potential problem areas. Each month the task managers will provide the program manager with status reports on cost, schedule, and technical progress for the subtasks for which they have responsibility.

Extensive use will be made of electronic communications for the day-to-day administration of the ATS program. A protocol will be established such that the Siemens Westinghouse program manager will be copied on all e-mail communications between the ATS team members, thus providing an electronic file of all activity.

Video conferencing will be used as much as possible when face-to-face meetings are necessary with the subcontractors and vendors. This communication medium allows for visual interaction among individuals and the ability to show sketches, drawings, outlines, etc. Most of the team subcontractors have access to this technology. Those who do not are exploring the use of such facilities within their respective localities. Video conferencing will also help minimize travel expenses and the loss of productive time used in traveling.

The ATS program manager is responsible for the direction of the program including: data management, monitoring program progress, cost and schedule requirements, and maintaining control over manpower allocation and expenditures.

The performance of all program activities is tracked relative to cost and schedule using a monthly performance review cycle. An existing computerized cost

control program provides timely incurred cost information by task. On a monthly basis, or as decided by the program manager, the program management team meets to consider schedule progress, cost status, percentage of work completed, assignment of appropriate corrective actions, and documentation status.

The Siemens Westinghouse Business Management System, that is used to track and control the program performance, is iterative and is based on five principal steps in program management:

- Step 1: Planning
- Step 2: Release
- Step 3: Tracking
- Step 4: Control
- Step 5: Recovery (return to Step 1)

These steps are driven by the program schedule and Work Breakdown Structure (WBS), which are established at the outset of the contract and govern all program activities by describing the tasks and subtasks that define the work to be performed.

In executing the management plan, each activity (as defined by the WBS, Program Schedule, and Task Descriptions) is planned, scoped and budgeted in Step 1 to achieve program technical, cost and schedule objectives. Work is released in Step 2 to initiate activity according to the program schedule and planned milestones.

The performance of all program activities are tracked in Step 3, relative to the cost and schedule, using a monthly review cycle. An existing computerized cost control program is specifically modified to accommodate each new contract. This cost control system provides timely incurred cost information.

The contract administration and cost control function provides the program manager with the ability to review contract fiscal operations, measure the attainment of program milestones against cost targets, and to oversee the progress of all program work in terms of the schedule and Work Breakdown Structure.

On a monthly basis, or as deemed necessary by the program manager, the program management team meets to consider the following agenda:

- Project progress as measured against the project schedule
- Cost status and percentage of work completed as measured against key schedule milestones
- Assignment of appropriate corrective action and status review of previously assigned tasks
- Engineering problems encountered and suggested solutions
- Documentation status

- Review of newly received correspondence and replies to previously received items

The program manager is provided with a monthly summary. An analysis is made of the status of performance, problems encountered, schedule, and rate of funds expended.

On the basis of this analysis, items requiring attention are identified with the emphasis on areas that are weak, low on manpower, or unusually difficult.

The program manager conducts formal program reviews with DOE every three months and initiates reviews internally as he determines necessary. He has the authority to utilize support personnel required for such purposes. Program reviews also are held, as necessary, to determine progress and to control technical adequacy and development.

Contract administration and cost control provides the program manager with the tools to review program milestones against cost targets and schedule, and to oversee the progress of all work according to the schedule and work breakdown structure established at the outset of the program.

The contract administration function is the overall administration of the terms and conditions of the contract with DOE, focusing primarily on customer interface and correspondence, contract changes, cost and schedule reporting, maintaining current contract records and supporting the program manager in areas of contract interpretation.

The charging of time and the monitoring of time spent on each task is done through time cards. Those personnel assigned to the various tasks submit time cards on a weekly basis. In addition, all other contract-related costs are collected. The contract administrator sees to it that these data are entered into the contract monitoring computer program. The computer produces data sheets showing the breakdown of accumulated costs in the various categories and tasks. The data is distributed to the appropriate management personnel for review. The program manager, in particular, reviews the information to confirm that project costs, particularly in the charging of time by assigned personnel, are realistic and correct.

Subcontract administration is the responsibility of the program contract administrator. In general, overall Siemens Westinghouse subcontracting policies are established and implemented through corporate guidelines and procedures. These formal subcontracting procedures are implemented by the purchasing department in coordination with the contract administrator.

A review board will be constituted to review program results and make recommendations regarding the program redirection, as may be required. The review board (Table 15) comprises of the Siemens Westinghouse program manager, the DOE ATS product manager, and interested utilities and independent power producers. The review board will meet at predesignated times that coincide with key decision points. The review board may be called at other times at the prerogative of the program manager.

#### **Table 15 ATS Advisory Board**

## COMPANY

Florida Power & Light

Allegheny Power

Houston Light & Power

Florida Power Corporation

National Power (UK)

Power Gen (UK)

Dow Chemical

L.G. & E

Siemens Westinghouse Electric Corporation

DOE/NETL

### 2.3.10 Tasks 9.0 and 12.0 Design, Test and Development of Critical Components

#### 2.3.10.1 Cooling Development

##### 2.3.10.1.1 Tasks 9.1 and 12.1.4 Closed-Loop Cooling Development/Vane Cascade Test

###### 2.3.10.1.1.1 Introduction

Successful development of a closed-loop cooling design for the ATS turbine airfoils was identified as one of the major technical barrier issues. The benefit of film cooling, which provides a protective layer between the hot gas and the airfoil surface, is excluded in closed-loop cooling. For closed-loop cooling to succeed, the cooling design must: (1) minimize external heat transfer coefficients by using optimized aerodynamic design, (2) use thermal barrier coatings to reduce heat load, (3) increase allowable surface metal temperature with an advanced anti-corrosion bond coat, (4) maximize cold side surface area, (5) enhance cold side heat transfer coefficients with turbulators, and (6) minimize airfoil wall thickness to reduce wall temperature gradients and hence the internal heat transfer coefficients required to cool the airfoil. To achieve the ATS program goals, thin wall cooling designs were generated for the first stage turbine vane and blade incorporating the previously described concepts. The objectives of this development program were to:

1. Verify first stage vane closed-loop cooling design
2. Confirm the capability of operating with either steam or air as coolant
3. Quantify the cooling performances of the various circuits
4. Provide data to refine and optimize the cooling designs
5. Verify steam cooled transition design
6. Verify transition mouth seal design

An integrated combustion/hot cascade test rig was designed to accommodate testing of the ATS first stage turbine vane, the steam cooled transition and the ultra low NO<sub>x</sub> combustor. The new test rig was to be installed in the Siemens Westinghouse high pressure combustion test facility located at the Arnold Engineering Development Center (AEDC), Arnold AFB, Tullahoma, Tennessee.

During the course of this project it was decided that provision should be made for a straight through combustion test rig with axial exhaust. Therefore, components for both the side exhaust vane cascade test rig and axial exhaust combustion test rig only were designed and manufactured.

#### 2.3.10.1.1.2 Design of Rig Components

Design was carried out on the integrated test rig components for the required operating conditions. The test cylinder was designed to withstand 500 psia (3.45 MPa) internal pressure. It was cooled with a water jacket cooling system. An access port and a rear dome cover were incorporated to facilitate the cascade holder removal. The steam cooled transition, and the steam cooled instrumentation section, which was located between the transition and the cascade holder, were designed with internal cooling channels to provide sufficient cooling at the ATS operating conditions. Designs were completed for the inlet air diffuser, transition support bracket, vane pack assembly carriage, exhaust elbow flanges and the "corn crib", which was an array of aerodynamic baffles for generating the correct inlet flow conditions to the combustor. The required valves for the different steam air and water circuits were specified. The design of the cascade holder, the water cooled instrumentation section and the exhaust duct have been partially completed. The cascade holder design included the centrally located instrumented test vane and two side walls representing the pressure and suction surfaces of the adjacent vanes. The side walls were water cooled and required a special cooling design to maintain allowable wall temperatures. When the test rig is used for combustion testing, the test vane will be replaced with a dummy vane, which uses a similar water cooling design as the side walls. The side walls and the dummy vane will be machined from two solid first stage vane castings produced during the Thin Wall Casting Development program (one casting will be cut in half to produce the two side walls). During combustion testing, the steam cooled instrumentation section will be replaced by a water cooled instrumentation section. This is necessary due to the different instrumentation requirements for the combustion testing and hence different axial length of the instrumentation section.

Figure 67 shows the schematic of the integrated combustion/hot cascade test facility, Figure 68 a cut-away of the integrated combustion/hot cascade test rig, and Figure 69 the axial flow combustion test rig.

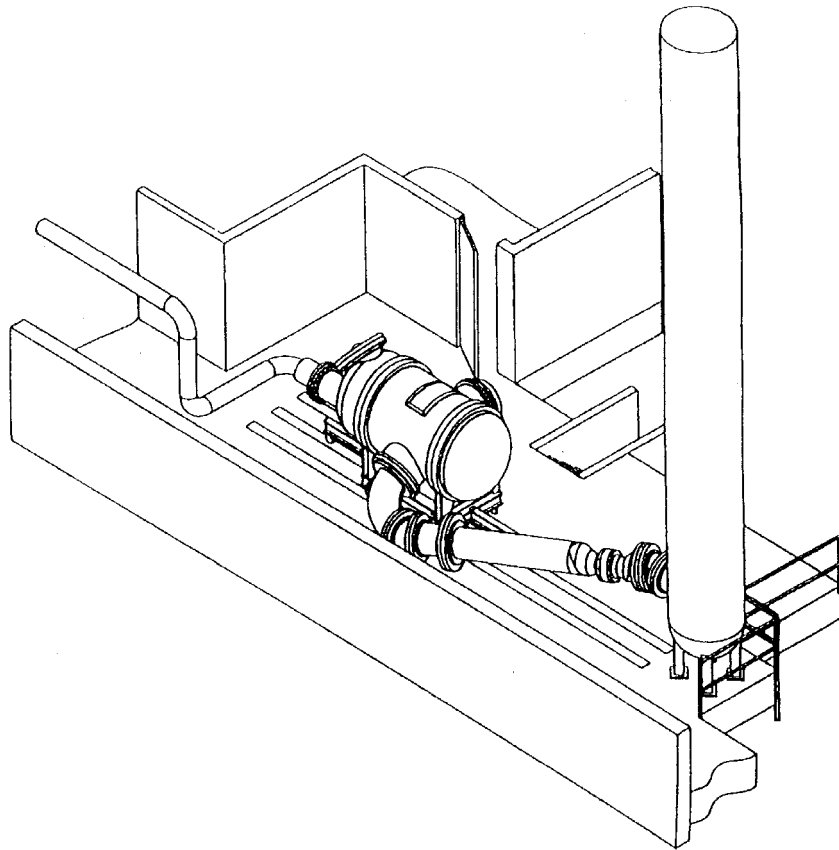


**Figure 67**     **Integrated Combustion/Hot Cascade Test Facility**

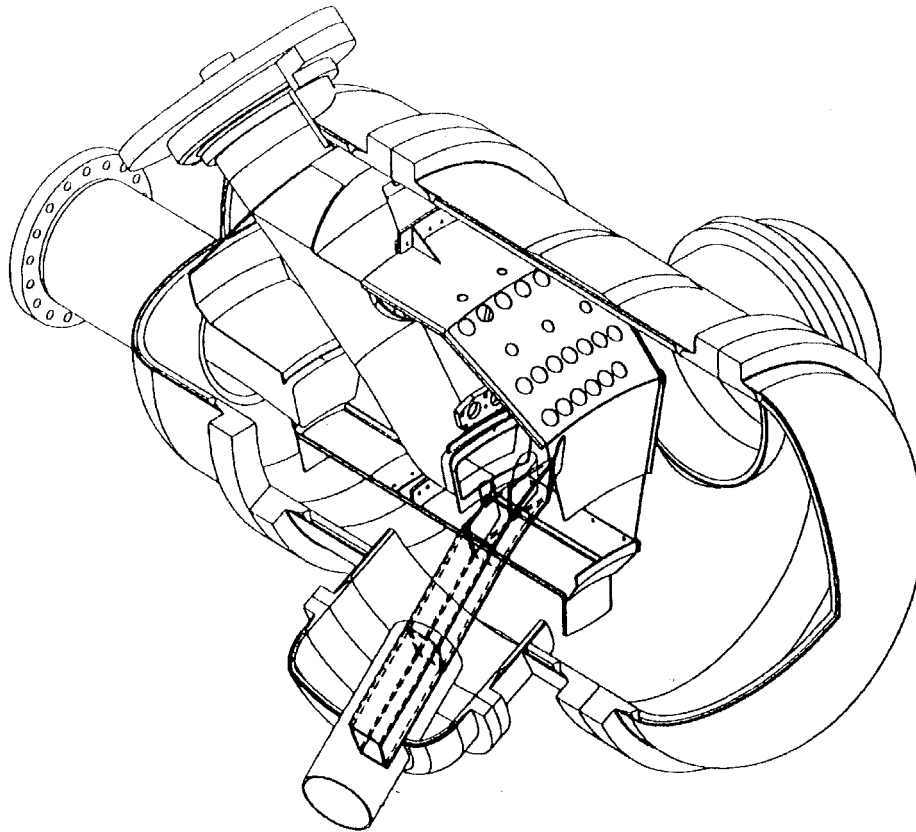


**Figure 68 Integrated Combustion/Hot Cascade Test Rig**

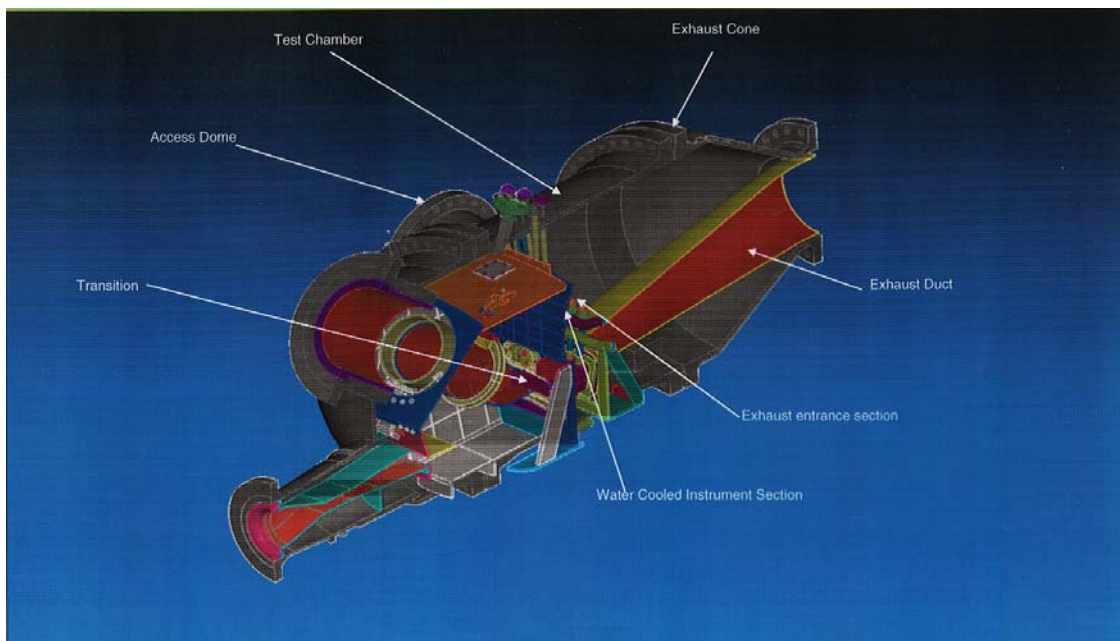


**Figure 69 Axial Flow Combustion Test Rig**

#### 2.3.10.1.1.3 Instrumentation

The integrated test rig, transition and test vane will be extensively instrumented. Three radially retractable water cooled temperature rakes, located in the steam cooled instrumentation section, will measure cascade inlet temperature distribution. Seven water cooled emissions probes, located in the water cooled instrumentation section, will monitor emissions during combustion tests. The transition will be instrumented with about 60 thermocouples. The test vane will have approximately 70 thermocouples and 10 static pressure taps. Thermocouples and static pressure taps will be installed on the test cylinder, baffles and components located inside the test cylinder, and the exhaust system. Flows, temperatures and pressures will be measured in the inlet air duct and all the steam, water and air cooling circuits. A total of about 270 temperatures and 30 pressures will be measured.

#### 2.3.10.1.1.4 Hardware Manufacture

The following new test rig components were manufactured:

- Test cylinder, (see Figure 70, which shows the axial exhaust configuration) with provision for side and axial exhaust
- Test rig support structure
- Instrumentation ring
- Steam cooled transition
- Transition support bracket
- Transition mouth seal
- Steam cooled instrumentation section
- Water cooled instrumentation section
- Inlet diffuser
- Corn crib
- Vane pack assembly carriage
- Exhaust elbow flanges
- Instrumentation probe actuators
- Probe seal assemblies
- Valves

Remaining components to be manufactured are cascade holder (including test vane, dummy vane and side walls) and exhaust diffuser.

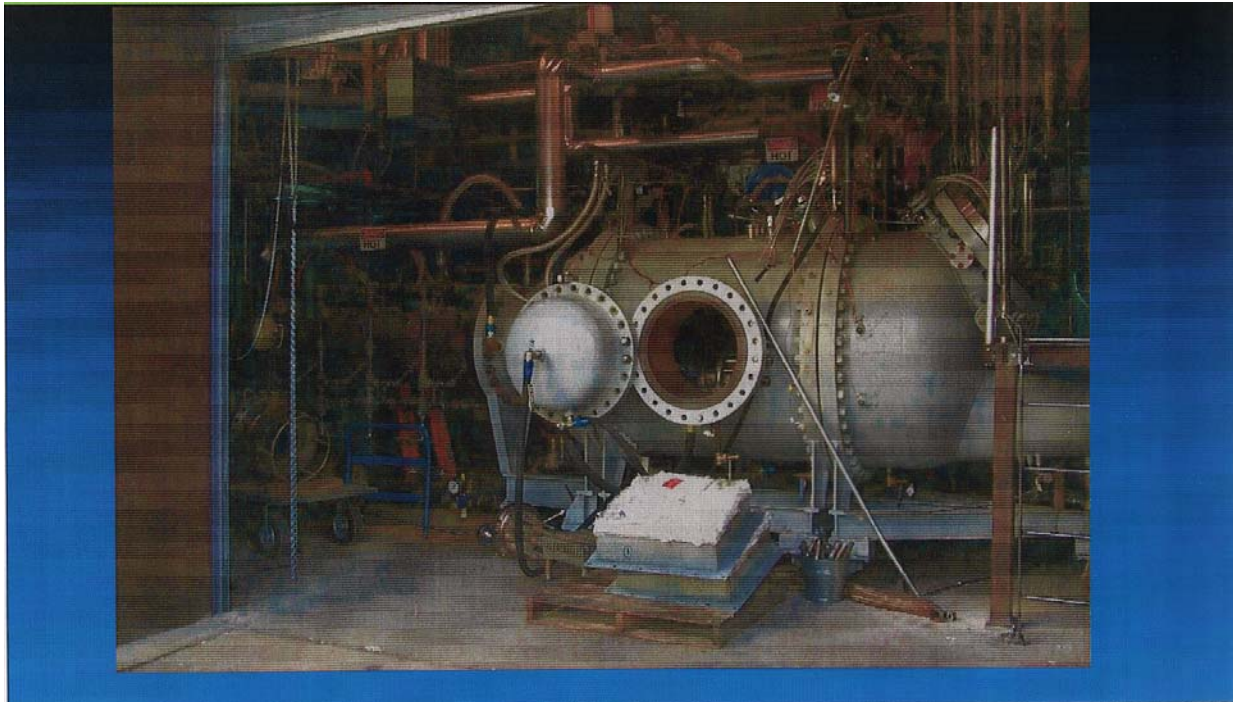


**Figure 70     ATS Combustion Test Rig**

#### 2.3.10.1.1.5 Combustion Test Rig Commissioning

The axial exhaust flow combustion test rig was commissioned and some W501G combustion system tests were carried out prior to the test rig being shipped to another location.

#### 2.3.10.1.1.6 Conclusions

The integrated combustion/hot cascade test rig was designed and most of the components were manufactured.

The axial exhaust flow combustion test rig was constructed and commissioned.

#### 2.3.10.1.2 Task 9.19 Closed-Loop Cooling Internal Heat Transfer Tests

##### 2.3.10.1.2.1 Introduction

The tasks performed in this study were directed towards the heat transfer and flow characterization of Siemens Westinghouse ATS combustion turbine Row 1 vane and blade cooling designs. Cooling of the airfoils uses a novel, closed-loop cooling system which is facilitated by complicated heat transfer geometry and various heat transfer enhancement techniques. A number of scaled plexiglass models were fabricated to simulate realistic aerodynamic and heat transfer conditions. Local heat transfer coefficients on all the participating surfaces were measured non-intrusively using a transient liquid crystal technique. The acquisition and analysis of liquid crystal images used a customer-developed software which consists of many automated and self-calibrated features designed exclusively for turbine cooling research. Data obtained in this study will provide the designers with a reference of performance and a guideline for further

improvements. The effort was divided into six major tasks representing various cooled sections of the vane and blade.

#### 2.3.10.1.2.2 Models Tested

A total of 10 plexiglass models, representing six cooling techniques used in the Row 1 vane and blade, were fabricated and tested. These models represented the following: vane airfoil, and trailing edge, vane shroud, blade airfoil, blade trailing edge, blade tip cap and blade platform.

#### 2.3.10.1.2.3 Test Results

Internal heat transfer and pressure loss tests were carried out at Carnegie-Mellon University. Transient liquid crystal technique was used in the heat transfer measurement. In some cases, the liquid crystal imaging method was complimented by the naphthalene sublimation technique based on a heat and mass transfer analogy.

Based on the test measurements, detailed internal heat transfer coefficients and pressure losses were estimated for the different cooling configurations. These results indicated which cooling configurations achieved the desired heat transfer coefficients and which needed further optimization to achieve design targets. The areas identified for further enhancement were the vane trailing edge turbulator design and vane shroud acute corner pedestal bank.

#### 2.3.10.1.2.4 Conclusions

Internal heat transfer performance of the ATS Row 1 vane and blade cooling designs was validated. The test results confirmed the anticipated performance in most cases and have identified potential shortfalls in some.

### 2.3.10.1.3 Task 12.1.9 Turbulator Model Tests

#### 2.3.10.1.3.1 Introduction

The objective of this program was to quantify heat transfer and pressure loss characteristics of turbine airfoil cooling holes with various non-ideal turbulator shapes as anticipated for the ATS turbine airfoil cooling design geometries. For optimum heat transfer enhancement the turbulators should have sharp edges and have the correct height and aspect ratio. The manufacturing techniques used in producing these turbulators result in turbulators with rounded edges, incorrect height, etc. This poses a problem in achieving successful turbine airfoil cooling designs, since the correlations used in the heat transfer analysis assumed ideal turbulator shapes. To obtain realistic heat transfer and pressure loss data nine scaled plexiglass configurations of cooling holes with non-ideal turbulator shapes were manufactured and tested over a wide range of expected engine Reynolds' numbers. The transient liquid crystal technique was used in the heat transfer measurements.

#### 2.3.10.1.2.2 Test Results

A test matrix of anticipated non-ideal turbulator shapes produced by standard STEM drilling or casting processes was generated and tested across a range of

Reynolds' numbers for evaluation of thermal performance using plexiglass models with the transient liquid crystal technique. Testing was performed at Carnegie-Mellon University. The test results generated a sufficient database needed for design purposes permitting determination of adjustment factors to heat transfer coefficient enhancement correlations intended for ideal turbulator shapes. Testing revealed an optimum turbulator shape based on thermal performance (including both HTC enhancement and pressure loss), differing from the ideal square shape for HTC enhancement alone. Data also indicated as much as a 60% reduction in heat transfer enhancement due to non-ideal turbulator shape without a significant reduction in pressure loss in worst case geometries. Only one of the nine turbulator geometries tested (square turbulators with aspect ratio of one) agreed with the available non-dimensional heat transfer and friction data.

### 2.3.10.2 Sealing Development

Minimizing air/gas leakages was very critical in achieving the ATS program performance, emissions and mechanical integrity goals. Therefore, a concerted development effort was carried out to reduce leakage in the different components of the ATS engine. Figure 71 shows the locations of advanced sealing development.

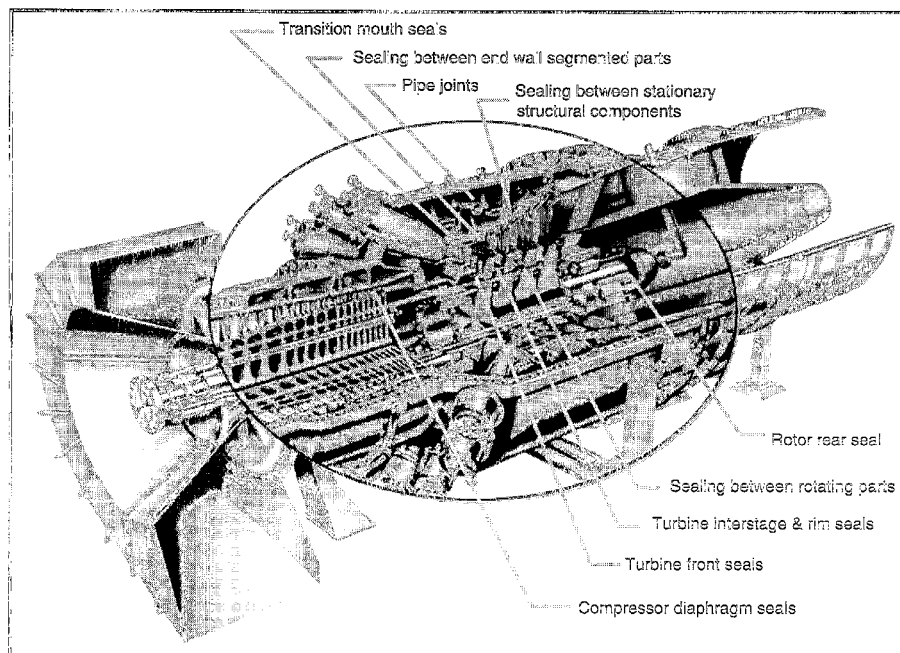


**Figure 71 W501ATS Sealing Focus Areas**

#### 2.3.10.2.1 Task 9.3 Rotor Sealing Development

##### 2.3.10.2.1.1 Introduction

This program addressed achieving low leakages in the closed-loop air rotor cooling flow system. This flow system provides cooled, high pressure air to the two rows of turbine blades for cooling, and then returns the air to the combustor shell. Tight sealing is required at interfaces in the flow circuits, i.e., where air

enters the rotor center at the rear; between rotor discs, i.e., “belly bands” between disc arms and at the blade roots; and at the blade roots where the blades are attached to the turbine rotor discs. Leakage is exacerbated by the high air pressure maintained throughout the circuit so that the air can be returned to the combustor shell.

In this task, design approaches were sought to meet the tight sealing requirements. For sealing between rotating parts, conceptual design schemes were devised and final approaches derived with consultation from seal vendors. This effort was done in concert with the turbine design.

The rotor rear seal, where the cooling air enters the rotor was an especially critical sealing location. Here, a near zero leakage, advanced air seal was needed. A key challenge to this sealing location was the large relative axial motion between the rotor and surrounding housing during engine start up and shut down. Advantages of this location were a low air temperature, seal not being segmented, and a relatively small size for minimal leakage area.

The prime candidate for the rotor rear seal was a face seal. Face seals are used in many aero gas turbines and other turbomachinery applications. They consist of two flat annular ring surfaces running in close proximity axially; one is attached to the rotating shaft and the other to a stationary housing. They are designed to have a very small axial clearance despite shaft movement, wobble (called “swash”), etc., in order to maintain near zero leakage rates. Hydrostatic or hydrodynamic approaches are employed to maintain the small clearances. One of the surfaces is usually made of carbon because of its excellent wear and machinability characteristics. Springs or other mechanical devices aid in maintaining a small gap.

The primary objective was designing and validating a rotor rear seal, since sealing between the rotating parts was done in concert with turbine design. The approach taken was to: (1) define the rear seal requirements; (2) solicit competing vendor proposals for the seal; (3) select a vendor via a detailed evaluation against the requirements; and (4) fund one vendor to design, build, and rig test two seals. The test hardware would subsequently be the prime and spare rear seals for the first ATS engine.

#### 2.3.10.2.1.2 Seal Design and Selection

A face seal was incorporated into the W501ATS engine at the rear of the rotor aft of the bearing. This type seal provides a low leakage for the closed-loop rotor cooling air as it enters the center of the rotating shaft. The seal operates with a pressure difference across its faces using hydrostatic lift forces to open or close the gap between them at maximum pressure levels. The narrow axial clearance (0.0001 to 0.0003 in. [0.00254 mm to 0.00762 mm] wide) is maintained by balancing pressure forces for a hydrostatic type seal, or balancing pressure and hydrodynamic lift forces for a hydrodynamic type seal. The latter forces come from shallow spiral grooves machined part way across the rotating (secondary) face. The grooves permit air flow towards the inner diameter where an ungrooved portion forms a sealing dam. This type of face seal can maintain low leakage rates even with very high pressure drops. Generally, face seals are not segmented and are applied to maximum rotor diameters of 10 to 15 in. (0.254 to

0.381m) because of size limitations of seal face materials. Thus, application of face seals is generally limited to the shaft regions of large gas turbines, such as at the W501ATS rotor rear.

Several seal companies were approached for their recommended best seal configuration for this location. In light of the above requirements, a labyrinth seal was rejected because it would not meet the leakage requirements, even with the smaller shaft diameter. Brush seals would have to be staged to handle the large pressure drop and would also pass too much leakage flow. Circumferential seals could readily meet most of the requirements except the high pressure drop. A compliant seal was a possibility, but it was too early in its development to be applied here. It could be a lower cost alternative sometime in the future.

The seal type selected by all the responding seal manufactures was a non-contacting, dry running, gas seal, i.e., a face seal. This type of seal has been used in many aero gas turbines and other turbomachinery applications. It was recommended primarily because the required diameter is small, the seal does not need to be segmented, and the leakage requirement is low. Also, a face seal can readily meet the pressure drop, temperature, and swash requirements. Development was necessary to demonstrate that such a seal can meet the life, durability, air contamination, and large axial movement requirements. John Crane Inc., was selected as the vendor for the development.

John Crane manufactures Type 28 Series dry-running gas seal cartridge systems. These systems have proven to be reliable because the seal is non-contacting which virtually eliminates seal wear while keeping parasitic power loss and leakages at minimum levels. Further, the hydrostatic lift component ensures smoother starts and stops.

Dry gas face seals are robust in design. They can withstand rapid speed and pressure changes and are relatively unaffected by shaft vibration. Standard seals of this type have a  $\pm 0.125$  in. (3.175 mm) float to accommodate axial thermal growth differences and ballooning of the surrounding casing. Allowance for radial shaft movement is 0.025 in. (0.635 mm). To minimize vibration, critical rotating seal components are single-plane dynamically balanced, and then the complete seal rotor assembly is dual-plane dynamically balanced. The seals, which are housed in protective cartridges, are subjected to a battery of static and dynamic performance tests prior to installation to ensure seal integrity.

The W501ATS rotor rear seal was designed especially to satisfy the requirement challenges for a larger axial movement, larger seal diameter, and larger angular swash. The larger seal diameter than standard seals (9-in max. [228.6 mm]) was designed using John Crane's proprietary design system. In the engine, a filtered, purged air system will supply air to the seal face region to prevent particles from lodging in the narrow gap (0.0002 in. [0.00508 mm] wide) between the faces and cause wear. To minimize the purge air flow rate requirements, a secondary labyrinth or brush seal is placed between the seal face region and main cooling air circuit to minimize reverse flow.

Two seals were needed in the test rig and the second seal also provided backup hardware for the first W501ATS engine application.

#### 2.3.10.2.1.3 Seal Validation Testing

The testing of the two face seals included:

- Performance evaluations at full pressure and speed
- Large axial travel evaluations (included in all the performance tests)
- Angular misalignment evaluations (included in all the performance tests)
- Over-speed spin testing of rotating components before assembly to ensure integrity
- Extended turning gear operation

The performance testing was completed with two seals installed in the test rig. The seals were in a back-to-back configuration with high pressure air introduced between them. A reverse direction, spiral-groove mating seal face was installed in the second (slave) seal. Two series of performance tests were run, with the seal positions reversed for the second test. A motor provided axial movement while the seals were being tested.

All aspects of the performance test procedure and test conformed to John Crane's standard test procedures. The gas used for the test was filtered shop air. Parameters measured included: pod gas temperature, test pressure, test speed, seal leakage, time, static torque, motor load, and relative axial shaft position. Digital photographs were taken of the seal faces before and after each test.

Turning gear operation was simulated in a separate rig, using the same test pod as in the prior performance tests. This rig was specially built for this test. The slow-roll testing was done at two rpm, at ambient temperature, and with no pressure drop across the seal, which are the engine conditions during turning gear operation. The test was run for 100 hours and the results extrapolated to expected engine time on turning gear before replacing or reworking the rear seal.

The performance testing showed that the rear seal: (1) leakage at steady-state would be about 2 scfm (0.0057 m<sup>3</sup>/min), or 1/40th of the leakage requirement, and (2) could readily handle the large angular swash and axial travel without any sign of wear on the seal faces. The turning gear evaluation showed similar seal face wear results with not even any scratch marks noted. The seal faces looked as if they had not been run.

#### 2.3.10.2.1.4 Conclusion

Three rotor face seals were evaluated and one design was selected for validation test. Two seals were manufactured and tested. Steady state leakage tests showed that air leakage was negligible. Ability to accommodate large axial travel and turning gear operation were demonstrated.

## 2.3.10.2.2 Tasks 9.6 and 12.2.3 Advanced Sealing Development

### 2.3.10.2.2.1 Introduction

The objective of this program was to develop, rig test and validate advanced air seals in engine and component tests. Air seals were to be developed for locations beneath the compressor diaphragms, along the torque tube, in the turbine interstages, and at the rims at the inner flow path upstream and behind the turbine blade rows. These seals were to pass significantly less leakage flow than current labyrinth seals while withstanding the large relative radial and axial movements during engine start-up and shut down without degrading seal performance at steady-state conditions. These seals also had to be rugged to be installed in an industrial engine environment without damage.

The prime candidates for advanced air seals are brush seals. They would replace or be in series with current labyrinth seals. Brush seals are being incorporated into aero gas turbines. Currently, they are proposed for use in over fifteen different aero engines. Brush seals restrict airflow between the mating rotating and stationary components by filling the gaps with a brush of very fine wire bristles, angled in the direction of rotation. Running line-to-line with the rotating surface, they have been found to leak considerably less than labyrinth seals with normal gap clearances. However, brush seals must be carefully designed so that they operate through the engine operation excursions without excessive wear or damage. Also, they must be designed to run against uncoated surfaces because it would be difficult to apply the hard coatings used in aero engines on the large gas turbine rotors.

Applying brush seals to large industrial gas turbines imposes several unique design constraints:

- 1) Seals must be durable to accommodate handling, field installation and operation, which leads to larger bristle diameters and a smaller frontplate inner diameter to protect the bristles. Weight is a lesser issue in industrial engines, so that seal containment plates can be heavy for ruggedness.
- 2) Seals must be segmented, i.e., split into two halves because of the engine's horizontally split casing; more than two segments are preferred for field handling and installation.
- 3) Seals should run against uncoated rotor surfaces. The rotors are very large and it is undesirable from cost and manufacturing standpoints to apply the hard face ceramic coatings normally used in aero gas turbines. However, rotor surface wear signatures created by the brush seals should not impact rotor life because of the large rotor section sizes and low stress levels at sealing locations.
- 4) Seals must be able to accommodate a large radial closure toward the rotor surface ( $> 1$  mm) during start up and shut down without excessive frictional heating of the bristles or rotor.
- 5) Component design life is at least 50,000 hours. Brush seals will survive this long, but the leakage rate will have increased. During the relatively short start up and shut down cycles, the seal's bristles wear because of

seal closure, thereby increasing leakage rate at operating conditions. Eventually the bristles wear line to line at the maximum closure point and the leakage reaches a maximum. This increased leakage however is still significantly less than that of a labyrinth seal.

- 6) Seal backplate radial gap must be large enough to avoid it touching the rotor surface even when the rotor is whirling during start up and shut down as the rotor passes through its critical speeds.

The focus of this program was development of brush seals for turbine interstages (under the stator assemblies), turbine front (where very high pressure drops occur), under compressor diaphragms, turbine rims (including investigation of higher temperature bristle materials, such as ceramic fibers), and transition mouth region (static brush seals).

#### 2.3.10.2.2.2 Development Program

Brush seals, much more than labyrinth seals, must be carefully designed in order to operate properly and meet design requirements. Consequently, a detailed development program was conducted, consisting of:

1. Performing analytical studies to determine transient and steady-state conditions for the selected engine locations
2. Conducting tribopair evaluations of candidate bristle materials running against uncoated rotor materials for the selected engine locations. From this testing, bristle materials are determined which produce low friction heating and polishing of the rotor surface
3. Designing and fabricating subscale candidate brush seals for the selected engine locations
4. Rig testing subscale seals for conditions modeling the engine locations as close as possible. Based on the results, determining the best brush seal design for each location
5. Fabricating brush seals with optimum design for engine hardware testing
6. Validating brush seal configurations in engine hardware testing, i.e., compressor diaphragm seals in the ATS compressor rig test, and turbine interstage, rim and transition mouth seals in a selected field engine

The initial study identified the potential risk/benefit of applying brush seals at various gas turbine locations. The turbine interstages were found to offer the maximum benefit, followed by the front turbine seal, turbine rim, and compressor diaphragm. For each of these seal locations, the transient operating conditions and seal radial and axial closure cycle during start up and shut down were calculated.

The preliminary effort (number 2 above ) was done with Cross Manufacturing to investigate running against uncoated rotors which is not normally done in aero engine brush seal applications. Two dynamic, subscale tests were run at ambient temperature with pressure drop and geometry conditions modeling the

turbine interstage location. One test was done with the rotor repeatedly offset to model engine start up and the other was with a constant interference of the order of 1 mm. The seals tested had similar stiffness, bristle pack thickness, backplate gap, etc., as would be expected for the full-size seal. Leakage, wear, and surface characterization results from this testing demonstrated an excellent potential of running brush seals against uncoated surfaces and that the service life could approach that required for large industrial gas turbines.

Based on the success of the preliminary effort, focused development efforts (number 3 above) were initiated for selected seal locations. These efforts addressed the technical challenges of sealing, i.e., (1) running a brush seal against an uncoated rotor, and (2) design optimization for negotiating the transient radial closure at that location to achieve minimal steady-state leakage. EG&G Sealol was selected as the seal vendor to assist in these efforts. They have had continuing brush seal design and development programs with two U.S. Air Force funded projects and internally funded ones to develop their manufacturing processes at EG&G Sealol's Engineered Products Division.

Based on the initial study, engine locations selected for brush seal application were the: (1) turbine interstages, (2) turbine front, (3) compressor diaphragms, and (4) turbine rims. Later, the static transition mouth seal development was added to the program. Development was initiated for the turbine interstage locations because of their larger expected performance benefit. This location has a modest pressure drop and large radial closure during start up. The turbine front seal location has a very large pressure drop; thus, two brush seals in series are probably needed there to reduce the pressure drop across each seal. The compressor diaphragm seal location is beneath the compressor diaphragms. This seal has a relatively small pressure drop across it, but limits the flow recirculating under the diaphragm vanes.

For each selected engine locations, five subtasks were pursued:

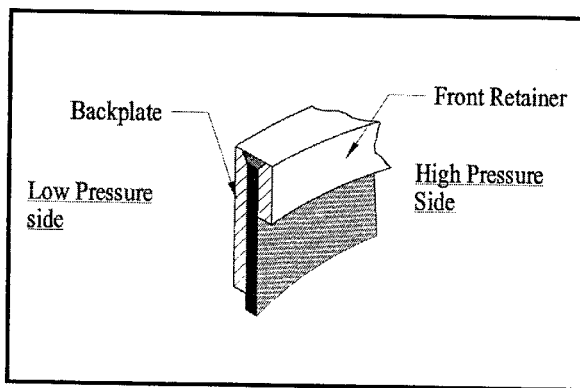
- 1) Design of subscale seals to meet operational requirements. These seals were designed specifically for rig testing, but were representative of actual engine seals.
- 2) Tribological study in which various bristle alloys were run against uncoated rotors made of current and anticipated materials for the W501ATS turbine.
- 3) Extensive subscale rig testing of subscale seals to assess performance of selected design configurations under simulated engine transient and steady-state conditions at the particular locations.
- 4) Design and fabrication of full-scale hardware
- 5) Rig validation testing

#### 2.3.10.2.2.3 Brush Seal Design

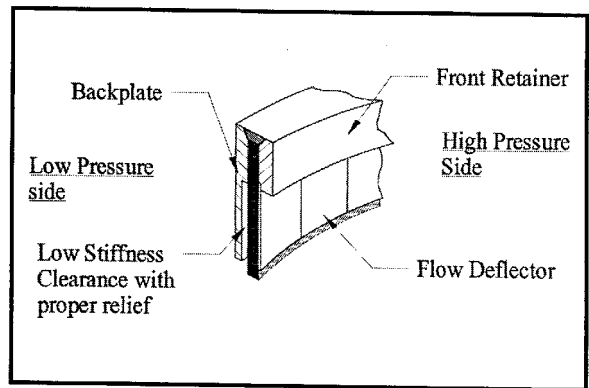
The brush seal design process considers the following variables for a particular sealing location: relative closure between the seal and rotor, pressure drop, rotor surface speed, and air temperature. The goal is to design a seal which will

exhibit minimal wear during interference operation, but have enough stiffness to support the required pressure drop at steady state. This then influences the bristle pack radial and axial stiffnesses, respectively. Design parameters selected are: bristle diameter, bristle length, bristle angle, bristle-pack width, bristle material, backplate gap with the rotor (called “fence height”), and initial seal interference. Figure 72 is a schematic of a generic (standard) brush seal with the various features identified.

In addition to these standard seal design parameters, EG&G has developed unique design features which stabilize the bristle pack so there is less stiffening at higher pressure drops and less bristle flutter. Hysteresis, the effect of the bristle pack hanging up in the pushed back condition after a shaft excursion, is reduced by providing a small relief in the back plate. Figure 73 shows EG&G’s advanced brush seal design. These features are added design parameters which are tailored to meet individual seal application requirements.



**Figure 72 Standard Brush Design**



**Figure 73 Advanced Seal Design**

EG&G’s testing has shown that airflow through the bristle pack causes a phenomenon called “bristle blow-down,” or “pressure closure.” Airflow through the bristle pack has both axial and radial components. Radial flow produces a net inward force causing the bristle pack to move toward the rotor. Bristle pack radial instability is a function of the seal design stiffness and the pressure drop across the bristle pack. As pressure drop increases, flow rate through the bristle pack increases and pressure closure occurs. The advanced seal design combines a flow deflector plate with a low stiffness feature to enhance bristle pack stability and to modify the flow pattern through the bristle pack to counter pressure closure and reduce pressure stiffening.

For large industrial gas turbines, the fence height is relatively large to accommodate large rotor perturbations and seal closures. But a large fence height exposes a long unsupported bristle pack length which reacts against the imposed pressure drop. In addition, the seal must be designed with a low radial stiffness to accommodate the large rotor excursions and closures expected. Consequently, the focus of brush seal design for large industrial engines has been to select the minimum stiffness that will seal against the required pressure drop with the large fence height.

#### 2.3.10.2.2.4 Tribological Testing

For high radial closure and high surface speeds the mechanical contact between the bristle and runner produces high frictional heating. To quantify friction and wear behavior under aggressive conditions, brush seal tribopair tests were run in the absence of a pressure drop (i.e., no cooling flow through bristles).

For aero-engine applications, brush seals consist of a runner with a coating applied to the rotor outer diameter and bristles made from selected wire alloys. Extensive tribopair studies of brush seals and coated runners have been previously presented. In an effort to develop high efficiency brush seals that can run at high speed on bare shafts, an extensive tribological characterization effort was conducted using a specially designed high speed tribology test rig. The test rig has a variable frequency AC drive converter to provide speed control to the direct drive shaft, which can be rotated at speeds up to 60,000 rpm. The rotor is fabricated from the same material as the actual engine rotor. The rotor has a diameter of 2.7 in. (68.6 mm) and develops surface speeds up to 700 ft/sec. (213 m/sec.). The rotor and brush seal are contained in a chamber which can be heated to engine operating temperature levels. A torque cell is used to measure rotational torque during each test, and the temperature at the brush seal backing plate is measured using a thermocouple. The test rig also has a dedicated computer to collect precise friction data on a real time basis.

Bristle packs made from up to five different alloys were tested in the tribopair tests for each location. The alloys were selected based on their physical and mechanical properties including melting point, tensile strength, hardness, and availability in wire form. The rotor material was the same as in the W501ATS engine at the respective locations. The test brush seals have inner diameters of 2.690 in. and 2.680 in. (68.3 mm and 68.1 mm) so that two interference levels between the bristle inner diameter and the rotor outer diameter could be evaluated. Each tribopair is first tested under cyclic conditions where the speed is ramped up to 700 ft/sec. (213 m/sec.), held constant for two minutes, and then ramped down. After ten cycles, each tribopair is tested for one hour at constant speed and temperature. Prior to each test, the rotor is precision balanced so that it runs smoothly at high speed. Rotors were run having two different surface roughnesses to determine the effect of roughness on frictional heating and wear of the bristle alloys. Friction coefficients were calculated from the mechanical contact pressure and the frictional torque.

For each cyclic test, the seal chamber was preheated to an elevated temperature, then the speed increased to a maximum value and allowed to run for a total of two minutes at the full speed condition before reducing the speed to zero. The chamber was allowed to cool, then the second cyclic test was conducted, etc. until a total of ten tests were run.

At the end of the tenth test, each sample was removed for dimensional measurements and surface characterization. The sample was then reinstalled, the chamber heated to a higher elevated temperature, the rotor speed increased to nominal speed, and the sample run for a one-hour endurance test. Subsequently, brush seal measurements and optical photographs of the wear surface were taken. For each test, the torque, backing plate temperature, and brush seal and rotor wear were measured.

A test matrix of two runner materials running against five different bristle materials was conducted. The tribopair giving the best results exhibited the lowest temperature rise measured, e.g., for the turbine interstage only 266°F (148°C) during the first cycle test and 165°F (92°C) during the tenth cycle. Generally, the torque remained in the 0.2 to 0.1 in-lbs. (0.023 N-m to 0.0113 N-m) range throughout all of the cyclic tests as well as the one hour endurance test.

Measurements of the brush seal inner diameter show that the brush seals lost an acceptable amount of material during the endurance tests. Profilometry traces of the runner show that a very small amount of wear occurs in the contact area. From a high magnification profile trace of the rotor surface in the axial direction, it was determined that the depth of the wear area is less than 0.0001 in. (0.00254 mm).

When the same bristles ran against a rotor with a rough surface finish, higher temperature from friction heating was generated and more wear of the brush seal was produced than when running against the smooth rotor. Profilometry measurements of the rough surface rotor show less than 0.0001 in. (0.00254 mm) of rotor surface wear occurs, which suggest that there is not higher wear on the rotor when the high surface roughness condition was used.

There were a few tests run in which the tribopairs showed exceptionally poor friction and wear performance. In one such tribopair, a brush seal ran against a smooth rotor. During the first cyclic test, the temperature at the brush seal backing plate rose more than the previously mentioned test and much more wear was measured. The rotor from this test showed no evidence of material loss, but the profilometry trace indicated that a transfer layer of smeared material had been deposited onto the runner. This layer of material produces like-on-like sliding contact which causes galling to occur.

It is recognized that accelerated conditions were used for the brush seal material screening tests. The amount of bristle wear produced during a single cyclic test exceeds that for a brush seal undergoing many excursion cycles when air is flowing through the seal. Thus, the qualitative priority ranking was used to select the optimum bristle material to run against the rotor material for a given engine location.

Two special series of test were run to supplement the tribological results. In the first test the effects of a corrosive environment on brush seal performance were investigated. It is desirable to run brush seals against uncoated surfaces to avoid the costs and manufacturing complexities of coating large rotors. The results of the tribological testing indicated the feasibility of this approach. However, current steel material rotors being used are subject to corrosion and oxidation which can cause scale build up and pitting of the rotor surface.

To investigate the effects of surface deterioration on brush seal operation, tribology tests were run after both the brush seals and rotors surfaces had been exposed to an accelerated corrosive atmosphere. Seal specimens were exposed to a salt air and oxidized air environment at elevated temperature to determine if the seal bristles or rotor rust or decay had any deleterious effects. Uncoated rotors and rotors coated with corrosion resistant coatings were tested.

Sermatech International Inc. applied plasma sprayed coatings to some of the test rotor surfaces. An undercoat was applied to protect the base material from any contaminants passing through the porous top coat. These same coatings, if found to be required, can be applied in situ by Sermatech with a portable robot. Sermatech has been doing such on site work for about ten years.

The results of this special study showed that brush seals exhibit excellent resistance to corrosion after the accelerated exposure to a corrosive environment. Steel rotor surfaces did exhibit extensive corrosion, but the presence of the rust like corrosion material on the surface did not degrade brush seal wear performance. The rotors with the standard Sermatech corrosion resistance coating did not experience corrosion in the accelerated exposure and the coating held up well when run against a brush seal.

The second special series of tests studied the possible benefits on seal wear rate of embedding solid lubricants into the bristle pack. Various solid lubricant, plus wax, the material used to protect seal bristles during shipping/installation, were investigated. The results were mixed but one lubricant material reduced the bristle wear rate by 50% for the first few minutes of operation. This result is helpful, but some of the greater local bristle wear will occur in the first few minutes of operation as a brush seal wears so the inner diameter is concentric with the rotor. The lower wear rate will lessen the chances of rapid bristle oxidation during the initial start up cycle.

#### 2.3.10.2.2.5 Subscale Seal Rig Testing

In general, subscale seals were fabricated and rig tested when one or more operating condition for the application was outside the design experience envelope. From subscale test results, seal design was optimized, and leakage performance and seal life characterized. For large industrial gas turbines, a primary operating condition outside of previous experience is the large radial closure cycle to be accommodated during startup and shutdown without excessive heat up or long term bristle wear after repeated cycles.

In the subscale effort, several candidate brush seal configurations for the different engine locations were evaluated. The testing was both static and dynamic. Initial subscale brush seal testing in ATS Phase 2 tasks demonstrated the feasibility of brush seals running against uncoated rotor surfaces and with large radial closure cycles. Also, preliminary characterization data were obtained for a standard and an advanced design brush seal. Based on these results, brush seal configurations were established for the turbine interstage, compressor diaphragm, turbine front, and turbine rim.

In Task 9.6, five additional brush seal configurations have been tested, i.e., two for the turbine interstage location, one for the compressor diaphragm, and two for the turbine front. One of the turbine interstage seals was a standard design and was the same as that tested in Phase 2. This seal was for control (bench marking) purposes. The other turbine interstage seal had EG&G advanced seal design features with a low hysteresis relief in the back plate and a flow deflector in front to reduce pressure closure. Each of the test seals was designed to accommodate large relative closures, i.e., had a large fence height, low radial stiffnesses, and larger bristle diameters.

#### 2.3.10.2.2.5.1 Static Leakage Flow

Static flow data were acquired for the test seals before, during, and after wear testing on EG&G's Aerospace rig. The dynamic rig has a seal downstream pressure that is close to ambient pressure. To model engine operation, seal wear data are obtained on the dynamic rig at representative seal pressure drops (to simulate forces on the seal bristle pack) and steady-state leakage performance data acquired with seal pressure ratio modeled. A static flow fixture was designed and built to measure static leakage of a single seal as a function of both pressure drop and downstream pressure level. Consequently, both seal pressure ratio and pressure drop can be modeled. A second reason for obtaining static flow data was to build a data base of static versus dynamic flow data for various brush seal configurations. This will assist in maintaining quality control of full-size segmented seals which cannot be readily flow checked dynamically.

Static seal leakage performance was determined in terms of flow parameter vs. pressure ratio. The data were obtained starting with a high pressure ratio data point and then taking successively lower pressure ratio points. This gave the most consistent data since the initial high pressure drop stabilized the bristle pack for the lower pressure drop measurements.

#### 2.3.10.2.2.5.2 Dynamic Rig Testing

EG&G's Advanced Aerospace seal rig was a multi-use, high speed, high temperature, dynamic test rig. At representative air temperature levels, this rig could independently simulate engine pressure drop, rotor surface speed, and relative seal closure cycle variations. The rig had maximum capabilities of 24,000 rpm rotor speed, 78 kW heating capacity, and 150 psig (1.034 MPa) supply pressure. It could accommodate seal diameters of 2.5 in to 14 in. (63.5 mm to 355.6 mm). The actual maximum achievable seal temperature and pressure drop levels varied with the rig total flow rate.

The dynamic rig used in Phase 2 testing was upgraded to allow the rig test pod containing the test and slave seals to be moved axially instead of the rotor. The total travel distance was much longer than the previous rotor movement. The result was that the precise engine closure cycle could be simulated.

Test results in the compressor diaphragm brush seal showed that for a total number of test start cycles (representative of the number of engine cycles between refurbishments for a base load power plant) the brush seal leakage flow was 60% lower than that of a four-knife labyrinth seal, normally employed in this location. Also, test data showed that a diaphragm seal incorporating advanced features, exhibited less wear than the control seal.

For the turbine interstage brush seal testing, both standard and advanced design seals were tested. The results for both seals demonstrated acceptable performance with the severe start-up conditions. However, seal performance degraded during the test. Both seals wore to the maximum line-to-line operating diameter condition after many start cycles. The standard seal design exhibited a non-uniform wear pattern; whereas the advanced seal wore more uniformly. Also, the standard seal wore beyond line-to-line in some locations. Inspection of the rotor surface was performed throughout the testing. Overall, the rotor

showed little wear or distress, however, the wear track did have bristle alloy transfer from the seal to the rotor. Even though a brush seal wears line to line at the maximum closure point after many cycles, it will still pass less leakage flow than a labyrinth seal for industrial engine applications.

Tests were carried out on the turbine front brush seals to determine their leakage characteristics. Figure 74 shows leakage results for the turbine front brush seals. At this location bristle wear is a lesser issue. A specific flow is desired at the turbine front to prevent ingress through the downstream rim seal. The horizontal line in this figure represents the desired leakage flow parameter through the turbine front brush seals. The plotted points are rig test data for a one- and two-stage brush seal. The dashed lines are best fit linear lines through the rig data. This plot has been used in engine design to select the hot-running clearance of the turbine front brush seal configuration.

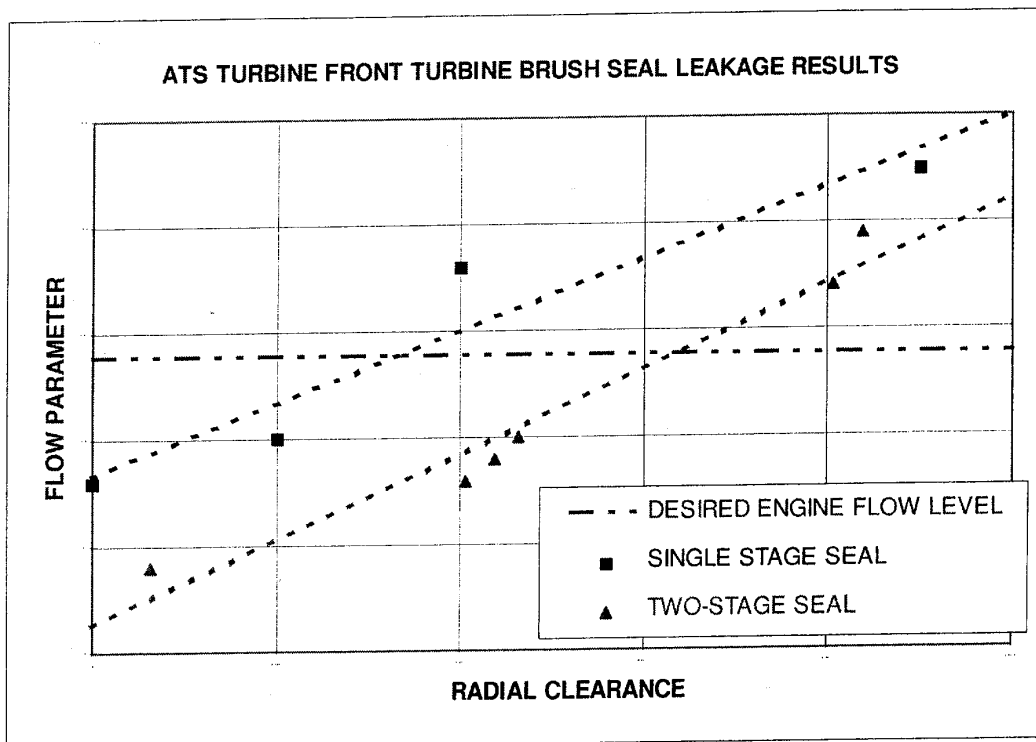


**Figure 74 Results from Turbine-Front Brush Seal Subscale Rig Testing**

#### 2.3.10.2.2.5.3 Transition Mouth Brush Seal

Development testing was carried out by Technetics Inc. on the stationary transition mouth brush seal design. Leakage and vibratory testing was performed. Turbine rim seal tests revealed that more wear was experienced at the turbine rim than at the interstage seal location due to the interrupted rotor surface. A significant pressure drop across the bristle pack was required to prevent bristle melting.

#### 2.3.10.2.2.6 Full-Scale Hardware Design/Fabrication

Results and “lessons learned” from fabricating and testing subscale brush seals led directly to defining design criteria for full-scale seals for each engine location.

The first full-size brush seals manufactured for the W501ATS engine were for several compressor diaphragm stages. The subscale seal testing for this location provided optimized seal parameter values and characterization of: 1) seal stiffness (it's effect on pressure drop capability, leakage, and life), (2) fence height (the effect of the large required fence height on leakage and pressure drop capability), and (3) advanced seal parameters (i.e., features controlling bristle hysteresis and pressure closure).

Design and fabrication of the full scale hardware required several considerations that depart from the standard aerospace type product. First, the split design of large industrial gas turbines dictates the use of a segmented brush seal. In this application, six segments form a single seal in order to simplify handling and installation of the relatively long segments. The ends form additional leak paths, but that leakage is small compared to the total seal leakage.

The second consideration is the effect of curvature on the bristle pack. Proper manufacturing process control is required to ensure bristle pack homogeneity. The fabrication process used has given such uniformity for a wide range of brush seal sizes.

The third consideration for full-scale seal fabrication is with the large dimensions and subsequent tolerancing. This is critical to properly locating the seal inside diameter which sets the initial seal interference. The stack-up of component mechanical tolerances, build-up tolerances, and operating clearances result in a sideplate inside diameter true position that can vary significantly. Verification of the dimensions of large-diameter, brush seal segments required inspection equipment capable of radially measuring "centerless" components. The challenge is to establish the center of a large arc without the aid of a fixed reference point. A large coordinate measuring device was adapted to measure solid as well as flexible surfaces. Flexible surfaces, such as along the bristle tips, were measured using a video system in conjunction with the coordinate measuring system.

A fourth consideration is to provide a contingency for the unlikely event that the rotor would rub the backplate with the large fence height. Thus, the seal backplate has a knife-edge profile to minimize damage to the rotor surface in case of a rub. Similarly, the front plate also has a knife-edge profile. It is extended to the same inner diameter as the backplate to protect the bristle pack when the seal segment is being handled and installed.

Beside W501ATS compressor diaphragm seals, other full-size brush seals were fabricated for installation into the combustion turbines. The turbine interstage was one of those applications. This seal had a bolted configuration to best fit the existing interstage seal assembly with a minimum hardware rework.

#### 2.3.10.2.2.7 Validation Testing

Proof of concept has been demonstrated with full-scale brush seal hardware. Brush seals have been installed in selected W501ATS compressor diaphragm stages and were evaluated in the compressor aero rig tests. The turbine interstage brush seals were evaluated in W501D5 and W501G engines.

In validation tests, brush seals were installed in series with labyrinth seals. Measured pressure drops across each of the two seals would indicate brush seal sealing effectiveness relative to the labyrinth seal. Monitoring leakage effectiveness over many engine starts and significant operation time would demonstrate brush seal wear. After testing, the brush seals were removed and inspected. Results from these tests would then confirm the designs based on the subscale seal testing and/or indicate changes to incorporate into future hardware. In the validation testing of the W501ATS compressor diaphragm brush seals, the seals operated well with a significant leakage reduction over the current labyrinth seal design. The compressor rig test time was limited so that seal wear life could not be evaluated.

#### 2.3.10.2.2.8 Conclusions

Brush seals were designed and developed for application in heavy duty industrial gas turbines.

Extensive testing was carried out to determine brush seal leakage and wear characteristics.

Compressor diaphragm brush seals were demonstrated in W501ATS compressor and turbine interstage seals on W501D5 and W501G engines.

#### 2.3.10.2.3 Task 9.17 Transition Mouth Seal Development

##### 2.3.10.2.3.1 Introduction

Transition mouth sealing was one specific focus for improved sealing between static components. There are several can-annular combustors in each combustion turbine. On the transition mouth sides, labyrinth seal teeth engage as adjacent transitions move together when the transitions heat up during engine operation. On the transition mouth top and bottom, connecting metal parts form seals between the transition mouth and the first-stage vane outer and inner endwalls. The transitions and connecting pieces are made of heavy metal to withstand:

- the hostile thermal and vibrational environment
- rugged field installation and handling
- periodic removal for turbine hardware inspections

Consequently, improved sealing concepts for the transition mouth must:

- (1) reduce leakage to an acceptable level to meet emissions requirements while providing minimum cooling levels
- (2) be robust for handling and the operational environment

The objective of this program was to develop a transition mouth seal design for the W501ATS engine which

- minimized leakage flow

- provided adequate cooling of the seal and adjacent parts
- met structural, manufacturing, in site installation, etc. requirements.

The task included:

- conceptual design of an improved transition mouth seal design
- fabrication of prototype seals for evaluation in the W501ATS hot cascade rig tests
- alternate seal designs as necessary.

#### 2.3.10.2.3.2 Seal Design and Manufacture

A cooled radial strut is placed between transition mouths in front of every other first stage vane. This is possible because there are twice as many first stage vanes as transitions and one vane lines up with the middle of a transition and one in between. Each transition mouth has a rectangular seal acting in the axial direction. The seal was envisioned to be a welded bellows type. Its design was based on discussions with EG&G Sealol and EG&G Pressure Science.

The transition mouth seal was required to operate with:

- a maximum material temperature set by the cooling air temperature on the high pressure side and hot gas temperature on the low pressure side
- pressure drop corresponding to the combustor pressure drop with its dynamic variation
- a design axial movement range including tolerances
- a design axial vibratory movement
- an initial operation life for rig testing and an ultimate service life between combustor/transition inspections.

It has a non-circular, welded construction which is fabricated from a higher temperature metallic alloy. The bellows has a sufficient number of convolutions to meet the expected axial movement with the design operating temperature and pressure drop. Slots have been added to the backing plate and flow deflectors placed on the seal inner side to provide a limited amount of cooling air to flow over the bellows surfaces to provide cooling and thermal protection from the hot gas path air. The seal ends were pressure balanced to prevent the seal opening during any sudden reverse pressure changes. Stress distributions in the bellows assembly were calculated using a 2-D finite element analysis. The specified seal free height and number of convolutions were established using a maximum bending stress limit. Two transition bellows seals were fabricated by EG&G Sealol. These two seals are available for evaluation in the W501ATS hot cascade rig or engine.

Using a bellows type seal approach was considered to be acceptable for the hot cascade rig testing, but there were concerns that the thin-metal structure would not be robust enough to withstand rough handling/installation at an engine site nor the high vibration environment at this location. Consequently, alternate transition mouth sealing approaches were investigated. A prime alternate approach has a seal carrier inserted between the transition outer hardware and the first stage vane end wall. Such a carrier would be placed both inside and outside of the flow path. Sealing is accomplished by brush seals on each side of the carrier. Sealing is also required on the transition mouth sides between transitions since there would not be any radial strut in front of the vanes to seal against. Sealing on the sides would be done using circumferentially directed brush seals. Requirements for the different brush seals are similar to that for the bellows seal. The axial brush seals would have to accommodate the axial relative movement depending upon location.

Two different brush seal manufacturers have reviewed the brush seal designs and requirements, and both feel that brush seals would work well.

#### 2.3.10.2.4 Task 9.7 Active Tip Clearance Control/Abradable Coating Development

##### 2.3.10.2.4.1 Introduction

Where possible, advanced coating/blade tip technology from aero and other industrial gas turbine engines was transitioned to the ATS engine. Development had been initiated in ATS Phase 2 Task 8.15, which focused on ceramic abradable coatings for turbine ring segments. Task 9.7 addressed:

- Improved compressor abradable coatings
- Turbine blade tip treatments.

Reducing compressor and turbine blade tip clearances is one critical area addressed in the ATS program to increase component and thus overall power plant performance. Abradable coatings are being used to reduce tip clearances by allowing decreased build clearances without fear of damaging hardware and by furnishing more uniform minimum tip clearances circumferentially. One sealing advancement introduced into the ATS engine is reduced hot-running clearances between the compressor and turbine blade tips and the outer air seal surfaces. This reduction gives significant increases in compressor and turbine efficiencies and thus overall plant performance. Also, an increase in output power is realized. For the ATS compressor section, a lower temperature coating was identified as the best erosion resistant, abradable coating to run against untreated blade tips for the earlier stages. For higher temperature stages in the compressor, a usable coating has been found, but work remains to determine a lower cost abradable coating/blade tip configuration. For the ATS turbine section, a high density TBC type tip coating has been identified to provide required blade tip insulation and good wear resistance.

##### 2.3.10.2.4.2 Abradable Coating Development

Abradable coatings were used in combustion turbines to run against uncoated blade tips. These coatings were placed on the stationary outer air seal surfaces

outside of the compressor and turbine blades. The coatings allowed bare blade tips to rub into them during engine startup and shutdown closure cycles with low tip wear. This provided minimum blade tip clearances at full load conditions where high engine performance was desired by: (1) allowing decreased cold build clearances without fear of damaging the blades and (2) furnishing more uniform minimum tip clearances circumferentially. Some blade tip wear was acceptable so that the blades would have a more uniform tip diameter. But the majority of the wear should occur in the outer abradable coating because of the larger circumferential variations of these surfaces caused by thermal distortions in the supporting blade ring structure.

A lower temperature abradable coating was applied to compressor outer air seal surfaces of the W501F engine and a "rub tolerant" metallic coating was applied to the early turbine stages of the W251 and W501D5 engines. The latter coating was abradable, but only for lower incursion levels with untreated blade tips. For advanced combustion turbines, the gas temperature in the early turbine stages is too high for metallic coatings. Instead, abradable ceramic coatings are being introduced onto the gas-side of the Row 1 and 2 turbine ring segments (i.e., outer air seals) of some upgraded engines. A ceramic coating not only provides an abradable surface, but also thermal insulation to minimize required ring segment cooling air flow. Both of these effects contribute to improved plant performance.

#### 2.3.10.2.4.3 Requirements

The general requirements for abradable coatings and mating blade tips are:

- Majority of the wear was to be in the abradable coating rather than the blade tips to minimize steady-state tip clearances (this may necessitate blade-tip treatments)
- Incursion rates are low compared to aero engines (maximum less than 0.0001 in/sec. [0.00244 mm/sec., which agrees with published test data for the W251 engine. Aero engines have an order of magnitude higher incursion rates)
- Two abrasion interference levels are of interest: a modest one for light rubs and a maximum one for heavy rubs.
- Set of maximum environment temperatures and air velocities at the tip for steady-state operation for the various compressor and turbine stages being considered.
- Operating life matching the same for replacement of outer air seals in the compressor and turbine (this implies erosion rate must be low).
- For the early turbine stages, provide thermal insulation for the ring segments.
- For the ATS Row 1 turbine blade tip, provide thermal insulation for the blade tip as well as an abrasive surface to rub against the abradable ring segment coating (tip treatment processing issues must be addressed since the blade airfoil surfaces will have TBC).

#### 2.3.10.2.4.4 Compressor Abradable Coatings

Compressor abradable coatings have been used in gas turbine engines for the last twenty years, especially in flight engines, to control blade tip clearances and thus improve compressor efficiency. Abradable coatings are increasingly being specified in the ground based gas turbine industry to meet demands for improved efficiency.

The current abradable coating specification for combustion turbines is a lower temperature one. The compressor blade tips are not treated to avoid adding processing costs. There are two issues relative to using this coating in the ATS compressor that led to a development effort. The first issue is erosion resistance. This type of coating has been used in flight gas turbines because of its good abradable characteristics. The coating appears to have a low risk when operating for relatively short times. There are no published erosion data to indicate this coating has an operational life sufficient for industrial turbine applications. The second issue is maximum operation temperature. The air temperature in the latter stages of the ATS compressor is above the current coating operating temperature. These two issues necessitated that alternate abradable coatings be identified for the ATS compressor.

The approach taken in this program was to: (1) select candidate abradable compressor coatings, (2) determine the best coatings to use from erosion and abradability rig testing of candidate coatings versus the current coating, and (3) validate coatings in the W501ATS compressor rig test. Sermatech International, the vendor applying the current coating to compressor hardware, was the primary vendor supporting the development efforts.

##### 2.3.10.2.4.4.1 Coating Selection

The operating conditions of the ATS compressor were taken from aerodynamic design data. Parameters considered at each compressor stage were: air temperature, air velocity, blade tip velocity, and incursion rate. Also the desired level of incursion versus stage number was estimated from design calculations. These parameters were of interest during the startup/shutdown closure cycle when maximum incursion occurs and at full-load operation where erosion is important.

The maximum air temperatures are below the lower limit of current coatings for the initial compressor stages. Based on a thorough search of available coating powders, an alternate coating was selected for the initial compressor stages which had an expected better erosion resistance than the current coating without sacrificing much abradability. For the latter stages, two higher temperature candidate clay type coatings were selected. Both of these latter stage coatings have the temperature capability, but are considerably more expensive than the lower temperatures varieties.

Test samples of each of the four coatings were applied to substrates during a single spray run to assure coating uniformity among the test samples. All coatings were applied using a robotic torch with established, proprietary parameter values. The microstructure and hardness of representative specimens for each coating type was evaluated to ensure proper sample quality.

The new lower temperature coating has a higher measured superficial hardness than the current coating.

#### 2.3.10.2.4.4.2 Erosion Testing

High temperature erosion testing was conducted at the University of Cincinnati. The test samples were trapezoidal in shape and had the test coating on one side. Each sample was placed in a holder to orient it at a specified angle to the erodent stream. The angle is based on the expected impingement angle of erodents hitting the compressor outer air seals. Once a sample was heated to the desired temperature, the erodent was introduced into the impinging gas stream. The sample was weighed before and after testing and the results were reported as a sample weight loss divided by the total weight of erodent material in the gas stream over the test time period. The rig parameters were based on the expected full-load conditions at each compressor stage where the test coating would be used. Two representative temperature levels were selected for each coating.

The results of the erosion testing showed that the erosion resistance of the two lower temperature coatings decreased with temperature, matching expectations. Also, the erosion resistance of the new coating was significantly better than the current coating at two different temperatures. The erosion resistance of the two higher temperature coatings was superior to the lower temperature ones, although they were tested at higher temperature levels.

#### 2.3.10.2.4.4.3 Abradability Testing

The incursion testing was conducted on a specially designed test rig at Sulzer Innotec Ltd., Winterthur, Switzerland. The test disc was made of steel and had slots for test blades to rub against the coated specimens. The specimens were mounted on a precision table driven by a motor capable of 0.15  $\mu\text{m}$  movement steps. The specimens were heated by a high velocity burner which produces a thermal gradient similar to that in the engine. The rotating disc and blade moved the hot gas against the flame guide and specimen. Cooling air was introduced directly above the specimen to avoid a hot spot on the top. By regulating the burner position, gas temperature, and cooling air flow rate, a wide range of specimen temperature levels and gradients was attained. Temperature calibrations were completed under real test conditions, using an instrumented calibration plate in place of a specimen. Backside thermocouples and a front-surface focused optical pyrometer were used to measure temperature. The optical pyrometer assured temperature measurements of the abradable surface and not the impinging gas. The specimen position relative to the rotating blade tip was controlled so that the desired incursion rate, incursion depth, and retraction rate at the end of the test were achieved. The specimen holder included piezo electric force sensors to measure the cutting forces tangentially and radially to the blade tip surface.

The parameters measured in the abradability testing were: blade tip velocity, temperature at the front and rear of the specimen, specimen wear track length, incursion depth, incursion rate, blade height variation, specimen wear track roughness, and wear mechanism. The total incursion depth was calculated accurately from measurements of the blade height change and specimen wear

track length. A comparison measure of abrasability for the material pair is the ratio of blade tip wear to total incursion depth.

Wear track roughness is also important because it gives an indication of the amount of grooving. Grooving is mostly a result of extreme build up or wear of the blade tip material and thus is a significant wear mechanism indicator. Deleterious mechanisms such as coating rupture were also noted. Typically, materials with higher surface roughness are preferred because they indicate clean cutting and removal of the coating; whereas, lower values may indicate glazing or densification at the surface.

The abrasability test matrix included: specimens with different coating types, two different blade materials, two different blade tip thicknesses, two different blade tip velocities, two different gas temperatures depending upon the coating type, and as coated and machined coating surfaces.

Inspection of the surface of a typical coated specimen after incursion testing with the new lower temperature coating showed that slight amounts of blade tip wear and coating densification occurred, depending upon the test conditions. However, the ratio of blade tip wear to total incursion depth was low. Thus, as expected, the new coating demonstrated good abrasability. Results for the higher temperature coatings showed that the first one produced a high level of blade tip wear compared to the incursion depth and thus was not a good candidate abrasable coating. The more expensive second coating produced blade tip wear comparable to that of the lower temperature coatings.

It was concluded from the rig testing that the new lower temperature coating is a suitable replacement for the current one. The new coating provides equivalent abrasability characteristics and much better erosion resistance in the initial compressor stages. For higher temperatures in the latter compressor stages, the second clay-type coating is a better choice than the first one because of its superior abrasability characteristics for comparable erosion resistance.

Subsequent to the rig testing, a concern was raised about the candidate coatings delaminating during occasional compressor washes. To simulate this event, samples of each coating type were soaked in room temperature water for a minimum of 30 minutes. The coating samples were then placed in a furnace and heated at a rate profile representative of an engine startup. The maximum temperature level reached was a function of the coating type. The samples were then held at the maximum temperature for 30 minutes and furnace cooled to room temperature. The samples were subsequently examined visually for delamination, and then mounted and polished in cross section to look for signs for delamination under magnification. The results showed that none of the candidate coatings had signs of delamination either at the bond line or within the coating.

#### 2.3.10.2.4.4.4 Coating Validation

Sermatech coated the outer air seals of ATS compressor test hardware. The earlier stages had the new lower temperature coating. The latter stages had the first clay-type coating. This coating was not the recommended one, but hardware cost and test rig schedule dictated that the less expensive, more readily available coating be used.

The compressor was successfully run with the coated air seals. Excellent performance was measured. Some rubbing of the blade tips with the outer air seals occurred during the test. After the compressor was dismantled, the hardware was carefully inspected. Examination of the hardware after the test showed that:

- The wear pattern in the lower temperature coating rows varied circumferentially, but the coating had good cut patterns and appeared to perform well
- Acceptable blade tip wear did occur in some rows with the lower temperature outer air seal coating
- In the rows where the outer air seals had the higher temperature coating, there was evidence of coating surface glazing and the wear occurred almost entirely on the blade tips and not in the coating.

The relatively short runtime of a test such as for the ATS compressor did not allow a confirmation of the erosion rig test results. However, the rub indications did validate the abrasability testing i.e., the new lower temperature coating is a good choice for the lower temperature stages, and the first clay-type coating should not be used for the higher temperature stages (at least with bare blade tips).

Consequently, further effort is needed to identify a better abradable coating/blade tip configuration for the higher temperature compressor stages. This effort would include investigating: (1) reducing the cost of the SAB-145 coating, (2) possible cost effective blade tip treatments to run against the SAB-135 coating, and/or (3) other outer air seal coatings and materials.

#### 2.3.10.2.4.5 Turbine Abradable Coatings/Tip Treatments

As noted earlier, turbine abradable coating system development was initiated in ATS Phase 2. That effort focused on ceramic abradable coatings for the ring segments in the first and second turbine stages. These types of coatings have been under development by aero gas turbine manufacturers and vendors for nearly two decades. The previous effort included: identifying the most cost effective abradable coating system, rig testing coated samples, and installing prototype coated ring segments into an operating combustion turbine.

A summary of the accomplishments is as follows:

- Testing of vendor coating system under combustion turbine conditions showed:
  - The coating shock resistance meet aero engine standards
  - Erosion rate was acceptable to met service life requirements
  - Blade tip treatments would be necessary to meet the requirement that the wear would be primarily in the coating (different than for aero engines because large industrial engines have low incursion rates)

- Eight Row 1 ring segments were coated and installed in a W501D5 engine operated by Dow Chemical. These segments were placed in pairs at the top, bottom, and horizontal joint locations with the coating penetrating into the flow path versus adjacent segment surfaces.
- The coated ring segments were inspected via borescope after approximately 8,000 and 16,000 hours of operation (1 and 2 years, respectively).
- The blade tips did not have any rubbing or wear indications (turbine tip clearances of this row could be closed down by the thickness of the coating with low risk of damage).
- Some erosion occurred on the coating edges but primarily on the sides facing an adjacent uncoated segment.
- Minor erosion swirl patterns were noted on the coating surfaces at the bottom.
- It was concluded that the selected ceramic abradable coating would work satisfactorily in higher turbine temperature engines with no blade tip treatments if the incursion level is expected to be small. However for tighter tip clearances, the blade tips should be treated.

#### 2.3.10.2.4.5.1 Turbine Blade Tip Treatment Development

A follow-on effort was conducted as part of Task 9.7 to develop abrasive blade tip treatments to rub against turbine ring segment abradable coatings. Pratt & Whitney's Talon testing showed that cubic boron nitride (CBN) blade tip treatments provide a good abrasive surface to rub against ceramic abradable coatings and their data quantified the tip-to-seal wear ratio as a function of the number of blade tips treated out of the stage. The CBN coating is sacrificial and oxidizes away after a few hours of engine operation, but the tip coating is thin enough so its disappearance only slightly increases blade tip clearance.

In this program, the blade tip treatment work was extended to developing a long life tip coating that is not only abrasive but provides thermal insulation of the metal blade tip. Tip insulation is required for the first and second ATS turbine blade rows because of their internal closed loop cooling. Praxair Surface Industries in Indianapolis, IN, supported this effort. They have a proprietary, high-density yttria-stabilized zirconia (YSZ) coating that has both insulating and abrasive properties.

Recent advances in thermally sprayed YSZ coatings have led to high-density coatings that have excellent erosion resistance and better thermal shock resistance than lower density zirconia coatings. Thermal shock resistance is obtained via a patented process to cause formation of vertical segmentation cells during the coating cycle. They found excellent performance of a shrouded plasma spray high density YSZ tip coating in aero engines running against various abradable seal materials. They can also produce the special YSZ structure using a detonation gun coating method.

Praxair's work was extended by testing their dense YSZ coatings against low-density YSZ seal coatings (comparable to Pratt & Whitney's Talon's porous TBC). To improve abrasability, coating density should be reduced, but that will also lower its erosion resistance. Consequently, Praxair's work included both erosion testing of the individual seal and blade tip coatings and the abrasability characteristics of the tribopair. Several seal and tip coating test samples were prepared covering a range of seal coating density and different coating application methods for the tip to obtain more wear resistance.

Duplicate seal and tip samples were erosion tested in both Praxair and University of Cincinnati rigs with particle velocities and impingement angles modeling that in the engine blade tip region.

Results from the erosion and abrasability testing demonstrated which tip treatment process gave the most wear resistant tip and the seal coating density compromise to give acceptable tip-to-seal wear ratios and still have acceptable erosion resistance.

After completion of the tip treatment development effort in Task 9.7, the ring segment design has progressed to the point that the abradable surface would require a rather thick layer to provide the desired running blade tip clearance after rubbing. Such thicknesses would lead to high porous TBC surface temperatures and the coating would sinter. Sintered TBC will spall from the ring segment surfaces leading to larger tip clearances and ring segment material loss from oxidation. Accordingly, additional work was planned to extend the current effort for a new high temperature, proprietary seal coating system under development for ATS ring segments. Initial rig testing showed that this coating had very good erosion resistance and abradable characteristics.

#### 2.3.10.2.4.6 Conclusions

Significant progress has been made in applying abradable coating sealing technology to combustion turbines for the purpose of reducing the compressor and turbine blade tip operating clearances. Such reductions will significantly improve component and thus power plant efficiencies.

Abradable coating development focused on improved tip clearance control. For compressor coatings, erosion and abrasability testing showed that a new lower temperature coating has equivalent abrasability characteristics as the currently used coating, but has much better erosion resistance. For the latter compressor stages, two candidate clay type coatings were found to have good erosion resistance at the higher temperatures experienced in the latter stages and the more expensive one of the two had better abrasability. The ATS compressor tests confirmed the abrasability findings of the rub tests. Overall, the compressor coating development effort showed that the lower temperature coating is a good candidate for earlier compressor stages; however, further work was needed to identify a lower cost abradable coating/blade tip configuration for the latter stages.

For the turbine, a long-life, wear resistant coating was identified for the blade tips when rubbing against available abradable porous TBC ring segment coatings. This blade tip coating is a high density, TBC type, that also provides thermal insulation required for the tips of the close-loop cooled blades in the ATS turbine.

Erosion and abrasability tests defined the process parameters/methods used to apply the coating to achieve the most wear resistant tip. Also the testing revealed the best ring segment coating to give acceptable tip-to-seal wear rates, while still having acceptable erosion resistance.

### 2.3.10.3 Aerodynamic Development

#### 2.3.10.3.1 Task 9.4 Compressor Aerodynamic Development

##### 2.3.10.3.1.1 Introduction

To verify the aerodynamic performance and mechanical integrity of the new high pressure ratio design, the full-scale W501ATS compressor was manufactured and tested in a specially designed facility constructed at the U.S. Navy Base in Philadelphia. The compressor test was carried out at subatmospheric inlet conditions to reduce the power required to drive the test compressor to that available at the test facility.

The project objectives were as follows:

1. Verify latest compressor design technology as it was applied to an industrial sized compressor. While the licensed Rolls-Royce computer codes and design system are well validated and calibrated for their size of engines, Siemens Westinghouse engines are typically beyond that range. Nevertheless, size effects were expected to work in the favor of the ATS compressor design. In addition, with actual detailed test data available, the Rolls Royce codes could be better calibrated for subsequent analysis and future design work.
2. Demonstrate that the compressor works, producing a 31:1 pressure ratio at a target adiabatic efficiency. Many traditional Siemens Westinghouse design features were retained in the ATS/W501G compressor design.
3. Verify the compressor starting characteristics. The starting schedule was determined by necessity from a meanline analysis, which was performed beyond the code's calibrated range. Obviously, test results would be invaluable in confirming the compressor starting characteristics and in further calibrating the meanline design system.
4. Determine the optimum efficiency variable stator schedule for both design and off-design conditions. This would be an opportunity to refine the design and to accumulate additional calibration data.
5. Investigate the compressor's sensitivity to aerodynamic fouling over time. This would determine how long the compressor could be expected to perform well. A simple test of introducing oil in the inlet to coat the downstream airfoils was planned. The anticipated degradation in aerodynamic performance would then be noted.

### 2.3.10.3.1.2 Description of Experimental Facility

#### 2.3.10.3.1.2.1 Compressor and Driver

The ATS compressor was designed to provide a 31:1 pressure ratio. The ATS compressor was based upon the W501G design. The front two-thirds are virtually identical. Alterations to the W501G included two variable stators up front, four more stages at the rear to achieve the higher pressure ratio, relocation of the third bleed to the exit of stator 14, and a commensurate redesign of all downstream airfoils.

Since this was a component test, the absence of a combustor and turbine necessitated additional modifications to the design. The standard combustor cylinder was replaced by a special compressor-combustor cylinder that would house a bearing to support the rotor and serve as a plenum chamber for the discharge air. The Siemens Westinghouse Science and Technology Center (STC) was responsible for this redesign. Figure 76 provides a schematic drawing of the ATS compressor test rig.

Compressor parts were produced all over the United States. The blades were machined in Hartford. The stator airfoils were formed in Winston-Salem, and the diaphragms were fabricated in Pensacola. The discs were forged in Boston; the cylinders were manufactured in Atchison and Shreveport. The rotor was stacked in Hamilton. The entire compressor test rig was initially instrumented and assembled in Houston. Then, the rig was shipped by rail to Philadelphia for testing.

There in building 77H the compressor was mated to and driven by an LM2500 engine. NAVSSES was responsible for the maintenance and control of the LM2500. At 3600 rpm, the LM2500 could deliver a maximum power of 32,000 hp (23,862 KW). This is about one-fifteenth of the power needed to drive the rig at the intended design point. Thus, the inlet had to be throttled in deference to the available power. The LM2500 consumed on average 30 gallons (113.6 Liters) of diesel fuel per minute.

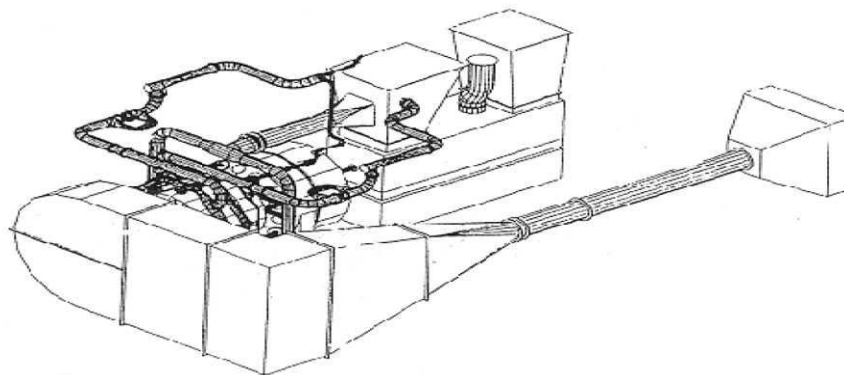


**Figure 76 Compressor Test Facility**

#### 2.3.10.3.1.2.2 Auxiliary Equipment

The test rig was supported by several major ancillary systems: an intake and bleed air system, an exhaust system, a hydraulic system, a lube oil system with a

backup, and a turning gear with a backup power supply. The intake system consisted of a filter house, a flow measurement device with upstream flow straighteners, a throttle valve, a transition duct, turning vanes, a silencer, and an inlet scroll. Mass flow rate was determined from a calibrated Annular transducer that was installed downstream of the inlet and a bundle of six foot-long flow straighteners. The throttle valve was 36 inches (914.4 mm) in diameter and had two hydraulically actuated louvers. The supersonic jet flow that exited the valve when nearly closed was redistributed downstream by two perforated steel plates in the transition duct. The hole pattern in the plates was specified to produce nearly uniform flow into the compressor. Intake traverse probes were available if an investigation of inlet flow distortion had become necessary. In addition, the plates were instrumented with strain gauges so that their mechanical integrity could be monitored throughout the test. If a plate had failed and its fragments were ingested into the compressor, a significant damage to the compressor would have resulted. The layout of the intake system was dictated by the available floor space. That is why a 90° turn was needed between the transition duct and the silencer. The turning vanes were simply curved plates that redirected the flow into the silencer with as little loss as possible. The silencer, also, was a typical Siemens Westinghouse design. The inlet scroll had a different aspect ratio but the same cross-sectional area as the regular ATS/W501G design. This was a consequence of shaft center-line clearance requirements.

Since the compressor inlet pressure was about one psia (6.895 Kpa), more than half of the compressor operated at subatmospheric conditions. This meant that a vacuum was needed on two of the bleed stages in order to remove flow for start-up. This was accomplished by routing the Stage six and 11 bleed lines back to the low-pressure intake system. But while the inlet pressure was low, the temperature was ambient. Therefore, after being heated while undergoing compression, the rejected flow had to be cooled down to near ambient temperature prior to return to the inlet. Two separate Unifin air-to-water heat exchangers handled this task. NAVSSES supplied ample cooling water to maintain acceptable cooler exit temperatures. Additionally, the low-pressure inlet system had other ramifications. The entire intake system had to be very well built to withstand a significant pressure differential (nearly 14 psi [97 kPa]). Due to the large surface areas of the intake components, loads were on the order of hundreds of tons.

The exhaust system consisted of the compressor-combustor shell, manifold piping, a back-pressure valve, and an emergency bypass valve. Compressed air discharged through the diffuser into the compressor-combustor shell, which was essentially a plenum. Eight pipes simulating the combustor layout vented the shell and then were combined into one 30-inch (762 mm) diameter exhaust pipe. A two-louver, high temperature valve connected to a hydraulic actuator, regulated the exit pressure. Since this valve operated slowly, a quick response “surge” bypass valve was also installed. Stainless steel pipe, designed to withstand 1200°F (649°C) discharge air temperatures, was used between the shell and the valve. Downstream of the valve, the flow was directed to and up the LM2500 exhaust stack. A steel transition duct connected the exhaust pipe to the stack. Since the Stage 14 bleed air pressure was above ambient, it was discharged into the LM2500 exhaust stack.

Each of the bleed lines had a hydraulically actuated, butterfly valve, a manually controlled gate bypass valve, and Annubar flow measurement devices installed in series. A hydraulic system supplied these valves along with the intake and exhaust valves and the inlet guide vane (IGV) and variable stator actuators. A W251B12 lube oil package supplied oil to the bearings. Lube oil was cooled in an oil-water heat exchanger. A DC backup power supply was available to supply critical oil to the compressor bearings in the event of a power failure. A W501D5 turning gear was installed on the front of the compressor. It was equipped with an emergency power supply as well as a manual crank. Lastly, an Allison gas turbine engine provided cooled, compressed air to the zero pressure drop seal and to the rotor torque tube cavity. The flow to the rotor torque tube was controlled to maintain an acceptable torque tube temperature of approximately 700°F (371°C).

#### 2.3.10.3.1.2.3 Control Room

The NAVSSES control room housed the LM2500 control console, the Navy's data acquisition system, the ATS compressor test rig programmable logic controller (PLC), and the Siemens Westinghouse performance monitoring equipment. NAVSSES personnel were responsible for operating the LM2500 and adjusting test rig valves and variable airfoil actuators at Siemens Westinghouse's behest. They monitored and recorded LM2500 engine performance as well as select ATS test rig instrumentation signals. The PLC, which proved to be troublesome, controlled the hydraulic actuators and monitored the compressor test rig's performance, providing warning and trip signals. A cluster of three computers connected to a local network provided real time test data reduction to Siemens Westinghouse site staff. This immediate performance information aided the test director in conducting the test.

#### 2.3.10.3.1.2.4 Instrumentation

The ATS compressor was instrumented with hundreds of transducers. For example, there were static pressure, total pressure, total temperature, and dynamic pressure transducers strategically located axially and circumferentially. Total pressure and temperature rakes were located at the inlet to the compressor (inlet flange) and at the diffuser inlet and exit (exit flange). Traverse probes and actuators were located downstream of stators one, nine, and 18. The traverse probe controller was located in the NAVSSES control room. During the course of testing, half of the available traverse probes were damaged for any number of reasons. Typically an inserted probe would encounter a moving rotor blade or pivoting IGV at an inopportune time.

Mechanical instrumentation consisted of thermocouples installed in the rotor bearings and torque tube cavity, strain gauges mounted on select stator diaphragms, blade vibration monitor (BVM) probes, and tip clearance probes. NAVSSES monitored the rotor shaft speed and provided that signal to the data acquisition system. In addition to the above instrumentation, dynamic pressure transducers were installed in and near all of the bleed cavities to ascertain the acoustic characteristics.

#### 2.3.10.3.1.2.5 Data Acquisition System

All of the hundreds of transducer signals traveling through thousands of feet of wire terminated their electronic journey in the Data Acquisition System (DAS) trailers. One of the trailers housed only the BVM system. The second trailer contained racks of the remaining signal processing and data capturing equipment, along with workbenches, tools, and supplies. In this second trailer, pressure transducer, thermocouple, mass flow rate, and NAVSSES relayed signals were collected into a VXI computer. The computer, in turn, converted the analog signals into digital data, applied calibration curves to transform the data into engineering units, displayed tables of the data, and then ultimately stored the data onto the computer's hard drive. At the conclusion of a day's testing, the data stored on the VXI hard drive was transferred onto two duplicate 100 Mb removable Zip discs.

While Siemens Westinghouse has previously used National Instruments' LabView software for data acquisition only, it is capable of doing much more. So, for the ATS test, the application of LabView was extended to instantaneous data reduction and graphically displaying any type of "virtual instrument." Ergo, a second computer, dedicated to data reduction and, also, local network support, was connected to the VXI computer. Accepting an array of data from the VXI computer, the second computer calculated pressure ratio, adiabatic efficiency, referred speed, and flow function. These parameters were plotted in various ways. Similarly critical temperature and vibration measurements were graphed as a function of time. The second computer could also process dynamic data and produce Fast Fourier Transform (FFT) displays. Besides that, the second computer provided data to a local ethernet network and a router connected to an ISDN line. This network allowed other authorized computers, running LabView, to display test data in real time anywhere. Thus, engineers in Orlando could monitor the test nearly as well as test engineers in Philadelphia in the NAVSSES control room. One last function of the second computer was to record test data once every minute. This data was transferred to Orlando at the conclusion of every test. It was also collected and archived onto a one Gb removable Jaz disc.

In addition, a third independent computer captured all of the transducer data and some dynamic data once every second. This computer functioned as a kind of "black box" or flight data recorder. The once-per-second data was written to Jaz discs and ultimately archived in Orlando.

To support subsequent post-processing analysis, analog dynamic signals, such as those from the Columbia acoustic probes, Kulite static pressure transducers, and the mechanical strain gauges, were recorded onto a digital audio tape. Three eight-channel recorders were used.

#### 2.3.10.3.1.2.6 Operation

Test engineers typically began their day in the afternoon for two reasons. First, the LM2500 could run at a higher power, because of the lower ambient temperature in the evening. Second, the high noise level of the compressor would be less disruptive to other NAVSSES projects housed in the same building. Test engineers would hold informal meetings amongst themselves and NAVSSES personnel to ascertain the condition of the test rig, the LM2500, and

the ancillary equipment. They would confer with Orlando regarding the previous evening's testing and decide upon objectives for that evening. Often the data reduction system was refined or improved during the day to meet current testing needs. Therefore, by late afternoon the latest version of LabView would be installed upon all of the support computers. LabView's functionality would be documented in a daily written report to the test director. The field engineer would provide a report confirming that the rig was ready to run. These reports were required before testing could commence.

Prior to testing the compressor, the intake, and exhaust valves were open, the IGV and variable stators were closed, and the bleed valves were open, and the turning gear had been running typically since the previous shutdown. With the go-ahead granted by the test director, NAVSSES would initiate LM2500 start. Rotor shaft speed would accelerate from approximately 3 rpm to 1000 rpm. At that time, the inlet valve would be closed down to drop the inlet pressure, thereby reducing the load on the LM2500, allowing it to accelerate to 3600 rpm (or test speed). At test speed, the bleed valves would be closed gradually. Then, the IGV and variable stators would be set to their respective nominal or test positions. Lastly, the exhaust valve would be closed to increase the back pressure on the rig. The intake and exhaust valves were adjusted to maintain the desired test pressure ratio and shaft speed while operating the LM2500 at maximum power.

After allowing the compressor to thermally stabilize, the evening's testing would begin. At a chosen speed, for example, traverse probes would be inserted into and retracted from the flow field, or IGV and variable stators would be adjusted systematically to achieve optimum efficiency.

At the conclusion of testing, the rig was shut down. First, the compressor was unloaded by fully opening the exhaust valve. Then, the bleed valves were opened, and the IGV and variable stators were closed. Running at 3600 rpm, the compressor would be spin cooled for approximately 10 minutes. After that, the shaft speed would be gradually reduced to about 1000 rpm, the intake valve would be opened, and the rig would spin cool for about another 10 minutes. Following spin cool, the compressor would be further decelerated to 600 rpm, where the LM2500 would trip. Consequently, the system would coast down slowly to 200 rpm, at which time the turning gear would start. The turning gear ultimately would maintain a three rpm shaft speed throughout the night and next day.

#### 2.3.10.3.1.3 Test Results

##### 2.3.10.3.1.3.1 Aerodynamic

The test results validated the latest aero engine design technology as applied to an industrial compressor. Compressor performance was demonstrated at the design point as well as at off-design conditions. The inlet mass flow and overall adiabatic efficiency were as expected. The compressor starting characteristics, especially with respect to the variable stators were optimized. The optimum variable stator schedule for both design and off-design conditions was determined. Compressor characteristics (maps) were generated at the design

IGV angle setting was well as at several other (closed) settings. Variation of compressor inlet flow versus IGV angle setting was determined.

#### 2.3.10.3.1.3.2 Mechanical

A multiprobe blade vibration monitor (BVM) test was performed on Rows 1, 3 and 4 of the ATS compressor rotor. The objective of the test was to measure blade frequencies. Synchronous responses at multiples of running speed were also measured during start-up and shutdown. The first mode vibration was observed in all three rows. The monitored blade rows were acceptably tuned, and the measured frequencies agreed with predictions. The synchronous vibration amplitudes measured were well below the test limits which were set at approximately one half the HCF endurance limit. Nonsynchronous responses at 3600 rpm and various operating conditions were also monitored on all three rows using the 2-probe BVM system. Response levels were small. Deflections were measured during several different surge events. The measured values were less than the predicted ones.

Compressor diaphragms Rows 3, 6 and 10 were strain gauged. The stages selected for instrumentation were based on analytical results showing the least amount of design margin. Although measured response was low level, typically 1 to 2 psi (6.9 MPa to 13.8 MPa) during start up transients, distinct resonant events were recorded throughout the operating range. As a result, natural frequency modes from first bending to fourth torsion were identified and compared to analytically predicted frequencies. The measured frequencies were within 10 percent of the predicted values.

The ATS Compressor blade-tip clearances were measured before and after the test. In addition, rub probes measured minimum running clearances. Abradable coating inspection provided a final indication of blade-tip clearance. Minimum running clearance was measured by rub probe pairs located in the base and cover flowpath at several axial positions.

#### 2.3.10.3.1.4 Conclusions

The ATS compressor test was completed successfully within the allotted time.

Test results showed that the compressor aerodynamic performance was as expected.

BVM and strain gauge measurement showed that blade and stator vibratory stresses were well within design limits.

Test results validated the latest aero engine design technology as applied to an industrial compressor.

#### 2.3.10.3.2 Tasks 9.5 and 12.1.5 Turbine Aerodynamic Development

##### 2.3.10.3.2.1 Introduction

The primary objective of the turbine test was to confirm the aerodynamic and heat transfer design of the ATS turbine. The test results will also lead to an expansion of heat transfer and aerodynamic knowledge of an advanced, highly

loaded turbine. The acquired knowledge from the test will also be applicable to updates and future developments. The objectives were to be achieved as follows:

- Provide external heat transfer coefficients that will be used to optimize and confirm cooling specifications.
- At design pressure ratio, increase of 1.0% point in turbine adiabatic efficiency through:
  - Indexing of turbine airfoils.
  - Reduced cooling flow requirements.
  - 3-D aerodynamic optimizations.
- Utilize test results to calibrate and develop unsteady CFD analysis system for aerodynamic and heat transfer design.

Clocking, also known as indexing, consists of adjusting the circumferential positions of vanes or blades in a downstream row relative to vanes or blades in an upstream row, respectively. The desired objective is to identify the vane/vane and blade/blade index position that will give the optimum performance and durability of the turbine. Some of the parameters that are commonly used to assess the effects of clocking on performance are overall turbine efficiency and heat transfer rate of clocked airfoils.

During the last decade, the subject of clocking became an area of interest for many gas turbine designers and manufacturers. As a result, various experimental investigations were conducted to study clocking and to identify turbine design areas where clocking may be beneficial. The major conclusion from these studies was that significant improvements in turbine efficiency could be achieved with careful indexing of the turbine airfoils.

An experimental investigation was conducted to explore the effects of clocking and explore the possibility of using clocking technology in advanced industrial gas turbine designs. The experiment was conducted to investigate the effects of clocking on turbine efficiency and heat transfer of clocked rows. This experiment is unique because it utilized a full two-stage turbine for which the first vane row was clocked relative to the second vane row and the first blade row was clocked relative to the second blade row. The ultimate objective was to develop design rules for turbine clocking that would help to achieve world-class gas turbine performance.

Although CFD analyses were performed to aid in the understanding of the flow physics and the experimental findings, only limited data is presented to support the discussion. The findings from the current investigation represent a significant addition to the very limited experimental data on clocking. It is hoped that this data can be used to validate CFD codes, which are currently used to assess the benefits of clocking.

### 2.3.10.3.2.2 Test Facility and Test Rig

The experimental program was performed at the Ohio State University Gas Turbine Laboratory. For these measurements, the facility was operated in shock-tube mode. The design of the facility is such that it can accommodate full-scale rotating turbines operating at non-dimensionally scaled aerodynamic conditions. Figure 77 shows a schematic of the test facility.

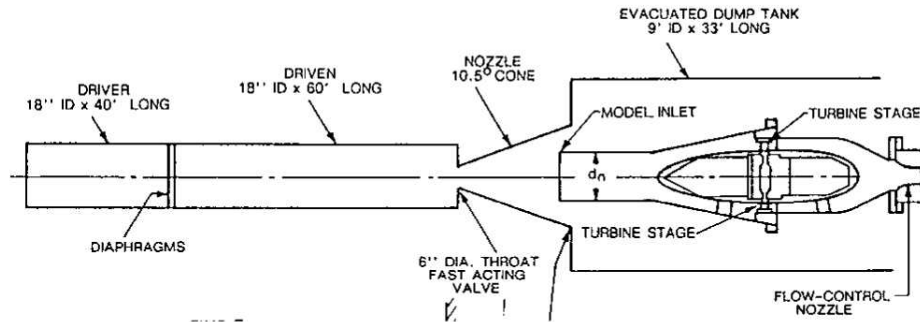


**Figure 77 Schematic of the Ohio State University Gas Turbine Shock Tube Facility**

A schematic of the test section configuration is shown in Figure 78. This configuration is a 1/3-scale model of stages one and two of the ATS turbine. The airfoil count for the model turbine is 32 first stage vanes, 48 first stage blades, 32 second stage vanes, and 48 second stage blades. A view of the airfoil geometry profiles is shown in Figure 79, along with the various clocking positions evaluated. Vane locations were referenced from a static location of “top dead center”; blade locations were referenced from a rotor location of “Slot A”. Data collected include inlet and exit total pressures and temperatures, turbine mass flow and shaft speed, airfoil leading edge temperatures, and inter-row endwall and airfoil surface static pressures and heat flux. In all, about 400 pressure transducers, thermocouples, and heat-flux gauges were used to instrument the turbine for detailed flow field measurements.

As shown in Figure 78, the inlet section was designed with contoured end-walls to maintain uniform inlet flow conditions into the turbine.

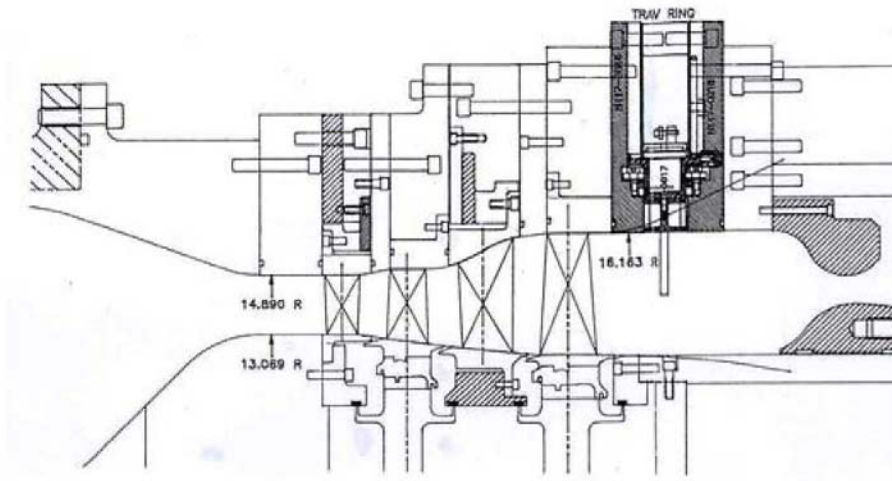


**Figure 78 Schematic Diagram of the Turbine Test Rig**

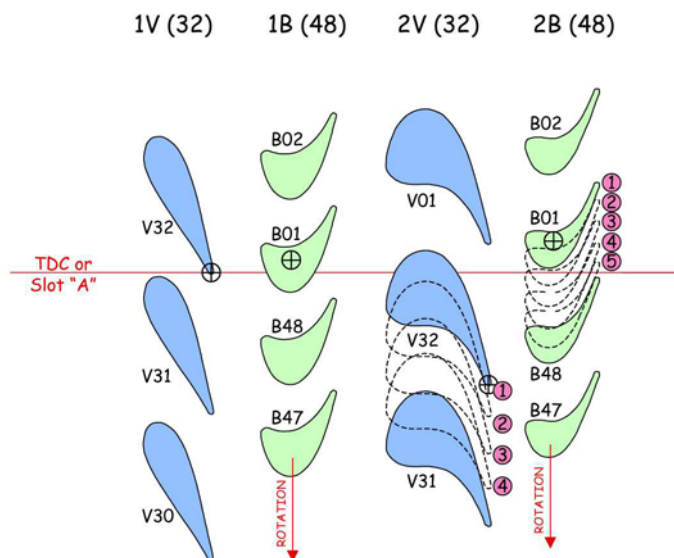


**Figure 79 Turbine Airfoil Geometries and Clocking Positions**

#### 2.3.10.3.2.3 Experimental Procedure

Measurements were obtained to investigate the effects of vane and blade clocking on turbine performance. At the upstream traverse plane, two rakes were used for total temperature and two rakes were used for total pressure measurements.

The pressure rakes were placed circumferentially 180° apart, and at 90° from the temperature rakes. A similar configuration was used at the downstream measurement plane. The total blockage area by the sensors was less than 0.07% relative to the flow area. The total blockage area set by the rakes was less than 0.5%, which is also negligible. The downstream rakes were located at a distance equal to one blade chord from the trailing edge of the Row two blade at the inner diameter.

Evaluations of four vane/vane clocking positions, spaced at 25% vane pitch per position, and five blade/blade clocking positions, spaced at 20% blade pitch per position, were conducted. When evaluating vane/vane clocking, the blade/blade position was set at index location one; likewise when evaluating blade/blade clocking, the vane/vane position was set at index location one. For the first vane/vane clocking position data were collected five times, each time indexing the exit traversing rake 25% of a second vane pitch, with exit traversing rake position five being a repeat of exit traversing rake position one displaced by one vane pitch. For all other vane/vane clocking positions data were collected at exit traversing rake positions one through four, without position five as a repeat. A repeat point was taken for the first blade/blade clocking position, which was identical to vane/vane clocking position one, before continuing with evaluation of the other blade/blade clocking positions two through five. Data for blade/blade clocking position two was not captured during the experiments and due to test scheduling was never re-attempted.

#### 2.3.10.3.2.4 Results and Discussion

Aerodynamic efficiency values at discrete radial heights were computed using the following equation:

$$\eta(r) = \frac{1.0 - \frac{T_{total\_exit}(r)}{T_{total\_inlet}}}{1.0 - \left( \frac{P_{total\_exit}(r)}{P_{total\_inlet}} \right)^{\frac{\gamma-1}{\gamma}}}$$

where P and T are the time and pitchwise average pressures and temperatures respectively, and r is the radial height. The above equation assumes that the inlet total pressure is uniform, which is the case in the present experiment. An uncertainty analysis was carried out, including the effects of individual sensor scatter, spatial variability, and boundary condition impacts on performance and wake windup was done; as well as performance calculation sensitivities due to shock tube specific concerns such as through flow time from inlet to exit plane, heat transfer, and the selection of a time window for data processing. The root-sum-square of all these uncertainties represents approximately 30% of the measured efficiency deltas due to airfoil clocking in these experiments, of which half of the uncertainty value is precision and the other half is bias.

The variation of efficiency was found to exhibit a sinusoidal shape for the two clocking pairs of approximately 4% points peak-to-peak in a relative basis, or a net benefit of 2% in a relative basis over that of a non-equal airfoil count turbine representative of random clocking. This is assumed to be the maximum efficiency benefit that may be achieved with clocking in this 2-D flow.

At the 90% position, it is hypothesized that the secondary flows are offsetting the wake position and therefore the clocking benefits are phase shifted. This is one area where a detailed CFD study will help to gain a better understanding of the flow physics.

#### **Figure 82      Effects of Clocking at Different Radial Heights, Blade Two Clocking**

The benefit for blade clocking is in phase and of similar magnitude at all spanwise locations, except at 90% span. However, this time at 90% span it is noted that the phasing is consistent with the mid-span, but the benefit magnitude for clocking is more than double that of the mid-span. It is hypothesized that this difference is primarily due to secondary flow or tip clearance effects. These hypotheses are being investigated more thoroughly via computational fluid dynamics (CFD).

#### 2.3.10.3.2.5 Conclusions

An experimental investigation was conducted to assess the effects of turbine airfoil clocking on aerodynamic efficiency for an advanced industrial gas turbine. It was found from the experiments and analyses that a significant gain in efficiency may be achieved by appropriately clocking vanes and blades of successive stages in a relative basis per clocked airfoil row for this configuration.

Moreover, the gain in efficiency was found to be similar for vane/vane and blade/blade clocking, and the gain was additive. Wake tracking analyses show that, wakes from an upstream vane or blade should impinge on the downstream vane or blade leading edge, respectively, for optimum performance.

#### 2.3.10.3.3 Task 9.18 Rotor Cooling Air Compression/Diffusion Development

##### 2.3.10.3.3.1 Introduction

The ATS turbine rotor parts are cooled with a unique closed-loop cooling scheme. In this unique turbine cooling air system, compressor discharge air is bled from the combustor shell, routed through a heat exchanger to reduce the temperature and introduced to the turbine rotor at the rear of the shaft. The cooling air is then injected into the bore region of the turbine rotor and pumped up to the blades using pumping vanes integral to the turbine discs and passages between turbine disc and nickel disc side plates. After cooling the blades, the majority of the air is then fed back into the combustor shell through a pressure recovery diffuser located just upstream of the Row 1 rotor.

There are two new features in the turbine rotor cooling air system. One is the finned disc cavity compression system and the other one is the pressure recovery diffuser located just upstream of the Row 1 disc cavity. The finned disc cavity is used to achieve maximum pressure rise and reduce the pressure loss as cooling air is pumped up to the turbine blades. The recovery diffuser/deswirl is used to recover a portion of the dynamic head from the returning cooling air coming off the rotor. These two new features are necessary to ensure that the rotor secondary air is pumped up to the required pressure, thus, avoiding or minimizing the use of an external compressor. By eliminating the external compressor, considerable costs (at least 1 million dollars) in hardware and control system could be saved. In addition, since the finned disc cavity compressor and the diffuser are integral parts of the engine, there will be virtually no unscheduled system shut down caused by an external compressor or associated control system malfunction. Further more, eliminating the power to drive an external compressor will also be beneficial to the overall performance of the ATS engine.

To achieve the above goal, a concerted development effort was required. By working together with Concepts ETI, a well recognized company in advanced technology development and testing of diffusers and centrifugal compressor designs, a model test program for the diffusion/compression system was setup. Series of tests were run and component performance was evaluated. Detailed CFD analyses were conducted, further improvement to the current system design was proposed, and future work planned.

#### 2.3.10.3.3.2 System Design

A design feasibility study was conducted on the pressure recovery systems for the rotor cooling air. The investigation was broken into two parts dealing with the rotor and diffuser geometry separately. Several different rotor configurations were evaluated. The rotor performance was evaluated by comparing the predicted rotor exit total pressure and absolute flow angle. The objective was to maximize exit total pressure while minimizing exit flow angle, since diffuser performance degrades rapidly as the absolute flow angle increases. The diffuser performance was greatly dependent on how the flow exited the rotor and entered the diffuser. The final design consisted of pumping vanes integral to the turbine discs.

Several diffuser designs were analyzed, using an empirical correlation. The requirement of zero exit swirl was eliminated to increase the margin for pressure recovery. The final design incorporated a channel diffuser.

#### 2.3.10.3.3.3 Rig Design

Concepts ETI designed a test rig which could model not only the coolant recovery system but also the pumping vanes and radial holes in the disc cavity. This test rig was able with separate builds to determine the performance of the radial pumping vanes, the pumping vanes plus two radial holes, and the cooling flow recovery system all on one rig. Separate builds were necessary both for instrumentation purposes and because different flow conditions were required depending on the subcomponent being tested. The flow passages in the rig were very similar to that of the full scale gas turbine but scaled down to a 0.3:1 scale to reduce the test rig weight and power requirement. The rig was fabricated out of aluminum wherever possible in order to reduce the weight and cost. A complete structural analysis of the test rig was performed using the ANSYS finite element analysis program. In addition, a thorough rotor dynamic analysis of the rotor system was performed to ensure that there were no problems with rotor dynamic instability, excessive bearing loading or forced response. The heat exchanger and the boost compressor were optional and could be used to run the test at different Reynolds numbers. In the actual tests conducted, these two devices were not used. A 75 horse power (55.9 kW) electric motor was used to drive the test rig with speed variation obtained by using a belt drive. After the rotor started, the ambient air was sucked into the test section through a bellmouth inlet (in the presence of the boost compressor, the ambient air was first compressed and cooled through a heat exchanger before entering the bellmouth inlet). After passing through the test section, the air was then dumped back into the ambient through two flow meters and valves. The primary flow was the flow through the recovery diffuser and the secondary flow was the leakage flow. The flow going through the test section could be adjusted by the two valves for the primary flow and the secondary flow.

#### 2.3.10.3.3.4 Test Results

A series of tests were carried out to evaluate the diffuser performance. The results showed that overall diffuser recovery coefficient was lower than expected and the cavity core rotation factor was lower than predicted, resulting in less

dynamic pressure available for recovery in the diffuser. After the first series of tests a 3-D CFD model was setup to investigate the cause of the low core rotation factor in the cavity. By matching the cavity pressure and mass flow rate to the diffuser the CFD results showed a much higher core rotation factor.

3-D streamline patterns revealed that tangential velocity in the cavity was reduced by the back sweep effect due to the pressure of the stationary wall on the diffuser side. However, it was concluded that the back sweep effect alone was not the sole reason for the low core rotation factor. Careful examination of the rig revealed a possibility of a large leakage through the left side brass seal. A follow-up test with additional instrumentation indicated that indeed there was a large leakage flow through the seal.

Based on the above, the test rig was modified and the tests were repeated. There was a substantial improvement in the overall diffusion recovery coefficient. The performance of the diffuser itself met the design requirement. Also, the core rotation factor was much improved and close to the target value. However, the overall diffusion recovery coefficient was still lower than expected. Further CFD analysis indicated a large boundary layer buildup from diffuser inlet to the diffuser throat, resulting in a large total pressure loss. The program was stopped due to a shift in emphasis in rotor closed-loop cooling.

#### 2.3.10.3.3.5 Conclusions

A novel rotor cooling air compression and diffusion system was designed for the ATS closed-loop air cooling circuit.

A rig was designed and constructed to verify the compression/diffusion concept.

Test results showed that the concept has promise, but required further fine tuning.

#### 2.3.10.4 Tasks 9.8 and 12.2.1 Combustion System Development

##### 2.3.10.4.1 Introduction

Due to the higher firing temperatures and the stringent emission requirements for the ATS engine, combustor development is one of the critical areas requiring significant effort and the incurring of significant costs.

The objectives of this program were as follows:

- Emissions:  $\text{NO}_x$  to be below 10 ppmv @ 15%  $\text{O}_2$  without the necessity of water injection or use of SCR
- Stable: Free of flameout and flashback, over operating range
- Stable: Acoustic oscillations low, within acceptable limits
- High efficiency
- Low combustor system aerodynamic pressure loss

Combustion development programs have been conducted to address these objectives. These programs included combustor flow visualization, combustion optical diagnostics probe development, combustion instability/noise investigation, catalytic combustion component development, and single combustor prototype fabrication and testing.

Air flows inside the combustor cylinder and into the combustor basket are very complex and have a significant effect on pressure losses and the combustion process, which directly affect engine performance. Air flow distribution is especially critical in the dry ultra low NO<sub>x</sub> lean premix combustors, which rely on correct fuel/air ratios within a very narrow tolerance band for low NO<sub>x</sub> production and operational flame stability. Flow tests were carried out on plastic models of the piloted ring combustor (PRC) baskets (i.e., combustors), in the single basket rig, and, as described in the next paragraph, in a multiple-basket rig.

Flow mapping and flow visualization tests were performed on a half-scale plastic model of a combustor cylinder at Clemson University. Detailed information on pressure, velocities and flow angles inside the combustor cylinder, and especially around the combustor baskets, were obtained, and used in the subsequent ATS combustion section design. Included in this investigation were the effect of struts, cooling air bleed ports, cooling air return pipes, diffuser exit swirl, flow shields around the combustor baskets, top-hat length, and the curved compressor exit diffuser. In addition to studying and optimizing the flow around the combustor baskets, the tests provided data for optimizing the performance of the compressor exit diffuser and reduce the diffuser exit dump loss and, hence, improve the ATS engine performance.

High firing temperatures are required to attain the challenging performance goals of the ATS program. The high firing temperature, which enhance NO<sub>x</sub> formation, have made the achievement of the NO<sub>x</sub> emission goals so difficult that only lean premix combustion systems can be employed. Very lean combustion, with its inherent flame instability, results in combustion generated noise and vibration in the combustion system as well as in the downstream components. Therefore, a sub-program to develop the theoretical background on combustion instabilities, and carry out experiments to aid in the understanding of the problem was a part of this effort.

Following completion of cold flow, low pressure, and other preliminary testing, high pressure testing was carried out at the AEDC test facility. One full-scale PRC is installed in the test rig, and subjected to the high pressures, flows, and temperatures representative of engine service. The interior of the test rig contains baffles to simulate the airflow in one segment of an engine. Downstream of the test combustor is a transition, meant to represent an engine transition, and at the transition exit is an array of emission probes. These are water cooled to allow operation at simulated ATS temperatures

Results from a typical high pressure test are shown in Figure 86. The horizontal, or X-axis is labeled Secondary Temperature, but it is also combustor outlet temperature, since the secondary state is at the exit of the combustor. The data can be grouped into two categories, consistent with the level of NO<sub>x</sub> observed. To the left, the four data points represent primary-only data. When only the primary is fueled, it is difficult to raise the secondary temperature, (burner outlet

temperature) without making the primary over-rich. The over-rich primary section exists because the unfueled secondary is sending a large volume of unheated air in, which cools the primary exit gases.

The five points grouped on figure 86 on the right are five points recorded with both primary and secondary fueled. The primary has been sufficiently de-fueled to lower its NO<sub>x</sub> output to approximately 20 ppmv. The secondary is very lean, contributing almost no NO<sub>x</sub>. The secondary exhibits an increase in the outlet temperature to attain over 2700°F (1482°C) without increasing NO<sub>x</sub> above 20 ppmv. Since the secondary adds no NO<sub>x</sub>, the route to lowering the overall outlet NO<sub>x</sub> of 20 ppmv is to improve primary performance, to allow it to operate leaner.

The CO emissions recorded simultaneously with the NO<sub>x</sub> were less than 3 ppmv. Combustion was stable, having pressure fluctuations of less than 0.15 psi (1.03 KPa). Burner outlet temperature reached 2710°F (1488°C), which because of the shape of the plot in the figure makes the goal of 2820°F (1493°C) attainable.

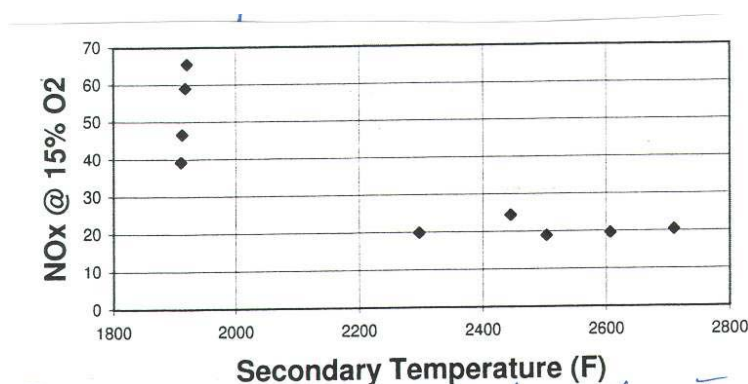


**Figure 86 NO<sub>x</sub> vs Secondary Flame Temperature**

#### 2.3.10.4.2 Piloted Ring Combustor

Combustor development for the ATS engine initially focused on a serial-staged premixing type combustor. It was believed that this type of combustor can achieve the difficult challenge of meeting lower emissions levels, while operating in an environment of much higher temperature and pressure than present machines. The concept selected for development was the piloted ring combustor (PRC), which has proven reliable in aeroderivative gas turbines under less stringent emissions. The concept was physically scaled-up (almost 2:1), and revised to meet the ATS applications. Prototypes were constructed and tested in single-combustor test rigs at conditions including high pressure and temperature. By the end of the period, the PRC concept had demonstrated stable, flashback-free operations at high pressures and temperatures, with exceedingly low emissions of carbon monoxide, and emissions of nitrogen oxides that were within ten parts per million of the goal. In parallel, a catalytic combustor program was conducted as a backup to the PRC, which promises to supply catalytic components, it could also be incorporated into the piloted ring combustor design.

After completion of the analytical and design tasks, multiple PRCs were fabricated. Each successive design iteration was evaluated in a single-combustor test rig. The test program consisted of cold-flow tests, employing transparent full-scale combustor models, full-scale fired tests in the Siemens

Westinghouse one atmosphere facility, and full-scale, full-temperature, high pressure tests in the Arnold Engineering Development Center (AEDC) of the US Air Force. At each stage of testing, the basic design was modified to incorporate the lessons learned from the previous test. Engine flow-visualization test data from Clemson University was incorporated in the later stages of the test program.

This design has been evaluated at high pressure and temperature, in the high pressure test rig, in the latter part of Phase 3. It is a “gas-only” combustor, in accordance with the fueling plan for the ATS engine; concentric to that, and surrounding it, is the array of gas jets for the diffusion flame pilot, which is referred to as “Central.”

Surrounding the diffusion flame pilot’s gas injector are the premix primary fuel-air passages. Combustion air flows around the outside of the combustor, and flows radially inward, through radial inflow swirlers, into the primary premixing passages. The combustion air is mixed with fuel gas from a series of “fuel pegs,” surrounding the entrance to the primary radial inflow swirlers, before changing direction, and flowing downstream, into the primary combustion zone. The diffusion-flame pilot ignites the premixed fuel and air entering the primary combustion zone. Although lean, the primary fuel air mixture is sufficiently flammable to sustain burning without the need for a pilot flame, once steady state has been attained. At a steady operation, fuel to the diffusion flame can be discontinued. With the diffusion flame extinguished, NO<sub>x</sub> production drops to the desired low level.

As engine load increases, fuel gas to the secondary premix fuel-air passage is started. This passage is an annulus surrounding the primary. Natural gas is injected just downstream of the annular cascade of swirl vanes, which appear at the entrance to the secondary fuel-air passage. Following injection, the secondary natural gas fuel has several inches to mix with the secondary air, before entering the combustion chamber. The secondary mixture is too lean to sustain combustion, but the presence of the flame from the primary keeps the secondary mixture burning. When operating at 75% base load, the diffusion-flame “Central” is discontinued, leaving only the lean primary and the very lean secondary burning. This mode of operation is necessary to achieve the program goal of less than 10 ppmv NO<sub>x</sub>.

Note that the length of the combustor is rather short downstream of the secondary mixture injection ports. By design, much of the combustion is completed in the transition duct, between the combustor and the turbine inlet. Because it is steam-cooled, the transition is sufficiently durable to serve this function.

#### 2.3.10.4.3 Active Control of Combustion Noise

In a parallel effort with Georgia Tech, a project controlling destructive acoustic combustor noise was continued. Georgia Tech has developed fuel controls which are capable of modulating the combustor fuel supply at frequencies equal to that of the most destructive acoustic modes of the combustor (the low frequencies). They have demonstrated hardware at the bench scale level. The hardware includes a microphone to pick up the acoustic waves, a computer to generate a fuel control command to counter the combustor pulses, and a fast-

acting fuel valve (see Figure 87). This set-up has proven it can quickly stabilize a combustor, at least at the bench scale level.

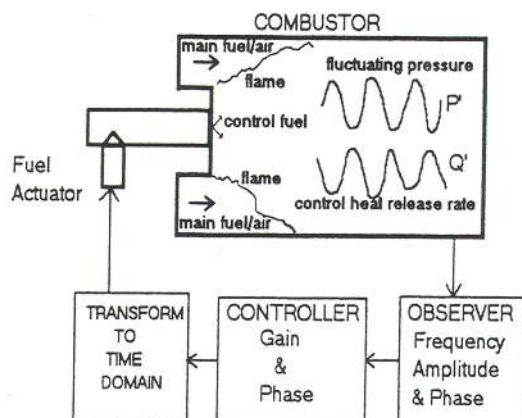


**Figure 87 Schematic of Active Combustion Noise Control System**

#### 2.3.10.4.4 Dry Low NO<sub>x</sub> Combustor Development

Near the end of the ATS Program, PRC development was terminated due to the high estimated production costs of this design and the breakthroughs achieved on the Dry Low NO<sub>x</sub> (DLN) combustor, which was being developed for both the W501F and W501G engines. Individual cans for the 16 can DLN combustion system incorporate eight premixed swirler assemblies arranged around a diffusion pilot nozzle swirler assembly. The premixed swirlers are designed to enhance mixing without recirculation, whereas the pilot swirler provides a strong swirl to produce a recirculation zone and therefore, good flame stability. The ultra lean, well premixed combustion in the DLN combustor results in low NO<sub>x</sub> emissions.

#### 2.3.10.4.5 Conclusion

The ATS combustion system development initially concentrated on the PRC combustor development and active combustion noise control. Rig tests demonstrated that low NO<sub>x</sub> emissions are achievable and that combustion instabilities are controllable with an active combustion noise control system. Due to high estimated production costs, the PRC development was stopped and further development effort concentrated on the DLN combustor. The DLN combustor demonstrated that it had great potential for achieving the ATS Program single digit NO<sub>x</sub> target.

#### 2.3.10.5 Materials Development

##### 2.3.10.5.1 Task 9.9 Ceramic Ring Segment Development

The program objectives were to develop a conceptual design of a CMC Row 1 ring segment for ATS, perform preliminary analyses, and develop base CMC technology to support implementation.

#### 2.3.10.5.1.1 Conceptual Design

Geometry and FE model: A number of geometries and attachment methods were evaluated on the bases of technical feasibility, manufacturability, performance and cost. The candidate design selected for further study was selected primarily for its manufacturing simplicity as well as the fact that it eliminates metallic parts exposed to the hot gas path, thus minimizing cooling.

#### 2.3.10.5.1.2 Analyses

##### 2.3.10.5.1.2.1 Heat Transfer and Thermal Stresses

Steady state heat transfer analysis was performed along with thermal and mechanical stress analysis from aerodynamic pressure loadings.

#### **Segment Under Steady-State Conditions**

##### 2.3.10.5.1.2.2 Mechanical and Combined Stresses

Mechanical stresses due to the pressure loadings were significant only in localized regions of the attachments. The stress concentration at the pinned holes was the highest stress level and was therefore examined further through focused analysis and subelement testing. Due to the complex state of stress in this region, a more complete model of the deformation behavior (elastic and inelastic) and failure criteria for the CMC are required. The combined overall stress state for the seal segment at steady-state is shown in Figure 90. This is a superposition of the thermal and mechanical stresses.

##### 2.3.10.5.1.2.3 Stress Summary and Comparison to Material Properties

Based on CMC stress-rupture data, mechanical stresses below 60 MPa are required to achieve life >10,000 hrs – this criteria is met. Thermal stresses are relenting due to stress relaxation, thus S/R data is an inappropriate criteria. A more rigorous analysis with more complete criteria is thus warranted

#### 2.3.10.5.1.3 Base Technology and Subelement Testing

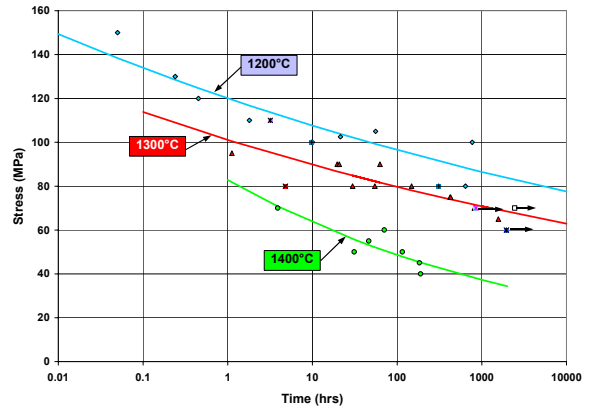
##### 2.3.10.5.1.3.1 Subelement Testing

The pinned joint attachment was an area where the stress state and failure criteria were not well understood. Subelements were therefore fabricated and tested to simulate the complex state of stress around the pin-loaded hole attachment area. Results of analysis and test data are shown in Figure 92.

### 2.3.10.5.1.3.2 Base Technology

Extensive high temperature characterization was performed, including LCF, HCF, stress-rupture and creep testing. Results of the stress-rupture testing are shown in Figure 93. Results of all these tests indicated that the CMC material was viable for high temperature oxidizing environments for many thousands of hours and cycles at reasonable stresses. However, interrupted fatigue tests showed that the material properties were significantly degraded after relatively short exposures to the environment. As a result of these tests, further work with this material was stopped.

**Figure 93 Stress-Rupture Test Data for Nicalon/Alumina CMC**



### 2.3.10.5.1.4 Conclusions

A design for a CMC turbine blade tip seal has been demonstrated to be feasible via analysis and subelement testing. Critical issues identified include:

- 1) Design issues: Control of cooling air leakage to minimize thermal stresses (sealing). Sealing concepts require further validation testing.
- 2) Material modeling issues: Need for comprehensive CMC deformation models for both elastic and inelastic (plastic and creep) behavior. This is needed to accurately predict complex, multiaxial stress states.
- 3) Life prediction capability: Effects of short term overstressing on long-term durability need to be addressed (relaxation of initially high thermal stresses). Localized inelasticity effects (plasticity and creep) under strain controlled loading need to be determined (is damage self-arresting?). Life prediction methods (damage accumulation models) need to be developed for multiaxial stress conditions.
- 4) Material stability: SiC fiber-reinforced alumina composites are shown to be unstable for long periods of time in the intended operating environment (oxidizing conditions at Temp >1000°C [>1832°F] for time >10,000 hrs).

### 2.3.10.5.2 Tasks 9.10 and 12.2.6 Advanced Coating Development

#### 2.3.10.5.2.1 Introduction

The Siemens Westinghouse Advanced Turbine System is designed to achieve a 60% thermal efficiency, less than 10 ppm NO<sub>x</sub> emissions and reliability-availability-maintainability (RAM) equivalent to the current advanced power generation systems. One of the many approaches to increase efficiency and reduce NO<sub>x</sub> emissions is by increasing rotor inlet temperatures at lower burner outlet temperatures. This can be achieved by utilization of a closed-loop steam

cooled Row 1 vane, with no film cooling air. This increases the rotor inlet temperatures, while maintaining a low burner outlet temperature without compromising the efficiency. Consequently, without film cooling, the TBC surface temperatures are now significantly higher than current advanced engines (see Figure 94). The bond coat temperatures can vary depending upon the TBC thickness, however, the average bond coat temperatures are expected to be higher than those of the F and G engines. The higher bond coat and TBC surface temperatures are challenging the limitations of the existing TBC system and new coating systems need to be identified to meet the increasing demands.

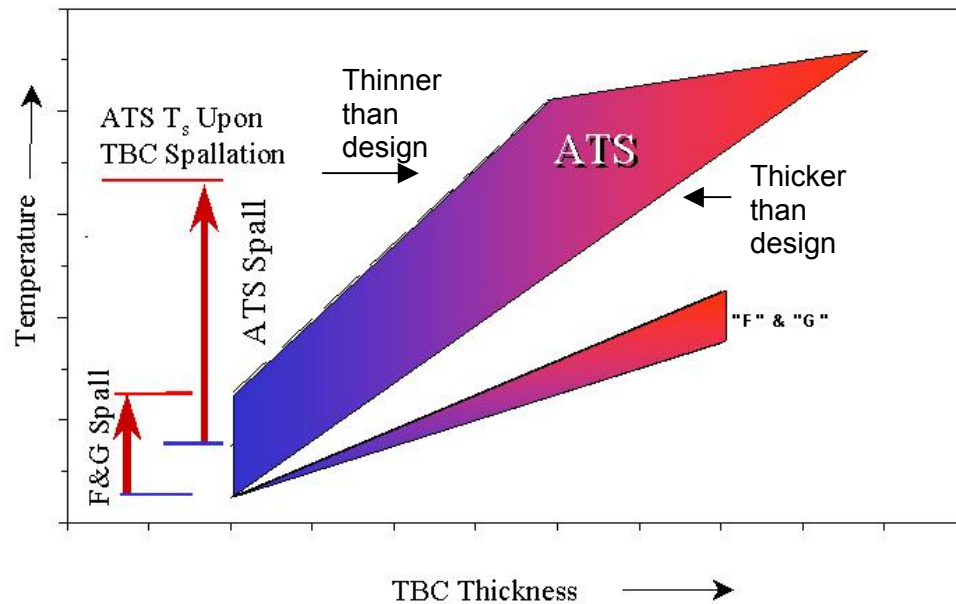


**Figure 94 Comparison of Temperature Gradients between the ATS and W501G (and F) Engines**

In addition, from Figure 94, demands on the reliability of a TBC system can also be ascertained. In the event of a TBC spallation in the G (and F) engines, the increase in component metal temperatures would still be within the design temperatures. However, a similar spallation in the ATS engine would result in component temperatures well in excess of the design allowable temperatures. This can, consequently, result in a rapid and severe degradation of the component properties. To realize the objective of maintaining reliability of an ATS engine equivalent to existing advanced engines, new TBC systems should be very dependable, so that a component can be designed with a guaranteed protection of the TBC system. This was attempted by adopting a complete coatings development approach which included the identification of an advanced thermal barrier coating system, a development of an analytical model to predict its life, identification of innovative NDE techniques to monitor the performance of the TBC system and development of a reliable, robust manufacturing process.

#### 2.3.10.5.2.2 The Complete Coatings Approach

A complete coatings approach was developed in his program to elevate the technology from the current W501F and W501G technology for application in the ATS engine. Several key areas of development and new ideas were generated during this program, of which some have already been transitioned to production and few other require some optimization before implementation in a next generation engine.

As a result of the program, several key recommendations are listed as guidelines in each of the critical areas discussed in the previous chapters along with a brief summary of the highlights. The program has also established a strong foundation for future TBC systems for industrial gas turbines and with new concepts and ideas for obtaining prime reliant coatings.

#### 2.3.10.5.2.3 Bond Coat Development

The development of bond coatings for the TBC systems has focused on identifying new bond coat chemistries, developing new concepts to maintain the aluminum reservoir and optimizing alternative cost-effective processes without compromising TBC life.

##### 2.3.10.5.2.3.1 New Bond Coat Chemistries

Due to the interdiffusion of elements between the substrate and the bond coat, the performance of the new bond coat systems is strongly dependent on the substrate alloy composition. The greatest improvements, about a factor of 2.5x in life over the baseline, can be realized by use of the high aluminum CA chemistry or the NY (modification to the commercially available NI-171) when using IN-939 substrates. Bond coats on MarM-002 benefit from a modification of both the cobalt or nickel based bond coats, high aluminum CA, and tantalum additions. Bond coat performance on CMSX-4 substrates showed considerable indifference to bond coat chemistry.

The high aluminum CoNiCrAlY composition CA provided a unilateral improvement in bond coat performance. The current program addressed improvements in the performance of the bond coat systems primarily from modifying the chemical compositions. However, further improvements are clearly possible by optimization of the mechanical properties of the bond coat – for instance, bond coat ductility. Since the performance benefit and the cost of the promising bond coat alloys are expected to be comparable to the baseline system, further consideration should be given to the development and optimization of the CA, NY and the bond coat with Ta.

##### 2.3.10.5.2.3.2 Diffusion Barriers

Diffusion barriers provide a benefit in inhibiting interdiffusion between the MCrAlY and the substrate and thus increase TBC life. Since the test temperatures were close to the base metal solution temperature, failure occurred due to solution of the barrier layer into the substrate and MCrAlY. Therefore, it would be more beneficial to evaluate the high diffusion barrier at test temperatures more indicative of engine operating conditions. Such an evaluation would also be beneficial for diffusion barriers.

#### 2.3.10.5.2.3.3 Composite Bond Coat

Incorporation of controlled amounts of oxides during APS depositions resulted in a significant increase in MCrAlY beta phase retention.

Further improvements may be realized by:

1. Increased the aluminum content in the barrier layer MCrAlY to accommodate losses from the formation of oxides during spraying.
2. Modification of APS deposition parameters and substrate temperature during coating to increase the continuity and thickness of planar oxides.
3. Use of finer MCrAlY powders to decrease spacing between oxides.
4. Providing an optimized bond coat surface finish and TBC.

#### 2.3.10.5.2.3.4 Bond Coat Processes

From the current study, results showed that HVOF should be considered as a substitute for LPPS where either cost or process flexibility indicate a clear advantage. Under optimized conditions, porosity and internal oxide content as determined from microscopy were comparable. As a result, TBC spallation life and failure mechanisms were comparable for the two processes. While no attempt was made to define the manufacturing window of the HVOF system, the process appears to be relatively insensitive to minor variation in control parameters.

Other processes such as APS, SPS, and Gator Guard bond coat deposition, all provide bond coats with significant levels of porosity and/or internal oxides. Despite the rapid internal oxidation particularly of the APS and shrouded plasma spray deposited coatings, the TBC spallation life was remarkably long. While oxidation attack of the substrate, prevents their use in the most demanding applications, the lower cost and impressive TBC adhesion makes them attractive for lower temperature applications where the primary function is to provide a surface for TBC adhesion. Alternatively, an LPPS or HVOF bond coat with an overlayer of APS, SPS or Gator Guard deposited bond coat may provide excellent adhesion in addition to the necessary component substrate protection.

#### 2.3.10.5.2.4 New TBC Development

By improving the temperature capabilities of the bond coat, benefits from reduced cooling air requirements, increased reliability and extended component life are realized. However, benefits from increased temperature capability are expected to be marginal, since these temperatures are already close to the superalloy design temperature limits. Therefore, further incremental benefits can be significant only if new TBC compositions are identified which can simultaneously withstand higher surface temperatures and provide larger thermal gradients. This would have a dual benefit of increased engine efficiency and increased reliability.

#### 2.3.10.5.2.4.1 APS of New Ceramics

New compositions for TBCs offer the possibility of increased sintering resistances and higher temperature gradient across the thickness. This will significantly increase the reliability of the coating system due to reduced oxidation of the bond coat. Several new ceramic compositions were evaluated for TBC applications by APS and EBPVD.

#### 2.3.10.5.2.4.2 Lab Scale Evaluation

A systematic lab evaluation approach was established in this program to identify new compositions that were more sinter resistant and phase stable than 8YSZ at temperatures of applications for the ATS engine. The approach was simple and very cost effective in screening out several oxide systems that showed both excessive phase instability and poor sintering resistance. Although, the technique allowed a quick ranking of the sintering resistance, one should realize that sintering resistance is significantly dependent on the microstructure. Therefore, this approach can eliminate oxide systems that are significantly worse than 8YSZ.

#### 2.3.10.5.2.4.3 EB-PVD of New Ceramics

Seven promising oxide compounds that were phase stable and sinter resistant were evaluated for feasibility for deposition by EB-PVD. This required identification of the melt pool stability and a match of the coating chemistry with the target composition. The coated substrates were then evaluated for sintering tendency and by cyclic furnace testing. One new chemistry was identified as a very promising material for application as an EB-PVD coating for ATS engine conditions. A desirable columnar microstructure with superior sintering resistance was obtained by modification of the deposition conditions, which included a combination of high substrate temperature and a low feed rate. The process parameters now need to be optimized and evaluated for cyclic life using a high heat flux rig.

EB-PVD of new compounds clearly demonstrated the need to understand the vaporization and condensation characteristics of the constituent oxides. The thermodynamics of the melt pool and the vapor constituents can significantly affect the chemistry of the coatings. A preliminary comparison of the vapor pressures of the constituents can provide a guidance to continue with the deposition process. It was also evident from this program that the microstructure of the deposited coatings was significantly affected by the crystal structure of the compounds. With increasing complexity of the crystal structure, the typical 8YSZ deposition temperatures resulted in the deposition of unstable coatings due to the inability of the coatings to crystallize completely into their desired structure. This implies that the deposition of new compounds would have to be aided by other innovative deposition techniques. It was also evident that the feed rate and substrate temperatures can control the growth of a columnar microstructure with superior sintering resistance.

#### 2.3.10.5.2.4.3 New TBC Concepts

In addition to new compositions, two new concepts were demonstrated to be capable for obtaining TBCs with very high temperature capability. In the first

concept, new ceramic compositions are deposited on to the substrate with modifications to the deposition process.

The other concept is the modification of the EB-PBD columns after the deposition process is complete.

Both the new designs are examples of a multiphase TBC with different phases performing key functions to enhance the applicability of the TBC for high temperatures. This is expected to be one of the key features of TBCs for application in future engines and this program has helped demonstrate the success of the first prototypes.

#### 2.3.10.5.2.5 High Heat Flux Rig Used in TBC Lifting Tests

Spallation of a TBC at high temperature and heat flux conditions was identified as a high risk factor in the design of engines with high turbine inlet temperature and high efficiency requirements. Therefore, successful testing under typical operating conditions prior to transferring the technology to production is essential.

Siemens Westinghouse designed and set up a high heat flux rig for thermal gradient thermal fatigue testing of TBCs which had the following features, considered to be one-of-a-kind facility capable for TBCs.

- Temperature: High uniform surface temperature (1400°C [2552°F] at the thermal barrier outer surface) can be obtained.
- Time at temperature: Thermal cyclic testing, with the specimen being brought up to temperature and held steady for a period of time (approximately 10 to 60 minutes) then cooled down to near ambient temperature, can be performed automatically.
- High Heat Flux: A large temperature gradient across the TBC layer, such that the bond coat/metal interface temperature is held at 950° C (1742°F) while the outer surface is held at 1350°C (2462°F) during the heating portion of the cycle, can be obtained. (This temperature gradient results in a heat flux of approximately 790,000 Btu/hr-ft<sup>2</sup> [8.06 x 10<sup>6</sup> KJ/hr-m<sup>2</sup>]).

This unique combination of capabilities and the requirement to impose such a high heat flux and external temperature on the specimen is a significant challenge.

In addition to validating the life prediction model, the purpose of the high heat flux rig test facility is also to screen candidate coating systems so that the best one can be selected for use in an engine.

Based on the results obtained from testing at the high heat flux rig, it has been established that the surface temperature can significantly affect TBC life. With increasing TBC surface temperatures, the failure of the coating initiates due to the sintering of the coating and spallation occurs layer-by-layer. These results were the first demonstration of the increased surface temperature on the reliability of the coating system. The data generated during the testing process was key for the validation of the life prediction model.

The first version of the life prediction model was developed at the South West Research Institute and was based on a mechanistic analysis. It provided the first insight into the ability of the models to predict the coating life. Upon comparing the prediction with the experimental data, it was evident that the failure times and mechanisms were in disagreement with some of the mechanistic analysis.

It is now clear that the model should address the interaction between TBC sintering and bond coat oxidation. A stored energy model is required to predict this interaction. It is also possible that the statistical nature of the ceramic failures is an important aspect for life prediction. Monte-Carlo simulations could be used in future programs in order to model the statistical nature of TBC failures. Monte-Carlo simulations could also account for multiple crack initiation and growth. From the experience in this program, it is imperative that life prediction should be performed in close conjunction with an experimental database, which can evaluate all the different failure modes and also their interaction.

#### 2.3.10.5.2.6 NDE, Maintenance and Repair

In addition to the development of new materials, NDE techniques both off-line and on-line are required to establish a pathway to prime reliance of the coating. Accurate process and manufacturing control is essential to obtain a performance with minimum scatter and this requires a reliable means to monitor the quality of the as deposited coatings. On-line monitoring is key to provide an advance warning system for the failure of the TBCs. Evaluations of both off-line and on-line monitoring were completed in this program.

##### 2.3.10.5.2.6.1 Off-line monitoring.

The program objectives for out of frame NDE also referenced as “off-line NDE” included investigations in two areas: 1. Thermal imaging method for TBC coating debonds and full field TBC thickness, and 2. Eddy current for local TBC thickness.

##### 2.3.10.5.2.6.2 On-line monitoring

As a result of the promising initial investigations regarding the possibility of monitoring TBC components for debond and spallation of the coating, an investigation was carried out into: 1. An on-line blade monitor based on real time, high speed thermal imaging, and 2. An on-line vane monitor based on thermally activated chemical emissions.

##### 2.3.10.5.2.6.3 Patch repair

Patch repair is critical to reduce the time to install components back after observing a defect during regular inspection or sometimes due to defects on new components resulting during installation. Patch repair allows repair to occur on-site. This possibility was investigated in this program and the results showed that the repaired coatings had nearly 82 % of baseline sample properties. These repairs may potentially be used to patch local areas of an APS coated turbine component instead of the general strip and recoat process currently used in the field.

For future programs, the results in this program can be used as a basis for transferring the technology to engine hardware. Also, in order to assess the true potential of these local repairs, a cost analysis comparing a local minor repair vs. a general strip and recoat will be advantageous.

Patch repair of EB-PVD was evaluated and determined to be ineffective from the initial trials. Future efforts should focus on other options for deposition of columnar microstructures locally.

#### 2.3.10.5.2.7 Manufacturing Issues

##### 2.3.10.5.2.7.1 Masking

Application of coatings to turbine component surfaces causes restriction of cooling holes and alters the heat management of the engine. The objectives of this program were to produce data to allow for compensated hole designs, to examine masking to prevent cooling hole blockage, and to examine the post machining to restore cooling hole tolerances.

Test panels with simulated cooling holes were produced to evaluate the extent of coating buildup and the reduction of cooling hole diameter. Data is presented as a function of hole size, hole angle, coating angle, and coating thickness.

Masking techniques were developed to prevent hole blockage by air plasma spray (APS) thermal barrier coatings (TBC). A number of systems were evaluated for ability to prevent APS buildup, ease of application, and ease of removal after coating. Qualification of masking for the W501F Row 1 turbine blade is complete. Several vanes for the W501F and W501G frames are being qualified as well. Improvements to the process are being implemented as part of vendor qualifications.

The feasibility of using post machining techniques to restore cooling hole tolerances after coating was determined. Water jet machining was selected as the most favorable candidate method. High pressure water jet parameters were tailored to efficiently remove coating, while leaving the underlying metallic coating unaffected. The major limitation of the technique is the ability to align the jet with the existing holes. Misalignment resulted in stripping TBC from the flat areas around the cooling holes. Improvements in hole finding capability are required to make water jet a production option.

##### 2.3.10.5.2.7.2 Coating Refurbishment On Surface Recrystallization Of Single Crystals

The above study was a key effort for deposition of advanced TBCs on to single crystal substrates. It was determined that coating refurbishment alone followed by a heat treatment on a cast ingot surface did not cause recrystallization. However, upon machining the surface or testing the sample in creep, the coating refurbishment resulted in a significant amount of recrystallization near the substrate/coating interface.

This leads to a conclusion that machining should be avoided in areas where recrystallization could compromise alloy performance.

### 2.3.10.5.2.8 Conclusion

The development of an advanced coating system has successfully resulted in several advanced bond coat and TBC materials, which have set a strong foundation for the utilization of coatings for very high temperature capability. This capability enables us to meet the objective of the ATS engine, which depends significantly on the reliability of coatings and their higher temperature capability. By taking a full circle approach (as shown in Figure 95), we have shown that development of advanced coatings also involves several key aspects to enable a component with high reliability and durability.

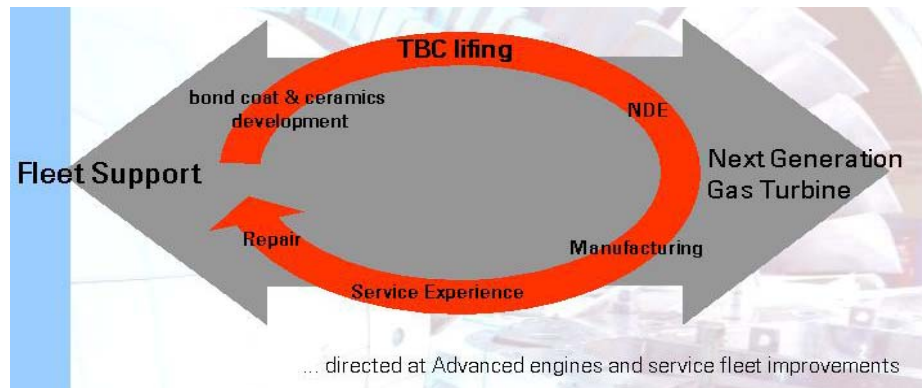


**Figure 95 A Full Cycle Approach To Development Of Advanced Coatings Technology**

### 2.3.10.5.3 Tasks 9.11 and 12.3.5 Steam Effects on Materials

The objectives of these tasks were to:

- Develop a steam chemistry model and evaluate effects of steam chemistry on cooling hole blockage and substrate alloy corrosion.
- Evaluate effect of time and temperature on steam corrosion with and without salt.
- Determine impact of salt concentrations on corrosion rate.
- Determine the effect of individual salt components on corrosion.
- Evaluate coating performance in a steam environment with and without salt.

Long term oxidation and corrosion testing was carried out at Southwest Research Institute and ORNL, using clean steam and in the presence of salt impurities. Different materials, representing turbine airfoils, transitions, cylinders, steam manifolds and steam piping were tested. Several different steam chemistries (with different percentages of impurities), steam temperatures, metal temperatures, two different steam flow rates, and two steam pressures (15 and 30 atmospheres) were tested.

Test results indicated the following:

1. Steam effects in the form of oxidation/corrosion/metal waste were observed on all materials exposed to high pressure and high temperature steam,
2. The extent of attack depended on the susceptibility of the alloy to such attack, level of impurities in the steam, temperature and exposure time, and,
3. Coatings such as aluminide and chromide, provided protection to the base alloy against steam effects.

The findings of these tests will be incorporated into ATS to meet steam oxidation and corrosion life objectives of the hot and components exposed to steam.

#### 2.3.10.5.4 Task 9.12 DS Blade Development

The alloy CM247LC has been widely used in aircraft engines as it offers excellent strength at elevated temperatures good oxidations resistance. In the conventionally cast and directionally solidified conditions, the alloy offers approximately 50°F and 90°F (28°C and 50°C) temperature advantage respectively compared to the current land based turbine blade alloy, IN 738. To qualify the alloy for application as large industrial turbine blades the following tasks were undertaken.

- Preliminary material property data for directionally solidified CM247LC were generated on cast bars and slabs.
- Evaluating the effect of casting withdrawal rate on mechanical properties.
- Evaluating the effect of coating on isothermal base metal properties.

The material property test results were analyzed and property curves were generated to support the design of large industrial gas turbine blades. Mechanical properties were determined to be relatively insensitive to the changes in withdrawal rates evaluated in the casting process trials. Isothermal mechanical properties were not greatly impacted by the coating.

#### 2.3.10.5.5 Task 12.3.4 DS/CC Properties

There were two areas of focus in this task: (1) verifying that data generated on cast slabs and bars accurately represented component properties, and (2) determining the influence of post-casting thermal cycles on mechanical properties.

##### 2.3.10.5.5.1 Validation Of Component Material Properties

The materials properties database for directionally solidified and conventionally cast blade and vane alloys was primarily based upon data generated from the testing of slabs and bars. However, it was recognized that size and geometry differences resulted in different cooling rates which in turn generated different microstructures in the test material compared with that of actual components.

Mechanical testing was performed on test pieces machined from blades and vanes. The results were compared with the existing data from slabs and bars, and reanalysis was performed to generate revised material property curves. The new curves were published in the materials properties database for use by Design. The results of the testing were also used to revise the material specifications, defining different requirements dependant upon the origin of the test material.

#### 2.3.10.5.5.2 Effect Of Processing Heat Treatments

Thermal history has a great influence on the microstructure and mechanical properties of nickel-base superalloys. Manufacturing operations such as welding, brazing and coating employ thermal cycles at temperatures that can significantly modify the shape and size of the strengthening gamma prime phase.

The effect of typical processing sequences on the tensile, creep and LCF properties were evaluated for the conventionally cast alloys IN 939 and IN 738 and the directionally solidified alloys CM247LC and MarM002. The effect of the best case processing scenario (once through each processing step) was compared with the worst allowable case where individual thermal treatments (i.e. tip brazing or coating diffusion) were performed up to three times (the maximum allowed by the specifications).

The results of the mechanical testing on processed materials were compared with the data contained within the materials properties database for material in the optimized condition (e.g. HIP, solution and aged) and the impact on component designs were evaluated.

#### 2.3.10.5.6 Task 12.3.11 LCF and TMF Properties of IN 939

The program objectives were:

- Generating LCF data and determine the potential impact on performance.
- Comprehensively characterizing the low cycle fatigue and thermo-mechanical fatigue properties of IN 939.
- Providing validated LCF and TMF data to support the development of predictive models.

Low cycle fatigue testing was performed at temperatures of 800°, 850° and 900°C (1472°F, 1562°F, and 1652°F) with dwell times of up to 1800 seconds. The majority of the tests were performed on uncoated test pieces with a strain ratio of  $R = -\infty$ . However, a limited amount of testing was performed on test pieces with a CN334 bondcoat and also on test pieces with a CN334 bondcoat + air plasma sprayed (APS) thermal barrier coating (TBC). In addition, a limited number of tests were performed with strain ratios of  $R = -1$  and  $R = 0$ .

Thermo-mechanical fatigue testing was performed using a 180° out-of-phase cycle with a minimum temperature of 100°C (212°F) and maximum temperatures of 800°, 850° and 900°C (1472°F, 1562°F, and 1652°F). The majority of test pieces were coated with a CN334 bondcoat, although a limited number of test

pieces were also tested in both the uncoated and the bondcoat + APS TBC condition.

#### 2.3.10.5.7 Task 12.3.6 SC Casting Production Development

The objective of the program was: (1) to provide production support for ATS single crystal blade and vane casting development, and (2) to perform long term creep rupture testing of CMSX-4.

Extensive material testing was performed on CMSX-4 cast materials. Tensile, creep rupture, LCF and HCF property data was generated. The data was analyzed and documented in Turbine Materials Manuals for design use with CMSX-4 material.

A material specification was written and issued for CMSX-4 alloy, which specified the chemistry, heat treatment and quality requirements for the material.

An Engineering Qualification Specification was written and issued, which described the technical and quality requirements for casting vendors to qualify ATS CMSX-4 SC Row 1 blade casting.

To investigate the stability of CMSX-4 during engine operation, long term creep rupture testing was performed. The longest testing time in one specimen surpassed 20,000 hours. After the creep rupture testing had been completed, the specimens were sectioned and prepared for metallographic examination by optical and scanning electron microscopes. The specimens demonstrated excellent long term microstructural stability. No detrimental phases were detected in these specimens.

#### 2.3.10.5.8 Task 12.3.15 Liquid Metal Cooling

Liquid metal cooling (LMC) offers two important advantages over the conventional directional solidification process. The first is the potential for a lower cost casting process. LMC increases the thermal gradient, which would allow for a higher withdrawal speed and shorter casting time. This is particularly important for long land based engine blades. The second advantage is higher casting quality. The higher cooling rate has been shown to improve the microstructure, such as dendrite arm spacing, segregation, eutectic formation and porosity, thus enhancing its mechanical properties.

The objective of this task was to explore the commercial feasibility of casting large SC components with a LMC process. The program plan included the development of a LMC casting process, aided by computer solidification modeling, casting trials of prototype turbine components, and cut-up evaluation and mechanical testing of the prototype components.

#### 2.3.10.5.9 Task 12.3.2 Bonded Vane Development

To achieve high efficiency in the ATS engine, front row vanes were sought that would be capable of withstanding higher than previously experienced gas path and, hence, metal surface temperatures. Even with the incorporation of thermal barrier coatings it became obvious that the temperatures imposed upon the metal sections of the vanes would significantly exceed the creep limit of conventional

materials. In the event of employing steam cooling the aggressive thermal gradients and thermally driven transient stresses that would be incurred by the vane airfoil and shroud walls could only be withstood by the most durable of vane materials, i.e., second generation nickel base single crystal. The implementation of second generation single crystals in ATS components was, however, constrained by the very limited ability of the casters to produce defect free castings of this size and complexity required for thin walled steam cooled components. Because these limitations were recognized to be size driven, the development of single crystal vanes using smaller cast segments and high quality single crystal bonding based upon Transient Liquid Phase bonding was investigated.

A Row 1 steam cooled vane was selected as the target component. A complete thermal and mechanical design was performed for the component resulting in the definition of a thin walled steam cooled structure with thin walled cooled channels in the shroud platforms and airfoil sections. The cooling hole geometry defined spanwise cooling holes along the axis of the airfoil and cooling channels extending from the airfoil fillets to the edges of the shroud platforms. Thermal and mechanical analyses indicated that the thermomechanical cycles that would be imposed upon the thin wall could be withstood, for reasonable component life, by a second generation single crystal alloy. The alloy CMSX-4 was selected as the single crystal alloy. Initial casting trials in this program and previous programs had demonstrated that single piece castings developed high levels of defects including freckles, stray grains and even cracked boundaries.

The development of the bonded component was pursued by simultaneously developing transient liquid phase bonding of the CMSX-4 alloy and casting of the shroud and airfoil sections in single piece SC forms and then combining the segments using the bonding process to produce complete single vane sections.

The transient liquid phase bonding development work built on previous work conducted under a NIST ATP program. In the previous program Siemens Westinghouse had demonstrated that well aligned single crystals could be bonded using transient liquid phase bonding to produce bond regions that were in many cases stronger than the original single crystal material but were at least as strong as 80% of the base material properties. In this program the bonding development work focused on identifying the tolerance allowables for bonding of single crystals and assessing the effects of bonding orthogonal single crystal structures. (This latter factor was pursued when the sectioning and casting efforts revealed that the most preferred growth of the separate shroud and airfoil section were in orthogonal directions.)

Extensive bonding and property evaluation work was conducted during the program. The work confirmed that the bonding process developed for bonding simply aligned single crystals was also the preferred bonding process for bonding "off-axis" specimens and orthogonal bonded specimens. The data developed for off-axis bonded specimens indicated that the tolerances for aligning single crystals to generate high property level bonds were identical to those that specify the allowable grain boundaries in such single crystals, i.e. in the 6-15 degree regime depending on the alloy. Since CMSX-4 is an alloy whose grain boundary tolerances are towards the more restrictive end of the tolerance band, the misalignments that can be tolerated between separately cast single crystals is

similarly low. Orthogonal bonding occurred in which nearly identical crystallographic orientation across, respectively, primary and secondary dendritic structures were bonded together using the originally defined processes. It was found that some modifications to the process were necessary to combat differences in interdendritic melting in the two orientations. Data were measured on the orthogonal bond specimens and these data were compared with those of the originally developed specimens. While the well aligned (crystallographically) orthogonal structure joints displayed similar properties to those of well aligned microstructurally similar joints, the data for crystallographically misaligned orthogonal joints showed greatly increased vulnerability to crystallographic misalignment. These data were not sufficient to validate orthogonal structure bonding and it was decided that more fundamental studies of the process should be conducted outside of the ATS program.

In order to apply the bonding process to the fabrication of single crystal vanes a "sectioning scheme" was developed for the complete vane. In this sectioning scheme the bond lines were placed in low stress locations. The initial sectioning scheme divided the vane into three parts, the airfoil and the inner and outer shroud sections. A bond line structure with the airfoil penetrating the shroud was designed. Schemes for the incorporation of cooling channels were investigated, i.e. casting the cooling channels into the original pieces or incorporating the cooling channels by secondary processing such as drilling. A key advantage of the sectioning of the complete vane was the ability to now cast the airfoil as a doubly oriented casting with primary growth along the axial direction of the airfoil while the shrouds could be grown with the primary growth direction in the plane of the shroud. This arrangement made the airfoils much less vulnerable to chord-wise grain boundary cracking of the airfoil (which was prevalent in single piece vane castings). While this arrangement would improve the castability of the airfoil structures, it did increase the severity of the constraints for crystallographic alignment of the orthogonally cast sections to generate high integrity joints – as discussed in the above section.

The incorporation of cooling channels in the airfoils and shroud segments was investigated by several different methods. Further resegmentation of the shroud and airfoil sections was investigated to develop methods to develop these segments by subsection casting and further bonding. While the ability to produce defect free sections by casting smaller sections did increase, the ability to maintain crystallographic matching was determined to become much more difficult as the number of parts to be bonded increased. Casting-in of cooling channels was addressed but core "Kissout" and nucleation of defects in the constrained thin walls was determined to be prohibitive for real manufacturing processes. It was eventually determined that STEM drilling of the straight line cooling channels in the airfoil was viable. For the shrouds, an innovative sectioning and rebonding approach was developed. In this approach, the shrouds were cast as solid segments. The surface regions in which the cooling channels were to be incorporated were sliced off by wire EDM and the cooling channels were counter sunk into the cut surfaces by EDM or ECM processes. The cleaned sections were then rebonded with the hollow sections forming the cooling channels. In this case, high integrity bonds were guaranteed because of the identical alignment of the surface and underlying shroud sections.

In the progression to developing final assembly and an overall manufacturing process for the bonded vane, fixturing and assembly routes were determined. A set of controlled thermal expansion fixtures were developed to control the bonding pressure on shroud rebond assemblies and full vane assemblies. Within the program only shroud rebonding was accomplished. One inner shroud was fabricated by this method. One full set of rebonded inner shroud, drilled airfoil section and a solid outer shroud was produced. Fixturing was developed to demonstrate proof of concept assembly on this structure, however the assembly was never fully bonded.

Because of the time and financial constraints the program did not meet the original goal of developing a manufacturing process for a bonded vane. The program did develop a method that could be applied to develop bonded vanes. It addressed and solved several key design and cooling channel incorporation issues but it did not resolve the parts' crystallographic orientation tolerance issues. Based upon the apparently restrictive tolerances of the parts' crystallographic mismatch for orthogonal bonded joints and revised cost payback estimates for the benefits of steam cooled single crystal vanes, the program was subsequently refocused outside of the ATS program to more rigorously address the constraints and implications of orthogonal structure single crystal bonding before it would be pursued for further parts fabrication programs.

#### 2.3.10.5.10 Tasks 9.14 and 12.3.8 Advanced Weldable Alloy Development

##### 2.3.10.5.10.1 Background

The goal of the ATS Advanced Weldable Vane Alloy Program was to modify the baseline IN-939 chemistry to enhance weldability while retaining current IN-939 mechanical properties. The initial phase of this effort, conducted at Oak Ridge National Laboratory (ORNL) during January 1996 to April 1998 concentrated primarily on modifying minor alloy additions such as zirconium and boron to improve weldability. A total of 45 small 1-2 pound (0.45 kg to 0.907 kg) experimental alloy heats were cast and tested for weldability using the Sigmajig test. This test places a uniaxial preload on a thin (0.030 in. [0.96 mm] thickness) specimen of the alloy to be tested. An autogenous, through-thickness GTA weld is then made on the specimen. The Sigmajig threshold stress for cracking is determined by the maximum stress that can be placed on the specimen without inducing cracking or failure. The results of the initial phase of testing identified optimum range of Zr and B to maximize the weldability of IN-939 was identified.

The second phase of this work, conducted under the ATS Phase 3 Extension program, was directed at producing larger heats of the modified IN-939 alloys to determine the effect of minor element content on mechanical properties. Seven heats of the modified IN-939 alloys were cast and six were selected for determination of mechanical properties.

Room temperature (70°F [21°C]) and 1200°F (649°C) tensile tests were run on cast-to-size tensile specimens with 0.25 in. (6.35 mm) diameter. Stress rupture tests were conducted at 1600°F (871°C) and 37 ksi (255.1 MPa), using identical 0.25 in (6.35 mm) diameter specimens. LCF tests were run using a strain ratio of minus infinity, 0.5% strain range, zero hold time and 1600°F (871°C). LCF

specimens were cast oversized and machined into 0.25 in. (6.35 mm) diameter test specimens.

#### 2.3.10.5.10.2 Discussion

The mechanical property data from the current investigation indicates that the room temperature and elevated temperature tensile properties generally varied little with changes in Zr and B content.

The stress rupture data from the modified alloys showed a definite trend toward increased rupture lives with increases in zirconium content. The replacement of zirconium with scandium was also beneficial in this regard, producing times to rupture in excess of 160 hours. It is believed that scandium behaves similarly to zirconium, terrelle the sulfur in the alloy as well as reducing the tendency for grain boundary cracking.

The results of the LCF tests showed less of a dependence on zirconium content, although scandium additions were still apparently beneficial. The effect of minor alloying element additions on the LCF life of nickel superalloys has been less well documented in the superalloys literature than the effect on creep properties. Since the cyclic frequency for the current tests was  $\sim 0.5$  Hz, the contribution of creep processes on LCF life should be less significant than at lower frequencies. The fracture surfaces from the various alloys were relatively flat, indicating transgranular crack propagation and no frequency dependence of crack growth rate. Of the twelve specimens tested, only one had a fracture surface sufficiently rough to suggest intergranular crack propagation. This specimen also had a lower LCF life, although the reason for this change in fracture morphology could not be explained on the basis of grain size. Measurement of grain size for each alloy showed that all but one had a uniform grain size of ASTM 4.1 – 4.9.

#### 2.3.10.5.10.3 Conclusions

The test results indicated that increasing zirconium levels are beneficial for increasing stress rupture life in IN-939. The rupture life was also enhanced by scandium additions, which may play a similar role to zirconium in terrelle the sulfur in the alloy. The effect of Zr and Sc on fatigue properties was less clear.

#### 2.3.10.5.11 Task 12.3.9 Thermal Barriers Coating Life Prediction

The objective of this task was to develop TBC service life prediction method for both APS and EB-PVD coatings. To provide experimental information cyclic tests, at different time periods and different bond coat and surface temperatures, were carried out on coated test pins at the Waltz-Mill High Heat Flux test rig. TBC sintering and bond coat oxidation were identified as being critical in TBC life determination. TBC life was found to be highly sensitive to surface temperature. Coating life could be predicted in temperature ranges where sintering and oxidation acted independently. A “stored energy” model was required to predict TBC life in the sintering/oxidation mixed mode region. Fatigue was not a relevant failure mechanism in the temperature range investigated. Reliability of the ceramic coating depended on thermally grown oxide thickness as well as coating compliance.

TBC life prediction models were developed for both the APS and EB-PVD TBC coatings based on time, bond coat temperature and coating surface temperature. The models accounted for surface fatigue limit, thermal cyclic fatigue, surface oxidation and surface sintering.

#### 2.3.10.5.12 Task 12.3.13 Back-Filled Honeycomb (BFH) Coating Development

##### 2.3.10.5.12.1 BFH as a Thick Thermal Barrier Coating

The ability to apply BFH coatings to components of complex geometry were successfully demonstrated in the fabrication of a BFH coated W501F combustor basket. Short-term testing of BFH coating under atmospheric (Casselberry Lab Test of Simple BFH Coated Cylinder) and full pressure (AEDC Test of BFH Coated W501F Combustor Basket) showed that BFH offers comparable performance improvement (in terms of short-term durability and emissions) to that of the current SWPC standard combustor coating, thick TBC.

In the testing of the simple cylinder coated with BFH, the component was tested under full air to fuel ratio conditions. As part of this testing, the cylinder was subjected to 100 full shutdown cycles, thereby experiencing maximum transient stress conditions. The BFH coating exhibited no visible signs of degradation and successfully demonstrated the durability of BFH under extreme transient conditions.

In the testing of the BFH coated W501F combustor basket, the BFH coating was subject to a full-scale rig test up to and including the baseload ATS conditions. During the test, the BFH coating exhibited comparable performance to the thick TBC coating but with the added potential benefit of reduced cooling air and hence  $\text{NO}_x$  reduction through reduced hot wall quenching. The short-term tests demonstrated the viability of BFH to be used as a thick thermal barrier coating in the combustor application and confirmed the performance benefits predicted by the thermal modeling of the BFH coating system. Longer term issues related to upper temperature limit and retention of the backfill under harsh mechanical conditions remain to be addressed. Initial data has indicated that the behavior of the system in a thermal gradient is not yet thoroughly understood.

Improvements to the baseline system in terms of adding a plasma sprayed overlayer and in chemically milling the metallic honeycomb surface have been identified as potential approaches to improving the surface temperature capability of the system. Both approaches rely on exposing only thermally stable ceramic material to the hot gas streams. Further work is required to verify these approaches, to determine ruggedized manufacturing procedures and to determine long term service related durability.

As part of the overall development program, full draft processing specifications were produced. A series of vendors were evaluated. One suitable vendor was selected and manufacturing work was conducted with that vendor. The vendor successfully demonstrated the ability to apply and inspect the BFH coating and, on this basis, was qualified for the combustor liner production.

## 2.3.10.5.12.2 BFH as an Abradable Coating

### 2.3.10.5.12.2.1 Engine Test of Baseline BFH Coated W501D5 Ring Segment

BFH based ring segments were developed during this program to the point where a series of such ring segments were installed in an operating turbine and were exposed to a 20,000 hour engine test. The engine was a W501D5 engine owned by Dow Chemical Company (gas path temperature of 1150°C [2102°F] with hot spots of 1316°C [2401°F]).

The objective of the 501D5 engine test of BFH coated ring segments was to evaluate several styles of BFH with respect to durability in a high temperature gas path environment. Specifically, some of the BFH coated ring segments were fabricated with a standard thickness BFH in such a way that the blade tip/ring segment interaction should have been minimal so that the blade tips would not intentionally abrade the ring segments. Other BFH coated ring segments were fabricated with thicker BFH so that the blade tips would intentionally interfere with the ring segment coating and the blade tips would actually abrade the BFH. Post test evaluation of the ring segments indicated degradation of the BFH both in regions where BFH/blade tip interactions had occurred and in regions that had been free from interference. A root cause analysis identified possible causes for the BFH degradation. These included:

- Fabricating, processing defects of the BFH
- Poor design of fabrication and inspection process
- Poor component and coating system design
- Turbulence due to coating surface roughness and increased erosion thereafter
- Thermal mismatch (between ceramic backfill and metal honeycomb) and the associated thermal stresses

### 2.3.10.5.12.2.2 Modifications to Improve BFH Abradability

Whereas prior generation engines such as the W501D5 avoid intentional blade tip/ring segment abrasion, advanced engines such as the ATS call for intentional rubbing of the blade tips into the coating surface (e.g. 1-2 mm) in order to minimize blade tip clearance and hence maximize efficiency. An abrasability test program was undertaken to improve the wear characteristics of BFH and to evaluate the abrasability of the base line and modified BFH coatings under the anticipated rub conditions for Row 1ring segments.

The coating modifications included: 1) a reduction in the metal surface area making contact with the blade tip during a rub and 2) alteration of the backfill constituents to weaken the ceramic backfill. The results demonstrated that a reduction in metal surface area making contact with the blade tip was beneficial to abrasability. Additionally, weakening the strength of the ceramic backfill (bond strength of matrix and/or reduction in sphere wall thickness and density) was found to significantly improve the abrasability of the BFH (this modification

provided the best volume wear ratio value of all tested variants). Unfortunately, SEM evaluation of the post-tested “weak ceramic backfill” BFH coating indicated that such coatings might be more prone to degradation (loss of ceramic backfill and hence insulating capability) than baseline BFH. The abrasability benefit derived from a “weak” ceramic backfill was believed to result from the generation of oxide particulates during the initial blade tip/shroud interaction – the oxide particles being available to assist the passing blade tip in cutting through the BFH coating. Even though the modified BFH compositions did not fully meet the desired wear characteristics, the generated data were sufficiently positive to warrant additional work.

The 2001 efforts focused on two main types of variants: 1) modification of the backfill composition so as to allow for abrasive or lubricating particles to be released from the coating surface during a rub and 2) elimination of metal honeycomb from the rub surface. The modified backfill BFH showed some improvement in abrasability over the baseline composition but unfortunately the required volume wear ratios were still not achieved. In addition to testing the variants under the anticipated rub conditions, additional tests (at varying incursion depths) were conducted to obtain additional information on the blade tip wear when worn against the BFH type coating. The results showed that using the prospective CBN blade tip coatings to wear against BFH the blade tip coating would be completely worn away at only very shallow incursion depths, i.e.  $\ll 0.4$  mm. Thus, BFH would not provide a properly abrasable coating for ring segments in advanced engine such as the ATS.

#### 2.3.10.5.12.3 Summary - Technology Status of BFH Coating

An alternative coating system to that of conventional thermal barrier coatings has been evaluated during this program. The potential to apply the coating to much greater thicknesses than are attainable for conventional TBC's offer the possibility of reduced backside cooling requirements. The system is currently constrained by restrictions on the hot surface temperature due to the metallic component of the system. Improvement based upon developing only ceramic-exposed structures have been identified but needs further development and verification. The ability to apply the coating to various component types has been demonstrated. Experience gained by exposing model ring segments in an operating turbine and laboratory abrasability test data indicate that the current manifestation of BFH must be improved if the system is to be employed as a high temperature abrasable coating for ring segments in an advanced engine such as the ATS.

#### 2.3.10.5.13 Nondestructive Evaluation (NDE) of ATS Components

##### 2.3.10.5.13.1 Introduction

##### 2.3.10.5.13.1.1 Background

Among the new materials and processes that the advanced turbine system (ATS) utilizes for component manufacture, the thermal barrier coating (TBC) process and the single crystal blades and vanes are the two most critical advancements in the turbine engine technology. Nondestructive evaluation (NDE) techniques were therefore investigated for the inspection of these ATS components of new advanced materials and processes including: (1) thermal barrier coated (TBC)

turbine blades, vanes, and transitions, and (2) single crystal (SC) turbine blades (Rows 1 & 2). The development efforts were focused on the following three most relevant NDE techniques: (1) pulsed infrared (IR) thermal wave imaging (TWI) for detecting various TBC failures such as disbond and spallation; (2) meandering winding magnetometer (MWM) for measuring primarily metallic bond coat (MCrAlY) thickness; and (3) x-ray diffraction (XRD) for measuring single crystal orientation and detecting unwanted secondary crystals within a single crystal blade. The techniques were developed in collaboration with a university research team (Johns Hopkins University for XRD) and NDE equipment manufacturers (Jentek Sensors, Inc. for MWM, and Thermal Wave Imaging, Inc. for TWI).

#### 2.3.10.5.13.1.2 Program Needs for NDE

The thermal barrier coating system provides essential insulation and protection of the metal substrate from the high temperature combustion gases. The TBC system consists of a substrate alloy, bond-coat (MCrAlY) and a thermal barrier ceramic top-coat (Yttria stabilized Zirconia containing 8wt% Y). While only the ceramic layer provides significant resistance to heat flow, the bond coat and the metal substrate play a major role in determining coating life. In the event of a TBC *failure* in ATS, the temperature of the exposed metal substrate would increase well in excess of the design temperatures. This can, consequently, result in a rapid and severe degradation of the component properties.

Thermally exposed coated components initially undergo micro-structural damages to the TBC system: e.g., formation of thermally grown oxide (TGO) between the bond coat and TBC layer; damages at TBC/TGO interface due to rumpling; and formation of voids and Ni/Co rich TGO at TGO/MCrAlY interface. TGO formation due to metal bond coat oxidation is a volumetric expansion process that occurs during high temperature exposure. The volumetric change is constrained in the plane of the interface because the stiffness of the TGO forms with a residual compressive stress.

In general, TBC failures could be conceived macroscopically in three stages: coating debond, surface cracking and spallation. Coating debond is the condition in which there is no adhesion between the bond coat and TBC layer, but the TBC layer is still physically intact and the layer will continue to function as a thermal barrier. Once the TBC layer is separated from the bond coat, the layer can easily crack to further release residual stresses. As the cracked layers continue to service under severe conditions, the layers will eventually be separated (chipped off) from the bond coat, and consequently, the component would totally lose the protection from the high temperature. Therefore, in service, it is important to detect TBC failures as early as possible (at least debond stage) in order to prevent the turbine engine from serious failures. Furthermore, *the thickness of the bond coat layer* should be carefully monitored during the manufacturing stage to meet the designer's requirement.

The MWM system, by Jentek Systems, Inc. is both unique and well suited for the measurement of coating system characteristics. The Jentek System is model-based and highly accurate at measuring conductivity, permeability and lift-off changes. Jentek uses a flat/conformable sensor with a square wave shaped winding that is highly predictable. Special training sets of nickel-based

superalloys were manufactured to develop measurement methods and calibration grids for measuring bond coat thickness.

Single crystal turbine blades (nickel-base superalloy) are being proposed in the first two stages of the ATS engine. Single crystal structure eliminates grain boundaries in the alloy, and offers superior creep characteristics. However, single crystal is elastically an isotropic in nature, and hence, the material's mechanical properties (e.g., tensile strength, yield strength, etc.) are different in different crystallographic directions. It is, therefore necessary to identify the crystallographic orientation to assure that a favorable crystallographic orientation has been maintained within the component structure. Furthermore, single crystal castings can contain unwanted secondary crystals (strays) that form during the solidification process. With these secondary crystals, components will not have the aforementioned benefits of single crystal structure, and therefore, the detection of secondary crystals within a single crystal component is also needed.

#### 2.3.10.5.13.1.3 Summary

Nondestructive evaluation (NDE) techniques were investigated for the inspection of ATS components of new advanced materials and processes: (1) pulsed infrared (IR) thermal wave imaging (TWI) for detecting various TBC failures such as disbond and spallation; (2) meandering winding magnetometer (MWM) for measuring primarily metallic bond coat (MCrAlY) thickness; and (3) x-ray diffraction (XRD) for measuring single crystal orientation and detecting unwanted secondary crystals within a single crystal blade.

The techniques were tested on a variety of test specimens as well as actual components. The thermal wave imaging (TWI) technique was applied for detecting TBC disbonds on blades, wall thinning and perforation on vanes, diffusion bond defects (debonds) on transitions. In addition, attempts were also made to measure thicknesses of TBC and TGO layers.

The MWM eddy current technique was tested on coupons of varying bond coat (MCrAlY) thicknesses ranging from 2 mils to 10 mils and the test results indicated an average measurement error of 1.6%.

The x-ray diffraction (XRD) technique was developed for the following capabilities: asymmetric crystal topography (ACT) for surface scanning, and through-transmission Laue imaging for volumetric scanning. The technique was evaluated on a special SX block with secondary crystal inserts.

#### 2.3.10.5.14 Task 9.16 Ni-Based Super Alloy Rotor Material Development

The objectives of this task were to evaluate candidate Nickel base alloys IN 718 and IN 706 for rotor discs and associated rotor components (sideplates etc.) by developing mechanical properties' databases for both alloys. Of particular concern was the ability to generate data that would be representative of the large size forgings that would be used for large ATS turbine discs. (It was known at the inception of the program that the properties of these forged alloys would be highly dependent on the forging and heat treatment processes that would be employed.)

Two suppliers of forged nickel base materials suitable for large disc production were identified. These suppliers were Wyman-Gordon and Alcoa. Initially work was focused on the IN706 alloy, but later work was directed towards the IN718 alloy. Initial work on the IN706 alloy was focused on a conventional two step heat treatment. Material from both suppliers was tested for tensile creep, high cycle fatigue and low cycle fatigue, crack growth and fracture toughness properties. An extensive database was developed for the IN706 alloy up to the 1300°F (704°C) temperature range. As part of Siemens Westinghouse's data development for disc materials the testing program was subsequently augmented to include notched specimens to determine the potential for notch sensitivity of the material under operating conditions, e.g. in the steeple locations of the discs.

Siemens Westinghouse investigated the potential for notch sensitivity of the IN 706 alloy using combination plain bar- notch bar specimens under creep and fatigue conditions. It was found that the alloy that had been forged and heat treated using the two step heat treatment exhibited significant notch sensitivity under creep loading. Microstructural evaluations and fracture surface and path evaluations confirmed that the IN706 microstructure developed by the forging and two stage heat treatment was notch sensitive under creep loading conditions. From a review of the available literature it was determined that the high temperature notch sensitivity was related to specific interactions of the material microstructure with the environment under the high local loadings imposed at notches and that, specifically, a modified form of the heat treatment would potentially alleviate this problem.

In order to overcome the high temperature creep notch sensitivity, a three step heat treatment which had been reported to alleviate this form of sensitivity was investigated. A segment of the original disc was reforged and heat treated with the new heat treatment. Combination bar creep rupture tests were conducted in the temperature regime that had given rise to the notch sensitivity. These initial experiments appeared to support the conclusion that the three step heat treatment would avoid the notch sensitivity issue. However, when attempts were made to compare the creep rupture data with the unnotched creep rupture data of the two step heat treated specimen, the strength of the base metal three step heat treated slabs was observed to be significantly different from the behavior of the original forged disc materials. Subsequent investigation determined that the tensile properties at room temperature and elevated temperature were different in the reforged and three step heat treated slab materials and the original forged and two step heat treated disc materials. Metallographic examination of the specimens traced this discrepancy to differences in the grain structure of the two sets of materials. These grain structure differences were concluded to arise from the differences in stored energy under the different forging conditions and the response of the material containing the different amounts of cold work to the solution heat treatment step of the post forging heat treatment process. The differences in grain size and grain shape could give rise to the difference in material properties: it is also probable that there existed differences in material crystallographic texture that would enhance these differences in properties. Thus, this portion of the work concluded that although the three step heat treatment should avoid the problems of creep notch sensitivity in alloy IN706, the property data developed by the investigation could not be used for design since they did not adequately represent the material structures that would be developed by forging and heat treating of a complete full sized disc.

A similar program of work was undertaken to investigate the properties of IN718. However, because the focus for this alloy was on application for side plate rather than complete discs the investigation did not address notch effects. Instead, the investigation focused on the baseline mechanical properties, tensile and fatigue in the temperature range from room temperature to 1200°F (649°C). The materials chemistry was well defined and as a result of this work a materials specification sufficient for the development of side plate components was developed. This specification was supported by extensive metallographic examinations and characterizations in order to define the required material microstructure that must be induced by the forging and heat treating cycle for alloy IN718.

As a result of the work in this task, it was concluded that IN718 provides a higher temperature capable material for side plate and small forging elements of turbine and compressor rotor assemblies and that the data developed and inputted into the Siemens Westinghouse database provide a reliable baseline for the further development of applications of this alloy. With respect to IN706 it was concluded that the alloy in the conventional 2 step heat-treated form would have the potential for notch sensitivity to induce non-conservatism in the design of disc steeples. On this basis, further work would be needed to determine the correct forging and heat treatment sequences for large discs and to develop the database to support implementation of the non-notch sensitive forms. Because of the high cost of the discs and the high cost of such a development program it was determined that the cost effectiveness of nickel alloy discs would be at best marginal. On this basis the program was terminated and the technology placed in abeyance until progress has been made (by manufacturers) on the forging/heat treatment issues and on the cost issues. When these issues have been resolved, further work should focus on expanding the mechanical properties database to reflect creep and fatigue properties and to verify that notch sensitivity is avoided in nickel disc alloys by the more judicious selection of heat treatments.

### 2.3.10.6 Mechanical Development

#### 2.3.10.6.1 Tasks 9.2 and 12.2.4 Thin Wall Casting Development

##### 2.3.10.6.1.1 Introduction

The primary purpose of the thin wall casting program was to develop thin wall airfoils that meet the following requirements:

- Allow closed-loop cooling to be used in an optimum fashion,
- Having capability to be manufactured in a production environment at a commercially feasible cost,
- Produce airfoils which maintain structural integrity for the required product life.

This section describes the designs and manufacturing effort for the ATS Row 1 vane and blade. These designs differ significantly from previous engines because they are entirely closed-loop cooled. Closed-loop cooling of these

components created new design challenges. These included: a strong dependence on TBC, high thermal gradients limiting thermo-mechanical fatigue life, and large single crystal castings that have come down in price since their initial commercial introduction.

The vane was designed as a single-crystal alloy component with superheated steam as the coolant. Pre-cooled air can also be used at the expense of vane life and cooling efficiency. Thermal analyses were performed using both internal Siemens Westinghouse computer codes and an aero-derivative suite of design codes. Steady state and transient temperatures were applied to a 3-D finite element model to calculate the stress fields and corresponding operating life at temperature. A creep analysis was performed and correlated with the thermal mechanical fatigue test program.

The blade was also designed as a single-crystal alloy component. The blade cooling was accomplished with the use of pre-cooled air. The complexities associated with internal coring required for the blade proved to be a significant design challenge. As with the vane, thermal analyses were performed using both the Siemens Westinghouse and an aero-derivative suite of design codes. These boundaries were then applied to a 3-D finite element model to calculate the stress field and operating life at design temperature. Thermal mechanical fatigue testing was carried out at operating conditions to verify longevity.

The vane design incorporated bonded inner and outer closure caps to contain the coolant. Coolant enters each vane segment through a piped connection created on the outer shroud closure cap and exits through a similar piped connection. There are 32 segments in the first stage. Each vane segment is supported axially at both the inner and the outer shroud closure caps. At the inner shroud, the vane segment is supported by a 360° ring, bolted to the downstream end of the torque tube seal housing.

The blade design does not require bonding or assembly. All internal blade coring is self supporting from the feed and exhaust locations. The use of advanced core attachment manufacturing methods as well as innovative design concepts have both been crucial to the blade design concept. There are 49 blades in the first stage. These blades feed and exhaust cooling media through the rotor.

#### 2.3.10.6.1.2 Casting Trials

The casting trials have proven that these components can be manufactured. Core attachment methods, shell system development, and the furnace cycle requirements have been established. The manufacturing development effort is ready for modifications that are anticipated to reduce production component costs. The casting of large single crystal components with complex coring is required for an effective closed-loop cooled design. The manufacturing of these castings must be accomplished at reasonable costs. The continuation of the manufacturing effort for the thin wall castings is required to progress into a production ready process.

#### 2.3.10.6.2 Task 12.1.6 Blade Root Verification Test

Low cycle fatigue (LCF) life prediction of blade attachments is based on: 1) analysis assumptions: 2D/3D, frictional/frictionless, plastic deformation, etc., 2)

material properties: fatigue curve, notch sensitivity, and 3) other factors, such as tolerances. In advanced engine designs the blade stress loading increases and approaches limit. Therefore, it is critical to understand the uncertainties associated with LCF calculation of blade attachment in order to ensure the accuracy of the calculation.

The objectives of the test program were to:

- Evaluate the performance of the ATS and W501G blade root/disc steeply attachment
- Ensure that 2350 design cycles can be achieved for both the blade root and disc steeply
- Calibrate and validate the methodology and tools used in design and analysis of blade attachment.

Stress analysis was carried on blade root/disc steeply interface to identify critical stress areas. This information was used to specify strain gauge locations on the test hardware. Dummy blades, with the correct root form and stubs representing the blade mass, and the test disc were machined. After the strain gauges were installed, the blade/disc assembly was installed in Siemens Westinghouse STC spin pit test facility. A series of cyclic spin tests were carried out and the strain gauge data were recorded. The test results will be used to calibrate and validate analysis tools used in turbine blade attachment design.

#### 2.3.10.6.3 Task 13.4.1 Closed-Loop Cooling Circuit Integrity and Vibratory Response

The ATS engine design incorporated closed-loop steam cooling in the transitions and first two stages of vanes. Steam flow had to be ducted through inlet and exhaust chambers, created with a blade ring sealing against the main engine cylinder. Flexible joints were employed between the blade ring and stationary parts, which were to be cooled, to allow for relative motion. This closed-loop cooling scheme presented many design challenges in effort to develop a system that would satisfy design requirements and be simple to assemble and maintain. One of the main challenges was to design a rugged long life, low leakage flexible joint for the piping connections. To help in selection of the flexible joint the focus of this task was redirected to an experimental integrity/leakage verification of two candidate flexible joints. The test program objective was to compare the performance of a standard piston ring seal Flex-Slide Joint to that of EG&G Pressure Science Tubeseal Flex-Slide Joint in a superheated steam environment. Both joints were designed for use in a 2 in. (50.8 mm) diameter pipe.

The test program consisted of two phases. The first phase was a static leakage test on the two types of joints carried out by EG&G. The objective was to provide a baseline leakages for subsequent vibratory leakage test. The EG&G test results showed their Flex-Slide Joint leakage was much lower than that of the piston ring seal.

The second phase testing was carried out at Siemens Westinghouse STC labs. The test procedure was as follows. For the low cycle test, two identical seals were tested under cycling conditions of 0.233 in. (5.9 mm) of axial displacement,

combined with 1 degree of angulation. The cyclic rate was 12 cycles per minute. Every 500 cycles leakage measurements were recorded. In the high cycle test, two identical joints were also tested simultaneously. This test consisted of a 0.010 in. (0.25 mm) movement at a frequency of 220 to 240 Hz. Leakage measurements were taken every 30 minutes. Test results demonstrated that the Tubeseal Flex-Slide seal had much lower leakage rates than the piston ring seal. The Tubeseal Flex-Slide seal leakage rate was less than specified in the ATS design for the duration of the tests.

#### 2.3.10.6.4 Task 12.4.3 Alternate Vane and Blade Design

The alternate first stage turbine vane and blade designs were carried out as a back up to the primary designs. The objective was to investigate design options for increasing vane and blade lives. An alternate first stage vane design was produced. The new core design included trailing edge features, such as double wall impingement cooling, target-wall turbulators and pressure side film ejection in a thin trailing edge configuration. A detailed heat treatment process was developed for manufacturing the vane from the time of the casting, through the coating cycle, assembly of parts and delivery for mounting in an engine. Several different alternate first stage blade designs and cooling schemes were also investigated.

#### 2.3.10.7 Technology Verification

##### 2.3.10.7.1 Task 14.1 Steam Cooled Component and Aerothermal Design Verification

###### 2.3.10.7.1.1 Introduction

The W501G engine (see Figure 101) was used as the platform to develop and validate ATS technology (see Figure 102), especially closed-loop steam cooling. In developing closed-loop steam cooling technology the deliberate plan was to introduce and verify one steam cooled component at a time. This development started in April 1999 with the steam cooled transition used in the W501G engine (Southall and McQuiggan, 1995). The development plan was to resolve all the technical issues with closed-loop steam cooling before proceeding further. This task proved to be much more challenging than originally anticipated. The learning curve took much longer and was more costly than planned. The following technical issues were identified and resolved: how to introduce steam into the engine, how to start the engine from cold start when no steam was available, how to bring the engine to base load, how to respond to emergency shut down, how to minimize joint leaks, what steam purity is required, what is the effect of steam on internal heat transfer, impact of steam on transition materials, and possibility of cooling hole blockage. All these issues were successfully overcome. Based on lessons learned from the W501G transition development the approach to closed-loop steam cooling of turbine stators was modified.

This section describes the W501G Prototype tests at the City of Lakeland McIntosh Plant in Florida (Bancalari, Diakunchak and McQuiggan, 2003).

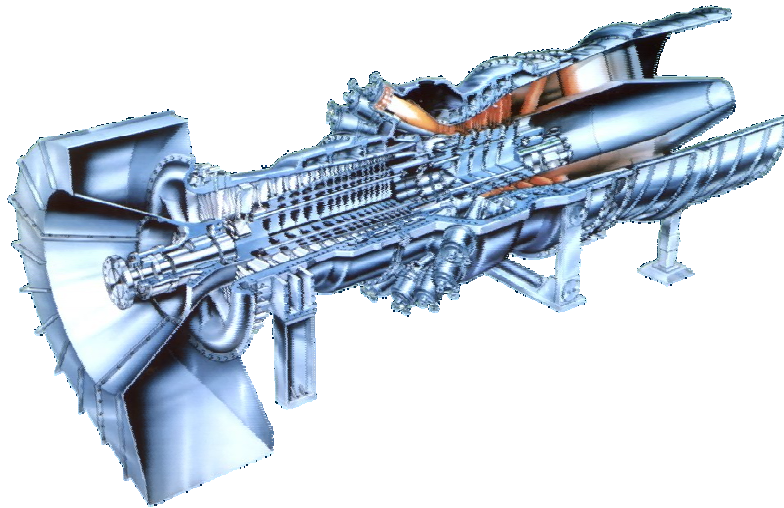


Figure 101 W501G Engine

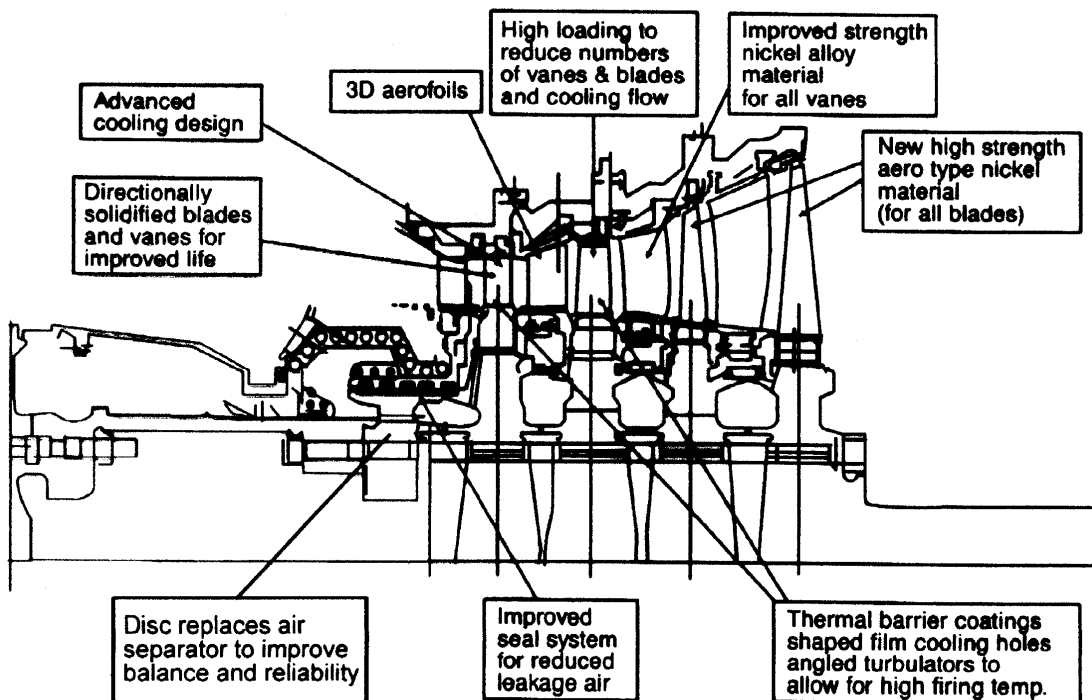
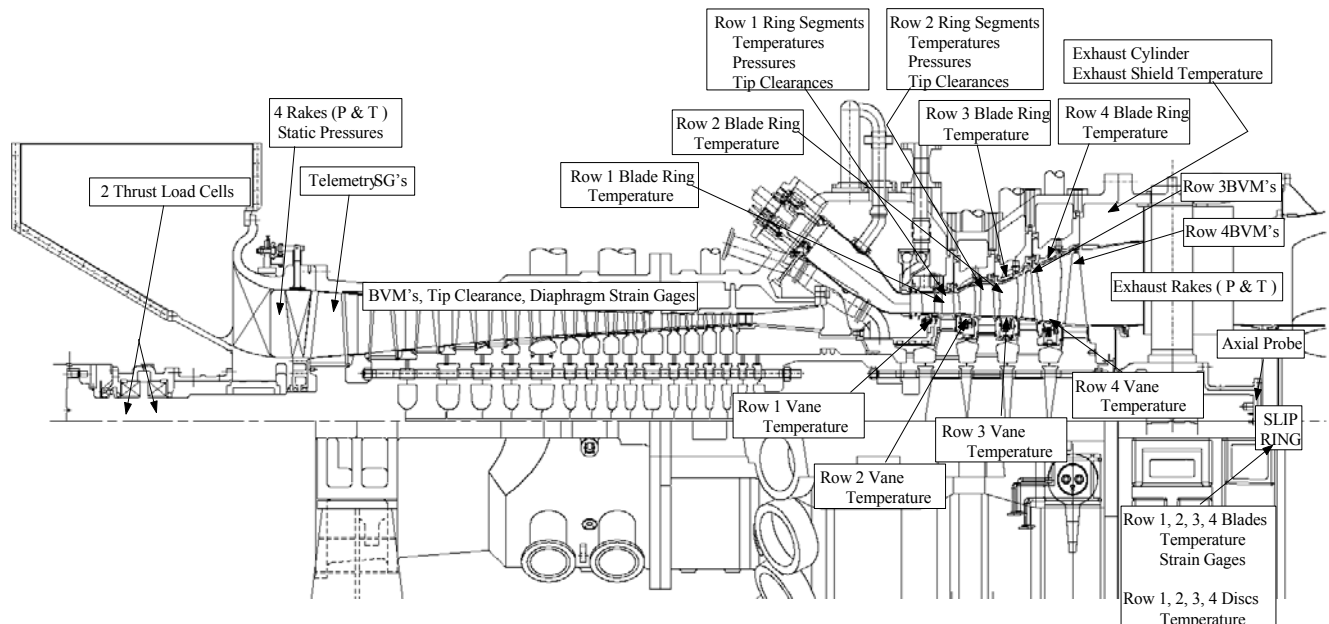


Figure 102 Advanced Technology Applied to W501G

#### 2.3.10.7.1.2 W501G Prototype Engine Tests

The W501G test program included starting optimization, performance and emissions verification, hot parts metal temperature measurement, including telemetry and thermal paint testing, vibration measurement, tip clearance measurement, etc. The telemetry system was employed to measure compressor blade vibratory stresses. A slip ring system, installed at the turbine back end, was used to measure the rotating blades' metal temperatures and vibratory stresses in critical areas. Tip clearance probes were installed to measure compressor and turbine blade tip clearances over the complete operating range, including transients. The engine instrumentation included over 3000 sensors and

measured parameters (1,200 thermocouples, 600 pressures and 200 strain gauges). An engine schematic showing the various sensors is shown in Figure 103. The test program consisted of two distinct phases: emissions/performance mapping phase and thermal paint testing. The emissions and performance mapping phase testing targeted combustion system variables and provided engine performance mapping for different operating conditions, such as IGV position and exhaust temperature. Test results demonstrated that the W501G engine achieved its performance, emissions and mechanical integrity design targets. Following the initial testing, turbine flowpath and combustion components were painted with thermal paints and installed into the engine. The thermal paint changes colors based on exposed temperature. This method is used extensively in aero engine validation since it provides a complete and accurate temperature map of the components at operating conditions. To react the thermal paint, the engine was ramped up to full load, run for approximately five minutes at full load and then shut down. The thermal paint test was conducted in two phases. In July, 2000, the transitions and first stage turbine vanes were painted and tested. These components are removable without a major cover lift. In October, 2000, a full paint test was carried out. This test included all turbine blades and vanes and areas of the rotor subjected to high temperatures. Figure 104 shows the scope of the painted components. Both tests were conducted successfully and results were evaluated in great detail to verify the hot parts' cooling design and to validate computer codes used in W501G engine design. Figure 105 shows the first stage turbine blade after the thermal paint test results have been interpreted. This testing also validated the transition duct closed-loop steam cooling concept in a commercial application (see Figure 106). Based on the test results, minor modifications were made to the first stage vane and blade to improve their service lives.



**Figure 103 W501G Prototype Test Instrumentation**

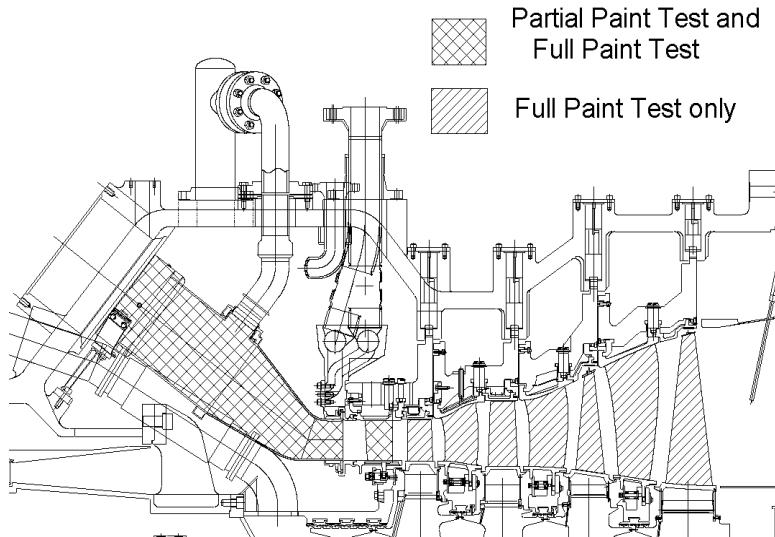


**Figure 104 Thermal Paint Test**



**Figure 105 Thermal Paint Test Results on First Stage Blade**

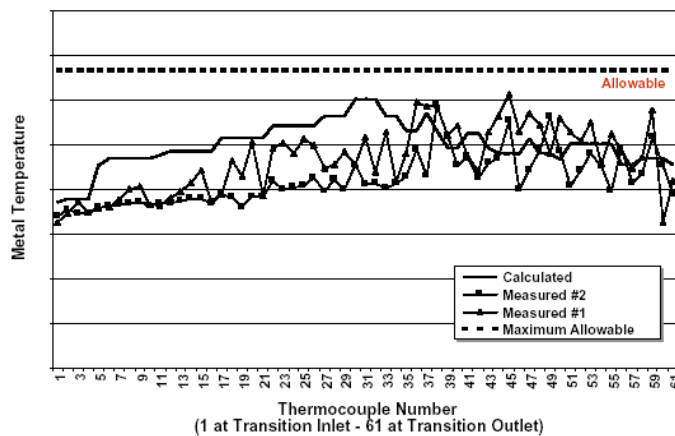


**Figure 106 Measured Transition Metal Temperatures**

2.3.10.7.1.3 Summary

The verification methodology employed for the W501G extended beyond just testing the engine and its components. Because the W501G was integrated into

the combined cycle for optimum performance, many of the support systems required verification. The Prototype W501G was exercised in various operational scenarios to verify the systems' behavior through a wide range of operating conditions. The correct operation of steam cooling, fuel gas heating, fuel oil, and cooling air systems were all verified. Fuel transfers between fuel gas and fuel oil were successful and operation on fuel gas at 204°C (400°F) were also proven. The extensive design verification and validation methodology used in W501G development proved beneficial and resulted in a high level of confidence that the W501G will succeed in today's competitive power generation environment, and serve as a platform for further ATS technology development.

#### 2.3.10.7.2 Task 14.2 Advanced Viscous Compressor Test Program

##### 2.3.10.7.2.1 Introduction

The objective of this program was to test the W501FD advanced viscous compressor design at the Empire Stateline Plant in Joplin, Missouri, so as to verify its performance and mechanical integrity.

The W501F compressor was designed in the early 1980's. It had 16 stages, a pressure ratio of 15:1 and a mass flow rate of 438 kg/sec (966 lb./sec) at its design point at ISO conditions. This compressor employed Double Circular Arc (DCA) technology for the front four (4) stages, and made use of standardized NACA-65 airfoil shapes (with a modification of the airfoil thickness distribution) for the remaining 12 stages and the two Outlet Guide Vanes. Starting with the eighth stage, every 3 stages were repeating stages, i.e., the airfoils were identical but were cut shorter to fit into the annulus. However, airfoil count was varied slightly to satisfy the tuning criteria. The stators of these stages were of constant cross section. Additionally, the inner diameter of stages 7 through 16 was constant, i.e., the discs were of the same diameter resulting in some savings during the design and manufacturing processes. All of the above resulted in an easy to build, lightly loaded compressor with sufficient surge margin.

The task of upgrading this compressor had two major objectives in mind. The first was a 6% increase in flow rate and the second was a 2% increase in Flange-to-Flange efficiency. It was immediately realized that the challenge lies in the efficiency requirement and not so much in the flow gain requirement. Furthermore, it was also requested that the upgrade be retrofittable into the older W501F engines should customers desire so. The retrofittability requirement restricted the problem severely and the design team was left with very few options.

##### 2.3.10.7.2.2 Aerodynamic Design

###### 2.3.10.7.2.2.1 Conceptual Design

The annulus area at the leading edge of the first rotor was increased by 9%, in order to facilitate the flow gain without compromising other relevant aerodynamics. This increase was tapered down to 0% at the leading edge of the third rotor. All discs, disc grooves, and axial gaps between airfoils were maintained, in addition to the outer diameter of stages 3 through 16, in order to satisfy the retrofittability requirement. This meant that the hub sections of the

newly designed rotor blades had to fit on the same platform as their predecessors. In addition the stator vanes could not exceed the axial space allowed to their predecessors. This in turn limited the axial loading redistribution to a minimum. The stator vane count was allowed to vary. However, due to strict tuning criteria, the vane count could not vary by radical amounts. In summary, stages 3 through 16 were designed to be completely interchangeable with the original design. Lastly, the original W501F compressor had 2 OGV's in addition to the last stator. This configuration was replaced by one that employs a single OGV and a single stator.

#### 2.3.10.7.2.2.2 The "Viscous" Method

Prior to the redesign of the upgrade, a thorough analysis of the existing W501FC compressor was performed. Shop test data existed for this design and the attempt to match it by the then current (S1-S2) analysis system did not yield acceptable results. Mass flow rate and efficiency calculated were different from measurements by as much as 2%. The calculated radial distribution of total pressure was remarkably flat, indicating that conditions at the end walls were completely missed. Attempts to remedy the situation by altering the blockage distribution were not successful as they also altered the mass flow rate. A different radial distribution of losses was employed and yielded somewhat better results, but this approach was later discarded in favor of the "viscous" method.

The "viscous" method simply replaced the then-current loss and deviation system, which was a 2-D inviscid blade-to-blade code (with simple boundary layer calculations), by a 3-D fully viscous Navier-Stokes CFD solution. The through flow code was then utilized as a bookkeeper, while the main source of aerodynamic input was the 3-D code. Losses and air angles were input directly into the through flow code upon attaining a converged 3-D solution. The compressor was then allowed to rematch using the newly generated input (of air angles and losses), and then a second iteration was performed. This method presented a totally different set of boundary conditions to the compressor, and the results were significantly more representative of actual test data, as shown in Figure 107. Additionally, the new mass flow and efficiency calculated were within the measurement tolerance, i.e., less than 0.3% different.

#### 2.3.10.7.2.2.3 Results and Discussion

The introduction of the 3-D solution into the design through flow of the upgrade compressor lead to improved boundary conditions for the stream section design. These new boundary conditions presented the endwall stream sections with increased incidence, and more severe diffusion requirements. The endwall sections were tailored to their new aerodynamic duties, and endbends were a direct consequence of that, as is shown in Figure 108, which shows the third stator of the W501FD as designed by the "viscous" method.

Another benefit of the endbends was increased mechanical strength. The endwall sections, as can be seen in the figure, are significantly more cambered than their predecessors, and have larger chords. This combination lead to a much higher minimum moment of area and a stronger, stiffer airfoil. This in turn allowed the designers to reduce thickness in the middle of the airfoil to gain more

efficiency. The end result was an increase of more than 10% in flow rate and 2% in efficiency.



**Figure 108 W501FD Compressor Third Stage Stator**

#### 2.3.10.7.2.3 Field Test

The advanced viscous design compressor test was performed on the W501FD engine, which was converted from the W501FC variant by incorporation of the new compressor hardware. The test objectives were to:

1. Verify engine performance with the advanced compressor.
2. Verify compressor aerodynamic performance and operational characteristics.
3. Verify compressor mechanical integrity.
4. Verify the viscous compressor methodology used in the W501FD compressor design.

The compressor was heavily instrumented with strain gauges (214) on different stator airfoils, BVM sensors (29) on some blade rows, tip clearance probes (8), accelerometers (16), fast response pressure sensors (12), thrust bearing load cells (8), mass flow measurements, inlet and exit total pressure and total temperature rakes (4 each), total temperature measurements on leading edges of two stator rows (two stators each), and endwall static pressure taps in most stator outer diameters at inlet and exit planes. Testing was completed over a period of about one month.

#### 2.3.10.7.2.4 Test Results

Test results demonstrated that there was 10.5% increase in compressor mass flow and 2 percentage points improvement in efficiency compared to the original compressor design, thus the validation viscous design methodology.

The monitored stator stress levels were either at or below expected values. Blade deflections for the compressor and turbine were within acceptable ranges. Stage one turbine vane temperatures were at expected values for the operating range that was experienced. Thrust bearing loads and temperatures were as expected. Crack indications were not reported for any of the stators or blades inspected. Standard blade rubbing was detected in rear stages but airfoil distress was not found.

#### 2.3.10.7.3 Task 14.3 Catalytic Combustor Development

Task objectives were to develop combustion technology to meet ATS program goals, i.e.,

- $\text{NO}_x < 10$  ppm at ATS firing conditions
- $\text{CO} < 10$  ppm
- Combustor Pressure Drop ( $Dp/P$ )  $< 4.5\%$
- 24,000 hour life with 8,000 hour service interval.

The combustor must achieve flame temperatures in excess of 1500°C (2732°F), maintain acceptable dynamics and remain stable over the entire engine operating range.

To achieve program goals the following approach was used: Two combustor concepts were developed and evaluated for ATS application: a lean premixed, dry low  $\text{NO}_x$  (DLN) design and a Catalytic Combustor. Early efforts focused on the DLN approach, utilizing design concepts already developed for the F-frame gas turbine engine technology. The severe operating environment of the ATS engine and the need to operate near “lean limit” to achieve desired emissions, limited the DLN technology. Although single digit  $\text{NO}_x$  should be achievable with the DLN approach, it was concluded that this design would offer little or no operating margin and no potential (without back-end cleanup) for achieving still lower  $\text{NO}_x$  emissions, a trend emerging in the market.

Working with Precision Combustion Inc. (PCI), SWPC developed a Catalytic Combustor to meet ATS program goals. This concept, illustrated in Figure 109, was demonstrated at full module scale. The module concept was developed to

fit into a conventional can annular basket design that permitted easy engine integration and retrofit.

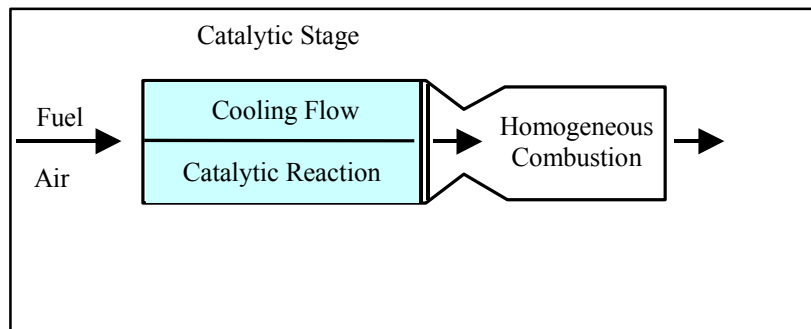


**Figure 109 ATS Catalytic Module Concept**

The Catalytic Module consists of a catalytic active stage that converts a portion of the inlet fuel to combustion products, generating significant temperature rise, and a homogenous burnout zone to complete combustion. No significant  $\text{NO}_x$  is generated in the catalytic active stage. The catalytic stage is designed to promote effective fuel-air mixing, cooling and burnout to minimize generation of thermal  $\text{NO}_x$ .

#### 2.3.10.7.3.1 Accomplishments

In the ATS program, efforts focused on the development of the Catalytic Module, including catalytic coatings, materials and performance testing in subscale and full scale modules. Table 17 summarizes the overall program scope and accomplishments.

**Table 17 Summary of Catalytic Combustor Development in ATS Program**

<b>Program Element</b>	<b>Scope and Approach</b>	<b>Accomplishments</b>
1. Catalytic Coatings Development	Screen and evaluate candidate precious metal catalysts and substrate materials, developing coatings to meet application objectives.	Coatings and substrate material systems were screened and down-selected. Catalytic active coating developed for ATS application and successfully applied to high alloy metal substrate.
2. Catalytic Reactor Technology	Qualify reactor performance and catalytic coatings materials durability in controlled sub-scale testing, simulating engine environment.	Base performance of selected catalytic material system demonstrated over load range. Light-off and conversion achieved. 100 and 500-hr materials durability tests completed.
3. Catalytic Module Development	Design and qualify a robust full-scale catalytic module and demonstrate performance in rig testing, simulating engine environment.	The design of the catalytic module was qualified through detailed thermal/mechanical analysis. Three full-scale modules were built and tested at full flow and pressure. Progressive improvement in module performance was demonstrated in the test program.
4. Development of a Catalytic Combustor	Design and qualify a full catalytic basket and demonstrate performance in rig testing, simulating engine environment.	Concept designs for a full-scale catalytic basket were developed, integrating six catalytic modules around a central pilot. Plans remain to test the basket under engine conditions.

#### 2.3.10.7.3.2 Catalyst Development

The catalyst should be active to “light-off” over a wide range of fuel air stoichiometries. This will ensure that adequate heat release occurs through the catalytic reactor, to ensure acceptable downstream flame stability. Catalyst light-off temperature is a function of many variables, usually those associated with the operating parameters of the engine (e.g., velocity or residence time across the catalyst, fuel-air concentration, fuel quality/composition, as well as ambient air composition). These parameters were explored in the ATS catalyst test program.

Catalyst testing involved the development of catalyst and substrate formulations for the reactor module. This included new formulation and process development addressing adhesion, materials and process compatibility as well as microstructural characterization of the catalyst and substrate.

For the catalyst screening, catalyst/substrate combinations were applied to flat, thin strips (or “coupons”) for rapid testing. The coupons were then installed in a simple test rig, and exposed to a flow of premixed, preheated fuel and air. Testing was done at both atmospheric and high pressure (10 – 15 atm [1.013 MPa to 1.52 MPa]). Catalyst performance was evaluated by the surface temperature rise due to catalytic surface reactions and pre/post gas analysis to measure fuel conversion and reaction rates.

#### 2.3.10.7.3.3 Sub-Scale Module Testing

Following coupons testing, promising catalysts were identified and tested at simulated operating conditions, in both sub-scale and full-scale modules at both atmospheric pressure and high (10 – 15 atm [1.013 MPa to 1.52 MPa]) pressure. Key test parameters included catalyst activity, selectivity and cooling design of the reactor. From this work, the preferred catalyst formulations were chosen for further performance and materials testing.

Utilizing the combustion rig located at the Siemens Westinghouse Science and Technology Center, performance and materials durability testing were conducted on a 1/40<sup>th</sup> scale catalytic module. Although sub-scale, the geometry and flow conditions represented full-scale module conditions.

Exhaust emissions including UHC, CO, CO<sub>2</sub>, O<sub>2</sub> and NO<sub>x</sub> were measured at a number of different steady state conditions in the sub-scale module test program. The data confirmed the low-NO<sub>x</sub> capability of the system, as well as operation at high firing temperature. For all data points, combustion was stabilized by catalytic pre-reaction from the reactor module. Large turndown from low, lean blowout to high firing temperature was achieved. Low single digit NO<sub>x</sub> emissions were obtained at flame temperatures up to approximately 1538°C (2800°F), meeting ATS goals.

Limited durability testing (10 to 50 hours) was conducted to evaluate the initial stability of catalyst formulations. The most promising formulation was tested at both 100 and 500 hour segments, at 15 atm (1.52 MPa). During this testing, catalyst surface temperatures were maintained at a constant value to allow interpretation and extrapolation of post-test materials analysis data. Performance testing and rig stabilization during the first 500 hours of testing led to some variation in catalyst surface temperature but results show consistent and steady temperature profile through the catalytic module over time. No degradation in catalyst performance was observed during the 500-hour high-pressure test. Performance testing and gas sampling were conducted both prior, during and subsequent to the durability testing period. Emissions and gas composition remained steady, which is consistent with stable module performance. Preliminary conclusions from material analysis of the 500-hour test module confirm the potential of achieving extended life and continued materials testing is recommended.

#### 2.3.10.7.3.4 Development of the Full-Scale Catalytic Module

A catalytic module concept was designed and developed utilizing the material systems qualified in the sub-scale testing. The module concept, illustrated in Figure 109, was designed and packaged to fit into the conventional Siemens Westinghouse can annular basket. Thus, no significant modifications to the engine casing are necessary.

Three full-scale catalytic modules were fabricated and tested as part of the ATS combustor program. The three modules differed only slightly in design, accomplishing improvements in both mechanical and aerodynamic (mixing) aspects. High pressure rig testing was conducted to evaluate performance. Key

performance parameters included emissions, pressure drop, dynamics, catalytic activity, peak metal temperatures and flame stability. Each module was operated over a range of temperature and load conditions. A brief summary of this testing is provided below:

*Module 1 Testing:* Four fired test runs were conducted, utilizing the GASL Blowdown Facility located in New York, to benchmark this initial design. Most of the identified performance parameters were met. NO<sub>x</sub> emissions ranged between 10 and 12 ppm, but were achieved at operating temperatures below ATS goals. Based on this testing, improvements in mechanical and aerodynamic design were identified and implemented into Module 2.

*Module 2 Testing:* Testing was again conducted at the GASL facility. In general, the module performed well, meeting most of the performance goals. NO<sub>x</sub> emissions below 10 ppm were achieved at nominal F-frame operating temperature, 1464°C (2668°F), but exceeded 10 ppm at targeted ATS conditions. In this test run, an over-pressure of the fuel feed line occurred causing mechanical deformation of the fuel manifold and possibly resulting in poor upstream air/fuel mixing. This would likely carry-through to the downstream, impacting emissions. Based on this testing, improvements in mechanical and aerodynamic design were identified and implemented into Module 3.

*Module 3 Testing:* This module was tested in the test rig at Solar Turbines in San Diego California at 10 bar. Two test runs were made, operating the module over a range of temperature and load conditions. At 1530°C (2785°F), NO<sub>x</sub> emissions were below 9 ppm and below 6 ppm under nominal F-frame conditions. Further reducing combustion temperatures also reduced NO<sub>x</sub>, but in this test rig relatively high dynamics were encountered under the lower temperature conditions. Post inspection showed no mechanical issues with the catalytic module.

#### 2.3.10.7.3.5 Combustion System Design

The module concept tested in this ATS program was sized to fit into a conventional can annular combustor with minimal modifications. Conceptual design studies were completed for the W501F engine to confirm the design basis (see Figure 111). Six catalytic modules are arranged around a central pilot to form the basket design. Preliminary thermal/mechanical studies were conducted to confirm mechanical feasibility. Air discharging from the compressor diffuser enters the engine casing and flows to the head-end of the catalytic module similar to conventional DLN basket designs. Fuel is distributed through a manifold to each catalytic module. The design concept appears feasible for both new and retrofit applications.

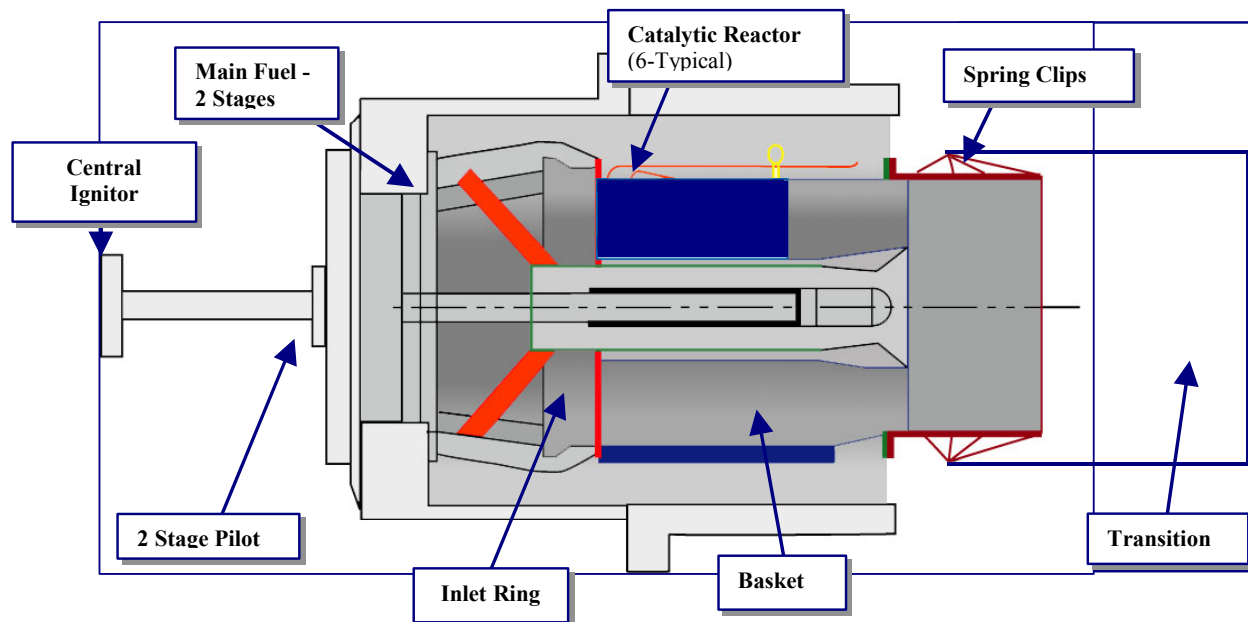


**Figure 111 Catalytic Combustor**

#### 2.3.10.7.3.5 Summary

Catalytic combustion technology has been developed to improve gas turbine engine emissions and performance and tested through sub-scale and full scale module component size. NO<sub>x</sub> emissions below 10 ppm were achieved under typical gas turbine engine operating conditions and temperature level consistent with ATS goals. Pressure drop, lightoff, catalyst activity, cooling design and stability criteria were also met. A full scale catalytic combustor concept design was prepared showing the feasibility of incorporating catalytic modules into a current engine casing using a standard can annular configuration. Further development of this technology is required to confirm long term catalytic coating life and combustion performance in a full basket arrangement.

#### 2.3.10 Conclusions

The ATS engine design specification was prepared and in conjunction with Siemens Westinghouse Design Criteria Manual and state-of-the-art computer codes, was used in the detail engine design. The design incorporated a mix of well proven design concepts and innovative advanced technology. The 20 stage compressor was based on the W501G compressor with additional stages and further enhancements. The combustor design was based on Siemens Westinghouse DLN technology. The four-stage turbine design employed 3D aerodynamic design technology and advanced materials and coatings.

The ATS plant design was derived from the 240 MW Reference Plant developed for the W501F product line. However, the ATS plant utilized the single shaft concept, which incorporated a gas turbine on one end of a common generator and a steam turbine on the other.

Application of ATS gas turbine for coal-fueled operation focused on Integrated Gasification Combined Cycle and the Advanced Pressurized Fluidized

Combustion concepts. Potential performances of these power plants were estimated and the required modifications to the ATS gas turbine were investigated. Adaptations for biomass application were also briefly considered.

An ATS Advisory Board, composed of 10 corporate and government members, was constituted to review program results and make recommendations regarding the program direction.

Integrated hot vane cascade/combustion test rig was designed and manufactured. This rig is capable of testing combustors, transitions and first stage turbine vanes at ATS operating conditions of temperature, pressure and air flow.

Internal heat transfer tests were carried out on plexiglass models representing the six different cooling techniques employed on the closed-loop, thin walled first stage turbine vanes and blades. Internal heat transfer coefficients and pressure drops used in the design of these components were validated.

Heat transfer coefficient and pressure drop characteristics of non-ideal turbulator shapes used in airfoil cooling holes were determined from tests on scaled up plexiglass models.

Extensive sealing development effort was carried out on different brush seals, face seal, rope seals and abradable coatings applied to stationary shrouds and air seals in the compressor and turbine. This effort focused on reducing leakages in different components of the gas turbine and hence on improving its performance.

To verify the aerodynamic performance and mechanical integrity of the new high pressure ratio design, the full-scale ATS compressor was manufactured and tested in a special facility constructed at the U.S. Navy Base in Philadelphia. Test results demonstrated that the design achieved its predicted aerodynamic performance and had lower than predicted vibratory stresses on airfoils instrumented with strain gauges.

The first two stages of the ATS turbine were tested at 1/3 scale in the shock-tube test facility at Ohio State University. Test results demonstrated a significant aerodynamic efficiency improvement resulting from optimum "clocking" of turbine vanes and blades.

A novel concept for compressing cooling air inside a closed-loop cooled turbine rotor/blade system (thus eliminating the need for an auxiliary compressor) was designed and rig tested. Test results validated the predicted pressure gain.

Combustion development focused on developing a combustion system that would meet the ATS Program emission goals. Rig testing of the Piloted Ring Combustor demonstrated that the emission goals are achievable. However, due to high estimated production cost of this concept, further development effort was redirected to the DLN combustor concept used on W501F and W501G engines. Parallel efforts with Georgia Tech on active combustion noise control, demonstrated on a test rig that the system under development can quickly stabilize a combustor after onset of instability.

Catalytic combustion technology has been developed to improve gas turbine engine emissions and tested through sub-scale and full scale module size. NO<sub>x</sub> emissions below 10 ppm were achieved. A full scale catalytic combustor concept design was prepared.

CMC turbine blade tip air seal design was demonstrated to be feasible by detail analysis and subelement testing.

Development was carried out on new bond coat chemistries and new TBCs for coating systems that would have long operating life at ATS temperatures. A series of TBC lifing tests were performed on the new High Heat Flux Rig. On-line and off-line TBC quality monitoring NDE techniques and TBC patch repair process were investigated.

Long term oxidation and corrosion testing, using clean steam and with salt impurities, was carried out on different materials used in the ATS engine cooling and steam piping designs. Oxidation, corrosion and metal waste were observed on all materials exposed to high pressure and temperature steam. The extent of the attack depended on the alloy, level of impurities test in the steam and exposure time. Coatings, such as aluminide and chromide, provided protection to the base alloy.

Material property data for directionally solidified CM247LC alloy were generated. The test results were analyzed and property curves were generated to support the design of large industrial gas turbines. Verified that data generated on cast slabs and test bars accurately represented components properties. Determined the influence of post-casting thermal cycles on mechanical properties. Low cycle fatigue and thermo-mechanical fatigue testing was performed on coated and uncoated IN 939 test pieces at different temperatures.

Extensive material testing was performed on single crystal CMSX-4 castings. The data were analyzed and documented in Turbine Materials Manual. To investigate CMSX-4 alloy stability during engine operation, long term creep rupture testing was performed.

Program plan was developed for liquid metal cooling process, which has considerable advantage over the conventional directional solidification process.

To achieve acceptable casting yields for large single crystal airfoil castings, the bonded vane development was carried out. The vanes were to be cast in smaller cast segments and then machined and fabricated using the transient liquid phase bonding.

Modified chemistry IN 939 alloy was developed for improved weldability, which is very important for repair of cracks in new castings, as well as for service run vanes.

TBC life prediction models were developed for APS and EB-PVD TBC coatings.

An alternative coating system to that of conventional thermal barrier coatings has been evaluated in rigs and an operating engine. This coating concept is based on ceramic filler inside a high temperature metallic honeycomb structure.

Non-destructive evaluation techniques were investigated for inspection of ATS components, such as TBC coated turbine airfoils and single crystal turbine blades. The development efforts focused on: (1) pulsed infrared thermal wave imaging for detecting various TBC failure mechanisms, (2) meandering winding magnetometer for measuring metallic bondcoat thickness, and (3) X-ray diffraction for measuring single crystal orientation and detecting unwanted secondary crystals.

Nickel base IN 718 and IN 706 alloys were evaluated for use in rotor discs and associated rotor components. Baseline mechanical properties were determined. It was concluded that IN 718 provides a higher temperature capability than IN 706 for side plates and small forging elements. For IN 706 it was concluded that it would have potential for notch sensitivity with the conventional two step heat treatment.

Thin wall first stage vane and blade single crystal casting trials have indicated that these components can be manufactured. However, further development is required to ensure they can be manufactured at a reasonable cost.

Spin pit tests were carried out to evaluate stresses in the turbine blade root/disc steeple attachment. Test results will be incorporated into the analytical tools used in turbine blade attachment design.

A rig test program was conducted on two types of flexible joints to be used in the closed-loop steam cooling piping system. Stationary and vibratory tests were carried out to measure steam leakage. Test results demonstrated that Tubeseal Flex-Slide Joint had a much lower leakage than the piston ring seal.

Alternate first stage turbine vane and blade designs were carried out as a back up to the primary designs.

An extensive test was carried out on the Prototype W501G engine at the City of Lakeland, Florida power plant to verify the ATS technology incorporated in its design. These technologies included the first sixteen stages of the ATS compressor, stage three turbine blade cooling, stage four turbine shrouded and snubbed blade, advanced turbine airfoil bond coat/TBC coating system, brush seals in the turbine interstage locations, and abradable coatings on compressor and turbine stationary air seals to reduce blade tip clearances without incurring severe blade tip rubs. More than 1,200 sensors were installed to measure temperatures, pressures, flow angles, emissions, stresses, tip clearances and blade vibration characteristics.

The advanced viscous compressor design was field tested in a W501F engine. The compressor efficiency was as predicted and the inlet mass flows exceeded prediction.

### **3.0 ATS TECHNOLOGY FLOWDOWN TO MATURE FRAMES**

To achieve the maximum benefits from reductions in energy use, emissions and cost of electricity resulting from the new technologies developed in the ATS Program, a concerted effort was made to incorporate these technologies into the entire Siemens Westinghouse gas turbine product line. Early introduction of new technologies, such as advanced aerodynamics, sealing, cooling concepts and

coating systems, as well as DLN combustion systems, would result in immediate public benefit prior to the ATS engine introduction. The Siemens Westinghouse design philosophy for product enhancements includes retrofitting improvements into older operating units, as well as incorporating them into current production units. This retrofitability allows existing customers to improve their assets' performance rather than wholesale replacement.

The ATS-developed compressor technology has been retrofitted into the W501F product line. Using the analytical techniques developed and proven in the ATS program, the W501F compressor was upgraded in the latest improvement to this successful frame. Field tests demonstrated that this design achieved significant improvement in massflow and efficiency. This advanced compressor is used on all new W501F engines. In addition, the redesigned compressor can be retrofitted to any of the 42 W501F engines that were built with the original W501F compressor. Applying this ATS technology to the W501F engine expands the benefit of the ATS program, since the W501F comprises more than 70% of future units that are sold or on order Siemens Westinghouse.

Brush seals in the transition inlet and turbine interstage seal locations have been incorporated into the W501F and W501G product lines, as well as retrofitted into the W501FD family. Rope seals are being considered for retrofit into interstage locations. Pre and post upgrade tests of installed interstage brush seals demonstrated performance improvement in retrofit applications.

The ATS developed abradable coatings have been incorporated into W501F and W501G compressors and front turbine stages to allow tighter blade tip clearances and hence improved performance, without the risk of tip rubs and consequential damages.

Advanced anti-corrosional and oxidation bondcoat developed for the ATS engine turbine airfoils has been applied to the W501G engine. TBC coating developed for ATS and W501G engines has been applied to the W501F engines.

Results of ATS compressor, model turbine, cooling, sealing, combustion, blade/disc attachment and material properties testing are being incorporated into the Siemens Westinghouse design system and will be used in future engine upratings and new engine designs to give further improvements in efficiency, emissions and mechanical integrity of our product line.

#### **4.0 PUBLIC BENEFITS**

The public benefits of the ATS program include lower cost of electricity through higher efficiencies, lower emission, and improved security (fuel use savings) while developing new high tech. jobs.

##### **Lower Cost of Electricity**

A number of key Siemens Westinghouse ATS component technologies have been incorporated into recent models of the W501F and W501G gas turbines. Today, technologies developed under the Siemens Westinghouse ATS Program are operating in over 130 power plants help them become lower cost producers of electricity for the American consumer.

These breakthrough technologies are expected to save \$7.0 Billion in consumer electricity savings by 2015. These public benefits are over and above the benefits of future ATS gas turbines entering the marketplace. The ATS gas turbine efficiency is over 70% higher when compared to the typical conventional coal fired steam plant efficiency of 35%.

#### Lower Emissions

The efficiency improvements derived from the technology portfolio developed under the Siemens Westinghouse ATS program set a new standard in environmental stewardship. An ATS gas turbine produces less NOx in one year than existing coal plants produce in under 2 weeks. There is less greenhouse gas, CO<sub>2</sub> produced in one year with an ATS gas turbine than the conventional coal plant produces in four months with the added benefit of no acid rain producing SO<sub>2</sub>.

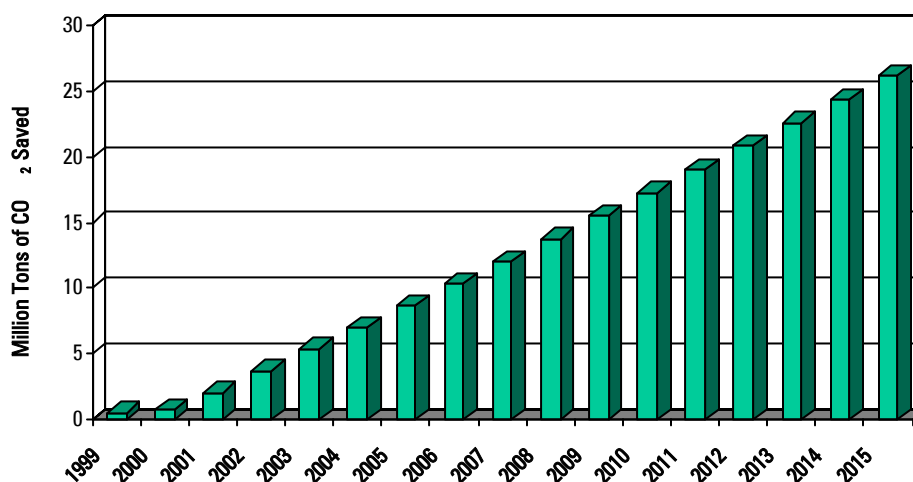


**Figure 112 Tons of CO<sub>2</sub> Saved**

#### Improved Security

The annual natural gas savings in efficient power generation is enough to heat over 17 million homes by 2015 and include savings of over 300,000 barrels of imported oil per day for the same time period.

Studies done under the ATS program confirmed the viability of the ATS gas turbine's fuel flexibility. Study results showed that the ATS gas turbine can be modified to operate on low to medium BTU syngas derived from coal, petcoke, or residual oil. Integration of an ATS gas turbine into tomorrow's Integrated Gasification Combined Cycle will lead to lower cost of electricity from these coal based plants as well.

#### More Jobs

The ATS program will help build U.S. economic strength by maintaining the competitiveness in an estimated \$80 Billion new capacity power market in America in the 2000-2015 time period. This supports thousands of jobs in the gas

turbine industry and related hardware manufacturing. The increase of U.S. export sales, estimated at \$260 billion for the same period reduces our trade deficit and creates additional jobs to support the international market. The ATS program was necessary to maintain the U.S. technology leadership against highly government subsidized foreign competitors.

#### Summary of Return on Investment

The return on investment for the U.S. with the ATS program supports a 60% efficient gas turbine technology saving 100 million barrels of oil equivalent per year by 2015. The reduced cost of electricity to the American consumer will amount to over \$7.0 by 2015 and allow continued competitiveness of U.S. industry in world markets. By maintaining American technology competitiveness in a \$350 billion world power market we create and preserve American jobs and increase our exports. The ATS program by being fuel flexible preserves future energy options and reduces climate change through global reduction in NO<sub>x</sub> and CO<sub>2</sub>.

## 5.0 OVERALL ATS PROGRAM CONCLUSIONS

Technology development efforts and detail component and engine designs have demonstrated that ATS Program goals are achievable. These goals will be demonstrated in the ATS engine when the market conditions are favorable for its introduction.

To achieve the maximum benefits from reductions in energy use, emissions and cost of electricity resulting from the new technologies developed in the ATS Program, a concerted effort was made to incorporate these technologies into the entire Siemens Westinghouse gas turbine product line. Early introduction of new technologies, such as advanced aerodynamics, sealing, cooling concepts and coating systems, as well as DLN combustion systems, would result in immediate public benefit prior to the ATS engine introduction. The Siemens Westinghouse design philosophy for product enhancements includes retrofitting improvements into older operating units, as well as incorporating them into current production units. This retrofitability allows existing customers to improve their assets' performance rather than wholesale replacement.

The major DOE/Siemens Westinghouse ATS Program accomplishments are listed below.

### TECHNOLOGY VERIFICATION

**Incorporated ATS technology into the Siemens Westinghouse gas turbine product line** - Technologies successfully developed in the ATS program were incorporated into the complete Siemens Westinghouse product line, including W501D, W501F, and W501G.

**W501G engine field testing to verify ATS technology** - An extensive test was carried out on the Prototype W501G engine at the City of Lakeland, Florida,

power plant to verify the ATS technology incorporated in its design. These technologies included the first sixteen stages of the ATS compressor, stage three turbine blade cooling, stage four turbine shrouded and snubbed blade, advanced turbine airfoil bond coat/TBC coating system, brush seals in the turbine interstage locations, and abradable coatings on compressor and turbine stationary air seals to reduce blade tip clearances without incurring severe blade tip rubs. More than 1,200 sensors were installed to measure temperatures, pressures, flow angles, emissions, stresses, tip clearances and blade vibration characteristics.

**Twenty-stage ATS compressor design and full scale verification test** - The twenty-stage 30 to 1 pressure ratio ATS compressor was designed using the latest viscous analysis codes available at the time. A test facility was designed and constructed at the US Navy Base in Philadelphia. A full scale ATS compressor test was then tested in this facility to verify the compressor starting characteristics, performance and mechanical integrity.

**W501F viscous compressor field verification** - To improve the W501F, which is the main production engine in Siemens Westinghouse, the compressor was redesigned using viscous design methods developed under the ATS program for increased flow and efficiency using further advances in viscous design philosophy, such as end bends. This compressor design was verified by a field test at a customer site.

## **GAS TURBINE COMBUSTION**

**Dry low NO<sub>x</sub> combustor development** - Development was carried out on several lean premixed dry low NO<sub>x</sub> combustors to ensure that low emissions can be achieved at ATS firing temperatures without combustion instabilities and flashback. The most successful concept is the Dry Low NO<sub>x</sub> (DLN) combustor, which consists of eight premixed swirler assemblies arranged around a diffusion/pilot nozzle/swirler assembly. Development tests were carried out in atmospheric, mid pressure, and high pressure test rigs, as well as in field engines.

**Test trials of catalytic combustor module** - In order to achieve single digit NO<sub>x</sub> emissions at ATS firing temperature without incurring combustion instabilities associated with very lean premixed frames, a catalytic pilot and a completely catalytic combustor are being developed. Tests were carried out to demonstrate catalyst performance characteristics over long periods of operation.

**Sub-scale demonstration of active combustion noise control** - An active combustion noise control system is being developed to allow safe lean premix combustor operation without resorting to catalytic components. Subscale tests were carried out on a system using a sensor located in the combustor, signal processor, actuator, and a control valve located in the fuel bypass line. Tests demonstrated a four-fold reduction in combustion dynamics.

**Non-intrusive laser-induced fluorescence probe development** - Controlling combustion dynamics in lean premix combustors requires very well mixed fuel/air mixtures. Poor mixing results in uneven flame temperatures, and hence in combustion instabilities and high NO<sub>x</sub> in regions of high flame temperatures. A

non-intrusive laser-induced fluorescence probe was developed for measuring fuel/air concentrations and combustion product concentrations. This probe was used in unfired and fired tests.

### **ADVANCED SEALING & COOLING**

**Advanced sealing development** - ATS engine performance and hot parts' mechanical integrity are detrimentally affected by cooling air or hot gas leaks. To reduce these leaks brush seals, rope seals, face seals, and abradable coatings were developed.

**Closed-loop steam cooling technology development** - One of the main contributors to the ATS engine performance is closed-loop steam cooling of turbine components. Designs were carried out for the first and second stage turbine closed-loop steam cooled stators and ring segments (air seals).

**Advanced Air Cooling Technology Development** - Tests were carried out to optimize turbine airfoil air cooling designs. These included multi-pass blade cooling, stator endwall cooling, third stage shrouded blade cooling, and effect on internal heat transfer coefficients of different turbulator shapes located in internal airfoil cooling passages.

### **ADVANCED MATERIALS & COATINGS**

**Advanced bond coat/TBC system development** - Long life bond coat/TBC systems are required to ensure the mechanical integrity of turbine airfoils. This is especially important for closed-loop steam cooled designs, which do not have protection of film cooling used in current gas turbine cooling designs. To address this issue an advanced high temperature bond coat/TBC system capable of 24,000 hour operation was developed.

**Effect of steam on turbine alloy materials** - Rig tests were carried out to investigate the effect of cooling steam on turbine components. These tests included fouling, scaling, oxidation, and corrosion characteristics of several alloys used in turbine airfoils, transitions, and steam pipes. Based on the results steam purity criteria and internal surface coating requirements were defined.

**Weldable turbine vane alloy development** - A more weldable version of IN939 alloy was developed to allow welding cracks in new turbine vane castings to improve casting yields and cracks in service run parts to reduce life cycle costs.

**Single Crystal casting technology development for large land based turbines** - Higher operating gas temperatures in the ATS application and the requirement to minimize coolant flows to improve performance necessitate the use of Single Crystal (SC) turbine alloys. Casting development was carried out on thin wall first stage vanes, first stage blades, second stage blades, and third stage shrouded blades to demonstrate the feasibility of SC castings for use in large utility gas turbines.

## REFERENCES

- Bajura, R.A., Webb, H. A., and Parsons, E. L., 1992, "A Proposed Plan for an Advanced Turbine Systems Program," Proceedings of Workshop to Define Gas Turbine System Research Needs 11, South Carolina Energy Research and Development Center, pp. 9-30.
- Bancalari, E., Diakunchak, I. S., McQuiggan, G., 2003, "A Review of W501G Engine Design, Development and Operating Experience," ASME Paper GT-2003-38843.
- Bannister, R. L., Cheruvu, N. S., Little, D. A., and McQuiggan, G., 1994 "Development Requirements for an Advanced Gas Turbine System," ASME paper 94-GT-388.
- Bannister, R. L., Newby, R. A. and Diehl, R. C., 1992, "Developing a Direct Coal-Fired Combined Cycle," Mechanical Engineering, Vol. 114, No. 12, pp. 64-70.
- Briesch, M. S., Bannister, R. L., Diakunchak, I. S., and Huber, D. J., 1995, "A Combined Cycle Designed to Achieve Greater than 60 Percent Efficiency," ASME Journal of Engineering for Gas Turbines and Power, Vol. 117, pp. 734-741.
- Diakunchak, I. S., Bannister, R. L., Huber, D. J., and Roan, D. F., 1996, "Technology Development Programs for the Advanced Turbine Systems Engine," ASME Paper GT-96-5.
- Jouini, D. B. M., Little, D., Bancalari, E., Dunn, M., Haldeman, C., and Johnson, P.D., 2003, "Experimental Investigation of Airfoil Wake Clocking Impacts on Aerodynamic Performance in a Two Stage Turbine Test Rig," ASME Paper GT-2003-38872.
- Khinkis, M. J., 1991, "Low Emission Combustion and Thermochemical Heat Recovery at IGT," Proceedings of Workshop to Define Gas Turbine System Research Needs, South Carolina Energy Research and Development Center.
- Levari, G. N., Jeffries, R.E., and Cohn, A., 1984, "Advanced Cooled First Stage Vane Design," ASME Paper 84-GT-219.
- Little, D. A., Bannister, R. L., and Wiant, B. C., 1993, "Development of Advanced Turbine Systems," ASME Cogen Turbo Power '93 Proceedings, IGTI Vol. 8, pp. 271-280.
- Southall, L., McQuiggan, G., 1995, "New 200 MW Class W501G Combustion Turbine," ASME Paper 95-GT-215.
- Webb, H. A., Parson, E. L., and Bajura, R. A., 1993, "Advanced Turbine Systems Program and Coal Applications," ASME Paper 93-GT-356.